

**A RENAISSANCE OF RADICAL FLUORINATION CHEMISTRY:  
METHODS, MECHANISMS, AND ADVANCES IN SELECTIVITY**

by  
Cody Ross Pitts

A dissertation submitted to Johns Hopkins University in conformity with the  
requirements for the degree of Doctor of Philosophy

Baltimore, Maryland

April 28, 2017

© 2017 Cody Ross Pitts  
All Rights Reserved

## Abstract

As taught in most introductory organic chemistry courses, a safe, selective "radical fluorination" of  $sp^3$  C-H bonds has been virtually absent from the synthetic toolbox for decades. In 2012, such radical monofluorination tactics came to fruition employing metal initiators and mild sources of atomic fluorine. Specifically, our laboratory, contemporaneous with Groves' report on a manganese-porphyrin/silver(I) fluoride approach, introduced a copper(I)/Selectfluor protocol for aliphatic fluorination. Beyond these pioneering examples, a number of methods have been reported from our laboratory, and others, that accomplish similar chemistry using different transition metals, radical initiators, and both ultraviolet and visible light photosensitizers. Although these represent a substantial leap in controlling *reactivity*, the issue of *selectivity* remains an even greater challenge. The original work in this area proved fit for selective fluorination of highly symmetric molecules and those containing more activated benzylic C-H bonds; yet, so-called scattershot fluorination may occur on more complex molecules with multiple, dissimilar C-H bonds, thus generating a large number of products. Through better mechanistic understanding of the existing protocols, we have begun to envision ways to *direct* radical fluorination more reliably to enable practical late-stage fluorination of biologically relevant molecules. In addition to guiding  $sp^3$  C-H functionalization through the use of directing groups, we have also discovered ways to fluorinate carbon-centered radicals generated from strained and unstrained  $sp^3$  C-C bond cleavage that, in turn, also led to the unveiling of an unanticipated aminofluorination reaction. This dissertation discusses the serendipitous discovery of initial reactivity with the copper(I)/Selectfluor aliphatic fluorination method and the ongoing method development and mechanistic investigations that have paved the way for 1) alternative approaches to practical radical fluorination chemistry (with a more recent emphasis on photochemical approaches) and 2) timely improvements in selectivity. Among other applications, this work highlights methods that may be used for the selective fluorination of amino acids, peptides, steroids, terpenoids, and other natural products. We are optimistic that this rebirth of radical fluorination may find near-term adoption in a medicinal chemistry setting, where fluorine plays a prominent role.

Advisor: Professor Thomas Lectka

Reader: Professor Gary H. Posner

Reader: Professor Craig A. Townsend

*For Poppy and Grandma*

## Acknowledgements

Every few months during my graduate career I would reflect on my progress. Explicitly, I would ask myself, "what am I capable of *now* that I was not *then*?" After several iterations, I have collected enough data to determine that this period of my life has been one of exponential personal and scientific growth. I understand that this type of acceleration would not have been possible without a constant applied force. That force was Professor Thomas Lectka. From the moment I joined the Lectka laboratory, Tom began to nurture my career continuously by pushing me outside of my scientific comfort zone, encouraging me through the lulls of research (what few there were), and inspiring me always to be better. Over the years he has trained me as a scientist, artist, businessman, advertiser, performer, writer, and teacher. Additionally, Tom has taught me the importance of *jazz* in chemistry and artful ways to turn lemons into lemonade. I am eternally grateful. Tom was an astounding advisor and, ultimately, an even better friend.

Beyond my advisor, two additional outstanding scientists have served as mentors to me: Professor Gary H. Posner and Professor Craig A. Townsend. Initially through joint group meetings and later in one-on-one interactions, Professor Posner has given me a new perspective on organic and medicinal chemistry and invaluable career advice. In particular, I appreciated hearing his firsthand accounts on developing organocopper methodologies and the medicinal chemistry success stories of vitamin D and artemisinin derivatives; I have learned a great deal from him. Notably, his generosity in sharing and donating chemicals, glassware, and equipment to the Lectka laboratory has opened up research opportunities that I could not have imagined earlier in my graduate career. On another front, Professor Townsend has inspired me through his work ethic, tenacity, curiosity, and sheer love of science. It is very easy to spend hours in Professor Townsend's office getting lost in the wonders of chemistry and biology. Beyond the classroom, he has taught me much in the way of natural products, biosynthetic pathways, mechanistic chemistry, writing grant proposals, and pursuing a career in academia. In all, I cannot express how fortunate I am to have had such a powerhouse of a thesis committee help construct the foundation of my future career. In addition, I would like to thank Prof. Lev Ryzhkov, Prof. Chris Falzone, and Prof. Lenny Brand for serving on my GBO committee.

Next, I would be remiss not to extend my gratitude to my fellow lab mates over the years. Though I did not overlap with Mike Scerba and Jeremy Erb for long, they helped me begin to establish a good mindset and proper technique when conducting dangerous or sensitive reactions. After Jeremy Erb left the Lectka laboratory in the summer of 2012, Steve Bloom, in his second year of graduate school, became the senior member of the laboratory alongside Mark Struble and me. Thus, Steve, Mark, and I had to figure out many things the hard way. I have always admired Steve Bloom's intense work ethic and creative thinking and Mark Struble's laser-sharp focus and unbelievably subtle wit. When given the option to sink or swim, the three of us helped each other stay afloat; consequently, we succeeded in pioneering some incredibly exciting research in fluorine chemistry, even if it meant working 80 hours in 5 days to submit a paper for publication on time.

After three years, the Lectka laboratory grew to include Desta Bume, Michelle Bloom, Liangyu Guan, and Max Holl (extending his term as a former undergraduate lab member). While I have had many delightful conversations with Max and Liangyu about computational and physical organic projects going on in their side of the lab, I worked more intimately with Michelle and Desta. I have enjoyed watching them grow as scientists and guiding them through the things that I had already learned the hard way, so they did not have to. In addition, Desta is one of the hardest workers I have seen in the lab to date and is a great friend for teaching me how to calculate *who minus who*. More recently, a new wave of graduate students arrived: Stefan Harry, Joe Capilato, and Fereshte Gorbani. I have had the opportunity to develop some very exciting chemistry with Stefan and establish another strong friendship over the last year. Although I will have spent much less time with Joe and Fereshte, I am very optimistic about Joe's unmatched creativity and Fereshte's determination. In all, I am thankful that the Lectka laboratory is well equipped with great people to continue doing great chemistry, but this also makes me sad to leave.

Additionally, from the early stages of my graduate career, I was tasked to train undergraduates in the laboratory. I would like to thank Dave Miller and Nathan Haselton, my first students, for being patient with me training them as I was in training myself. In many ways, they helped me start to figure out how to be a better teacher in the lab. In the next couple years, I had the pleasure of working with Andy Griswold, Ryan Woltornist, Dillon Auvenshine, Levi Knippel, Ran Liu, Arthur Zhang, and Bill Ling. I have spent memorable years watching each of them grow in the lab, and I am both honored to call them friends and

genuinely excited for their future careers. More recently, I have worked with Josh Zhu, Ben Park, Rayyan Jokhai, Javier Casado-Cocero, Hunter Pool, and Wei Hao Lee, all of whom are good people and show great potential. I can go on for pages about my lab mates and still not do them justice, so I hope it is enough to state that I am extremely thankful and proud of everyone. I am excited for our paths to cross again.

It is also important to acknowledge that I have received very helpful advice and experimental assistance from members of each the Posner, Townsend, Bragg, Yarkony, Karlin, Goldberg, Toscano, Fairbrother, Tovar, Klausen, and Greenberg laboratories. The collegiality of the Johns Hopkins Chemistry Department is part of what makes it great. I am thankful for what I have learned about NMR spectroscopy from Dr. Cathy Moore and later from Dr. Joel Tang and Dr. Ananya Majumdar, and I commend Dr. Maxime Siegler for his excellent X-ray crystallographic data contributions to our publications. I also appreciated the opportunity to serve as a teaching assistant for Prof. Chris Falzone, who gave me a fresh perspective on teaching organic chemistry. Beyond the science, I believe Boris Steinberg is worthy of the highest praise. He is an honest, reliable, caring, hard-working handy man that physically keeps this department running; I pray he never goes underappreciated. In addition, I thank the administrative staff – John Kidwell, Lauren McGhee, Rosalie Elder, Meghan Carter, and particularly Jean Goodwin – for their helpfulness on the non-scientific end of graduate studies. I thank Johns Hopkins for the Ernest M. Marks, Gary H. Posner, and Glen E. Meyer '39 Fellowships.

Of course, I would not have made it to Johns Hopkins without an exceptional undergraduate experience, so I have a number of people to thank from Monmouth University. I owe my sincerest gratitude to Prof. Massimiliano Lamberto (my former advisor) and Prof. Theresa Zielinski (my physical chemistry professor). Prof. Lamberto inspired me to be an organic chemist in the first place and took me under his wing. In my senior year, Prof. Zielinski gave me necessary the direction and confidence to think independently as a scientist. I also extend my thanks to Prof. Tongesayi, Prof. Kucharczyk, Prof. Topper, and Prof. Schreiber, among others, for being great teachers. Beyond the science, I have had tremendous support from the Honors School, especially from Prof. Garvey, Prof. Mitchell, Reenie Menditto, Erin Hawk, and both Elizabeth and Jane Freed. They are like family. Lastly, in the arts department, I never cease to be inspired by my good friend, Prof. Michael Thomas, and I am grateful for my involvement in the

theatre department (particularly with Prof. Sheri Anderson) that has helped shape my presence at the front of a classroom.

Above all, I would be nowhere if it were not for my family. It is difficult to forget how lucky I am to have such great parents (and not just because my mother does a great job reminding me), as they have provided me with great advice and wonderful opportunities over the years. Mom and dad, along with my brother, Casey, and my sister, Kendelle, are extremely supportive of everything I do. Graduate research is not always a glamorous undertaking, and the importance of emotional support can be overlooked. Therefore, it is important to recognize that they have kept me smiling, laughing, and confident in my abilities throughout this whole process, and I love them dearly. I was also blessed with great grandparents – Beverly and Gerald Pitts and Julia and Rosario "Sal" Marangio. The latter two passed away during my graduate career and mean the world to me; it is to them that this thesis is dedicated. Lastly, I have received no greater support than from my wife, Katrina Lynne Pitts. I cannot express my love enough for this woman, who is the most patient, understanding, kind, fun, and loving human being in the entire world. Through the trials and tribulations of graduate research, she has always been my rock.

Last but not least, I would like to thank myself; I could not have done it without me.



### Publications Drawing Upon this Dissertation

- 1) Bloom, S.; **Pitts, C. R.**; Miller, D. C.; Haselton, N.; Holl, M. G.; Urheim, E.; Lectka, T. "A Polycomponent Metal-Catalyzed Aliphatic, Allylic, and Benzylic Fluorination." *Angew. Chem. Int. Ed.* **2012**, *51*, 10580-10583.
  
- 2) Bloom, S.; **Pitts, C. R.**; Woltornist, R.; Griswold, A.; Holl, M. G.; Lectka, T. "Iron(II)-Catalyzed Benzylic Fluorination" *Org. Lett.* **2013**, *15*, 1722-1724.
  
- 3) **Pitts, C. R.**; Bloom, S.; Woltornist, R.; Auvenshine, D.; Ryzhkov, L. R.; Siegler, M. A.; Lectka, T. "Direct, Catalytic Monofluorination of  $sp^3$  C-H Bonds: A Radical-Based Mechanism with Ionic Selectivity." *J. Am. Chem. Soc.* **2014**, *136*, 9780-9791.
  
- 4) **Pitts, C. R.**; Ling, B.; Woltornist, R.; Liu, R.; Lectka, T. "Triethylborane-Initiated Radical Chain Fluorination: A Synthetic Method Derived from Mechanistic Insight" *J. Org. Chem.* **2014**, *79*, 8895-8899.
  
- 5) Bloom, S.; Bume, D. D.; **Pitts, C. R.**; Lectka, T. "Site-Selective Approach to  $\beta$ -Fluorination: Photocatalyzed Ring Opening of Cyclopropanols" *Chem. Eur. J.* **2015**, *21*, 8060-8063.
  
- 6) **Pitts, C. R.**; Bloom, M. S.; Bume, D. D.; Zhang, Q. A.; Lectka, T. "Unstrained C-C Bond Activation and Directed Fluorination through Photocatalytically-Generated Radical Cations" *Chem. Sci.* **2015**, *6*, 5225-5229.
  
- 7) **Pitts, C. R.**; Ling, B.; Snyder, J. A.; Bragg, A. E.; Lectka, T. "Aminofluorination of Cyclopropanes: A Multifold Approach through a Common, Catalytically Generated Intermediate" *J. Am. Chem. Soc.* **2016**, *138*, 6598-6609.

8) Bume, D. B.; **Pitts, C. R.**; Jokhai, R. T.; Lectka, T. "Direct, Visible Light-sensitized Benzylic C-H Fluorination of Peptides using Dibenzosuberone: Selectivity for Phenylalanine-like Residues" *Tetrahedron* **2016**, 72, 6031-6036.

9) **Pitts, C. R.**; Bume, D. D.; Harry, S. A.; Siegler, M. A.; Lectka, T. "Multiple Enone-Directed Reactivity Modes Lead to the Selective Photochemical Fluorination of Polycycles" *J. Am. Chem. Soc.* **2017**, 139, 2208-2211.

10) **Pitts, C. R.**; Siegler, M. A.; Lectka, T. "An Intermolecular Aliphatic C-F---H-C Interaction in the Presence of 'Stronger' Hydrogen Bond Acceptors: Crystallographic, Computational, and IR Studies" *J. Org. Chem.* **2017**, 82, 3996-4000.

### Publications Not Included in this Dissertation

- 1) **Pitts, C. R.;** Lectka, T. "Chemical Synthesis of  $\beta$ -Lactams: Asymmetric Catalysis and Other Recent Advances." *Chem. Rev.* **2014**, *114*, 7930-7953.
  
- 2) Bume, D. D.; **Pitts, C. R.;** Lectka T. "Tandem C-C Bond Cleavage of Cyclopropanols and Oxidative Aromatization by Manganese(IV) Oxide in a Direct C-H to C-C Functionalization of Heteroaromatics" *Eur. J. Org. Chem.* **2016**, *2016*, 26-30.
  
- 3) **Pitts, C. R.;** Lectka, T., "Allylic Fluorides," In *Science of Synthesis Knowledge Updates*, (2017), *In Press*.

## Table of Contents

Title Page	i
Abstract	ii
Dedication	iv
Acknowledgements	v
Publications Drawing upon this Dissertation	ix
Publications Not Included in this Dissertation	xi
Table of Contents	xii
List of Tables	xviii
List of Figures	xxi
List of Schemes	xxvii
List of Abbreviations	xxxii

## **Chapter 1: Introduction**

1.1 On Practical Radical Fluorination.	1
1.2 Organization of Chapters.	1
1.3 Brief Overview.	1
1.4 References.	4

## **Chapter 2: A Polycomponent Metal-catalyzed Aliphatic, Allylic, and Benzylic Fluorination**

2.1 Introduction.	6
2.2 Screening for Reaction Conditions (Adamantane Fluorination).	6
2.3 Optimization of Reaction Conditions for Secondary Alkanes.	8
2.4 Evaluation of Substrate Scope.	9
2.5 Conclusion.	12
2.6 References.	12

## **Chapter 3: Iron(II)-catalyzed Benzylic Fluorination**

3.1 Introduction.	14
3.2 Screening for Reaction Conditions.	15
3.3 Evaluation of Substrate Scope.	15
3.4 Conclusion.	18
3.5 References.	19

## **Chapter 4: Direct, Catalytic Monofluorination of $sp^3$ C-H Bonds: A Radical-based Mechanism with Ionic Selectivity**

4.1 Introduction.	21
4.2 Simplified Protocol.	23
4.3 Loss of Fluoride from Copper(I)-Selectfluor Interaction.	25
4.4 UV-vis Spectroscopy.	26
4.5 X-band CW EPR Flat-Cell Experiments.	27

4.6 Solid-state X-band CW EPR.	27
4.7 Initiation by Single-Electron Transfer.	31
4.8 Outer-sphere SET.	31
4.9 Inner-sphere SET.	32
4.10 Involvement of Alkyl Radicals.	34
4.11 Induction Period.	37
4.12 Rate Dependence.	39
4.13 KIE.	40
4.14 Proposed Mechanism.	41
4.15 Role of Valence Bond "Ionicity" in Reaction Selectivity.	43
4.16 Polar Effect.	44
4.17 Conclusion.	47
4.18 References.	47

**Chapter 5: Triethylborane-initiated Radical Chain Fluorination: A Synthetic Method Derived from Mechanistic Insight**

5.1 Introduction.	51
5.2 Screening for Reaction Conditions.	52
5.3 Preliminary Mechanistic Investigation.	53
5.4 Evaluation of Substrate Scope.	55
5.5 Conclusion.	57
5.6 References.	57

**Chapter 6: A Site-selective Approach to  $\alpha$ -Fluorination: Photocatalyzed Ring Opening of Cyclopropanols**

6.1 Introduction.	59
6.2 Reaction Design.	60

6.3 Evaluation of Substrate Scope.	61
6.4 Preliminary Mechanistic Investigation.	64
6.5 Conclusion.	64
6.6 References.	65

**Chapter 7: Unstrained C-C Bond Activation and Directed Fluorination through Photocatalytically-generated Radical Cations**

7.1 Introduction.	67
7.2 Screening for Reaction Conditions.	68
7.3 Evaluation of Substrate Scope.	70
7.4 Preliminary Mechanistic Investigation.	73
7.5 Conclusion.	74
7.6 References.	74

**Chapter 8: Aminofluorination of Cyclopropanes: A Multifold Approach through a Common, Catalytically Generated Intermediate**

8.1 Introduction.	77
8.2 Reaction Discovery.	78
8.3 Product Distribution Studies.	79
8.4 Linear Free Energy Relationships.	81
8.5 On Photoinduced Electron Transfer.	84
8.6 Fluorescence and Time-Resolved Spectroscopy.	86
8.7 Alternative Photosensitized Initiation.	89
8.8 Alternative Chemical Initiation.	90
8.9 Kinetic Isotope Effects.	92
8.10 Drawing a Unified Mechanism.	93
8.11 As a Synthetic Method.	96
8.12 Conclusion.	99

8.13 References.	100
------------------	-----

**Chapter 9: Direct, Visible Light-sensitized Benzylic C-H Fluorination of Peptides Using Dibenzosuberenone: Selectivity for Phenylalanine-like Residues**

9.1 Introduction.	104
9.2 Screening for Reaction Conditions.	105
9.3 Evaluation of Substrate Scope.	106
9.4 Preliminary Mechanistic Investigation.	110
9.5 Conclusion.	111
9.6 References.	111

**Chapter 10: Multiple Enone-directed Reactivity Modes Lead to the Selective Photochemical Fluorination of Polycyclic Terpenoid Derivatives**

10.1 Introduction.	114
10.2 Classification of Reactivity Modes.	115
10.3 Evaluation of Substrate Scope.	116
10.4 Preliminary Mechanistic Investigation.	119
10.5 Conclusion.	121
10.6 References.	121

**Chapter 11: An Intermolecular Aliphatic C-F...H-C Interaction in the Presence of "Stronger" Hydrogen Bond Acceptors: Crystallographic, Computational, and IR Studies**

11.1 Introduction.	123
11.2 Synthesis of Parent Molecule.	124
11.3 Discovery and Computational Investigation of C-F...H-C Interaction.	124
11.4 Characterization as Blue-shifted H-bond by IR Spectroscopy.	126
11.5 C-F...H-C Interaction in the Presence of Potentially Stronger H-bonding Interactions	128
11.6 Conclusion.	129



11.7 References.	129
<b>Chapter 12: Experimental Methods</b>	
7.1 General Methods.	131
7.2 Experimental Details for Chapter 2.	132
7.3 Experimental Details for Chapter 3.	133
7.4 Experimental Details for Chapter 4.	137
7.5 Experimental Details for Chapter 5.	157
7.6 Experimental Details for Chapter 6.	159
7.7 Experimental Details for Chapter 7.	166
7.8 Experimental Details for Chapter 8.	174
7.9 Experimental Details for Chapter 9.	203
7.10 Experimental Details for Chapter 10.	212
7.11 Experimental Details for Chapter 11.	241
7.12 References.	248
Vita	253

## List of Tables

<b>Table 2.1</b> Screening conditions for adamantane fluorination.	7
<b>Table 2.2</b> Optimization of fluorination conditions for a secondary alkane.	9
<b>Table 2.3</b> Substrate scope.	11
<b>Table 3.1</b> Survey of benzylic substrates.	16
<b>Table 4.1</b> EPR parameters for complexes in Figures 4.5 and 4.6.	29
<b>Table 4.2</b> Radical clocks.	35
<b>Table 4.3</b> Isodesmic reactions.	44
<b>Table 5.1.</b> Screening for reaction initiation conditions.	53
<b>Table 5.2</b> Substrate scope.	56
<b>Table 6.1</b> Survey of $\alpha$ -fluoro ketones and $\gamma$ -fluoro alcohols.	62
<b>Table 7.1</b> Screening for photoxidants.	68
<b>Table 7.2</b> Screening for substituents.	70
<b>Table 7.3</b> Substrate scope.	71

<b>Table 7.4</b> Application to 5-, 7-, 8-, and 12-membered rings.	72
<b>Table 8.1</b> Rehm-Weller estimation of PET free energies.	85
<b>Table 8.2</b> Excited-state lifetimes ( $t_0$ ) measured by nanosecond transient absorption spectroscopy and quenching constants ( $k_q$ ) from Stern-Volmer analysis.	87
<b>Table 8.3</b> Intramolecular and intermolecular competitive KIE's.	93
<b>Table 8.4</b> Scope of aminofluorination reaction for Selectfluor and NFSI under 300 nm irradiation.	98
<b>Table 9.1</b> Photochemical fluorination optimized for dipeptides.	106
<b>Table 9.2</b> Protecting group compatibility.	107
<b>Table 9.3</b> Substrate scope: phenylalanine-like residues targeted for fluorination in amino acids and dipeptides.	108
<b>Table 9.4</b> Regioselective fluorination showcased in tripeptides.	110
<b>Table 10.1</b> Directed photochemical $sp^3$ C–H fluorination of bioactive polycyclic terpenoid derivatives.	117
<b>Table 11.1</b> DFT and AIM computational analyses.	126
<b>Table 12.1</b> Intrinsic relative hexyl acetate radical stabilities.	147

<b>Table 12.2</b> Isodesmic reactions: predictive properties of radical cations.	149
<b>Table 12.3</b> Compiled initial rate data.	150
<b>Table 12.4</b> Compiled initial rate data (metal initiation procedure).	189
<b>Table 12.5</b> Intermolecular competition with Selectfluor (para substituent effects).	190
<b>Table 12.6</b> Intermolecular competition with Selectfluor (meta substituent effects).	190
<b>Table 12.7</b> Intermolecular competition with NFSI (para substituent effects).	190
<b>Table 12.8</b> Intermolecular competition with NFSI (meta substituent effects).	191
<b>Table 12.9</b> Intermolecular competition with triethylborane (para substituent effects).	191
<b>Table 12.10</b> Intermolecular competition with copper (para substituent effects).	191
<b>Table 12.11</b> Intramolecular competition with Selectfluor (para substituent effects).	192
<b>Table 12.12</b> Intramolecular competition with NFSI (para substituent effects).	192
<b>Table 12.13</b> Crystallographic data for <b>2</b> :CHCl <sub>3</sub> .	242

## List of Figures

<b>Figure 3.1</b> Retrosynthetic 1,4-conjugate addition of fluoride.	17
<b>Figure 4.1</b> Common "N-F" reagents.	22
<b>Figure 4.2</b> UV-vis spectra of CuI, ligand, and Selectfluor.	26
<b>Figure 4.3</b> Flat-cell liquid phase spectra of copper(II) over time.	27
<b>Figure 4.4</b> Isotopically enriched ligand for solid state EPR.	28
<b>Figure 4.5</b> Solid-state spectra of copper(II) in the absence of a substrate at 8 K.	28
<b>Figure 4.6</b> Solid-state spectra of copper(II) after 180 min. with (C1) and without (C2) substrate present at 8 K.	29
<b>Figure 4.7</b> Sample rate of fluorination plot displaying induction period.	38
<b>Figure 4.8</b> Competitive KIE <sup>19</sup> F NMR overlay of the formation of 3-fluoro-3-phenylpropyl acetate ( <i>left</i> , ddd, $J = 47.4, 30.9, 14.4$ Hz) and 3-fluoro-3-phenylpropyl-3- <i>d</i> acetate ( <i>right</i> , ddt, $J = 30.9, 14.4, 7.2$ Hz).	40
<b>Figure 4.9</b> Mechanistic hypothesis based on experimental results.	42
<b>Figure 4.10</b> Free-energy profile for the monofluorination of cyclodecane through our proposed catalytic cycle.	42

<b>Figure 4.11</b> Application of Donahue's theory.	45
<b>Figure 4.12</b> Transition state calculations and charge distributions alongside isoenergetic scenarios.	46
<b>Figure 5.1</b> Hypothesized alternative initiation to $sp^3$ C-H fluorination method.	52
<b>Figure 5.2</b> Proposed initiation through formation of ethyl radicals.	54
<b>Figure 5.3</b> Energetic landscape of ethyl radical-initiated fluorination of cyclodecane at B3PW91/6-311++G**(MeCN).	55
<b>Figure 6.1</b> Calculated structure of trans-1,2-dimethylcyclopropanol radical cation (wb-97xD/cc-pVTZ, MeCN dielectric).	60
<b>Figure 8.1</b> Kinetic profile of 4-fluorophenyl cyclopropane, Selectfluor, and aminofluorination product.	82
<b>Figure 8.2</b> Intermolecular (top row) and intramolecular (bottom row) Hammett plots. Conditions: <b>A, B</b> = Selectfluor and 300 nm irradiation, <b>C, D</b> = NFSI and 300 nm irradiation, <b>E, F</b> = Selectfluor and catalytic $BEt_3$ .	83
<b>Figure 8.3</b> Stern-Volmer plots for fluorescence quenching of arylcyclopropanes by Selectfluor.	87
<b>Figure 8.4</b> Time-resolved transient absorption spectroscopy of phenylcyclopropane following 266-nm excitation; radical cation ( $PCP^{*+}$ , $\lambda_{max} = 545$ nm) is generated in the presence of Selectfluor. The upper panel has been referenced to a $\Delta OD$ of 0 to highlight the spectral evolution.	88

<b>Figure 8.5</b> Kinetics of the phenylcyclopropane radical cation (PCP <sup>•+</sup> ) generated in presence of Selectfluor according to nanosecond-resolved transient absorption at 520 nm.	89
<b>Figure 8.6</b> Solvent-assisted ring opening transition state at wB97XD/6-311++G** (MeCN).	96
<b>Figure 9.1</b> Benzylic selectivity strategy toward "directed" fluorination within peptide natural products.	105
<b>Figure 10.1</b> Classification of reactivity modes (I-IV) that lead to selective $\gamma$ -, $\beta$ -, homoallylic, and allylic photochemical fluorination.	115
<b>Figure 10.2</b> Fluorination of triterpenoid saponin derivative 15 in an extreme illustration of selectivity.	119
<b>Figure 10.3</b> Preliminary mechanistic hypothesis for enone-directed photochemical sp <sup>3</sup> C-H fluorination using Selectfluor.	120
<b>Figure 11.1</b> A C-F...H-C interaction observed in the presence of traditionally stronger oxygen-based hydrogen bond acceptors.	123
<b>Figure 11.2</b> Crystal structure determined from single-crystal X-ray diffraction (displacement ellipsoids given at 50% probability level) with hydrogen atoms refined using a riding model.	125
<b>Figure 11.3</b> Zoomed in overlay of the IR spectra of the 1:1 parent molecule 2:CDCl <sub>3</sub> crystal and pure CDCl <sub>3</sub> , highlighting the blue shift in the C-D stretch vibration frequency.	127

<b>Figure 11.4</b> Relative energies of O-bound chloroform complexes to the observed F-bound chloroform complex, calculated at B3LYP/6-311++G**.	128
<b>Figure 12.1</b> Plot of formation of fluorocyclodecane over time by $^{19}\text{F}$ NMR.	139
<b>Figure 12.2</b> Plot of disappearance of Selectfluor N-F signal over time by $^{19}\text{F}$ NMR.	140
<b>Figure 12.3</b> Overlay of Selectfluor and 1:1 Selectfluor:CuI $^{19}\text{F}$ NMR spectra.	140
<b>Figure 12.4</b> Second derivative graph of spin trapped copper(II) post-induction period.	141
<b>Figure 12.5</b> Plot of intensity vs. time of a standard reaction in a flat-cell monitored at room temperature by EPR.	142
<b>Figure 12.6</b> Overlay of differential pulse voltammograms.	143
<b>Figure 12.7</b> UV-vis spectra of CuI and Selectfluor over time.	144
<b>Figure 12.8</b> Overlay of $^{19}\text{F}$ NMR spectra for reactions using a Mosher ester substrate.	145
<b>Figure 12.9</b> $^{19}\text{F}$ NMR spectrum of crude reaction mixture from 2-phenylbenzylcyclopropane fluorination.	146
<b>Figure 12.10</b> Relative n-fluoro-hexyl acetate $^{19}\text{F}$ NMR integrations.	148
<b>Figure 12.11</b> Representative plot for initial rate of formation of 3-fluoro-3-phenylpropyl acetate ( <i>top</i> ) vs. 3-fluoro-3-phenylpropyl-3- <i>d</i> acetate ( <i>bottom</i> ) by $^{19}\text{F}$ NMR.	152



<b>Figure 12.12</b> Representative plot for initial rate of formation of fluorocyclohexane ( <i>top</i> ) vs. fluorocyclohexane- <i>d</i> <sub>11</sub> ( <i>bottom</i> ) by <sup>19</sup> F NMR extrapolated from sigmoidal fit equations.	153
<b>Figure 12.13</b> Sigmoidal fit for appearance of fluorocyclohexane by <sup>19</sup> F NMR.	153
<b>Figure 12.14</b> Sigmoidal fit for appearance of fluorocyclohexane- <i>d</i> <sub>11</sub> by <sup>19</sup> F NMR.	154
<b>Figure 12.15</b> Sample <sup>19</sup> F NMR of competitive KIE experiment following the rate of appearance of fluorocyclohexane vs. fluorocyclohexane- <i>d</i> <sub>11</sub> .	154
<b>Figure 12.16</b> Displacement ellipsoid plot (50% probability level) of 2CuI•bis(imine) complex at 110(2) K.	155
<b>Figure 12.17</b> Kinetic profile (4-fluorophenyl cyclopropane and Selectfluor under 300 nm hv).	188
<b>Figure 12.18</b> UV-vis spectra of phenylcyclopropane, NFSI, and Selectfluor (in MeCN).	189
<b>Figure 12.19</b> <sup>19</sup> F NMR spectrum of reaction with 1:1 acetonitrile:pivalonitrile; putative pivalonitrile-trapped product from phenylcyclopropane observed.	194
<b>Figure 12.20</b> <sup>19</sup> F NMR spectrum of reaction with 1:1 acetonitrile:pivalonitrile; putative pivalonitrile-trapped product from 1,2-diphenylcyclopropane observed.	195
<b>Figure 12.21</b> fs-TAS of PCP in acetonitrile following 266 nm photoexcitation to illustrate the evolution of S <sub>1</sub> PCP (no quencher).	196

<b>Figure 12.22</b> Comparison of $S_1$ lifetime of PCP at 700 nm in the absence and presence of Selectfluor following 266 nm excitation.	197
<b>Figure 12.23</b> $\mu$ s-TAS of PCP/Selectfluor in ACN following photoexcitation with 266 nm.	198
<b>Figure 12.24</b> Comparison of the PCP <sup>++</sup> absorption spectrum as probed $\Delta t=50$ ns following 266 nm photoexcitation of PCP/Selectfluor and 350 nm photoexcitation of PCP/BDTA,	199
<b>Figure 12.25</b> ns-TAS (probed at 639 nm) of PCP and derivatives (no added quencher) following photoexcitation with 266 nm.	200
<b>Figure 12.26</b> Temporal profile of the $\mu$ s-TA LED probe light source.	201
<b>Figure 12.27</b> Fluorescence quantum yield ( $\Phi_f$ ) of PCP determined using aerated naphthalene as a reference.	202
<b>Figure 12.28</b> Packing diagram screenshot for <b>2</b> :CHCl <sub>3</sub> crystal.	244
<b>Figure 12.29</b> Thermal ellipsoid plot for <b>2</b> :CHCl <sub>3</sub> crystal (50% probability level).	244
<b>Figure 12.30</b> AIM analysis screenshot.	245
<b>Figure 12.31</b> AIM analysis screenshot (zoomed in).	245
<b>Figure 12.32</b> Pruned parent molecule <b>2</b> (CAM-B3LYP/6-311++G**) electrostatic potential.	246
<b>Figure 12.33</b> Overlay of IR spectra of CDCl <sub>3</sub> and 1:1 parent molecule <b>2</b> :CDCl <sub>3</sub> .	247

## List of Schemes

<b>Scheme 3.1</b> Effect of catalyst on substrate scope.	14
<b>Scheme 3.2</b> Iron(II)-promoted reversal in selectivity.	17
<b>Scheme 3.3</b> Isodesmic reaction for dehydrofluorination of coumarin at B3LYP/6-311++G**.	18
<b>Scheme 4.1</b> Concept for mild $sp^3$ C-H fluorination method.	21
<b>Scheme 4.2</b> Simplified protocol for Selectfluor/copper(I) system.	24
<b>Scheme 4.3</b> Possible identities of copper(II) species observed in EPR spectra.	30
<b>Scheme 4.4</b> Inner-sphere and outer-sphere SET pathways.	31
<b>Scheme 4.5</b> Preliminary evidence for triethylborane as an alternative reaction initiator.	33
<b>Scheme 4.6</b> Analogy to Hoffmann-Löffler-Freytag reaction.	34
<b>Scheme 4.7</b> Radical scavengers.	35
<b>Scheme 4.8</b> Role of copper(II) in Baran's system versus our proposed fluorination pathway.	37
<b>Scheme 4.9</b> Cation formed through direct hydride transfer and stabilized as oxonium.	37
<b>Scheme 4.10</b> Observed KIEs.	41

<b>Scheme 5.1</b> Ethyl radical probe experiment.	54
<b>Scheme 6.1</b> Site-selective $\alpha$ -fluorination of cyclopropanols.	59
<b>Scheme 6.2</b> Tandem ring expansion/ $\alpha$ -fluorination to access cycloheptanone or cycloheptanol core.	63
<b>Scheme 6.3</b> Proposed mechanism for photocatalyzed site-selective $\alpha$ -fluorination.	64
<b>Scheme 7.1</b> Concept for selective C-C fragmentation/C-F formation.	67
<b>Scheme 7.2</b> Control reaction.	69
<b>Scheme 7.3</b> Standard reaction conditions.	69
<b>Scheme 7.4</b> Intermolecular competition experiments.	73
<b>Scheme 7.5</b> Isodesmic analyses at B3PW91/6-311++G**(MeCN).	74
<b>Scheme 8.1</b> Four unique aminofluorination tactics provide a synergistic approach to mechanism elucidation.	77
<b>Scheme 8.2</b> Discovered aminofluorination reaction.	79
<b>Scheme 8.3</b> Diastereoselectivity and regioselectivity probes.	80
<b>Scheme 8.4</b> Hammett plot competition experiments.	82

<b>Scheme 8.5</b> Relative rates via competition experiments.	86
<b>Scheme 8.6</b> Alternative photochemical initiation.	90
<b>Scheme 8.7</b> Electron relay at B3PW91/6-311++G** (MeCN).	90
<b>Scheme 8.8</b> Elongation/cleavage of N-F bond upon reduction at B3PW91/6-311++G** (MeCN).	91
<b>Scheme 8.9</b> Alternative chemical initiation.	92
<b>Scheme 8.10</b> Proposed initiation mechanisms.	94
<b>Scheme 8.11</b> Calculated phenylcyclopropane oxidations ( $\Delta G_{\text{calc}}$ ) at B3PW91/6-311++G** (MeCN).	94
<b>Scheme 8.12</b> Oxidation, aminofunctionalization, fluorination, and propagation.	95
<b>Scheme 8.13</b> Acetonitrile-assisted ring opening.	95
<b>Scheme 8.14</b> Potential synthetic utility of Selectfluor adducts.	97
<b>Scheme 9.1</b> Competition experiments.	111
<b>Scheme 11.1</b> Synthesis of the parent molecule 2 (major diastereomer depicted with respect to C-F bond).	124

**Scheme 12.1** (A) Products of reaction on a Mosher ester substrate. (B) Achiral and chiral ligands employed. 146

**Scheme 12.2** Syntheses of (4-fluorobut-1-ene-1,4-diyl)dibenzene isomers. 147

## List of Abbreviations

Å	Angstroms
Ac	acetyl
acac	acetylacetonate
Ada	adamantyl
AgRE	silver reference electrode
AIBN	azobisisobutyronitrile
AIM	atoms in molecules
Ala	alanine
atm	atmosphere
ATR-IR	attenuated total reflection infrared resonance
aq	aqueous
BCP	bond critical point
BHT	2,6-di- <i>tert</i> -butyl-4-methylphenol
Boc	<i>tert</i> -butyloxycarbonyl
BPMED	<i>N,N</i> -bis(phenylmethylene)-1,2-ethanediamine
BTDA	3,3',4,4'-benzophenonetetracarboxylic dianhydride
°C	degrees Celsius
cat	catalyst
Cbz	carboxybenzyl
CFL	compact fluorescent light
cm <sup>-1</sup>	wavenumbers
CP	crossing point
CSD	Cambridge Structural Database
CV	cyclic voltammogram
CW	continuous wave
Cy	cyclohexyl

DABCO	diazabicyclooctane
DAST	diethylaminosulfur trifluoride
DCC	<i>N,N'</i> -dicyclohexylcarbodiimide
DCM	dichloromethane
DFT	density functional theory
DI	deionized
DMAP	4-dimethylaminopyridine
DMF	<i>N,N</i> -dimethylformamide
DMSO	dimethylsulfoxide
DPV	differential pulse voltammogram
dr	diastereomeric ratio
$\Delta E$	change in energy (enthalpy)
$E_a$	activation energy
$E^0_{(A/A\cdot)}$	acceptor one-electron redox potential
$E^0_{(D\cdot/D)}$	donor one-electron redox potential
$E^*_{(0,0)}$	excited state energy
EAS	electrophilic aromatic substitution
EIE	equilibrium isotope effect
EPM	electrostatic potential map
EPR	electron paramagnetic resonance
ESI	electrospray ionization
Et	ethyl
EtOAc	ethyl acetate
EtOH	ethanol
equiv	equivalent(s)
$\Phi_f$	fluorescence quantum yield
$F_0$	fluorescence intensity (absence of quencher)
F	fluorescence intensity (presence of quencher)



Fmoc	fluorenylmethyloxycarbonyl
fs	femtosecond(s)
FT-IR	Fourier transform infrared
$\Delta G_{\text{calc}}$	calculated change in Gibbs free energy
$\Delta G^0_{\text{ET}}$	Gibbs free energy of electron transfer
g	gram(s)
G	Gauss
GC/MS	gas chromatograph/mass spectrometer
GHz	gigahertz
Glu	glutamic acid
Gly	glycine
h	hour(s)
$\Delta H_{\text{REACT}}$	enthalpy of reaction
H-TEDA-BF <sub>4</sub>	1-chloromethyl-1,4-diazabicyclo-[2.2.2]octane-1,4-dium bis(tetrafluoroborate)
HCV	hepatitis C virus
HIV	human immunodeficiency virus
HOBt	1-hydroxybenzotriazole
HOMO	highest occupied molecular orbital
HPLC	high-performance liquid chromatography
HRMS	high-resolution mass spectrometry
Hz	Hertz
iPr	isopropyl
iPrOH	isopropanol
IR	infrared
$k_q$	quenching rate constant
K	Kelvin
kcal	kilocalorie
kcal/mol	kilocalorie per mole

kHz	kilohertz
KIE	kinetic isotope effect ( $[k_H]/[k_D]$ or $[P_H]/[P_D]$ )
$\lambda_{\max}$	maximum wavelength
LED	light-emitting diode
Leu	leucine
LFER	linear free energy relationship
Lys	lysine
$\mu\text{s}$	microsecond(s)
$\mu\omega$	microwave
m/z	mass to charge ratio
M	molar(ity)
Me	methyl
MeCN	acetonitrile
MeNO <sub>2</sub>	nitromethane
MeOH	methanol
mg	milligram
MHz	megahertz
min	minute(s)
mL	milliliter(s)
mm	millimeter(s)
mM	millimolar
mmol	millimole(s)
mol	mole(s)
m.p.	melting point
MP2	second order Møller–Plesset perturbation theory
ms	millisecond(s)
MS	mass spectrometry
mV	millivolt(s)

NCS	<i>N</i> -chlorosuccinimide
NBO	natural bond orbital
NBS	<i>N</i> -bromosuccinimide
n.d.	not determined
NDHPI	<i>N,N</i> -dihydroxypyromellitimide
NFPy	<i>N</i> -fluoropyridinium
NFSI	<i>N</i> -fluorobenzene sulfonimide
NHPI	<i>N</i> -hydroxyphthalimide
nm	nanometer
NMR	nuclear magnetic resonance
ns	nanosecond(s)
Nuc	nucleophile
$\Delta$ OD	change in optical density
PCC	pyridinium chlorochromate
PCP	phenylcyclopropane
PET	photoinduced electron transfer (or positron emission tomography)
Ph	phenyl
Phe	phenylalanine
Phth	phthalimido
PINO	phthalimide <i>N</i> -oxyl radical
ppm	parts per million
ps	picosecond(s)
$\Delta$ q	change in net charge
Q	quencher
R <sup>2</sup>	coefficient of determination
R <sub>f</sub>	retardation factor
rt	room temperature
S <sub>1</sub>	singlet excited state

S <sub>N</sub> 1	unimolecular nucleophilic substitution reaction
S <sub>N</sub> 2	bimolecular nucleophilic substitution reaction
S <sub>H</sub> 2	homolytic nucleophilic substitution reaction
s	second(s)
SCE	saturated calomel electrode
Selectfluor	1-chloromethyl-4-fluoro-1,4-diazoniabicyclo-[2.2.2]octane bis(tetrafluoroborate)
SET	single electron transfer
τ <sub>0</sub>	innate lifetime of excited state
T <sub>1</sub>	triplet excited state
t	time
TA	transient absorption
TAS	transient-absorption spectroscopy
TBABF <sub>4</sub>	tetrabutylammonium tetrafluoroborate
TBAClO <sub>4</sub>	tetrabutylammonium perchlorate
tBu	<i>tert</i> -butyl
tBuOH	<i>tert</i> -butanol
TCB	1,2,4,5-tetracyanobenzene
TEA	triethylamine
TEMPO	2,2,6,6-tetramethylpiperidine 1-oxyl
TFA	trifluoroacetate
THF	tetrahydrofuran
TLC	thin-layer chromatography
TMS	tetramethylsilane
Trt	trityl
TS	transition state
TTBNB	2,4,6-tri- <i>tert</i> -butyl nitrosobenzene
UV-vis	ultraviolet-visible
v/v	volume to volume ratio

V	volt(s)
Val	valine
w	solvent-dependent work function
W	watt
wt	weight

## Chapter 1

### Introduction

#### 1.1 On Practical Radical Fluorination.

Despite the profound impact of fluorine-containing molecules on medicinal chemistry, agrochemistry, materials science, and biology, fluorination reactions seem to remain elusive in most introductory organic chemistry course curricula to date. Students are often taught, however, that practical radical fluorination using  $F_2$  gas (unlike an  $sp^3$  C-H functionalization using  $Cl_2$ , NCS,  $Br_2$ , or NBS) is *impossible*. This is for a simple reason –  $F_2$  is far too reactive. Although most would agree that the use of  $F_2$  or (other high-energy fluorinating reagents) precludes "practicality," useful radical fluorination chemistry has become both *possible* and *controllable* using mild sources of atomic fluorine (the so-called "N-F" reagents) in the last 5 years. Consequently, fluorination no longer represents a missing link in radical halogenation chemistry. In this dissertation, select methods, mechanistic studies, and advances in selectivity are discussed that have helped radical fluorination become a valuable synthetic approach. As the chapters progress, the direction of the work noticeably and rapidly shifts from reactions of academic interest to reactions with more practical applications.

#### 1.2 Organization of Chapters.

Herein, each chapter represents a previously *published* body of work with only minor alterations made to fit the format of the dissertation. Accordingly, they contain more detailed introductory material and references specific to each body of work. The chapters are presented in chronological order of publication.

#### 1.3 Brief Overview.

The story begins with reaction discovery, as the first observation of  $sp^3$  C-H bond fluorination in the Lectka laboratory was not intentional. Following a publication by Steven Bloom and coworkers on  $\alpha,\alpha$ -difluorination of arylacetyl acid chlorides in late 2011,<sup>1</sup> efforts were made to make this method amenable to long-chain aliphatic acid chlorides. Upon screening for transition metals to supplant the tin catalyst of the former system, an interesting result was found when employing a copper(I) species

alongside Selectfluor. That is, by  $^{19}\text{F}$  NMR analysis of the crude reaction mixture, both the expected  $\alpha$ -monofluorinated and  $\alpha,\alpha$ -difluorinated products were observed from the caproyl chloride starting material (in minor amounts) along with *other* secondary fluoride signals. Intrigued, the next round of screening involved substoichiometric copper(I) compounds (whatever was lying around the laboratory), Selectfluor, and an alkane, namely, adamantane. Before further optimization, we found that stirring this alkane substrate with Selectfluor and copper(I) iodide in acetonitrile at room temperature produced 1-fluoroadamantane in 18% yield. This was one of the first aliphatic monofluorination reactions discovered at the time; such an exciting result single-handedly altered the direction of chemistry in the Lectka laboratory for the next several years.

In Chapter 2, the development of this copper(I)/Selectfluor aliphatic monofluorination method is presented.<sup>2</sup> At the time, there was no clear hypothesis for a reaction mechanism, so a full mechanistic study was initiated immediately thereafter. While this study was underway, we recognized that the copper(I)/Selectfluor protocol performed less admirably on benzylic substrates. Without knowing the exact mechanism, we reasoned that if one transition metal has this interesting interplay with Selectfluor in effecting C-H bond fluorination, there must be another. Upon screening for benzylic C-H bond fluorination with other redox-active transition metals, we found rapid success with an iron(II) salt. The details of this iron(II)/Selectfluor benzylic fluorination are discussed in Chapter 3.<sup>3</sup> Although a complete follow-up study was not conducted on this method, we have preliminary evidence that the iron(II) system is mechanistically distinct from the copper(I) system.

In Chapter 4,<sup>4</sup> a full mechanistic analysis of the copper(I)/Selectfluor system is revealed. It was found to operate through a radical chain mechanism whereby copper acts as an initiator and Selectfluor acts as both the precursor to the chain carrier and as an atomic source of fluorine. (In order to study the mechanism, a simplified protocol was also developed that, in turn, aided the practicality of the method.) Additionally, theoretical analyses offered insight into the importance of "the polar effect" in affording selective monofluorination over any significant polyfluorination. With this insight, we were able to rationally design new  $\text{sp}^3$  C-H bond fluorination methods. On one hand, Steven Bloom and coworkers pursued alternative ways to generate alkyl radicals photochemically using 1,2,4,5-tetracyanobenzene (a powerful oxidant in the excited state) and 300-nm irradiation.<sup>5</sup> On the other hand, the employment of

transition metal-free radical initiators was pursued as an alternative approach to generating the chain carrier from Selectfluor. In Chapter 5, the triethylborane/Selectfluor radical initiation system is shown to effect the desired C-H bond fluorination, likely through an identical mechanism to the copper(I)/Selectfluor method beyond initiation.<sup>6</sup> This metal-free and ultraviolet light-free method of generating the *N*-centered radical intermediate also proved invaluable as a control experiment in later work.

At this juncture, previous methods had only demonstrated selective  $sp^3$  C-H bond fluorination on highly symmetric substrates or those containing more activated benzylic C-H bonds. Moving forward, there was an immediate emphasis on *directing* radical fluorination effectively to extend its practicality to selective complex substrate fluorination. We envisioned primarily two routes: (1) exploring C-C bond fragmentations that could direct formation of an alkyl radical and (2) employing "directing groups" for selective C-H bond cleavage. In Chapters 6 and 7, selective fluorination methods born of strained and unstrained C-C bond mesolytic cleavage tactics are presented. The cyclopropanols of Chapter 6 allow formation of  $\beta$ -fluoro-carbonyl-containing compounds,<sup>7</sup> while the appropriately aryl-substituted ketals of Chapter 7 allowed formation of even more complex, distally fluorinated structures.<sup>8</sup> Both methods introduce and exemplify the great potential of photochemistry in radical fluorination methods. The latter method also highlights the use of a photosensitizer that can be activated by a 14-Watt compact fluorescent light (CFL) as a safe and economical replacement for ultraviolet light.

Inspired by the cyclopropanols, we wondered if direct photolysis of diarylcyclopropanes in the presence of an N-F reagent would lend a way to difluorination of a biradical. Although puzzling, we discovered instead a unique aminofluorination reaction that is remarkably efficient. In Chapter 8, the mechanism of this aminofluorination reaction is explored in detail.<sup>9</sup> Along the way, control experiments revealed multiple ways to effect the same reaction; in turn, this allowed a multifold approach to mechanistic elucidation and unveiled the essential role the *N*-centered radical intermediate as a chain carrier in a sequence of cyclopropane ring oxidation/three-electron nucleophilic substitution/radical fluorination. This project also inspired an important and fruitful collaboration with the Bragg laboratory that provided spectroscopic observation of our proposed reactive intermediates, as well as indisputable kinetic evidence for the chain propagation mechanism.



Beyond these C-C bond cleavage approaches, we began to focus more intently on selective  $sp^3$  C-H fluorination methods that specifically target biologically relevant molecules. In Chapter 9, the selective fluorination of phenylalanine-like amino acid residues in di- and tripeptides using a visible light-sensitized protocol is discussed.<sup>10</sup> *Prima facie* it represents another of (now) many extant benzylic fluorination methods in the literature; however, preliminary competition experiments and other mechanistic experiments suggest that the amide may play a role in directing C-H bond fluorination. Subsequently, another carbonyl functional group was found to have directing capability upon direct photolysis. In Chapter 10, an enone-directed photochemical fluorination tailor-made for steroids and other terpenoids is presented.<sup>11</sup> Based on orientation of the enone oxygen atom and C=C bond, the enone-directed fluorination is classified into four reactivity modes whereby  $\gamma$ -,  $\beta$ -, homoallylic, and allylic fluorination are possible and predictable in rigid polycyclic substrates.

Lastly, while screening substrates for enone-directed fluorination, we found that a hecogenin acetate derivative elicited selective fluorination, but not at any site we would have expected it. To confirm the structure, we submitted a sample for single-crystal X-ray crystallography (grown from hexanes and chloroform) and discovered quite serendipitously a unique C-F...H-C interaction between the aliphatic fluoride and the chloroform molecule. Thus, in Chapter 11, this C-F...H-C interaction is discussed and characterized as a weak-moderate blue-shifted hydrogen bond.<sup>12</sup>

Future directions in the Lectka laboratory based on the work in this dissertation will likely maintain an emphasis on carbonyl-directed  $sp^3$  C-H fluorination and/or selective fluorination ensuing biradical or radical cation rearrangement processes.

#### 1.4 References.

---

<sup>1</sup> Bloom, S.; Scerba, M. T.; Erb, J.; Lectka, T. *Org. Lett.* **2011**, *13*, 5068-5071.

<sup>2</sup> Bloom, S.; Pitts, C. R.; Miller, D.; Haselton, N.; Holl, M. G.; Urheim, E.; Lectka, T. *Angew. Chem. Int. Ed.* **2012**, *51*, 10580-10583.

<sup>3</sup> Bloom, S.; Pitts, C. R.; Woltornist, R.; Griswold, A.; Holl, M. G.; Lectka, T. *Org. Lett.* **2013**, *15*, 1722-1724.

<sup>4</sup> Pitts, C. R.; Bloom, S.; Woltornist, R.; Auvenshine, D.; Ryzhkov, L. R.; Siegler, M. A.; Lectka, T. *J. Am. Chem. Soc.* **2014**, *136*, 9780-9791.

<sup>5</sup> Bloom, S.; Knippel, J. L.; Lectka, T. *Chem. Sci.* **2014**, *5*, 1175-1178.

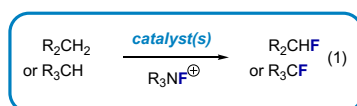
- 
- <sup>6</sup> Pitts, C. R.; Ling, B.; Woltornist, R.; Liu, R.; Lectka, T. *J. Org. Chem.* **2014**, *79*, 8895-8899.
- <sup>7</sup> Bloom, S.; Bume, D. D.; Pitts, C. R.; Lectka, T. *Chem. Eur. J.* **2015**, *21*, 8060-8063.
- <sup>8</sup> Pitts, C. R.; Bloom, M. S.; Bume, D. D.; Zhang, Q. A.; Lectka, T. *Chem. Sci.* **2015**, *6*, 5225-5229.
- <sup>9</sup> Pitts, C. R.; Ling, B.; Snyder, J. A.; Bragg, A. E.; Lectka, T. *J. Am. Chem. Soc.* **2016**, *138*, 6598-6609.
- <sup>10</sup> Bume, D. B.; Pitts, C. R.; Jokhai, R. T.; Lectka, T. *Tetrahedron* **2016**, *72*, 6031-6036.
- <sup>11</sup> Pitts, C. R.; Bume, D. D.; Harry, S. A.; Siegler, M. A.; Lectka, T. *J. Am. Chem. Soc.* **2017**, *139*, 2208-2211.
- <sup>12</sup> Pitts, C. R.; Siegler, M. A.; Lectka, T. *J. Org. Chem.* **2017**, *82*, 3996-4000.

## Chapter 2

### A Polycomponent Metal-catalyzed Aliphatic, Allylic, and Benzylic Fluorination

#### 2.1 Introduction.

The selective incorporation of fluorine into organic molecules has advanced in dramatic ways over the last 30 years.<sup>1</sup> Although arene<sup>2</sup> and alkyne<sup>3</sup> fluorination using metal catalysis has received much attention, corresponding methods for metal-*catalyzed* alkane fluorination remain only a promising goal (Eq. 2.1).<sup>4</sup> To date, the most notable methods for alkane fluorination<sup>5</sup> involve the use of stoichiometric quantities of difficult-to-handle or indiscriminate reagents such as elemental fluorine,<sup>6</sup> cobalt trifluoride (polyfluorination),<sup>7</sup> or potentially explosive cesium fluoroxysulfate.<sup>8</sup> We were particularly interested in the question of whether alkane fluorination could indeed be selectively catalyzed under mild conditions, thus perhaps opening up a realm of fluorination catalysis in addition to much-studied aromatic fluorination. What is more, a mild procedure using safe, commercially available alternatives would be complementary to pioneering methods, and potentially be applicable to closely related allylic and benzylic substrates. In this chapter, we report the fluorination of a series of aliphatic, benzylic, and allylic substrates using a polycomponent catalytic system that involves commercially available Selectfluor, putative radical precursor *N*-hydroxyphthalimide (NHPI), an anionic phase transfer catalyst (KB(C<sub>6</sub>F<sub>5</sub>)<sub>4</sub>), and a copper(I) bisimine complex.<sup>9,10</sup>



#### 2.2 Screening for Reaction Conditions (Adamantane Fluorination).

For the purposes of this study, we chose first to focus our efforts on the well-characterized adamantane system **1** and its fluorinated derivatives. Initial catalyst screening employed a variety of transition metal salts, Selectfluor, and adamantane in dry MeCN (1 mL) stirred over 24 h at room temperature. Most notably, 10 mol% CuI turned out to be a competent lead, yielding 1-fluoroadamantane **2** in 18% yield and in good selectivity (8:1 with respect to 2-fluoroadamantane **3**). It should be noted that in the absence of metal catalyst, the reaction produced no fluorinated products under the specified conditions. At this point,

a number of other copper(I) salts were screened (CuBr, CuCl, CuClO<sub>4</sub>), but CuI proved to be the most effective. For example, CuCl afforded only trace amounts of product, whereas CuClO<sub>4</sub> resulted in a complex mixture of highly fluorinated adamantane-based products in variable quantities.

**Table 2.1** Screening conditions for adamantane fluorination.

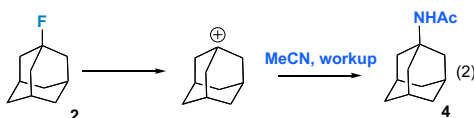
catalyst	solvent	ligand	T (°C)	2:3	yield % 2
-	MeCN	-	25	-	0 <sup>[a],[b]</sup>
CuI	MeCN	-	25	8:1	18 <sup>[a],[b]</sup>
CuI	MeCN	BPMED	25	7:1	28 <sup>[a],[b]</sup>
CuI	MeCN	BPMED	25	5:1	35 <sup>[a]</sup>
CuI	MeNO <sub>2</sub>	BPMED	25	-	trace <sup>[a]</sup>
CuI	MeCN	BPMED	25	3:1	12 <sup>[c]</sup>
<b>CuI</b>	<b>MeCN</b>	<b>BPMED</b>	<b>25</b>	<b>8.4:1</b>	<b>75<sup>[d]</sup></b>

[a] Yield without KB(C<sub>6</sub>F<sub>5</sub>)<sub>4</sub>; [b] MeCN was not degassed; [c] Yield after 1 h; [d] Yield after 3 h; Otherwise yields were determined after 24 h by <sup>19</sup>F NMR using 2-fluorobenzonitrile as an internal standard, and also by column chromatography.

Our laboratory has shown that reactions employing Selectfluor concomitant with a metal co-catalyst can be accelerated by the addition of a phase transfer catalyst as a solubilizing agent and presumed metal counteranion exchanger.<sup>10</sup> To this end, we added KB(C<sub>6</sub>F<sub>5</sub>)<sub>4</sub> (10 mol %) to our reaction and were gratified to find a substantial increase in the rate of formation and yield of **2** (Table 2.1).<sup>11</sup> In a parallel effort toward making the reaction more homogeneous, we also sought the use of a ligand to bring CuI into solution more effectively and to modulate its reactivity. Bisimine-derived ligands are well established in copper catalysis, so we tried them at the outset.<sup>12</sup> For example, addition of *N,N*-bis(phenylmethylene)-1,2-ethanediamine (BPMED) (10 mol %) to our reaction afforded a further increase in the yield of **2**. We then examined the effects of time, temperature, solvent, and the amount of Selectfluor on the reaction. Immediately, we found the reaction proceeded well when MeCN was used as a solvent, and the yield of the desired fluorinated product depended significantly on time. In this respect, longer reaction times were shown to give lower yields of **2** counterbalanced by increased formation of the corresponding acetamide **4** (Eq. 2.2). Furthermore, heating the reaction proved deleterious, while cooling of the reaction to 0 °C remarkably

yielded increased quantities of **3** over anticipated **2** (40%). Stopping the reaction after 3 h at room temperature provided an optimal yield of **2** (75%; Table 2.1).

Although a detailed mechanistic study is forthcoming, a few observations point to the putative participation of radicals<sup>5</sup> (either free or metal-based) or single electron transfer (SET) during fluorination: 1) Yields in the strict absence of O<sub>2</sub> are much higher than in its presence.<sup>13</sup> 2) Interference from the MeCN solvent is minimal (at least during the *initial* fluorination), consistent with its sluggish reaction with free radicals.<sup>14</sup> 3) Finally, there is precedent for Selectfluor engaging in SET chemistry.<sup>15</sup> On the other hand, bare fluoro radicals are unlikely major participants in the optimized reaction; we would expect them to abstract H atoms with virtually equal facility from both tertiary and secondary alkyl sites in adamantane.<sup>16</sup> One final piece of evidence in support of the involvement of radicals may be discerned through the use of a radical trapping agent such as TEMPO. When the reaction is performed under optimized conditions using a stoichiometric amount of adamantane and TEMPO, only trace amounts of **2**, **3**, and **4** are evident.

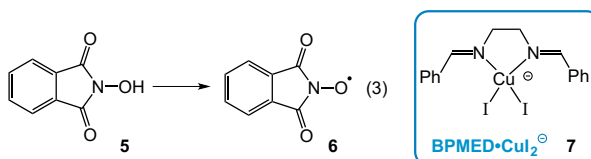


Depletion of **2** involving a putative S<sub>N</sub>1 solvolysis is likewise expected based on the formation of the corresponding acetamide following work-up (Eq. 2.2).<sup>17</sup> Adamantyl cations are well-established intermediates in solvolysis reactions;<sup>18</sup> the higher stability of the 1-adamantyl cation relative to the 2-isomer would explain the relative depletion of product **2** vs. **3** during longer reaction times. For example, at B3LYP/6-311++G\*\*, the 1-adamantyl cation is more stable than the 2-isomer by almost 11.3 kcal/mol.<sup>19</sup>

### 2.3 Optimization of Reaction Conditions for Secondary Alkanes.

We turned our attention to an investigation of the reaction's scope. A variety of aliphatic, allylic, and benzylic substrates were investigated. Unfortunately, upon initial screening, the conditions optimized for reactive adamantane yielded only trace amounts of the desired fluorinated products on a variety of substrates. At this point, we chose to focus our efforts on a less reactive model substrate such as cyclododecane (**8**). We found that heating the reaction increased the yield greatly (43%) - a likely result

from increased reaction rate - and as the product is a secondary fluoride, solvolysis in MeCN was not such a serious problem. In an effort to improve both the yield and the rate of reaction, *N*-hydroxyphthalimide (10 mol %), which is known to form the "PINO" radical **6** in situ in the presence of redox active metals (Eq. 2.3),<sup>20</sup> was examined as a possible cocatalyst.



Interestingly enough, addition of NHPI provided further increases in yield of **9** (63%), and along with additive KI to form the putative Cu(I) ate complex **7** (10 mol %), afforded optimal yield of **9** (72%, Table 2.2).<sup>21</sup> When longer reflux times were employed, 1,1-difluorocyclododecane began to form in appreciable amounts (18% after 24 h).

**Table 2.2** Optimization of fluorination conditions for a secondary alkane.

catalyst	cocatalyst	cocatalyst	yield %
(BPME)CuI	-	-	26
(BPME)CuI	KB(C <sub>6</sub> F <sub>5</sub> ) <sub>4</sub>	-	44
(BPME)CuI	KB(C <sub>6</sub> F <sub>5</sub> ) <sub>4</sub>	NHPI	63
(BPME)CuI	KB(C <sub>6</sub> F <sub>5</sub> ) <sub>4</sub>	NHPI <sup>[a]</sup>	72

All reactions were performed at reflux for 2 h and yields were determined by <sup>19</sup>F NMR using 3-chlorobenzotrifluoride as an internal standard and isolation of the product by chromatography; [a] Reaction performed with KI (10 mol %) as additive.

## 2.4 Evaluation of Substrate Scope.

Straight chain substrates such as *n*-dodecane **20** give rise to a virtual 1:1:1:1 mixture of monofluorinated products in 63% yield, although the necessity of 1.2 equiv KI at reflux may reflect their

less reactive nature (entry 10).<sup>22</sup> Allylic substrates proved to be interesting in their own way. For example,  $\alpha$ -methylstyrenes are known to fluorinate in MeCN to form fluoroacetamides (under so-called electrophilic conditions), admixed with variable quantities of allylic fluorides.<sup>23</sup> Under catalytic conditions at room temperature, as demonstrated herein, the allylic fluorides predominate to the virtual exclusion of the fluoroacetamides. This would seem to bolster the case for a different (non-electrophilic) mechanistic pathway, as well.

A benzylic substrate, ethylbenzene **26**, fluorinated to provide  $\alpha$ -fluoroethylbenzene **27** (entry 13, Table 2.3) in 28% yield (56% based on recovered substrate). Once again, this product is unlikely to form by a strictly electrophilic process under these conditions. Although the yield of this reaction is modest, only very minor amounts of ring fluorinated products were observed. Especially intriguing results are shown in entries 14-16, in which oxygen containing substrates (esters) fluorinate productively. For example, n-hexyl acetate **28** fluorinates predominately on the 4- and 5-positions of the hexyl chain (72%; 81% total fluorination, entry 14), whereas dihydrocoumarin **30** reacts in its benzylic position to afford product **31**, which is the equivalent of a *conjugate addition* of fluoride to coumarin (entry 15).<sup>24</sup> On the other hand, lactone **32** fluorinates exclusively on its side chain (entry 16).

At this point we undertook a preliminary UV-vis study of the components of the catalytic system. The main observations include: 1) Bisimine ligand (BPMED) + CuI affords a spectrum consistent with a Cu(I) complex; 2) addition of KI maintains the oxidation state of copper at (I); 3) addition of Selectfluor gives rise to weak bands indicative of Cu(II) that disappear rapidly, concomitant with the appearance of a prominent  $I_3^-$  band.<sup>25</sup> In turn, addition of NHPI results in consumption of  $I_3^-$ .<sup>26</sup> Presumably, Cu(I) is regenerated, as well. Thus, along with electron transfer to Selectfluor from the Cu-ate complex, the addition of KI may aid in the production of PINO radicals and in regeneration of the catalyst, allowing less reactive substrates to convert smoothly.

**Table 2.3** Substrate scope.

entry	substrate	product	yield %	time (h)	T (°C)
1			75 [c]	3	25
2			40 [c]	3	0
3			72 [a]	2	81
5			66 [b]	1	81
6			41 [b]	0.5	81
7			47 [b]	0.5	81
8			52 [b]	2	25
9			33 [b]	1	81
10			63 [b]	2	81
11			53 [c] (88)	24	25
12			42 [c] (70)	24	25
13			28 [c] (56)	24	25
14			81 [b]	1.5	81
15			47 [b]	3	25
16			62 [b]	5	81
17			55 [b]	3	81

[a] 10 mol % KI; [b] 1.2 equiv KI; [c] No KI. Yields in italics for entries 11-13 based on recovered starting materials. All reactions were monitored by <sup>19</sup>F NMR and yields determined using 3-chlorobenzotrifluoride as an internal standard and/or isolation of the product by column chromatography.



## 2.5 Conclusion.

This method represents one of the first catalytic sp<sup>3</sup> C-H monofluorination methodologies in the chemical literature. Further investigations will prove essential to the elucidation of a reaction mechanism and additional study will address the utility of the reaction and its application to complex substrates and natural products.

## 2.6 References.

---

<sup>1</sup> a) Purser, S.; Moore, P. R.; Swallow, S.; Gouverneur, V. *Chem. Soc. Rev.* **2008**, *37*, 320-330; b) Cahard, D.; Xu, X.; Couve-Bonnaire, S.; Pannecoucke, X. *Chem. Soc. Rev.* **2010**, *39*, 558-568.

<sup>2</sup> a) Watson, D.; Mingjuan, S.; Teverovskiy, G.; Zhang, Y.; Jorge, G. F.; Kinzel, T.; Buchwald, S. L. *Science* **2009**, *325*, 1661-1664; b) Furuya, T.; Klein, J. E. M. N.; Ritter, T. *Synthesis* **2010**, *11*, 1804-1821; c) Anbarasan, P.; Neumann, H.; Bellar, M. *Angew. Chem. Int. Ed.* **2010**, *49*, 2219-2222; d) Ye, Y.; Lee, S.; Sanford, M. S. *Org. Lett.* **2011**, *13*, 5464-5467; e) Loy, R. N.; Sanford, M. S. *Org. Lett.* **2011**, *13*, 2548-2551.

<sup>3</sup> a) Akana, J. A.; Bhattacharyya, K. X.; Müller, P.; Sadighi, J. P. *J. Am. Chem. Soc.* **2007**, *129*, 7736-7737; b) Gorske, B. C.; Mbofana, C. T.; Miller, S. J. *Org. Lett.* **2009**, *11*, 4318-4321.

<sup>4</sup> Considerable progress has been made in aliphatic C-H bond activation, see: Davies, H. M.; Dick, A. R. *Topics in Current Chemistry: C-H Activation* **2010**, 303-346; and for a representative example, see: Chen, M. S.; White, M. C. *Science*, **2007**, *318*, 783-787.

<sup>5</sup> Fluorination of alkane derived free radicals has been recently observed: Rueda-Becerril, M. Sazepin, C. C.; Leung, J. C. T.; Okbinoglu, T.; Kennepohl, P.; Paquins, J.-F.; Sammis, G. M. *J. Am. Chem. Soc.* **2012**, *134*, 4026-4029.

<sup>6</sup> a) Miller, W. T.; Dittman, A. L. *J. Am. Chem. Soc.* **1956**, *78*, 2793-2797; b) Miller, W. T.; Koch, D. D.; McLafferty, F. W. *J. Am. Chem. Soc.* **1956**, *78*, 4992-4995; c) Miller, W. T.; Koch, S. D. *J. Am. Chem. Soc.* **1957**, *79*, 3084-3089. d) Barton, D. H. R.; Hesse, R. H.; Markwell, R. F.; Pechet, M. M.; Toh, H. T. *J. Am. Chem. Soc.* **1976**, *98*, 3034-3035. e) Rozen, S. *Acc. Chem. Res.* **1988**, *21*, 307-312.

<sup>7</sup> a) Fowler, R. W.; Burford, W. B.; Hamilton, J. M.; Sweet, R. G.; Weber, C. E.; Kasper, J. S.; Litant, I. *Preparation, Properties and Technology of Fluorine and Organic Fluoro-compounds* New York, **1951**, 349-371; b) Joyner, B. D. *J. Fluorine Chem.* **1986**, *33*, 337-346; c) Burdon, J.; Creasey, J. C.; Proctor, L. D.; Plevey, R. G.; Yeoman, J. R. N. *J. Chem. Soc. Perkin Trans 2* **1991**, 445-447.

<sup>8</sup> a) Furin, G. G. *New Fluorinating Agents in Organic Synthesis* Berlin, **1989**, 35-68; b) Zupan, M.; Stavber, S. *Tetrahedron* **1989**, *45*, 2737-2742.

<sup>9</sup> For our interest in polyfunctional catalysis, see: a) Paull, D. H.; Scerba, M. T.; Alden-Danforth, E.; Widger, L. R.; Lectka, T. *J. Am. Chem. Soc.* **2008**, *130*, 17260-17261; (b) Erb, J.; Paull, D. H.; Belding, L.; Dudding, T.; Lectka, T. *J. Am. Chem. Soc.* **2011**, *133*, 7536-7546.

<sup>10</sup> Bloom, S.; Scerba, M. T.; Erb, J.; Lectka, T. *Org. Lett.* **2011**, *13*, 5068-5071.

- 
- <sup>11</sup> Toste et al. have recently developed a system involving an asymmetric phase transfer catalyzed fluorination of silyl ethers, see: Rauniyar, V.; Lackner, A. D.; Hamilton, G. L.; Toste, F. D. *Science* **2011**, *334*, 1681-1683.
- <sup>12</sup> CuI•bisimine complexes are known: Toth, A.; Floriani, C.; Pasquali, M.; Chiesi-Villa, A.; Gaetani-Manfredotti, A.; Guastini, C. *Inorg. Chem.* **1985**, *24*, 648-653.
- <sup>13</sup> Okamura, K.; Takahashi, Y.; Miyashi, T. *J. Phys. Chem.* **1995**, *99*, 16925-16931; b) Wikinson, F. *Pure & Appl. Chem.* **1997**, *69*, 851-856. On the other hand, this observation may also be explained by suppression of the formation of catalytically deactivated Cu-O<sub>2</sub> complexes, see: c) Kitajima, N.; Moro-oka, Y. *Chem. Rev.* **1994**, *94*, 737-757; d) Tyeklar, Z.; Jacobson, R.; Wei, N.; Murthy, N. N.; Zubieta, J.; Karlin, K. D. *J. Am. Chem. Soc.* **1993**, *115*, 2677-2689.
- <sup>14</sup> Engel, P. S.; Lee, W. K.; Marschke, G. E.; Shine, H. J. *J. Org. Chem.* **1987**, *52*, 2813-2817.
- <sup>15</sup> a) Nyffeler, P. T.; Durón, S. G.; Burkhart, M. D.; Vincent, S. P.; Wong, C. H. *Angew. Chem. Int. Ed.* **2005**, *44*, 192-212; b) Zhang, X.; Wang, H.; Guo, Y. *Rapid Commun. Mass Spectrom.* **2006**, *20*, 1877-1882; c) Serguchev, Y. A.; Ponomarenko, M. V.; Lourie, L. F.; Fokin, A. A. *J. Phys. Org. Chem.* **2011**, *24*, 407-413.
- <sup>16</sup> Poutsma, M. L. in *Free Radicals* J. K. Kochi (Ed.) John Wiley and Sons, New York, 1973, vol II.
- <sup>17</sup> Michaudel, Q.; Thevenet, D.; Baran, P. S. *J. Am. Chem. Soc.* **2012**, *134*, 2547-2550.
- <sup>18</sup> Schleyer, P. V. R.; Fort, R. C.; Watts, W. E.; Comisarow, M. B.; Olah, G. H. *J. Am. Chem. Soc.* **1964**, *86*, 4195-4197.
- <sup>19</sup> Geometry optimizations were performed using the Spartan '06 program, Wavefunction, Inc.
- <sup>20</sup> a) Coseri, S. *Catalysis Reviews: Science and Engineering* **2009**, *51*, 218-292; b) Coseri, S. *Eur. J. Org. Chem.* **2007**, 1725-1729; (c) Orliska, B.; Romanowska, I. *Cent. Eur. J. Chem.* **2011**, *9*, 670-676.
- <sup>21</sup> It is known that aqueous solutions of CuI and KI react to form a host of copper halide species in which the ate complex CuI<sub>2</sub><sup>-</sup> predominates: Endo, K.; Yamamoto, K.; Deguchi, K.; Matsushita, K. *Bull. Chem. Soc. Jpn.* **1987**, *60*, 2803-2807.
- <sup>22</sup> A recommended conditions chart based on substrate reactivity is provided in the Supporting Information.
- <sup>23</sup> Yadav, J. S.; Subba Reddy, B. V.; Narasimha Chary, D.; Chandrakanth, D. *Tetrahedron Lett.* **2009**, *50*, 1136-1138.
- <sup>24</sup> Compound **31** is prone to dehydrofluorination over time.
- <sup>25</sup> Similarly, unstable CuI<sub>2</sub> rapidly disproportionates to give a mixture of CuI and soluble I<sub>2</sub> in acetonitrile, see: Wang, Y.-L.; Wang, X.-B.; Xing, X.-P.; Wie, F.; Li, J.; Wang, L.-S. *J. Phys. Chem. A* **2010**, *14*, 11244-11251.
- <sup>26</sup> Selectfluor is also known to react with I<sub>3</sub><sup>-</sup> and I<sup>-</sup>: a) Banks, R. E.; Besheesh, M. K.; Mohialdin-Khaffaf, S. N.; Sharif, I. *J. Chem. Soc. Perkin. Trans. 1* **1996**, 2069-2076; b) Stavber, S.; Kralj, P.; Zupan, M. *Synlett* **2002**, *33*, 598-600.

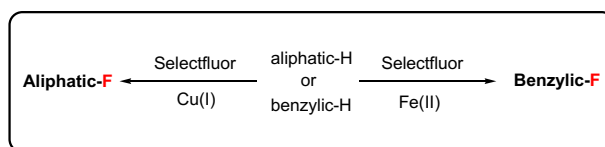
## Chapter 3

### Iron(II)-catalyzed Benzylic Fluorination

#### 3.1 Introduction.

Practical, direct conversions of benzylic  $sp^3$  C-H bonds into C-F bonds offer a potentially valuable addition to the category of C-H functionalization.<sup>1</sup> Despite developments in site-specific oxygenation,<sup>2</sup> amination,<sup>3</sup> and other halogenation methods,<sup>4</sup> innate benzylic fluorination remains an underdeveloped synthetic transformation – thus far relying almost entirely on the use of electrochemical methods<sup>5</sup> or harsh, unselective reagents.<sup>6</sup> Considering the growing importance of fluorinated compounds in drug discovery, a mild benzylic fluorination method may prove itself a useful instrument for the medicinal chemist (e.g. potentially by allowing inhibition of cytochrome P450 oxidation and increasing the lifetime of a drug *in vivo*, among other applications).<sup>7</sup> Thus, our laboratory has recently taken an interest in the development of a straightforward, metal-catalyzed benzylic fluorination method.

Both we (copper(I) bisimine, Selectfluor<sup>8</sup>) and the Groves group (manganese porphyrin, fluoride ion, iodosobenzene<sup>9</sup>) have reported unique catalytic systems for the selective fluorination of aliphatic C-H bonds. In our original copper system, we found that, although applicable to a select few benzylic substrates, fluorination proved somewhat difficult, notwithstanding the enhanced reactivity of benzylic C-H bonds. Inspired by the oxidation capabilities of certain biological catalysts, cost-effectiveness, commercial availability and/or ease of preparation, we turned our attention to prospective iron catalysts (Scheme 3.1). Herein, we report our studies on a catalyzed fluorination of benzylic substrates using an inexpensive iron(II) salt, iron(II) acetylacetonate ( $Fe(acac)_2$ ), and commercially available Selectfluor, under mild conditions.



**Scheme 3.1** Effect of catalyst on substrate scope.

This unique system produces an array of benzylic fluorinated products in good to excellent yields and in outstanding selectivity. Moreover, we demonstrate the possibility for a strategically placed carbonyl group to result in site-specific fluorination in the  $\beta$ -position, a potentially desirable synthetic transformation. Further study of this and similar systems may also provide a more clear understanding of halogenase enzymes<sup>10</sup> and potential use of ketones as directing groups in C-H bond activation.<sup>11</sup>

### 3.2 Screening for Reaction Conditions.

Noting previous success in the literature in C-H functionalization by non-heme iron catalysts,<sup>12</sup> we reasoned that iron(II) salts could be effective for this transformation. We began our initial survey of iron salts as potential catalysts with 3-phenylpropyl acetate **1a** as a model substrate (Table 3.1). Among the iron salts screened, only Fe(acac)<sub>2</sub> yielded the desired 3-fluoro-3-phenylpropyl acetate **2a**. The use of other iron salts, e.g. halides, sulfates, and nitrates, failed to yield any fluorinated products under our specified conditions. Perhaps this can be explained by the fact that hard, polydentate *O*-donor ligands, such as anionic acetylacetonate, allow easy access to higher oxidation states, facilitating oxidative functionalization. Accordingly, several late transition metal complexes containing one or more acetylacetonate (acac) ligands have appeared in recent years capable of C-H bond activation.<sup>13</sup>

### 3.3 Evaluation of Substrate Scope.

Subsequently, we evaluated the scope of our system by screening a series of benzylic substrates. To our satisfaction, several substrates underwent sufficient benzylic fluorination in good yields and in excellent selectivity (Table 3.1). Electron-poor or more neutral alkyl benzenes proved most promising, whereas electron-rich aromatic systems lead to varying quantities of polyfluorinated products, often ring fluorination adducts.<sup>14</sup> A particularly interesting case, cymene, **1b**, afforded fluorinated **2b** *exclusively*, in direct contrast to our previously reported copper system in which fluorination of the tertiary carbon is preferred. The formation of **2b** may be suggestive of a change in mechanism whereby steric constraints influence selectivity more so than trends in radical stability. Additionally, carbonyl-containing compounds demonstrated a notable shift in selectivity to benzylic fluorination over an expected background reaction (Scheme 3.2).

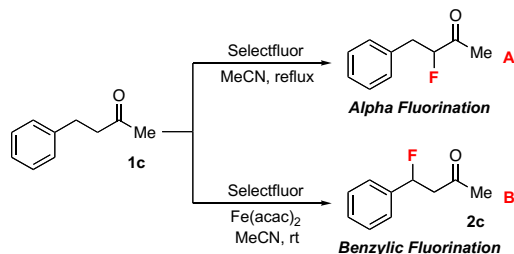
**Table 3.1** Survey of benzylic substrates.

entry	substrate	product	yield %
1			71
2			66
3			76
4			64 <sup>b</sup>
5			52
6			35 <sup>a</sup>
7			61
8			41 <sup>b</sup>
9			58 <sup>a</sup>
10			57
11			59
12			65 <sup>a</sup>
13			68 <sup>a</sup>

<sup>a</sup>Yields determined by <sup>19</sup>F NMR using 3-chlorobenzotrifluoride as an internal standard. <sup>b</sup>Isolated as major benzylic product with minor fluorinated isomers

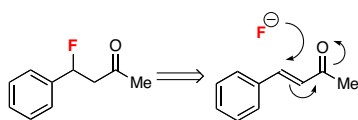
Traditionally, Selectfluor is known to react with carbonyl-containing compounds to yield  $\alpha$ -fluorinated products.<sup>15</sup> For example, benzylacetone **1c** reacts readily with Selectfluor at elevated temperatures in acetonitrile to yield  $\alpha$ -fluorinated ketone (Scheme 3.2, path A). Interestingly enough, under our catalytic

conditions, benzylacetone reacts at room temperature to give solely benzylic fluorinated compound **2c** (Scheme 3.2, path B).



**Scheme 3.2** Iron(II)-promoted reversal in selectivity.

What is more, **2c** resembles the retrosynthetic product of a 1,4-conjugate addition of a fluoride anion to the analogous  $\alpha,\beta$ -unsaturated ketone (Figure 3.1), an attractive transformation in modern synthetic chemistry. In a similar instance, ibuprofen methyl ester **1d** affords predominantly benzylic fluorinated **2d** under our conditions, potentially a pharmaceutically interesting transformation, rather than the  $\alpha$ -fluorinated ketone.

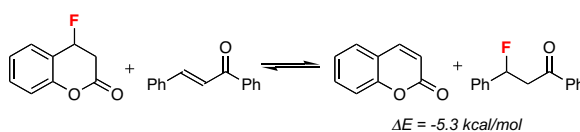


**Figure 3.1** Retrosynthetic 1,4-conjugate addition of fluoride.

It stands to reason that iron is crucial in reaction selectivity and that the carbonyl may even provide a directing effect toward the benzylic position over chemistry at the more acidic  $\alpha$ -carbon. This notion may be further supported by the ease at which 3-arylketones undergo benzylic fluorination in light of changes in the identity of the carbonyl containing functional group. As evidenced, the system tolerates aryl ketones, esters, aliphatic ketones, amides, and other halogens with near equal propensity. It is important to note that the majority of our substrates do not undergo dehydrohalogenation upon workup, a common problem in

benzylic halogenation. Surprisingly,  $\beta$ -fluoroketones proved particularly stable, contrary to our previous finding that 2-fluorodihydrocoumarin **2f** readily dehydrofluorinates.

In this instance, analysis of an isodesmic reaction between a compound that readily dehydrofluorinates, dihydrocoumarin **2f**, and one that does not, dihydrochalcone **2g**, offers some insight (Scheme 3.3). At the B3LYP/6-311++G\*\* level of theory,  $\Delta E$  of the isodesmic reaction is -5.3 kcal/mol,<sup>16</sup> suggesting a more exothermic process whereby fluorine is lost in favor of desaturation and resultant gain in aromatic character.



**Scheme 3.3** Isodesmic reaction for dehydrofluorination of coumarin at B3LYP/6-311++G\*\*.

Nitrogen-containing compounds (such as amines) were likewise problematic. In most cases, *N*-fluorination of the starting compound inhibits desired functionalization,<sup>17</sup> instead leading to *N*-oxidized products through a putative iminium intermediate.<sup>18</sup> We gathered that a compound in which direction from the ketone in concert with lowered basicity of the nitrogen (e.g. through amide resonance) would be primed for fluorination, such as **1h**. Indeed, **1h** proved most amendable providing fluorinated **2h** in 41%.

### 3.4 Conclusion.

Future studies will seek to elucidate the mechanism of this reaction through kinetic, isotopic, and spectroscopic analysis. Additionally, efforts will be made in the way of rendering the reaction enantioselective, an important goal in direct fluorination methods, and determining the role of carbonyls as C-H bond directing groups.

### 3.5 References.

- <sup>1</sup> (a) Brückl, T.; Baxter, R. D.; Ishihara, Y.; Baran, P. S. *Acc. Chem. Res.* **2012**, *45*, 826-839. (b) Labinger, J. A.; Bercaw, J. E. *Nature* **2002**, *417*, 507-514. (c) Wencel-Delord, J.; Dröge, T.; Liu, F.; Glorius, F. *Chem. Soc. Rev.* **2011**, *40*, 4740-4761.
- <sup>2</sup> (a) Newhouse, T.; Baran, P. S. *Angew. Chem. Int. Ed.* **2011**, *50*, 3362-3374. (b) Guoyong, S.; Fen, W.; Xingwei, L. *Chem. Soc. Rev.* **2012**, *41*, 3651-3678. (c) Chen, M. S.; White, M. C. *Science* **2007**, *318*, 783-787. (d) Fung, Y. S.; Yan, S. C.; Wong, M. K. *Org. Biomol. Chem.* **2012**, *10*, 3122-3130.
- <sup>3</sup> Nishioka, Y.; Uchida, T.; Katsuki, T. *Angew. Chem. Int. Ed.* **2013**, *52*, 1739-1742. (b) Jordan-Hore, J. A.; Johansson, C. C. C.; Gulias, M.; Beck, E. M.; Gaunt, M. J. *J. Am. Chem. Soc.* **2008**, *130*, 16184-16186. (c) King, E. R.; Hennessy, E. T.; Betley, T. A. *J. Am. Chem. Soc.* **2011**, *133*, 4917-4923. (d) Takeda, Y.; Hayakawa, J.; Yano, K.; Minakata, S. *Chem. Lett.* **2012**, *41*, 1672-1674.
- <sup>4</sup> (a) Liu, W.; Groves, J. T. *J. Am. Chem. Soc.* **2012**, *132*, 12847-12849. (b) Goldsmith, C. R.; Coates, C. M.; Hagan, K.; Mitchell, C. A. *J. Mol. Catal. A: Chem.* **2011**, *335*, 24-30. (c) Do, H.-Q.; Daugulis, O. *Org. Lett.* **2009**, *11*, 421-423. (d) Hull, K. L.; Anani, W. Q.; Sanford, M. S. *J. Am. Chem. Soc.* **2006**, *128*, 7134-7135.
- <sup>5</sup> (a) Toshiki, T.; Ishii, H.; Fuchigami, T. *Electrochem. Commun.* **2002**, *4*, 589-592. (b) Hou, Y.; Higashiya, S.; Fuchigami, T. *Electrochim. Acta* **2000**, *45*, 3005-3010.
- <sup>6</sup> (a) Fowler, R. W.; Burford, W. B.; Hamilton, J. M.; Sweet, R. G.; Weber, C. E.; Kasper, J. S.; Litant, I. *Preparation, Properties and Technology of Fluorine and Organic Fluoro Compounds*; McGraw Hill: New York, 1951; pp 349-371. (b) Furin, G. G. *New Fluorinating Agents in Organic Synthesis*; Springer: Berlin, 1989; pp. 135-168.
- <sup>7</sup> Liu, P.; Sharon, A.; Chu, C. K. *J. Fluorine Chem.* **2008**, *129*, 743-766. (b) Park, B. K.; Kitteringham, N. R. *Drug Metab. Rev.* **1994**, *26*, 605-643. (c) Smart, B. E. *J. Fluorine Chem.* **2001**, *109*, 3-11. (d) Ojima, I. *Fluorine in Medicinal Chemistry and Chemical Biology*; Wiley-Blackwell: Chichester, U.K., 2009. (e) Chambers, R. D. *Fluorine in Organic Chemistry*; Wiley: New York, 1973.
- <sup>8</sup> Bloom, S.; Pitts, C. R.; Miller, D. C.; Haselton, N.; Holl, M. G.; Urheim, E.; Lectka, T. *Angew. Chem. Int. Ed.* **2012**, *51*, 10580-10583.
- <sup>9</sup> Liu, W.; Huang, X.; Cheng, M.-J.; Nielsen, R. J.; Goddard, W.; Groves, J. T. *Science* **2012**, *337*, 1322-1325.
- <sup>10</sup> For a review of halogenase enzymes see: Vaillancourt, F. H.; Yeh, E.; Vosburg, D. A.; Gameau-Tsodikova, S.; Walsh, C. T. *Chem. Rev.* **2006**, *106*, 3364-3378.
- <sup>11</sup> (a) Gandeepan, P.; Parthasarathy, K.; Cheng, C.-H. *J. Am. Chem. Soc.* **2010**, *132*, 8569-8571. (b) Patureau, F. W.; Besset, T.; Glorius, F. *Angew. Chem. Int. Ed.* **2011**, *50*, 1064-1067. (c) Xiao, B.; Gong, T.-J.; Xu, J.; Liu, Z.-J.; Liu, L. *J. Am. Chem. Soc.* **2011**, *133*, 1466-1474.
- <sup>12</sup> (a) Xiaoli, S.; Li, J.; Huang, X.; Sun, C. *Curr. Inorg. Chem.* **2012**, *2*, 64-85. (b) Enthaler, S.; Junge, K.; Beller, M. *Angew. Chem. Int. Ed.* **2008**, *47*, 3317-3321.
- <sup>13</sup> (a) Ess, D. H.; Gunnoe, T. B.; Cundari, T. R.; Goddard, W. A. III; Periana, R. A. *Organometallics* **2010**, *29*, 6801-6815. (b) Bischof, S. M.; Ess, D. H.; Meier, S. K.; Oxgaard, J.; Nielsen, R. J.; Bhalla, G.; Goddard, W. A. III; Periana, R. A. *Organometallics*, **2010**, *29*, 742-756. (c) Salavati-Niasari, M.; Elzami, M. R.; Mansournia, M. R.; Hydarzadeh, S. *J. Mol. Catal. A: Chem.* **2004**, *221*, 169-175.



---

<sup>14</sup> Selectfluor is known to fluorinate activated aromatic compounds without virtue of a catalyst.

<sup>15</sup> (a) Stavber, S.; Zupan, M. *Tetrahedron Lett.* **1996**, *37*, 3591-3594. (b) Stavber, G.; Zupan, M.; Stavber, S. *Synlett* **2009**, *4*, 589-594.

<sup>16</sup> Geometry optimizations were performed using the Spartan '10 program, Wavefunction, Inc.

<sup>17</sup> (a) Singh, R. P.; Shreeve, J. M. *Chem. Commun.* **2001**, *13*, 1196-1197. (b) *Advances in Organic Synthesis, Vol. 2, Modern Organofluorine Chemistry. Synthetic Aspects*; Rahman, A.-U., Laali, K.K., Eds.; Bentham: Hilversum, The Netherlands, 2006.

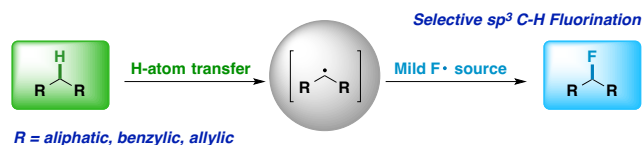
<sup>18</sup> Jin, Z.; Xu, B.; Hammond, G. B. *Tetrahedron Lett.* **2011**, *52*, 1956-1959.

## Chapter 4

### Direct, Catalytic Monofluorination of $sp^3$ C-H Bonds: A Radical-based Mechanism with Ionic Selectivity

#### 4.1 Introduction.

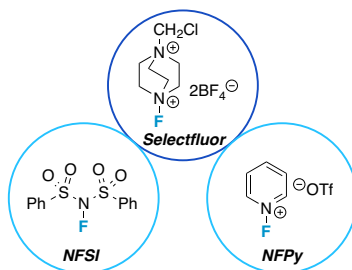
Selective functionalization of  $sp^3$  C-H bonds represents an area of invaluable and economical chemistry. The direct formations of alcohols, alkenes, alkyl halides, and other functional groups from unactivated C-H bonds are impressive, seemingly effortless reactions accomplished by enzymes that are often challenging to effect in a laboratory setting. However, selective *fluorination* has proven an arduous undertaking for both Nature and the synthetic chemist alike. Biologically, very few fluorinase enzymes are known, and none of them operates on the basis of direct C-H functionalization.<sup>1</sup> Synthetically, a conceivable radical fluorination method using hazardous and difficult-to-use  $F_2$ , similar to the well-established bromination and chlorination reactions, is actually highly exothermic, which causes great selectivity and safety concerns.<sup>2</sup> For organofluorine chemists, this issue and other existing challenges call for a more innovative approach to C-H fluorination (Scheme 4.1).



**Scheme 4.1** Concept for mild  $sp^3$  C-H fluorination method.

Arguably one of the most significant developments in the field of organofluorine chemistry was the advent of the N-F reagents (containing a nitrogen-fluorine bond) intended as mild sources of electrophilic fluorine in the late 1980s.<sup>3</sup> Considering that these reagents were solid, stable, and effective compounds, they quickly superseded the use of the high-energy electrophilic fluorinating reagents such as fluorine gas, xenon difluoride, perchloryl fluoride, and hypofluorites, making fluorination reactions significantly more accessible to the synthetic chemist.<sup>4</sup> Among the top ranks of the N-F reagents are *N*-fluorobenzene sulfonimide (NFSI), *N*-fluoropyridinium salts (NFPy), and 1-chloromethyl-4-fluoro-1,4-diazoniabicyclo-

[2.2.2]octane bis(tetrafluoroborate) (Selectfluor) *vide infra* (Figure 4.1). These unique and versatile compounds have proven their worth as reagents for fluorofunctionalization as mediators and catalysts, but are also ideal candidates for mechanistic studies.<sup>5</sup>



**Figure 4.1** Common "N-F" reagents.

Recent findings suggest that some of these so-called "electrophilic" N-F reagents can also act as F-atom transfer reagents. Sammis et al. have reported the ability of NFSI to react with alkyl radicals,<sup>6</sup> Baran et al. have suggested the ability of Selectfluor to participate in single-electron transfer (SET) chemistry and the homolytic cleavage of C-H bonds,<sup>7</sup> and within the last year both our laboratory and the Groves laboratory have independently published methods on metal-catalyzed sp<sup>3</sup> C-H monofluorination. Where the Groves system utilizes silver(I) fluoride (a nucleophilic fluorine source) and iodosobenzene to generate a manganese(IV) fluoride porphyrin catalyst *in situ* instead of an aforementioned N-F reagent,<sup>8</sup> our system, as will be shown in this full paper, relies fundamentally on radical-based chemistry between Selectfluor and a copper(I) promoter to effect both H-atom abstraction and subsequent installation of fluorine.<sup>9</sup>

Groves's and our work were among the first direct, catalytic methodologies for the monofluorination of aliphatic substrates. These discoveries prompted further investigations in our laboratory, *viz.* 1) simplification of the conditions for our originally fairly complex system, 2) exploration of the chemistry of other redox-active transition metals with Selectfluor,<sup>10</sup> and especially 3) in-depth mechanistic studies of the system(s) we devised. In this article, we propose a detailed mechanism for the copper-initiated aliphatic fluorination method that is consistent with exhaustive EPR, <sup>19</sup>F NMR, UV-vis, electrochemical, kinetic,

synthetic, and computational studies. Furthermore, we offer a possible explanation for the notable, useful, but curious preference for monofluorination.

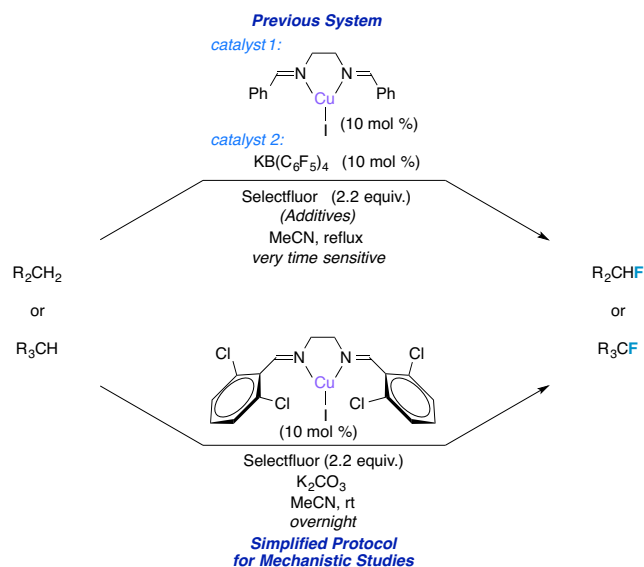
The chapter is structured to present a logical narrative whereby the mechanistic studies were conducted. With this regard, it is organized respectively as to 1) establish the simplified protocol used for mechanistic analysis, 2) discuss the experiments used to determine the role of copper as an initiator, 3) examine the H-atom abstraction/fluorination steps of the mechanism (illuminating the involvement of radical intermediates), 4) illustrate our conclusions drawn from kinetic analyses, 5) propose a reasonable mechanism in accord with all experimental observations, and 6) offer an explanation for the observed selectivity of our reaction as a manifestation of the "polar effect" by ascribing an ionic character to the H-atom abstraction transition state and, finally, subjecting the system to computational analysis to confirm experimental results.

#### **4.2 Simplified Protocol.**

Our original discovery combined Selectfluor and transition metal catalysts (especially copper(I) based complexes) in effecting direct aliphatic, benzylic, and, in special cases, allylic monofluorination.<sup>9,10</sup> However, the copper system that focused on aliphatic fluorination, albeit intriguing, is admittedly less practical for large-scale applications as it involves the use of several additives. Thus, our immediate goal was to establish a simplified protocol that is more accessible, cost-effective, scalable, less time-sensitive, and easier to subject to mechanistic studies. A logical approach was to strip the system back down to the minimum number of necessary components (i.e. Selectfluor, a copper salt, acetonitrile) and address possible problems more directly.

Previously, we observed that our newly fluorinated substrates were prone to ionization *in situ* over time, which led to a decrease in product yields if the reactions were not quenched at the appropriate time intervals. Perhaps this is attributed to a gradual accumulation of hydrogen fluoride (HF) as a byproduct of the reaction, which was observed by <sup>19</sup>F NMR under our published conditions. To prevent the buildup of HF, we screened a variety of bases and noted that whereas amines often impede the reaction altogether, 0.1 equiv. of potassium carbonate is often enough to effect the reaction and eliminate any traces of HF by <sup>19</sup>F NMR for 16-24 h. This small modification allows us to let a variety of substrates stir at room

temperature for longer, generalized periods of time without having vigilantly to monitor and optimize each one individually. To our satisfaction, we also obtained comparable conversions to monofluorinated products in the presence of potassium carbonate. However, at this time we did not conclude anything about the true role of the potassium carbonate in the system.



**Scheme 4.2** Simplified protocol for Selectfluor/copper(I) system.

Hoping to circumvent the dependency on potassium tetrakis(pentafluorophenyl)borate, *N*-hydroxyphthalimide, and potassium iodide for higher yields, we decided to focus on modifying the ligand. In the original system, we had the most success with *N,N'*-bis(benzylidene)ethane-1,2-diamine. Making minor modifications to the ligand scaffold, we quickly found a substantial increase in percent conversions at room temperature by using *N,N'*-bis(2,6-dichloro-benzylidene)-ethane-1,2-diamine instead.<sup>11</sup> At this juncture in our laboratory, we have established that a standard reaction using 2.2 equiv. Selectfluor, 0.1 equiv. cuprous iodide, 0.1 equiv. of the aforementioned ligand, and 0.1-1.0 equiv. potassium carbonate in MeCN under N<sub>2</sub> at room temperature overnight was a suitable, generalized protocol for aliphatic and benzylic monofluorination (Scheme 4.2). Under these conditions, the reaction has also proven amenable to gram-scale synthesis of monofluorinated products (e.g. 1-fluorocyclododecane was obtained in 50% yield after 8 h). Using this simplified protocol, we sought to address the most fundamental concerns surrounding

the reaction mechanism, i.e. the role of copper, how the fluorine atom is installed, how the reaction kinetics behave, and the preference for monofluorination.

### 4.3 Loss of Fluoride from Copper(I)-Selectfluor Interaction.

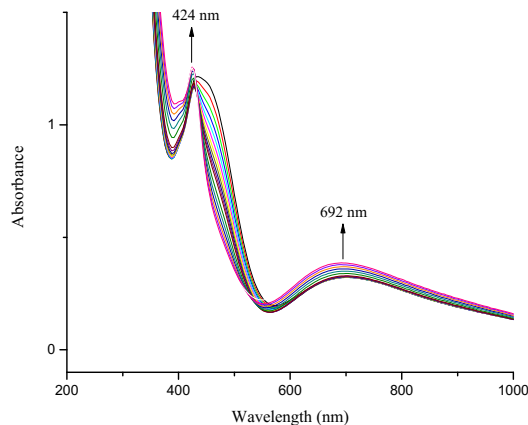
Intuitively, copper can either be a species actively involved in the catalytic cycle or an initiator to the reaction. With these potential roles in mind, a large array of experiments was designed to probe the behavior of copper over the course of the reaction. Considering that the minimum necessary components to effect  $sp^3$  C-H fluorination are simply Selectfluor and copper(I), we first studied their interaction by NMR. A  $^{19}\text{F}$  NMR spectrum of Selectfluor in  $\text{CD}_3\text{CN}$  displays an N-F signal at +47.1 ppm and a  $\text{BF}_4$  signal at -152.1 ppm, relative to 3-chlorobenzotrifluoride.<sup>12</sup> A spectrum of a 1:1 mixture of Selectfluor and cuprous iodide in  $\text{CD}_3\text{CN}$ , taken after 45 min of stirring, displays a  $\text{BF}_4$  signal at -152.4 ppm and the standard peak. No N-F fluorine signal is observed at +47.1 ppm, nor are any additional signals from +400 ppm to -300 ppm present.

Preliminary EPR experiments reveal the formation of a copper(II) species, but no Cu-F coupling is observed at room temperature, as well. So where did the fluorine atom go? The most logical scenario is the formation of a copper fluoride species that is undetectable by  $^{19}\text{F}$  NMR due to extreme signal broadening induced by the paramagnetic copper(II) center (unlikely), formation of a copper(II) bifluoride exhibiting fluxional behavior in solution,<sup>13</sup> or the fact that after rapid solvolysis, it exists as a solvent separated ion pair.<sup>14</sup> Attempts were made to "freeze out" a copper(II) bifluoride signal at -10°C and -40°C, but no evidence for this type of species or any other signal was seen. Notably, a simple  $^{19}\text{F}$  NMR of cupric fluoride in MeCN supports the notion of solvent separation – no fluorine signal is observed.

To rule out the possibility of a copper fluoride formed *in situ* being the key player for H-atom abstraction and subsequent installation of fluorine, several control experiments were run using preformed copper fluorides (cupric fluoride and  $(\text{PPh}_3)_3\text{CuF}\cdot 2\text{MeOH}$ )<sup>15</sup> in the absence of Selectfluor.<sup>16</sup> Although these experiments provide no evidence for/against a copper fluoride as the source of fluorine during the fluorination step of the mechanism,<sup>17</sup> they do help confirm that an interaction between copper and Selectfluor is necessary to generate the species responsible for effecting H-atom abstraction.<sup>18</sup>

#### 4.4 UV-vis Spectroscopy.

This copper(I)-Selectfluor interplay may best be elucidated by direct observation of copper. Formation of a copper(II) species was recognized early on in the investigation by UV-vis and EPR analyses, and was subsequently studied intently.

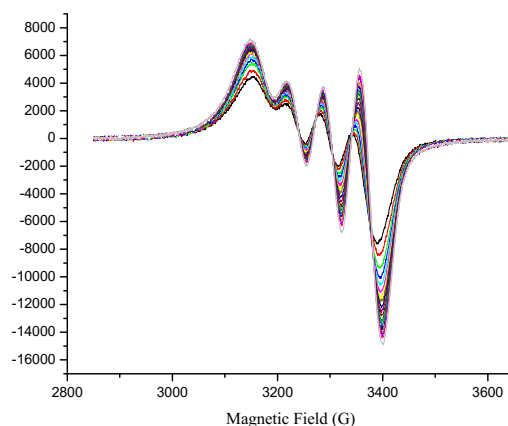


**Figure 4.2** UV-vis spectra of CuI, ligand, and Selectfluor.

UV-vis spectroscopy was used to monitor changes in the copper species early in the reaction (ca.  $t = 5$  min to  $t = 15$  min displayed in Figure 4.2). Figure 4.2 displays visible bands at 426, 456, and 692 nm upon the addition of cuprous iodide and our bis(imine) ligand to Selectfluor in MeCN under  $N_2$ . The broad band at 692 nm, a new copper(II) absorbance, grows in concomitantly with the sharp absorbance at 426 nm, which disappears in the absence of ligand and is conceivably a charge-transfer band from a copper-ligand interaction. The decreasing absorbance at 456 nm was determined to result from an interaction between iodide and Selectfluor - this absorbance was duplicated when taking a UV-vis spectrum upon mixing Selectfluor with tetrabutylammonium iodide (note that the interaction between iodide and Selectfluor alone will not effect the fluorination reaction; copper is necessary). Interestingly, when the reaction was run in a cuvette under standard conditions (in the presence of substrate), the spectrum obtained was virtually identical. Furthermore, a UV-vis spectrum taken after several hours still shows a strong copper(II) absorbance.

#### 4.5 X-band CW EPR Flat-Cell Experiments.

The formation of a paramagnetic copper(II) species presents an opportunity for analysis via EPR spectroscopy. For liquid phase EPR experiments, a flat-cell was used in place of a cylindrical sample configuration in order to minimize the absorption of microwaves by the solvent.<sup>19</sup> The copper(II) spectra of reaction conditions with and without a substrate present consist of four hyperfine lines (from copper;  $I = 3/2$ ) of unequal intensities that grow in and *persist* over time. Subsequent observation of a reaction in the absence of a substrate over time revealed gradual shifts in intensities and resonances (Figure 4.3). This could indicate a change in geometry or ligand environment of the original copper(II) species formed. For better clarification, we turned to solid-state EPR.



**Figure 4.3** Flat-cell liquid phase spectra of copper(II) over time.

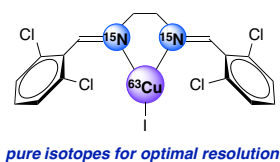
#### 4.6 Solid-state X-band CW EPR.

The added complexity of solid-state EPR spectra due to anisotropic effects can illuminate details about the geometry of a complex, symmetry, and the nature of any neighboring atoms.<sup>20</sup> In an attempt to achieve optimal resolution, spectra were collected at 8 K using isotopically enriched  $^{63}\text{CuI}$  and  $^{15}\text{N}$ -labeled ligand (Figure 4.4).<sup>21</sup> To our knowledge, this is the best approach to determine definitively whether a direct Cu-F interaction is characteristic of the copper species at any point in the reaction.

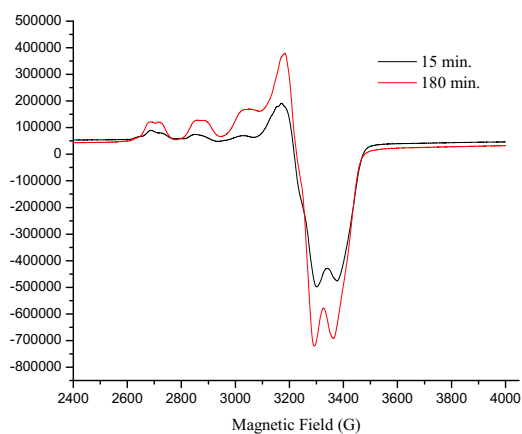
Solid-state spectra of the reaction in the absence of a substrate display an interesting feature. An equilibrium of two copper(II) species is well resolved in a spectrum taken after 3 h (Figure 4.5). The



signatures indicate that both species are monomeric, solely surrounded by nitrogen-containing ligands, and tetragonal in coordination geometry ( $g_x > g_y > g_z$ ; see Table 4.1).<sup>22</sup> Although it is tempting to mistake the separation of the hyperfine resonances for each species as "splitting," perhaps due to a Cu-F interaction, none is observed – these are two separate copper complexes that both lack coupling to fluorine. Regarding the implausibility of a Cu-F interaction, Weltner et al. reported a hyperfine coupling constant of  $A(^{19}\text{F}) = 115 \text{ G}$  derived from EPR spectra of cupric fluoride at 4 K in argon and neon matrices, which is significantly higher than any supposed splitting observed in these complexes, but may not be the most appropriate comparison.<sup>23</sup> In another scenario, by exposing ceruloplasmin to 15 equiv. of fluoride, Gray et al. reported  $A(^{19}\text{F}) = 40 \text{ G}$  for a cupric fluoride,<sup>24</sup> which seems on par with the separation between our observed hyperfine resonances. Yet, the additional  $g_3$  resonance that appears in our spectra shatters the appeal of perceiving this as Cu-F coupling and solidifies the notion of two separate copper(II) complexes.<sup>25</sup>

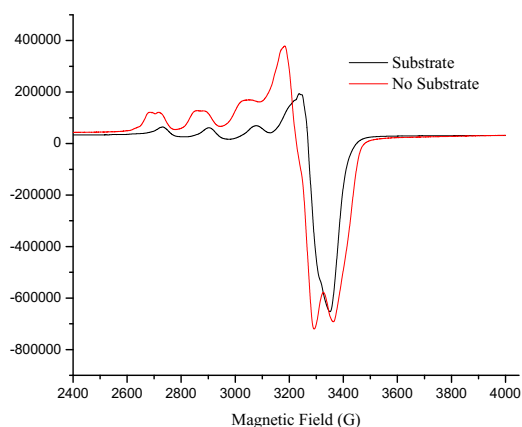


**Figure 4.4** Isotopically enriched ligand for solid state EPR.



**Figure 4.5** Solid-state spectra of copper(II) in the absence of a substrate at 8 K.

In the presence of substrate (under standard reaction conditions), something even more interesting is observed – the presence of only one of the two copper(II) species (Figure 4.6). This is likely an issue of dynamic ligand activity between the putative complexes **1** and **2** (Scheme 4.3). A higher concentration of an additional amine ligand **3** (Selectfluor minus F<sup>+</sup>) is formed under reaction conditions, which shifts the equilibrium preferentially toward only one of the copper(II) species.



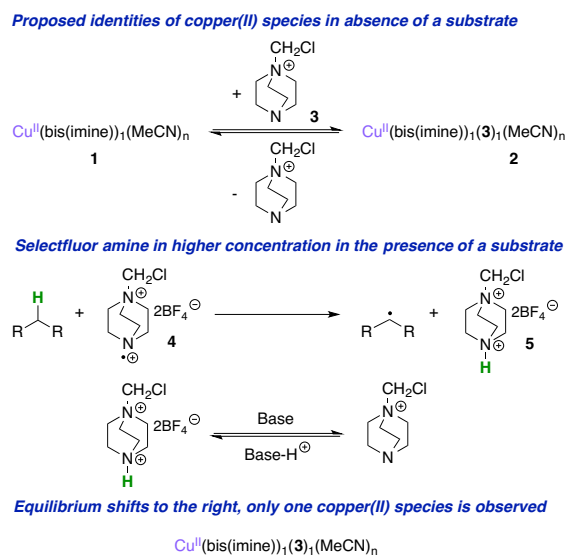
**Figure 4.6** Solid-state spectra of copper(II) after 180 min. with (C1) and without (C2) substrate present at 8 K.

**Table 4.1** EPR parameters for complexes in Figures 4.5 and 4.6.

Complex	$g_{\parallel}$	$g_{\perp}$	$A_{\parallel}$ (G)	$A_{\perp}$ (G)	$g_{iso}$	$A_{iso}$ (G)
<b>C1</b>	2.27	2.04	170	12.5	2.12	65
<b>C2a</b>	2.30	2.12	177	16.5	2.18	70
<b>C2b</b>	2.28	2.07	167	14.0	2.14	65

In the catalytic cycle we ultimately propose, radical dication **4** abstracts a hydrogen atom from an alkane to form ammonium salt **5**, which would easily be deprotonated in the presence of potassium carbonate (Scheme 4.3). The corresponding amine **3** would be a suitable ligand for copper(II). If an alkane substrate is not present, the formation of **5** is significantly slower, the concentration of the amine significantly lower, and thus, there is a mixture of amine-ligated copper(II) **2** and non-amine-ligated copper(II) **1**. This is consistent with the EPR parameters for the complexes (Table 4.1), which indicate that

both copper species are surrounded solely by nitrogen-containing ligands. Under any circumstance, there is no observed Cu-F interaction, characteristic of a copper(II) bifluoride or otherwise. It is crucial to highlight that this by no means rules out the possibility of a solvent separated copper(II) fluoride being formed as a product of the reaction, which can be inferred reasonably from our NMR experiments.

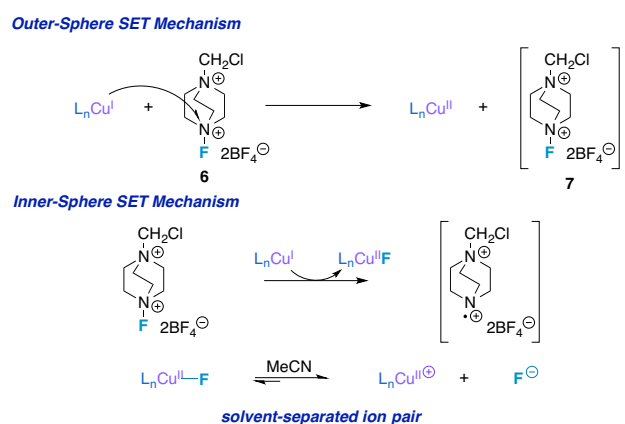


**Scheme 4.3** Possible identities of copper(II) species observed in EPR spectra.

Lastly, hoping for more clarification, several attempts were made to grow single crystals suitable for X-ray structure determination of the unoxidized copper(I)-bis(imine) complex and the oxidized copper(II) species observed by EPR. In the former scenario, an interesting polymeric structure was obtained exhibiting 2:1 cuprous iodide:bis(imine) ligand stoichiometry. However, this polymer is likely just a thermodynamic sink for the copper(I):bis(imine) ligand interaction and does not play an active role in the chemistry; EPR signatures of the copper(II) species observed over the course of the reaction do not resemble those of dimeric or polymeric copper species.<sup>26</sup> In the latter scenario, any attempt to grow crystals of the oxidized copper species (in the presence of Selectfluor) only afforded the ammonium salt **5** - H-TEDA-BF<sub>4</sub> - previously reported by the Baran group.<sup>7</sup>

#### 4.7 Initiation by Single-Electron Transfer.

Evidence of a rapid growth and persistence of copper(II) over the course of the reaction was observed in the liquid phase EPR studies, whereby copper(II) is formed rapidly over the first hour of the reaction (~85% conversion from copper(I)) and asymptotically approaches 100% conversion thereafter.<sup>27</sup> It is very possible that the copper species plays a *laissez-faire* role beyond initiating the reaction and generating an unstable Selectfluor derivative that serves as the H-atom abstractor and propagator in the reaction mechanism. Taking into account previous observations by both our laboratory and the Baran laboratory, we explored the supposed SET chemistry between copper and Selectfluor. There are two potential scenarios to consider under the reaction conditions, resembling either an outer-sphere or inner-sphere electron transfer mechanism (Scheme 4.4).<sup>28</sup>



**Scheme 4.4** Inner-sphere and outer-sphere SET pathways.

#### 4.8 Outer-sphere SET.

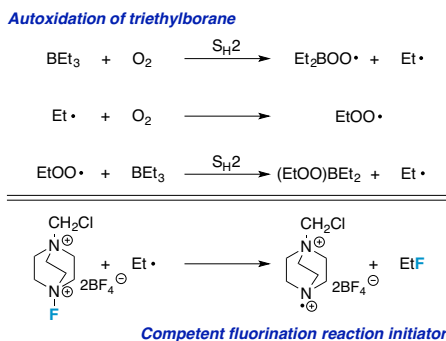
In the instance of an outer-sphere mechanism, the copper species and Selectfluor **6** would remain separate and otherwise unchanged throughout the course of an event where copper(I) transfers an electron to Selectfluor, generating copper(II) and Selectfluor radical cation **7**. One could draw out a mechanism where radical cation **7** performs H-atom abstraction, forming HF and an alkyl radical, and the newly formed alkyl radical reacts with Selectfluor to generate a fluorinated product and a radical dication species (**4**) that would be responsible for subsequent H-atom abstraction. However, a few experimental findings discount this possibility. First of all, if this outer-sphere mechanism holds true for initiating the reaction,

other known, highly competent outer-sphere single-electron transfer reagents, such as ferrocene, should be able to produce similar results upon reaction with Selectfluor.<sup>29</sup> Running the reaction with ferrocene instead of cuprous iodide (despite the promising color change to dark green, indicating formation of the ferrocenium ion) gave very poor results, yielding only a trace amount of the desired fluorinated product. Tris(bipyridine)ruthenium(II) also proved incompetent in effecting the reaction. Secondly, a controlled potential electrolysis experiment was attempted in the presence of an electrolyte, Selectfluor, and cyclododecane, but was unsuccessful in reducing Selectfluor while producing any detectable fluorinated products. Third of all, in the absence of base (i.e. potassium carbonate), we should be able to detect an initial burst of HF by <sup>19</sup>F NMR at room temperature, but this was not observed. Lastly, a differential pulse voltammogram (DPV) of a 1:1 mixture of copper:bis(imine) ligand reveals an oxidation potential of +0.87 V vs. SCE for the copper(II/I) transition; however, the reported reduction potential of Selectfluor, -0.296 V vs. AgRE,<sup>30</sup> would suggest an unfavorable flow of electrons by an outer-sphere electron transfer mechanism and further aid in the nullification of this type of process. Thus, an inner-sphere mechanism whereby radical dication **4** is formed may be the more likely of the two.

#### 4.9 Inner-sphere SET.

Still, a more convincing argument would be to show an example where the reaction *proceeds* through another inner-sphere electron transfer event. Thus, we examined an initiator that cannot fathomably form radical dication **4** through an "outer-sphere" process accompanied by loss of fluoride: a primary alkyl radical. The formation of ethyl radicals *in situ* is well established upon reaction of triethylborane with oxygen.<sup>31</sup> Applying this chemistry to our system, an ethyl radical could reasonably form **4** and fluoroethane upon interaction with Selectfluor (Scheme 4.5). To our satisfaction, adding a catalytic amount of triethylborane to a solution of Selectfluor and cyclododecane in MeCN, with no measures taken to remove O<sub>2</sub>, resulted in the formation of 1-fluorocyclododecane in 50% yield after 4 h. The involvement of ethyl radicals in initiating the reaction is supported by detection of fluoroethane by <sup>19</sup>F NMR. Furthermore, a few other synthetic methods have been published since our original copper system that effect an analogous fluorination reaction using catalytic amounts of iron,<sup>10</sup> vanadium,<sup>32</sup> and organic-based reagents<sup>33</sup> that conceivably participate in inner-sphere electron transfer chemistry with Selectfluor. (Note that other

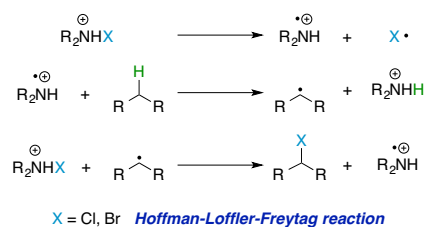
methods have also been published recently using photocatalysts that likely operate under much different initiation mechanisms.<sup>34</sup>)



**Scheme 4.5** Preliminary evidence for triethylborane as an alternative reaction initiator.

Additional efforts were made to probe the role of copper as an initiator by attempting to remove or sequester copper during the course of the reaction and also suggest the reaction does not need copper to proceed beyond initiation (see Chapter 12 for details). Lastly, an experiment probing the potential for asymmetric induction - using a chiral variant of our bis(imine) ligand (derived from *trans* 1,2-cyclohexanediamine)<sup>35</sup> and the Mosher ester of 3-phenylpropanol<sup>36</sup> (as benzylic fluorination of this substrate establishes spectroscopically distinct diastereomers by <sup>19</sup>F NMR)<sup>37</sup> - resulted in a distribution of fluorinated products that was identical to the distribution when an achiral ligand was employed. In a small way, this helps support the notion that fluorine may not be transferred from a copper catalyst. All things considered, the evidence overwhelmingly insinuates that copper(I) is, in fact, an initiator in our system that operates through an inner-sphere electron transfer mechanism with Selectfluor, as opposed to being necessary throughout the catalytic cycle.

As suggested in Scheme 4.4, copper(I) is used to generate what we propose to be the true "catalyst" from Selectfluor – a radical dication (**4**).<sup>38</sup> Conceptually, if this radical dication acts as an H-atom abstractor, an alkyl radical would be generated that could feasibly react with Selectfluor to form the fluorinated product and regenerate the radical dication. This idea is akin to the mechanism established by Corey and co-workers for the Hoffman-Löffler-Freytag reaction (Scheme 4.6).<sup>39</sup> Correspondingly, the next set of experiments discussed focus on probing the involvement of radicals.



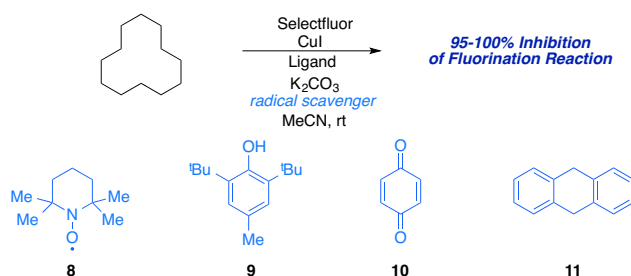
**Scheme 4.6** Analogy to Hoffmann-Löffler-Freytag reaction.

#### 4.10 Involvement of Alkyl Radicals.

The reaction was run in the presence of four radical scavengers to explore the involvement of radical intermediates: 2,2,6,6-tetramethylpiperidine 1-oxyl (TEMPO) **8**, 2,6-di-*tert*-butyl-4-methylphenol (BHT) **9**, *p*-quinone **10**, and dihydroanthracene **11** (Scheme 4.7).<sup>40</sup> Subjecting cyclododecane to normal reaction conditions with an added 1.2 equiv. of each radical scavenger, the formation of fluorocyclododecane was inhibited by 95% in the presence of *p*-quinone, 97% with BHT, and completely in the presence of either TEMPO or dihydroanthracene. One potential criticism of these experiments may be that some of these compounds do not solely act as radical scavengers; rather, some will likely also be fluorinated or oxidized, consuming a significant amount of Selectfluor, and thus inhibiting fluorination through another venue. To elucidate the primary role of these compounds as radical inhibitors, we also found that 1) merely 0.15 equiv. of TEMPO and dihydroanthracene - leaving a fifteen-fold excess of Selectfluor - also resulted in significant reaction inhibition (85% with TEMPO and 70% with dihydroanthracene) without any substantial amount of fluorinated variants of the scavengers detected and 2) if dihydroanthracene is added at any point after fluorinated products start to appear by <sup>19</sup>F NMR, the fluorination reaction stops. These experiments strongly infer the shutting down of a radical pathway. Note that oxygen also quenches the reaction – typical of many radical chain reactions.

Although we have shown the ability to interrupt the proposed radical pathway, these experiments do not necessarily allude to the scavenging of *alkyl* radicals. In fact, the aforementioned compounds and oxygen are likely to inhibit the reaction via cessation of the radical dication. The best way to probe the involvement of alkyl radicals is to run the reaction with substrates that notoriously rearrange to provide more stable radicals or release ring strain, such as those containing a cyclopropyl moiety. The rates of

rearrangement have been studied for several "radical clocks," and under certain circumstances allow the possibility of extrapolating rate information from the reaction. We studied a small family of cyclopropane-based radical clocks, spanning rearrangement rates over a few orders of magnitude (Table 4.2).



**Scheme 4.7** Radical scavengers.

**Table 4.2** Radical clocks.

	<i>Rearrangement</i>	<i>Rearranged Fluorinated Product</i>
 <b>12</b>	$k_r < 2.0 \times 10^5 \text{ s}^{-1}$	 <i>Not observed</i>
 <b>13</b>	$k_r \sim 1.0 \times 10^8 \text{ s}^{-1}$	 <i>Not observed</i>
 <b>14</b>	$k_r = 2.0 \times 10^8 \text{ s}^{-1}$	 <i>Not observed</i>
 <b>15</b>	$k_r = 3.6 \times 10^8 \text{ s}^{-1}$	 <b>16</b> <i>Observed</i>

The first three radical clocks studied – benzylcyclopropane, thujone, and norcarane<sup>41</sup> – showed evidence of fluorinated product mixtures by <sup>19</sup>F NMR, but no detectable amount of the expected "rearranged" fluorinated products following the putative formation of radicals **12**, **13**, and **14**, respectively.<sup>42</sup> However, the rate of fluorination may be significantly faster than their rates of rearrangement, and the latter two clocks have multiple competing sites for H-atom abstraction that would not allow for a rearranged product anyway. Accordingly, we examined another slightly faster clock with one favorable benzylic site for H-atom abstraction under our reaction conditions –

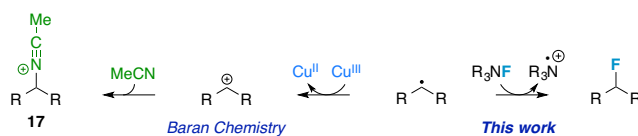


2-phenylbenzylcyclopropane (to form radical **15**).<sup>43</sup> A <sup>19</sup>F NMR analysis revealed that the reaction yielded four fluorinated products in a total yield of 18.2% – one of these signals may correspond to the (*E*)-isomer of rearranged product **16** ( $\delta = -172.53$  ppm, ddd,  $J = 47.4, 24.8, 16.5$  Hz) and another signal also has the characteristics of an "opened" fluorinated clock ( $\delta = -178.69$  ppm, ddd,  $J = 48.5, 39.2, 14.4$  Hz).<sup>44</sup> The two additional signals have slightly more difficult splitting to decipher, but have chemical shifts that reasonably match up with two benzylic fluorinated isomers that contain an intact cyclopropane ring ( $\delta = -179.81$  ppm, m and  $\delta = -185.33$  ppm, m). The identification of these compounds is also supported by a crude GC/MS analysis where four similar fragmentation patterns were found with  $m/z = 226.3$ . The ratio of total rearranged products to intact cyclopropane products is ca. 1:1.09. This rearrangement is strong evidence for a stepwise fluorination mechanistic pathway and for the involvement of short-lived alkyl radicals.

As an aside, the fact that the reported rates of rearrangement for norcarane and 2-phenylbenzylcyclopropane are very similar, yet we found no rearranged norcarane products, is a noteworthy result. As either rearrangement or fluorination of the radical happens *after* the rate-determining step (*vide infra*), this observation indicates that secondary alkyl radicals fluorinate faster than the more delocalized secondary benzylic radicals in this reaction.

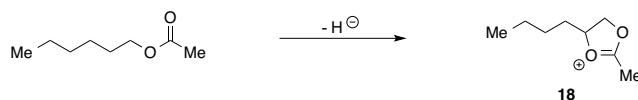
Thus far, these experiments paint a reasonably convincing picture whereby radical dication **4** generates an alkyl radical, which may react homolytically with Selectfluor to yield a fluorinated product and regenerate **4**. One alternative to consider is the role that carbocations may play in the mechanism, as cationic intermediates may also result in the opening of the cyclopropane ring. For example, can an alkyl radical sacrifice another electron to a suitable acceptor and then trap fluoride? There are a number of factors from theoretical and experimental standpoints that militate against this possibility. Most of all, we would be considering secondary cations, whose free existence in solution is at the very least unfavorable, and somewhat debatable.<sup>45</sup> In any case, a secondary cation in MeCN solvent would rapidly collapse to the nitrilium as opposed to trapping fluoride. Nitrilium adducts **17** – rather, acetamides upon aqueous workup – were observed by Baran and co-workers in a copper(II)-Selectfluor based system.<sup>7</sup> However, their postulated mechanism, involving a copper(II) reagent that is subjected to harsher conditions in the presence of Selectfluor, invokes formation of a precedented copper(III) species that is much more likely to be reduced by an alkyl radical than our observed copper(II) species (Scheme 4.8). The fact that nitrilium-

derived products are minimal in our system (aside from *ex post facto* solvolysis) would seem to indicate that cations play a minor role.



**Scheme 4.8** Role of copper(II) in Baran's system versus our proposed fluorination pathway.

What about direct formation of cations through hydride transfer? Take the well-behaved substrate 1-hexyl acetate, which fluorinates predominately in the 5-position, as a model. Hexyl acetate should donate hydride preferentially from the 2-position, as this would form, after anchimeric assistance, a stable cyclic oxonium **18** that could trap fluoride (Scheme 4.9). This product is not observed to any significant extent.



**Scheme 4.9** Cation formed through direct hydride transfer and stabilized as oxonium.

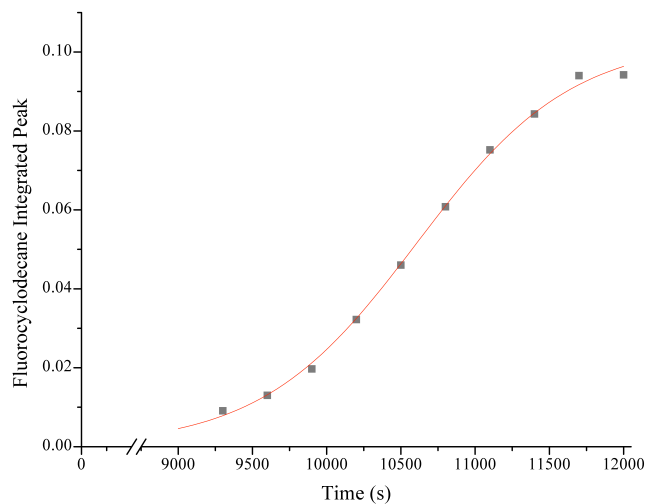
#### 4.11 Induction Period.

A mechanistic study would not be complete without an analysis of reaction kinetics. A preliminary kinetic study to monitor the rate of appearance of the fluorinated product of 3-phenylpropyl acetate by  $^{19}\text{F}$  NMR under standard reaction conditions revealed a significant induction period before the desired 3-fluoro-3-phenylpropyl acetate began to form. Over the course of our studies, we have noted induction periods for this same compound varying anywhere from 20 min to 2.5 h. We also found that the length of this induction period can vary greatly among all substrates; for instance, the induction periods for monitored reactions with cyclodecane or cyclohexane have varied in length on the orders of minutes to hours, just as 3-phenylpropyl acetate has. (A sample plot of the rate of fluorination of cyclodecane is provided below, illustrating the induction period (Figure 4.7).)

To determine whether the substrate itself plays a significant role in the induction period of the reaction, we looked at the consequences of "aging" the catalyst in six reactions set up in parallel. In this

experiment, 3-phenylpropyl acetate was added at six different time intervals ( $t = 0, 15 \text{ min}, 30 \text{ min}, 1 \text{ h}, 2 \text{ h},$  and  $4 \text{ h}$ ) into six different reaction flasks, and an aliquot was taken from each flask at the  $4.5 \text{ h}$  mark. In every instance where the starting material was added at/prior to  $2 \text{ h}$ , the percent yields of the fluorinated products by  $^{19}\text{F}$  NMR relative to an internal standard were virtually identical. However, in the reaction where the starting material was added at  $4 \text{ h}$ , well past any previously observed induction period, the fluorinated product had already appeared after only  $30 \text{ min}$  of stirring, and in half the percent yield of the other reactions. Thus, the induction period does not appear to be substrate dependent.

We noticed shorter induction periods as technique improved, presumably with respect to excluding oxygen from the system. In fact, suspecting the involvement of radical species, we noted that the reaction is greatly hindered in the presence of an  $\text{O}_2$  atmosphere and also found that the induction period is typically shorter using degassed anhydrous MeCN (with  $\text{N}_2$ ) over simply anhydrous MeCN (with no measures taken to remove dissolved oxygen).<sup>46</sup> If oxygen is quenching **4**, then the origin of the induction period is likely attributed to a slower build-up in concentration of **4**, the effective catalyst, *in situ*.<sup>47</sup> Even after rigorous efforts to exclude oxygen, a small concentration was present in each reaction – the induction periods shortened significantly, but never disappeared.



**Figure 4.7** Sample rate of fluorination plot displaying induction period.

#### 4.12 Rate Dependence.

We next sought to determine the overall order of the reaction using the method of initial rates; however, it is very challenging if not impossible to obtain quantitative rate dependencies for this reaction, given its induction period and the limited solubility of several components.

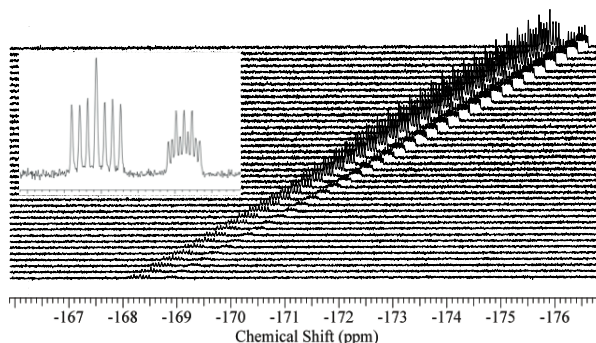
Our model thus far involves three steps: 1) an inner-sphere SET event between Selectfluor and copper(I) generates copper(II) and a radical dication; 2) this radical dication performs H-atom abstraction on an alkane, which generates an ammonium salt and an alkyl radical; and 3) the resultant alkyl radical abstracts a fluorine atom from Selectfluor, which regenerates the radical dication to enter the catalytic cycle. Since the radical dication is believed to be the true catalyst (or chain carrier), and if H-atom abstraction is a rate-limiting step, the rate of product formation (studied by  $^{19}\text{F}$  NMR) would likely have a first-order dependence on both the alkane and the radical dication. Our data show that the rate of product formation is, in fact, strictly first-order with respect to the substrate.

The rate of radical cation formation is dependent on the concentrations of copper(I) and Selectfluor, but the observed induction period seriously complicates the picture. Qualitatively, the length of the induction period is inversely proportional to the concentration of copper and proportional to the concentration of oxygen. We also observed that copper(I) is not entirely expended as the reaction rate accelerates. The total concentration of radical cation, and thus product, is dependent on a first order term in Selectfluor and a reciprocal first order term (reflecting the production of the radical dication). An accurate mathematical analysis of the rate dependencies of Selectfluor and copper(I) is less feasible under these circumstances, but qualitatively they should both be  $< 1$  (depending on the relative contributions of the two terms), which proved to be the case. The proposed rate equation is illustrated below (Eq. 4.1).

$$\begin{aligned} \frac{d[\text{fluoroalkane}]}{d[t]} &= k[\text{alkane}][\text{radical dication}] \\ \frac{d[\text{radical dication}]}{d[t]} &= k_1[\text{Selectfluor}][\text{Cu}] - k_2[\text{Selectfluor}][\text{Cu}][\text{quencher}] \end{aligned} \quad (1)$$

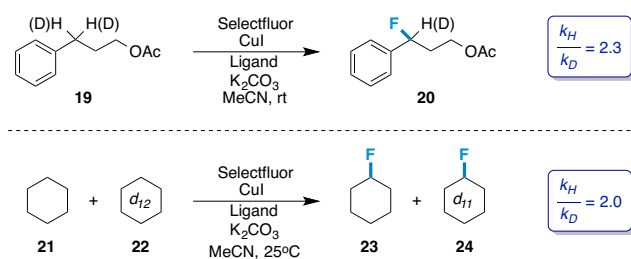
#### 4.13 KIE.

Kinetic isotope effect (KIE) experiments are also capable of providing a wealth of knowledge about a reaction mechanism, from information about the rate-determining step to intimate details about the nature of the transition state.<sup>48</sup> An appropriate benzylic substrate for this experiment would be 3-phenylpropyl acetate, as it yields only one fluorinated product (in the benzylic position) and the corresponding mono/dideutero species **19** is easily accessible.<sup>49</sup> The appearance of fluorinated products **20** was monitored by <sup>19</sup>F NMR in a competitive KIE experiment, as the deuterium-induced <sup>19</sup>F isotopic shift is significant enough to allow independent observation of the geminal protio- and deuterio- products ( $\Delta\delta = 0.59$  ppm; Figure 4.8).<sup>50</sup> This method also obviates misleading results from potential inconsistencies in induction periods.



**Figure 4.8** Competitive KIE <sup>19</sup>F NMR overlay of the formation of 3-fluoro-3-phenylpropyl acetate (*left*, ddd,  $J = 47.4, 30.9, 14.4$  Hz) and 3-fluoro-3-phenylpropyl-3-*d* acetate (*right*, ddt,  $J = 30.9, 14.4, 7.2$  Hz).

Comparison of the initial rates revealed an average kinetic isotope effect of 2.3, which is a superposition of a moderate primary KIE and a secondary effect from the dideuterio species (Scheme 4.10). This diminished putative primary KIE value appears to be consistent with an early or bent transition state if the rate-limiting step is, in fact, H-atom abstraction.<sup>51</sup> A transition state calculation of the radical dication **4** engaging in H-atom abstraction at B3LYP/6-311++G\*\* supports this notion ( $d(\text{C-H}) = 1.17$  Å,  $d(\text{N-H}) = 1.69$  Å). (In order to simplify the calculation, the aliphatic substrate used was propane. Counterions were included in an MeCN dielectric, as otherwise without counterions present the barrier to H-atom transfer diminished to zero).

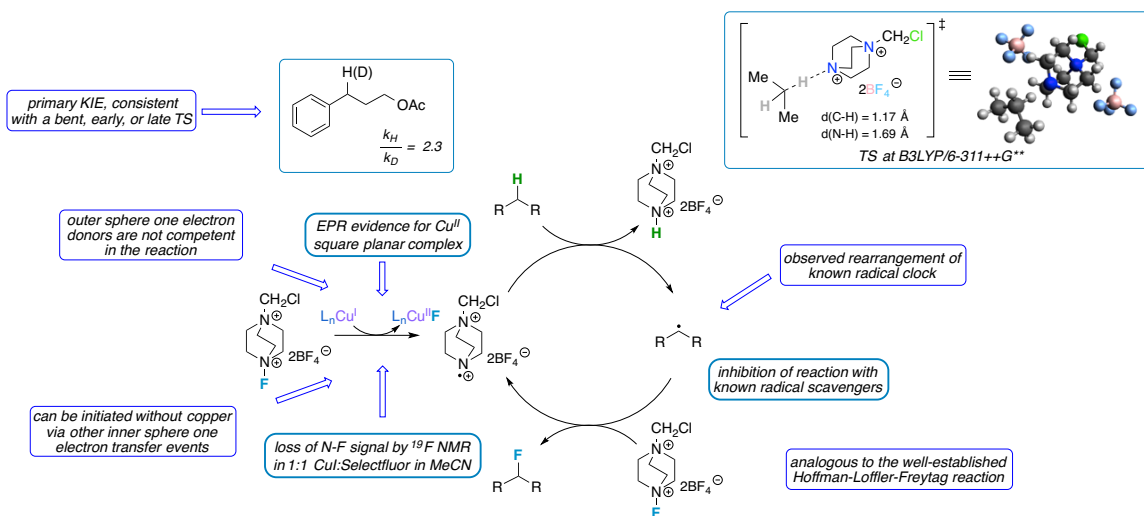


**Scheme 4.10** Observed KIEs.

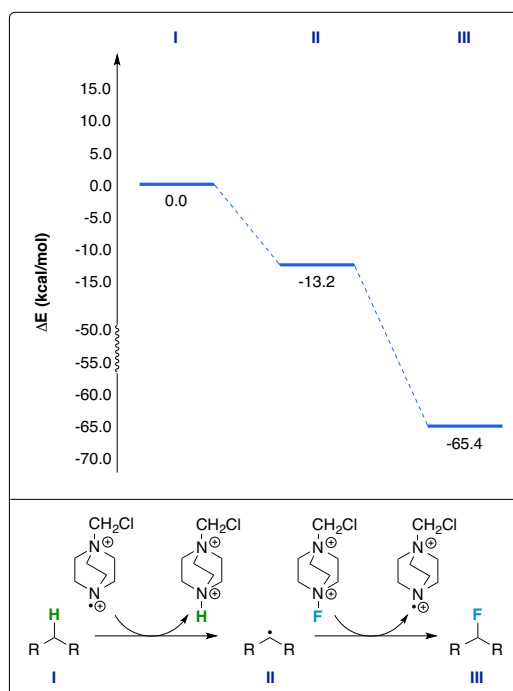
A second competitive KIE experiment was also conducted using a purely aliphatic substrate, *viz.* a 1:1 mixture of cyclohexane (**21**):cyclohexane- $d_{12}$  (**22**) to provide **23** and **24**, which provided a slightly smaller average value of 2.0 (Scheme 4.10). Similar to the 3-phenylpropyl acetate result, there is a moderate primary isotope effect and small secondary effect from the geminal deuterium atom. On the other hand, cyclohexane- $d_{12}$  has four vicinal deuterium atoms that have an inverse secondary effect on the rate that accounts for a notable diminution of the phenomenological KIE value.<sup>48</sup>

#### 4.14 Proposed Mechanism.

Based on experimental observations thus far, we can propose a reasonable mechanism. EPR, UV-vis, <sup>19</sup>F NMR, and several synthetic experiments point to an inner-sphere SET reaction between copper and Selectfluor whereby copper(I) is oxidized to copper(II) accompanying a loss in fluoride from Selectfluor. As determined by the aforementioned KIE experiments and transition state calculation, the resultant radical dication species from the SET reaction **4** is a reasonable actor in H-atom abstraction that occurs through an early transition state and is postulated to be rate-determining. Radical scavenger and radical clock experiments confirm the involvement of alkyl radicals that would be formed along with ammonium salt **5** (observed) upon H-atom abstraction. Furthermore, the notion that fluorine is being transferred directly from Selectfluor is logical, as this would regenerate the radical dication and complete a catalytic cycle/radical chain reaction similar to the Hoffman-Löffler-Freytag reaction (Figure 4.9). We have also provided an energy profile of the reaction intermediates in the catalytic cycle that illustrates a largely exothermic reaction pathway (Figure 4.10).



**Figure 4.9** Mechanistic hypothesis based on experimental results.



**Figure 4.10** Free-energy profile for the monofluorination of cyclodecane through our proposed catalytic cycle.

Overall, this picture appears to be a reasonable mechanism for this system. However, perhaps the most difficult question to answer pertaining to the selectivity of the reaction still remains: *why is*

*monofluorination preferred?* Finally, we turned our attention to a more in-depth theoretical analysis to try to complete the puzzle.

#### 4.15 Role of Valence Bond "Ionicity" in Reaction Selectivity.

One of the most enlightening features regarding the selectivity of this reaction is in the highly reproducible product distribution of 1-hexyl acetate. Fluorination of this substrate predominates in the 5-position, yields of the other monofluorinated isomers largely decrease moving down the chain, and there are trace (if any) monofluorinated products in the 1-position, 6-position, and  $\alpha$ -position to the carbonyl. Compare this to the outcome of a reaction using n-dodecane, where an almost equal distribution of monofluorinated products on the methylene sites is observed. It is clear that the reaction is sensitive to substituent effects that will provide some potent clues.



From one vantage point, as we propose a mechanism involving a radical chain process, we conducted a computational experiment early on that interestingly suggested the observed distribution of n-fluoro-1-hexyl acetate isomers correlates with the calculated relative stabilities of the corresponding hexyl acetate radicals. If the selectivity of the reaction is based solely on radical stability though, which is characteristic of a purely covalent valence bond model for the rate-determining H-atom abstraction transition state,<sup>52</sup> then geminal difluorination should be favored. Also consider the isodesmic analyses of cyclohexane and cyclodecane (Table 4.3) that indicate favorable formations of 1,1-difluorocyclohexane and 1,1-difluorocyclodecane over monofluorination based on thermodynamic considerations; yet, *geminal difluorinated products are not observed experimentally*, except to a minor extent when we apply forcing conditions (but even then, ionization/trapping of acetonitrile is a more competitive process). The desire to analyze this reaction in terms of generating the most stable radical, a bond dissociation energy argument, is thus a misguided instinct.

Instead, if we revisit the substituent effect observed in 1-hexyl acetate as an effect resembling that of a radical reaction with *ionic* character in the transition state, then we can begin to rationalize the selectivity. In this light, the deactivation of  $sp^3$  C-H sites proximal to an electron-withdrawing group toward fluorination agrees nicely with our proposed mechanism. The species we suggest is responsible for H-atom



abstraction, radical dication **4**, is an electron deficient radical that would much prefer interaction with the more electron rich C-H sites (hence the starting material over the newly-formed fluorinated products).

**Table 4.3** Isodesmic reactions.

Isodesmic Reaction		$\Delta E$ (kcal/mol)
	0.8	
	0.2	

All geometry optimizations were performed at B3PW91/6-311+G\*\*(MeCN).

#### 4.16 Polar Effect.

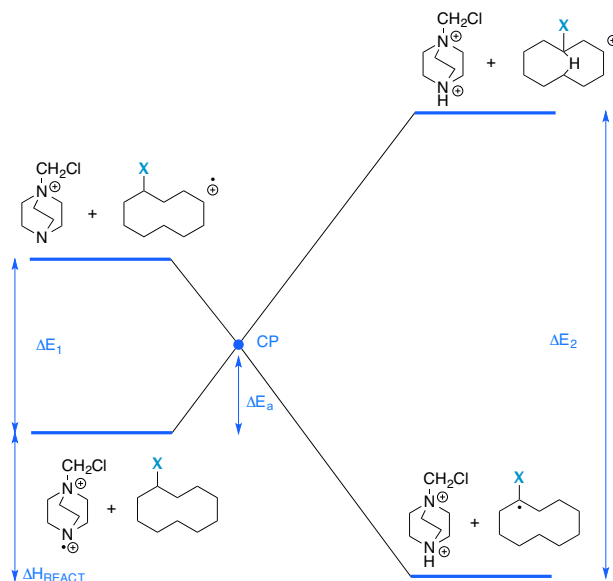
Ionic-like selectivity is not unheard of in radical reactions; there are several accounts of this phenomenon in the literature, first noted by Walling and Mayo<sup>53</sup> in free radical polymerization reactions and since referred to as "the polar effect." By analogy of our reaction to the Hoffman-Löffler-Freytag reaction, reports demonstrating that this polar effect, putatively at play in our fluorination reaction, is similarly observed in free radical chlorination<sup>54</sup> and bromination<sup>55</sup> reactions involving intermolecular H-atom abstraction also by amine radical cations make an extremely convincing argument for our case. These reports also indicate an overwhelming preference for the penultimate  $sp^3$  C-H site on n-alkyl esters, which they attribute to such polar (and also minor steric) effects.

The last piece of the puzzle lies in further examining the effect of ionicity on the H-atom abstraction transition states of the alkane versus the monofluorinated product. Postulating the role of the ionic potential energy surface on dictating selectivity and given the complexity of transition state calculations, we first turned to Donahue's seminal ionic curve crossing theory as a way to study the nature of the transition states – only geometry optimization calculations are necessary by this analysis.<sup>56</sup> This theory indicates that the lowering in energy of the saddle point on the ground state potential energy surface results from an avoided curve crossing with the ionic potential energy surface. Succinctly stated, lower ionic state energies correlate with lower transition state energies. Boundary conditions for an avoided curve crossing are derived from plotting the evolution of the ground and ionic state energies as reactants approach each

other (bear in mind that for radical cation abstraction reactions, the ground state is ionic, as well). In our system,  $\Delta E_1$  is the calculated difference between ground and "ionic" states of the reactants,  $\Delta E_2$  is the same for the products,  $\Delta E_a$  is the activation energy,  $\Delta H_{\text{REACT}}$  is the reaction enthalpy, and CP is the potential energy surface crossing point (Eq. 4.2).

$$\text{CP} = \frac{\Delta E_1(\Delta E_1 + \Delta H_{\text{REACT}})}{\Delta E_1 + \Delta E_2} \quad (2)$$

For cyclodecane, CP is calculated to be 4.6 kcal whereas fluorocyclodecane as a precursor to the more stable 1-fluorocyclodecyl radical, leads to CP = 5.4 kcal (B3PW91/6-311++G\*\*/MeCN), implying a higher activation energy for its formation - consistently accounting for the observed selectivity from this reaction (Figure 4.11).

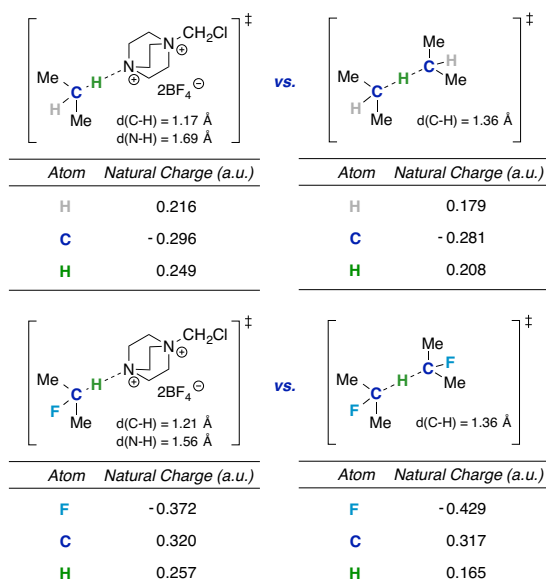


**Figure 4.11** Application of Donahue's theory.

The calculations in Figure 4.11 include optimized geometries of the 1-fluorocyclodecyl and cyclodecyl cations, both of which are found to be hydrido-bridged employing the MeCN continuum. This model is consistent in predicting the observed preference for monofluorination of cyclohexane, as well. For

cyclohexane, CP is calculated to be 3.4 kcal, which is a lower barrier than that of fluorocyclohexane at 5.5 kcal.

Additionally, we calculated the transition states for formation of the isopropyl radical and the 2-fluoro-isopropyl radical, representing pruned substrates for ease of calculation. The result is in excellent agreement with the curve crossing analysis *vide supra*, as the transition state for the formation of the isopropyl radical is earlier and calculated to be 2.2 kcal lower than for the formation of the 2-fluoro-isopropyl radical at B3LYP/6-311++G\*\*. An NBO analysis also confirms that a positive charge has developed in the transition state (relative to an isoenergetic H-atom abstraction) that is accentuated on the hydrogen atom. A strong electron-withdrawing group such as fluorine would destabilize this positive charge, advocating again for H-atom abstraction of an alkane over a fluoroalkane (Figure 4.12).



**Figure 4.12** Transition state calculations and charge distributions alongside isoenergetic scenarios.

Finally, note that all attempts to calculate the transition state whereby Selectfluor fluorinates the isopropyl radical repeatedly collapsed to the products, potentially signifying a barrier-less reaction.

#### 4.17 Conclusion.

Through in-depth analysis of experimental and theoretical data, we are able to propose a mechanistic scenario of the copper-initiated  $sp^3$  C-H fluorination methodology. Spectroscopic evidence and synthetic experiments confirm a radical chain mechanism initiated by an inner-sphere SET from copper(I) to Selectfluor (as opposed to a mechanism where copper plays a role in the catalytic cycle), but this alone does not explain the observed preference for monofluorination. Analyzing the influence of the ionic potential energy surface and applying Donahue's ionic curve crossing theory has allowed us to offer a reasonable explanation for the energetics and selectivity of the reaction.

#### 4.18 References.

---

<sup>1</sup> (a) Eustáquio, A. S.; O'Hagan, D.; Moore, B. S. *J. Nat. Prod.* **2010**, *73*, 378-382. (b) O'Hagan, D.; Schaffrath, C.; Cobb, S. L.; Hamilton, J. T. G.; Murphy, C. D. *Nature* **2002**, *416*, 276.

<sup>2</sup> The chain propagation steps in the radical fluorination of an alkane using  $F_2$  (H-atom abstraction and subsequent fluorination) have an overall change in enthalpy of approximately -103 kcal/mol.

<sup>3</sup> For examples: (a) Differding, E.; Lang, R. W. *Tetrahedron Lett.* **1988**, *29*, 6087-6090. (b) Umemoto, T.; Kawada, K.; Tomita, K. *Tetrahedron Lett.* **1986**, *27*, 4465-4468. (c) Davis, F. A.; Han, W. *Tetrahedron Lett.* **1991**, *32*, 1631-1634. (d) Banks, R. E. *J. Fluorine Chem.* **1998**, *87*, 1-17, and references cited therein.

<sup>4</sup> Kirsch, P. Synthesis of Complex Organofluorine Compounds. In *Modern Fluoroorganic Chemistry: Synthesis, Reactivity, Applications*; Wiley-VCH Verlag GmbH & Co. KGaA: Weinheim, Germany, 2004; pp 203-278, and references cited therein.

<sup>5</sup> For some examples of studies and applications of N-F reagents, particularly Selectfluor, see: (a) Stavber, S.; Zupan, M. *Acta Chim. Slov.* **2005**, *52*, 13-26. (b) Stavber, S. *Molecules*, **2011**, *16*, 6432-6464. (c) Vincent, S. P.; Burkart, M. D.; Tsai, C.-Y.; Zhang, Z.; Wong, C.-H. *J. Org. Chem.* **1999**, *64*, 5264-5279. (d) Oliver, E. W.; Evans, D. H. *J. Electroanal. Chem.* **1999**, *474*, 1-8.

<sup>6</sup> Rueda-Becerril, M.; Sazepin, C. C.; Leung, J. C. T.; Okbinoglu, T.; Kennepohl, P.; Paquin, J.-F.; Sammis, G. M. *J. Am. Chem. Soc.* **2012**, *134*, 4026-4029.

<sup>7</sup> Michaudel, Q.; Thevenet, D.; Baran, P. S. *J. Am. Chem. Soc.* **2012**, *134*, 2547-2550.

<sup>8</sup> Liu, W.; Huang, X.; Cheng, M.-J.; Nielsen, R. J.; Goddard III, W. A.; Groves, J. T. *Science* **2012**, *337*, 1322-1325.

<sup>9</sup> Bloom, S.; Pitts, C. R.; Miller, D.; Haselton, N.; Holl, M. G.; Urheim, E.; Lectka, T. *Angew. Chem. Int. Ed.* **2012**, *51*, 10580-10583.

<sup>10</sup> Bloom, S.; Pitts, C. R.; Woltornist, R.; Griswold, A.; Holl, M. G.; Lectka, T. *Org. Lett.* **2013**, *15*, 1722-1724.

<sup>11</sup> Both *N,N*-bis(benzylidene)ethane-1,2-diamine and *N,N*-bis(2,6-dichloro-benzylidene)ethane-1,2-diamine were synthesized according to literature procedure. See: Liu, H.; Zhang, H.-L.; Wang, S.-J.; Mi, A.-Q.; Jiang, Y.-Z.; Gong, L.-Z. *Tetrahedron: Asymmetry* **2005**, *16*, 2901-2907.

<sup>12</sup> Naumann, D.; Kischkewitz, J. *J. Fluorine Chem.* **1990**, *47*, 283-299.

- 
- <sup>13</sup> Roe, C. D.; Marshall, W. J.; Davidson, F.; Soper, P. D.; Grushin, V. V. *Organometallics* **2000**, *19*, 4575-4582.
- <sup>14</sup> Baxter, A. C.; Cameron, J. H.; McAuley, A.; McLaren, F. M.; Winfield, J. M. *J. Fluorine Chem.* **1977**, *10*, 289-298.
- <sup>15</sup> For syntheses of stabilized copper(I) fluoride complexes, see: (a) Jardine, F. H.; Rule, L.; Vohra, A. G. *J. Chem. Soc. (A)* **1970**, 238-240. (b) Gulliver, D. J.; Levason, W.; Webster, M. *Inorg. Chim. Acta* **1981**, *52*, 153-159.
- <sup>16</sup> Another control experiment was also designed to probe the involvement of a copper(III) fluoride by applying a (2-pyridyl)methylamine ligand to the system, which has been shown to promote two-electron chemistry in copper(I) complexes, but no positive ligand effects were observed. See: Osaka, T.; Karlin, K. D.; Itoh, S. *Inorg. Chem.* **2005**, *44*, 410-415.
- <sup>17</sup> Another control experiment conducted was a thermolysis of *tert*-butyl 2-phenylpropaneperoxoate in the presence of cupric fluoride under Sammis's conditions (ref. 6) that could conceivably illuminate how an alkyl radical reacts with a copper(II) fluoride. No 1-fluoroethylbenzene was observed; however, these conditions do not directly mimic the reaction conditions.
- <sup>18</sup> Note that the reaction does not produce fluorinated products under the reaction conditions with Selectfluor in the absence of copper either; this control reaction was conducted.
- <sup>19</sup> MeCN is a high dielectric solvent and makes for a "lossy" sample, which can be overcome with a flat-cell. See: (a) Hyde, J. S. *Rev. Sci. Instrum.* **1972**, *43*, 629-631. (b) Mett, R. R.; Hyde, J. S. *J. Magn. Reson.* **2003**, *165*, 137-152. (c) Sidabras, J. W.; Mett, R. R.; Hyde, J. S. *J. Magn. Reson.* **2005**, *172*, 333-341. (d) Eaton, S. S.; Eaton, G. R. *Anal. Chem.* **1977**, *49*, 1277-1278.
- <sup>20</sup> Bennati, M.; Murphy, D. M. Electron Paramagnetic Resonance Spectra in the Solid State. In *Electron Paramagnetic Resonance: A Practitioner's Toolkit*; Brustolon, M.; Giamello, E., Eds. John Wiley & Sons, Inc.: Hoboken, NJ, 2009; pp 195-250.
- <sup>21</sup> The natural abundance of <sup>63</sup>Cu:<sup>65</sup>Cu is about 70:30 ( $I = 3/2$  in both instances) and <sup>14</sup>N:<sup>15</sup>N is over 99:1, but <sup>15</sup>N ( $I = 1/2$ ) gives rise to a simpler (doublet vs. triplet for <sup>14</sup>N), more pronounced superhyperfine pattern ( $A(^{15}\text{N})/A(^{14}\text{N}) = 1.4$ ). For some applications, see: (a) Yuan, H.; Collins, M. L. P.; Antholine, W. E. *Biophys. J.* **1999**, *76*, 2223-2229. (b) Lemos, S. S.; Collins, M. L. P.; Eaton, S. S.; Eaton, G. R.; Antholine, W. E. *Biophys. J.* **2000**, *79*, 1085-1094.
- <sup>22</sup> Majahan, M.; Saxena, K. N.; Saxena, C. P. *J. Inorg. Nucl. Chem.* **1981**, *43*, 2148-2152.
- <sup>23</sup> Kasai, P. H.; Whipple, E. B.; Weltner, W. *J. Chem. Phys.* **1966**, *44*, 2581-2591.
- <sup>24</sup> Dawson, J. H.; Dooley, D. M.; Gray, H. B. *Proc. Natl. Acad. Sci. USA* **1978**, *75*, 4078-4081.
- <sup>25</sup> Despite optimal conditions with pure isotopes, no additional information on ligand binding could be obtained via EPR spectroscopy without access to instrumentation capable of ENDOR.
- <sup>26</sup> For instance: Moncol, J.; Mudra, M.; Lönnecke, P.; Hewitt, M.; Valko, M.; Morris, H.; Svorec, J.; Melnik, M.; Mazur, M.; Koman, M. *Inorg. Chim. Acta.* **2007**, *360*, 3213-3225.
- <sup>27</sup> Determined by EDTA titration.
- <sup>28</sup> For some of the original discussion of outer-sphere and inner-sphere electron transfer mechanisms, see: (a) Marcus, R. A. *J. Chem. Phys.* **1956**, *24*, 966-978. (b) Marcus, R. A. *J. Chem. Phys.* **1956**, *24*, 979-989. (c) Taube, H.; Myers, H.; Rich, R. L. *J. Am. Chem. Soc.* **1953**, *75*, 4118-4119.
- <sup>29</sup> Clegg, A. D.; Rees, N. V.; Klymenko, O. V.; Coles, B. A.; Compton, R. G. *J. Electroanal. Chem.* **2005**, *580*, 78-86.
- <sup>30</sup> Oliver, E. W.; Evans, D. H. *J. Electroanal. Chem.* **1999**, *474*, 1-8.

- 
- <sup>31</sup> Ollivier, C.; Renaud, P. *Chem. Rev.* **2001**, *101*, 3415-3434.
- <sup>32</sup> Xia, J-B.; Ma, Y.; Chen, C. *Org. Chem. Front.* **2014**, *1*, 468-472.
- <sup>33</sup> Amaoka, Y.; Nagatomo, M.; Inoue, M. *Org. Lett.* **2013**, *15*, 2160-2163.
- <sup>34</sup> For examples: (a) Bloom, S.; Knippel, J. L.; Lectka, T. *Chem. Sci.* **2014**, *5*, 1175-1178. (b) Kee, C. W.; Chin, K. F.; Wong, M. W.; Tan, C-H. *Chem. Commun.* **2014**, DOI: 10.1039/C4CC01848F. (c) Xia, J-B.; Zhu, C.; Chen, C. *J. Am. Chem. Soc.* **2013**, *135*, 17494-17500.
- <sup>35</sup> For some applications of N,N'-bis(2,6-dichlorobenzylidene)cyclohexane-1,2-diamine in asymmetric catalysis, see: (a) Evans, D. A.; Lectka, T.; Miller, S. J. *Tetrahedron Lett.* **1993**, *34*, 7027-7030. (b) Li, Z.; Conser, K. R.; Jacobsen, E. N. *J. Am. Chem. Soc.* **1993**, *115*, 5326-5327. (c) Wu, J.; Chen, Y.; Panek, J. S. *Org. Lett.* **2010**, *12*, 2112-2115.
- <sup>36</sup> The Mosher ester, 3-phenylpropyl (*S*)-3,3,3-trifluoro-2-methoxy-2-phenylpropanoate, was synthesized via standard DCC coupling chemistry. See: Neises, B.; Steglich, W. *Angew. Chem. Int. Ed.* **1978**, *17*, 522-524.
- <sup>37</sup> (a) Dale, J. A.; Mosher, H. S. *J. Am. Chem. Soc.* **1973**, *95*, 512-519. (b) Gorkom, M. v.; Hall, G. E. *Quart. Rev. Chem. Soc.* **1968**, *22*, 14-29.
- <sup>38</sup> Radical dication **3** was observed by UV-vis spectroscopy in a spectroelectrochemical experiment (procedure described in supporting information) whereby the corresponding amine, 1-(chloromethyl)-1,4-diazabicyclo[2.2.2]octan-1-ium tetrafluoroborate, is oxidized in MeCN via controlled potential electrolysis. Over 1 h, a new absorbance grew in at 273 nm. It is impossible to observe this absorbance under the normal reaction conditions/concentrations.
- <sup>39</sup> For example: Corey, E. J.; Hertler, W. R. *J. Am. Chem. Soc.* **1960**, *82*, 1657-1668.
- <sup>40</sup> Save the experiment with dihydroanthracene, a similar study was done in: Vincent, S. P.; Burkart, M. D.; Tsai, C-Y.; Zhang, Z.; Wong, C-H. *J. Org. Chem.* **1999**, *64*, 5264-5279.
- <sup>41</sup> Benzylcyclopropane and norcarane were synthesized according to literature procedure. See: Simmons, H. E.; Smith, R. D. *J. Am. Chem. Soc.* **1959**, *81*, 4256-4264.
- <sup>42</sup> For respective rates of rearrangement of benzylcyclopropane, thujone, and norcarane, see: (a) Bowry, V. W.; Ingold, K. U. *J. Am. Chem. Soc.* **1991**, *113*, 5699-5707. (b) He, X.; Ortiz de Montellano, P. R. *J. Org. Chem.* **2004**, *69*, 5684-5689. (c) Auclair, K.; Hu, Z.; Little, D. M.; Ortiz de Montellano, P. R.; Groves, J. T. *J. Am. Chem. Soc.* **2002**, *124*, 6020-6027.
- <sup>43</sup> 2-Phenylbenzylcyclopropane was synthesized according to literature procedure. See: Aguila, M. J. B.; Badieli, Y. M.; Warren, T. H. *J. Am. Chem. Soc.* **2013**, *135*, 9399-9406. For rate of rearrangement, see: Hollis, R.; Hughes, L.; Bowry, V. W.; Ingold, K. U. *J. Org. Chem.* **1992**, *57*, 4284-4287.
- <sup>44</sup> Although it is difficult to isolate the low-yielding products under the reaction conditions, we confirmed the presence of the (*E*)-isomer of **16** in the reaction mixture by synthesizing each isomer by other means and comparing <sup>19</sup>F NMR shifts, splitting, and coupling constants.
- <sup>45</sup> Hydrido-bridged secondary cations are considered more stable, viable intermediates in solution. For direct observation of this phenomenon with secondary cycloalkane cations, see: Kirchen, R. P.; Sorensen, T. S. *J. Am. Chem. Soc.* **1979**, *101*, 3240-3243.

- 
- <sup>46</sup> For some examples of oxygen consumption causing induction periods and retarding reaction rates in radical processes, see: (a) Cunningham, M. F.; Geramita, K.; Ma, J. W. *Polymer* **2000**, *41*, 5385-5392. (b) Okubo, M., Ed. *Polymer Particles (Advances in Polymer Science)*; Springer-Verlag Berlin Heidelberg: The Netherlands, 2010.
- <sup>47</sup> For some examples of induction period dependences on catalyst concentration, see: (a) Singh, U. K.; Strieter, E. R.; Blackmond, D. G.; Buchwald, S. L. *J. Am. Chem. Soc.* **2002**, *124*, 14104-14114. (b) Ishiyama, T.; Takagi, J.; Ishida, K.; Miyaura, N.; Anastasi, N. R.; Hartwig, J. F. *J. Am. Chem. Soc.* **2002**, *124*, 390-391. (c) Márta, F.; Boga, E.; Matók, M. *Discuss. Faraday Soc.* **1968**, *46*, 173-183.
- <sup>48</sup> (a) Anslyn, E. V.; Dougherty, D. A. *Modern Physical Organic Chemistry*; University Science Books: Sausalito, CA, 2006. (b) Giagou, T.; Meyer, M. P. *Chem. Eur. J.* **2010**, *16*, 10616-10628.
- <sup>49</sup> Kurita, T.; Hattori, K.; Seki, S.; Mizumoto, T.; Aoki, F.; Yamada, Y.; Ikawa, K.; Maegawa, T.; Monguchi, Y.; Sajiki, H. *Chem. Eur. J.* **2008**, *14*, 664-673.
- <sup>50</sup> For instance, see: Osten, H. J.; Jameson, C. J.; Craig, N. C. *J. Chem. Phys.* **1985**, *83*, 5434-5441.
- <sup>51</sup> (a) More O'Ferrall, R. A. *J. Chem. Soc. B* **1970**, 785-790. (b) Strong, H. L.; Brownawell, M. L.; San Filippo, Jr., J. *J. Am. Chem. Soc.* **1983**, *105*, 6526-6528. (c) Westheimer, F. H. *Chem. Rev.* **1961**, *61*, 265-273.
- <sup>52</sup> Hiberty, P. C.; Megret, C.; Song, L.; Wu, W.; Shaik, S. *J. Am. Chem. Soc.* **2006**, *128*, 2836-2843.
- <sup>53</sup> See: C. Walling. "Free Radicals in Solution." Wiley: New York, N. Y., 1957; pp. 132-140, 365-369, 375-376, 474-491.
- <sup>54</sup> (a) Minisci, F.; Galli, R.; Galli, A.; Bernardi, R. *Tetrahedron Lett.* **1967**, *23*, 2207-2209. (b) Bernardi, R.; Galli, R.; Minisci, F. *J. Chem. Soc. B* **1968**, 324-325.
- <sup>55</sup> Minisci, F.; Galli, R.; Bernardi, R. *Chem. Commun.* **1967**, 903-904.
- <sup>56</sup> Donahue, N. M.; Clarke, J. S.; Anderson, J. G. *J. Phys. Chem. A* **1998**, *102*, 3923-3933.

## Chapter 5

### Triethylborane-initiated Radical Chain Fluorination: A Synthetic Method Derived from Mechanistic Insight

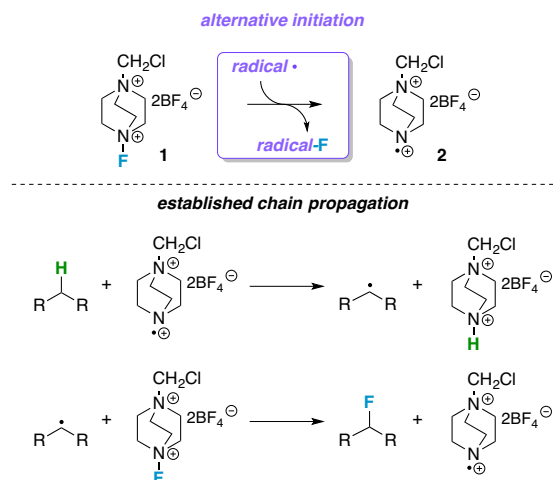
#### 5.1 Introduction.

Though the elucidation of a reaction mechanism can be troublesome, it can provide the insight to develop a new synthetic method that would otherwise remain undiscovered. For example, our laboratory recently investigated the mechanism of the copper(I)/Selectfluor  $sp^3$  C-H fluorination system.<sup>1</sup> We reported a detailed scheme whereby Selectfluor **1** is used to generate a radical dication species **2** (via inner-sphere electron transfer from copper(I), accompanied by loss of fluoride) responsible for H-atom abstraction, generating an alkyl radical. This radical, in turn, reacts homolytically with Selectfluor to yield the desired fluorinated product and to regenerate the radical dication, which propagates the chain. Considering that copper(I) proved to be unnecessary during the H-atom abstraction and fluorination stages of the mechanism and the radical dication chain propagator is generated by a homolytic cleavage of the N-F bond in Selectfluor, we gathered that a catalytic amount of an established "radical initiator" in the presence of Selectfluor and a substrate should also effect C-H fluorination in a similar fashion (Figure 5.1). If true, this mechanistic hypothesis permits us to design a new radical chain fluorination method rationally by choosing an appropriate initiator. Beyond proof-of-concept, alternative manners of initiating the same chain propagation can be envisioned that are advantageous over existing methods.

A number of radical initiators that might be suitable surrogates come to mind, including (but not limited to) halogens, AIBN, organic peroxides, and inorganic peroxides;<sup>2</sup> however, more punishing conditions such as heat or ultraviolet light are typically necessary to generate the radicals, which may also foster issues regarding selectivity. On the other hand, triethylborane famously undergoes a homolytic substitution ( $S_H2$ ) reaction with triplet  $O_2$  at room temperature (or lower) from which an ethyl radical is liberated.<sup>3</sup> Conceivably, this ethyl radical will behave like any other alkyl radical in our system to create the volatile and easily removed fluoroethane upon reaction with Selectfluor and the desired radical dication **2**, thus initiating the fluorination reaction. Furthermore, in an industrial setting,  $BEt_3/O_2$  is the preferred radical initiator wherever possible, as the reagent is atom-economical, low in toxicity, and lends way to



easier work-up.<sup>4</sup> Accordingly, we explored the possibility of effecting this reaction by implementing a catalytic amount of triethylborane, Selectfluor, and a substrate.



**Figure 5.1** Hypothesized alternative initiation to  $sp^3$  C-H fluorination method.

## 5.2 Screening for Reaction Conditions.

We examined a variety of conditions with cyclododecane **3** as a test substrate (Table 5.1) and were satisfied to find that stirring 1.0 equiv. cyclododecane with 20 mol% of triethylborane (administered as a 1.0 M solution in hexanes) and 2.2 equiv. Selectfluor in anhydrous MeCN (with no measures taken to remove dissolved  $O_2$ ) at room temperature under  $N_2$  will produce 1-fluorocyclododecane in 50% yield after 4 h.<sup>5</sup> The same reaction was attempted using *N*-fluorobenzene sulfonimide (NFSI), another precedented source of atomic fluorine by Sammis and coworkers,<sup>6</sup> but no 1-fluorocyclododecane was observed, indicating that Selectfluor is a necessary player for H-atom abstraction. The Inoue<sup>7</sup> and Chen<sup>8</sup> laboratories similarly observed this dependence on Selectfluor in their aliphatic fluorination systems (using NDHPI and  $V_2O_3$ , respectively), as have others using photochemical approaches.<sup>9</sup> Other trialkylborane reagents such as tri-*sec*-butylborane were also screened and afforded no fluorinated products. As triethylborane has also proven effective for the generation of tin and silyl radicals from trialkyltin hydrides and trialkylsilanes, we examined the reaction in the presence of each of these species but found significant depletions in yield. However, evidence of the Si-F bond being formed can be seen in the crude  $^{19}F$  NMR spectra, which may indicate that the silyl radicals were at least formed over the course of each reaction. Lastly, diethylzinc was

employed as an alternative initiator to triethylborane;<sup>10</sup> the reaction provided 1-fluorocyclodecane in a low yield and is also a less desirable alternative, as dialkylzinc species are notably harsher reagents than trialkylboranes.

**Table 5.1.** Screening for reaction initiation conditions.

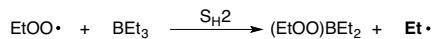
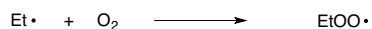
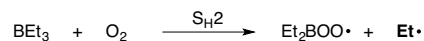
Entry	Initiator	F-source	% Yield
1	—	Selectfluor	0
2	BEt <sub>3</sub>	Selectfluor	50
3	B( <i>sec</i> -butyl) <sub>3</sub>	Selectfluor	0
4	BEt <sub>3</sub>	NFSI	0
5	BEt <sub>3</sub> /Ph <sub>3</sub> SnH	Selectfluor	4
6	BEt <sub>3</sub> /R <sub>3</sub> SiH	Selectfluor	8
7	ZnEt <sub>2</sub>	Selectfluor	4

### 5.3 Preliminary Mechanistic Investigation.

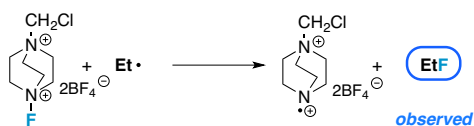
The success of the fluorination reaction appeared to rely intimately on 1) the purity of the triethylborane reagent and 2) the amount of O<sub>2</sub> present. Regarding the latter, product yields diminished using acetonitrile that was subjected to rigorous *freeze-pump-thaw* degasification, and, notably, the reaction completely shut down in the presence of air or an O<sub>2</sub> atmosphere. If the fluorination reaction is, in fact, initiated by release of ethyl radicals via autoxidation of triethylborane (Figure 5.2), this result should be anticipated - O<sub>2</sub> reacts with triethylborane to produce the ethyl radicals responsible for initiation but also inhibits propagation of the H-atom abstraction/fluorination steps. Whereas O<sub>2</sub> played a solely deleterious role as a quencher in the copper(I)/Selectfluor system, the BEt<sub>3</sub>/O<sub>2</sub> radical chemistry assigns it a productive role in reaction initiation. Moreover, the previously observed induction period due to O<sub>2</sub> quenching in the copper system has virtually disappeared. In turn, overall reaction times have satisfyingly decreased. Fortunately, we found that the amount of dissolved O<sub>2</sub> in the solvent at 1 atm ([O<sub>2</sub>] ≈ 8 mM)<sup>11</sup> was enough to produce satisfactory results in a standard organic laboratory setting, obviating the need for a more sophisticated set-up controlling [O<sub>2</sub>]. While we believe product yields and reaction efficiency could benefit

greatly from a detailed kinetic study on the most optimal  $[O_2]$  based on our proposed mechanism, such a study is beyond the scope of this work.

*Established autoxidation initiation/propagation mechanisms*



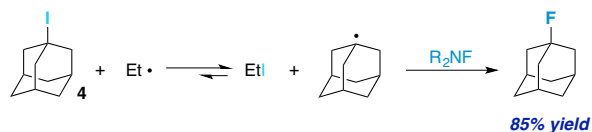
*Putative involvement in radical chain fluorination initiation*



**Figure 5.2** Proposed initiation through formation of ethyl radicals.

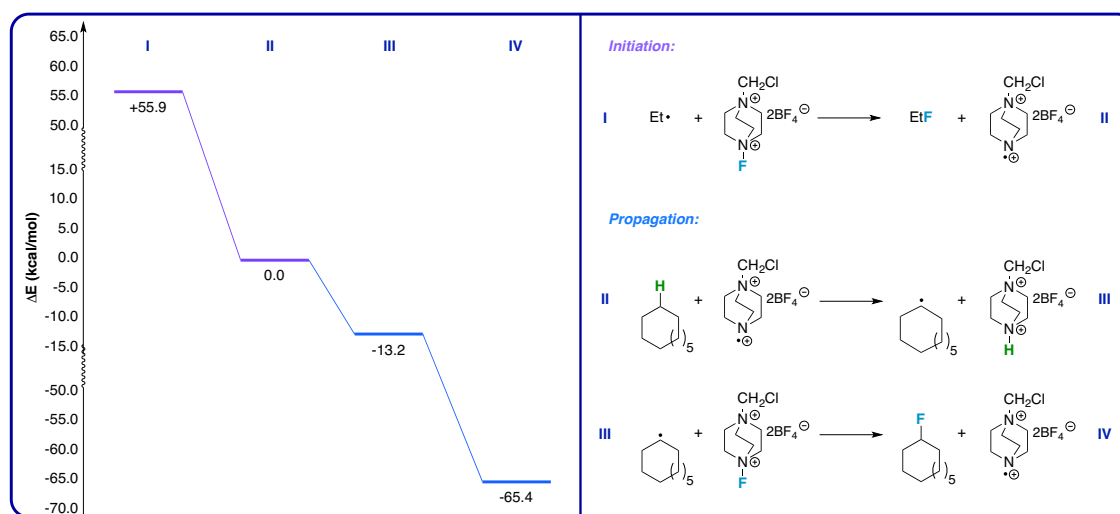
In support of our claim for reaction initiation by ethyl radicals, we found two particularly convincing artifacts that signify autoxidation of triethylborane. First, fluoroethane is unambiguously observed as a triplet of quartets ( $^2J = 47.4$  Hz,  $^3J = 26.8$  Hz) at  $-212.5$  ppm in the crude  $^{19}F$  NMR spectra of all fluorination reactions.<sup>12</sup> Second, monitoring the reaction by  $^{11}B$  NMR in  $CD_3CN$  revealed a rapid formation of  $B(OEt)(Et)_2$  at  $+56$  ppm, a typical byproduct of the autoxidation reaction.<sup>13</sup> Furthermore, considering the  $BEt_3/O_2$  interplay is utilized in iodine-atom abstraction of alkyl iodides,<sup>14</sup> we designed a system to probe the presence of ethyl radicals under our reaction conditions using 1-iodoadamantane **4** and NFSI in place of Selectfluor, as NFSI will act only as a source of atomic fluorine and will not propagate a chain reaction. We found that 1-fluoroadamantane was produced in 85% yield based on triethylborane, feasibly as a result of iodine-atom transfer to the ethyl radical and subsequent fluorination of the adamantyl radical (Scheme 5.1).

*Known triethylborane-mediated iodine atom transfer*



**Scheme 5.1** Ethyl radical probe experiment.

Lastly, the reaction of an ethyl radical with Selectfluor to produce fluoroethane and the radical dication was calculated at B3PW91/6-311++G\*\*(MeCN) to be a substantial 56 kcal/mol downhill,<sup>15</sup> demonstrating a highly favorable reaction (Figure 5.3). Thus, this method very likely operates as a radical chain reaction initiated via a well-precedented autoxidation mechanism and propagated in an analogous manner as the previously reported copper(I)/Selectfluor system.



**Figure 5.3** Energetic landscape of ethyl radical-initiated fluorination of cyclodecane at B3PW91/6-311++G\*\*(MeCN).

#### 5.4 Evaluation of Substrate Scope.

Upon evaluating the scope of the reaction, we found trends in selectivity very similar to those of the copper(I)/Selectfluor method. Aliphatic substrates, *viz.* the cyclic alkanes in Table 5.2 (**5-10**), provided monofluorinated adducts in better yields relative to benzylic substrates (**11-15**). This may suggest a minor steric influence of the phenyl ring in the transition state, characteristic of H-atom abstraction by *N*-radical cations.<sup>16</sup> In almost every instance, *strictly* monofluorination is observed, which we have previously attributed to a manifestation of "the polar effect."<sup>17</sup> A minor amount of difluorination only materialized in the adamantane-based substrates **9** and **10** in the methine positions (as previously noted in other Selectfluor-based systems<sup>18</sup>). On more complex substrates, *i.e.* the androsterone **16** and progesterone **17** derivatives *vide infra*, a good degree of site-selectivity is observed inherent to the parent molecules.

**Table 5.2** Substrate scope.

Entry	Substrate	Product	% Yield
1			47
2			41
3			40
4			50 <sup>a</sup>
5			42 (50) <sup>b</sup>
6			37 (45) <sup>b</sup>
7			30
8			38 <sup>a</sup>
9			36 <sup>a</sup>
10			31 <sup>a</sup>
11			41 <sup>a,c</sup>
12			47
13			28 <sup>a</sup>

Product yields determined by <sup>19</sup>F NMR using 3-chlorobenzotrifluoride as an internal standard unless otherwise stated. <sup>a</sup>Isolated yield. <sup>b</sup>Yield including 1,3-difluorinated products. <sup>c</sup>Isolated as a 1.4:1 *cis:trans* mixture of diastereomers.

Interestingly, fluorination was favored primarily in the C2 and C3 positions on the androsterone derivative<sup>19</sup> and occurred solely in the benzylic position on the progesterone derivative. We noted that the reaction conditions generally endure oxygen-containing substrates well and tend to falter in fluorinating most nitrogen-containing compounds, likely due to *N*-oxidation over desired reactivity.<sup>20</sup> Lastly, note that the product yields are mostly comparable to those reported for the copper(I)/Selectfluor system as well as other sp<sup>3</sup> C-H fluorination methods in the literature to date. Beyond mild reaction conditions and short reaction times, the virtue of using BEt<sub>3</sub> and Selectfluor lies in the minimal contamination from byproducts upon workup/isolation – starting materials can be easily recovered and fluorinated products can be obtained in high purity via chromatography.

## 5.5 Conclusion.

These parallels to the copper(I)/Selectfluor system and the aforementioned experiments maintain the notion that the ethyl radical liberated by BEt<sub>3</sub>/O<sub>2</sub> acts as an initiator in what we previously established to be a radical chain fluorination mechanism propagated by a radical dication. Although the reaction inherently has a two-edged sensitivity for [O<sub>2</sub>], under optimal conditions it provides a mild, cheap, and easy alternative to sp<sup>3</sup> C-H fluorination methods requiring transition metals, ultraviolet light, or "catalysts" that are not commercially available.

## 5.6 References.

---

<sup>1</sup> Pitts, C. R.; Bloom, S.; Woltornist, R.; Auvenshine, D.; Ryzhkov, L. R.; Siegler, M. A.; Lectka, T. *J. Am. Chem. Soc.* **2014**, *136*, 9780-9791.

<sup>2</sup> For a fairly comprehensive introduction to radical initiators, see: Denisov, E. T.; Denisova, T. G.; Pokidova, T. S. *Handbook of Free Radical Initiators*; John Wiley & Sons, Inc.: Hoboken, NJ, 2003.

<sup>3</sup> Ollivier, C.; Renaud, P. *Chem. Rev.* **2001**, *101*, 3415-3434, and references cited therein.

<sup>4</sup> Brotherton, R. J.; Weber, C. J.; Guibert, C. R.; Little, J. L. Boron Compounds. In *Ullman's Encyclopedia in Industrial Chemistry*; Wiley-VCH: 2000.

<sup>5</sup> Regarding optimization of our reaction conditions, we found that heating was unnecessary and promoted ionization over time, which was deleterious to product yields. Colder temperatures (e.g. 10 °C) are viable, but there is an increase in reaction times with no

---

increase in yield. Reactions were monitored at room temperature by TLC and/or  $^{19}\text{F}$  NMR; we found that 4 h is a reliable, generalized time period to accomplish this reaction across all substrates (in some instances, the reaction may be done sooner). Lastly, given solubility issues with Selectfluor in most organic solvents and its unique reactivity in acetonitrile, this is the solvent de choix for aliphatic fluorination.

<sup>6</sup> Rueda, Becerril, M.; Sazepin, C. C.; Leung, J. C. T.; Okbinoglu, T.; Kennepohl, P.; Paquin, J-F.; Sammis, G. M. *J. Am. Chem. Soc.* **2012**, *134*, 4026-4029.

<sup>7</sup> Amaoka, Y.; Nagatomo, M.; Inoue, M. *Org. Lett.* **2013**, *15*, 2160-2163.

<sup>8</sup> Xia, J-B.; Ma, Y.; Chen, C. *Org. Chem. Front.* **2014**, *1*, 468-472.

<sup>9</sup> However, some of these photochemical approaches may be operating very different mechanistically. For some examples: (a) Bloom, S.; Knippel, J. L.; Lectka, T. *Chem. Sci.* **2014**, *5*, 1175-1178. (b) Kee, C. W.; Chin, K. F.; Wong, M. W.; Tan, C-H. *Chem. Commun.* **2014**, *50*, 8211-8214. (c) Xia, J-B.; Zhu, C.; Chen, C. *J. Am. Chem. Soc.* **2013**, *135*, 17494-17500.

<sup>10</sup> (a) Bertrand, M. P.; Feray, L.; Nougier, R.; Perfetti, P. *J. Org. Chem.* **1999**, *64*, 9189-9193. (b) Ryu, I.; Araki, F.; Minakata, S.; Komatsu, M. *Tetrahedron Lett.* **1998**, *39*, 6335-6336.

<sup>11</sup> Achord, J. M.; Hussey, C. L. *Anal. Chem.* **1980**, *52*, 601-602.

<sup>12</sup> Tanuma, T.; Ohnishi, K.; Okamoto, H.; Morikawa, S. *J. Fluorine Chem.* **1996**, *76*, 45-48.

<sup>13</sup> Zhang, Z-C.; Chung, T. C. M. *Macromolecules* **2006**, *39*, 5187-5189.

<sup>14</sup> (a) Byers, J. In *Radicals in Organic Synthesis*; Renaud, P., Sibi, M. P., Eds.; Wiley-VCH: Weinheim, Germany, 2001; Vol. 1, p 72. (b) Curran, D. P.; Chen, M.-H.; Spetzler, E.; Seong, C. M.; Chang, C.-T. *J. Am. Chem. Soc.* **1989**, *111*, 8872-8878.

<sup>15</sup> Gaussian 09, Revision A.1: Frisch, M. J. et al. Gaussian, Inc., Wallingford CT, 2009.

<sup>16</sup> Bernardi, R.; Galli, R.; Minisci, F. *J. Chem. Soc. B* **1968**, 324-325.

<sup>17</sup> For a more extensive discussion on the ionic-like selectivity of recent  $\text{sp}^3$  C-H fluorination methods, see reference 1 and works cited therein.

<sup>18</sup> For example: Xia, J-B.; Ma, Y.; Chen, C. *Org. Chem. Front.* **2014**, *1*, 468-472.

<sup>19</sup> Similar site selectivity was observed on the same substrate by Groves et al. in a different approach to  $\text{sp}^3$  C-H fluorination: Liu, W.; Huang, X.; Cheng, M-J.; Nielsen, R. J.; Goddard III, W. A.; Groves, J. T. *Science* **2012**, *337*, 1322-1325.

<sup>20</sup> See discussion and references in: Bloom, S.; Pitts, C. R.; Woltornist, R.; Griswold, A.; Holl, M. G.; Lectka, T. *Org. Lett.* **2013**, *15*, 1722-1724.

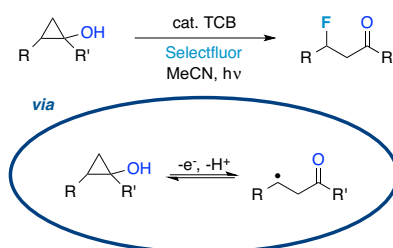
## Chapter 6

### A Site-selective Approach to $\beta$ -Fluorination: Photocatalyzed Ring Opening of Cyclopropanols

#### 6.1 Introduction.

Over the last two years, great strides have been made in the development of direct  $sp^3$  C-H monofluorination methods. However, the methods we<sup>1</sup> and others<sup>2</sup> have reported are often limited to the derivatization of highly symmetric compounds, such as cycloalkanes, or those containing one activated site (e.g. benzylic). In substrates that contain many distinct carbon atoms, the problem of "scattershot" fluorination often arises, leading to undesirable mixtures of products. Expanding upon these pioneering initial discoveries, the most logical next step is to focus on *directing*  $sp^3$  C-F bond formation more effectively, which will allow new and desirable passageways to complex, selectively fluorinated molecules.

Conceptually, two potential routes for a site-selective fluorination event may involve (1) employing a directing group for C-H activation or (2) exploring selective C-C activation. In the latter scenario, the use of C-C activation as a means to guide  $sp^3$  fluorination is, to our knowledge, uncharted territory.<sup>3</sup> To examine this possibility, we envisioned that the one-electron oxidation of highly strained cyclopropanes might serve as an excellent mode for directing fluorination, as long as selective formation of the radical cation that prompts C-C bond scission can be achieved. Furthermore, expanding on new advancements in the field, we gathered that photochemistry could play a pivotal role in the development of this tandem ring-opening/fluorination reaction. Accordingly, we report a site-selective photochemical approach to synthesizing a variety of  $\beta$ -fluorinated carbonyl-containing compounds from cyclopropanols (Scheme 6.1).

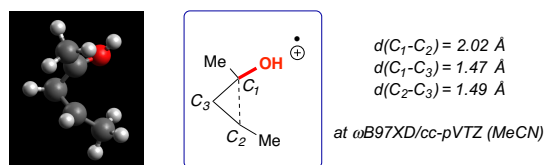


**Scheme 6.1** Site-selective  $\beta$ -fluorination of cyclopropanols.



## 6.2 Reaction Design.

Our laboratory recently unveiled a photocatalyzed procedure for the monofluorination of aliphatic<sup>1d</sup> and benzylic<sup>1g</sup> substrates using the inexpensive photosensitizer 1,2,4,5-tetracyanobenzene (TCB) along with Selectfluor as a source of atomic fluorine.<sup>4</sup> This work was accompanied by a number of alternative sp<sup>3</sup> C-H fluorination methods using photosensitizers such as fluorenone,<sup>2d</sup> acetophenone,<sup>2f</sup> anthraquinone,<sup>2h</sup> and decatungstate ions.<sup>2k</sup> Preliminary mechanistic experiments on our benzylic substrates suggest that the reaction proceeds through the formation of a radical cation intermediate that is rapidly (if not simultaneously) deprotonated to the corresponding benzylic radical (subsequently fluorinated by Selectfluor).<sup>1g</sup> With this in mind, we deduced that a similar photochemical system may be amendable to substituted *cyclopropanol-based* starting materials as 1) these compounds are known to form radical cations under mild irradiation in the presence of photooxidants due to their high-lying HOMOs<sup>5</sup> (release of strain energy being the thermodynamic driving force) and 2) the ring-opening of radicals generated from cyclopropanols followed by halogen atom transfer is a well-documented process to access  $\beta$ -halo ketones (or enones).<sup>6</sup> Consider the calculated structure of the representative radical cation shown in Figure 6.1 - elongation (to 2.02 Å) of the weakest C-C bond between the C(Me)(OH) and C(H)(Me) fragments is observed. Thus, proton loss should regioselectively afford  $\beta$ -carbonyl radicals that can be subsequently fluorinated. Additionally, cyclopropanols represent attractive substrates for fluorination because they are readily accessible (e.g. through the Simmons-Smith<sup>7</sup> and Kulinkovich<sup>8</sup> reactions) and are suitably reactive, a feature borne of their high strain energy.



**Figure 6.1** Calculated structure of trans-1,2-dimethylcyclopropanol radical cation ( $\omega B97XD/cc-pVTZ$ , MeCN dielectric).

Beyond proof-of-concept, note that the target  $\beta$ -fluorinated carbonyl-containing compounds are synthetically and medicinally useful. For example, the incorporation of a single fluorine atom at the  $\beta$ -

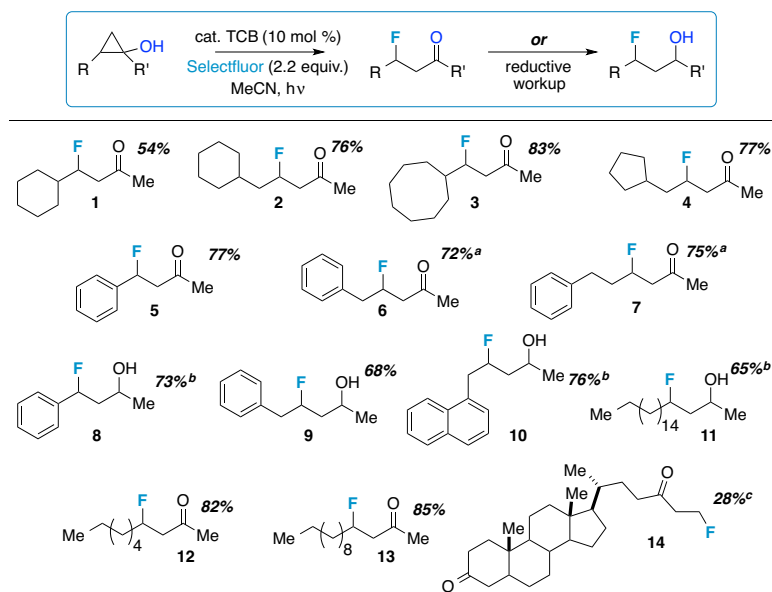
position has been shown to influence the conformational integrity of cyclic amines and amides,<sup>9</sup> prevent mitochondrial  $\beta$ -oxidation of fatty acids,<sup>10</sup> and serve as an adequate positron emission tomography (PET) probe for elucidating a number of biosynthetic and metabolic pathways.<sup>11</sup> Consequently, a number of methods have emerged pertaining to the targeted synthesis of  $\beta$ -fluorinated carbonyl compounds.<sup>1c,1f,1g,12,13</sup> It stands to reason that the development of an alternative, photocatalytic route to  $\beta$ -fluorides from cyclopropanols would be highly desirable, providing a much needed tool in the armamentarium of the medicinal chemist.

### 6.3 Evaluation of Substrate Scope.

To begin our studies, we selected 2-cyclohexyl-1-methylcyclopropanol for screening purposes. Gratifyingly, UV irradiation (302 nm) with catalytic TCB (10 mol %) and Selectfluor (2.2 equiv.) at room temperature provided the  $\beta$ -fluoride **1**, derived from preferential scission of the most substituted C-C bond, in 54% yield. Note that in the absence of TCB, no fluorinated products were observed. In addition, heating of 2-cyclohexyl-1-methylcyclopropanol and Selectfluor in MeCN provided a ~1:1 mixture of  $\alpha$ - and  $\beta$ -fluorinated ketones and other fluorinated products; evidently, selective  $\beta$ -fluorination is only achievable under photocatalytic conditions. Moreover, other N-F reagents were also examined and found to give lower yields. With these findings in mind, we decided to examine a variety of cyclopropanols derived from vinyl and allyl cycloalkanes, as well as aryl compounds. In each instance,  $\beta$ -fluorinated products were obtained in good to moderate yields and with excellent regioselectivity (Table 6.1).

Remarkably, the reaction is highly selective toward C-C bond cleavage/fluorination over direct  $sp^3$  C-H fluorination, despite the previous application of a similar system to aliphatic fluorination.<sup>1d</sup> Compounds **1-4** contain multiple potential fluorination sites on the cyclopentane, cyclohexane, and cyclooctane rings, but only trace ring fluorination products are observed in the <sup>19</sup>F NMR spectra of the crude products, avoiding the aforementioned issue of scattershot fluorination. Additionally, the selective formation of  $\beta$ -fluorinated compounds **5-7** reflects the tendency of cyclopropanols to direct the fluorination event. Benzylic starting compounds of **6** and **7** offer a much tougher test than **5**, but even in the presence of a more activated benzylic site, C-C bond cleavage *is still favored*, providing  $\beta$ -fluorinated products in upwards of 72% yield, although trace amounts of putative benzylic products are observed in some cases.

**Table 6.1** Survey of  $\beta$ -fluoro ketones and  $\gamma$ -fluoro alcohols.



All reactions were performed under an inert atmosphere of N<sub>2</sub> and irradiated with either a UV pen lamp (302 nm) or Rayonet reactor (300 nm) for 16 h. <sup>a</sup> Isolated as the major fluorinated product with minor fluorinated isomers. <sup>b</sup> Crude reaction mixture redissolved in THF and stirred with 5.0 equiv. LiAlH<sub>4</sub> for 2 min. Isolated as a mixture of diastereomers. <sup>c</sup> Substrate for which xanthone was used as the photocatalyst.

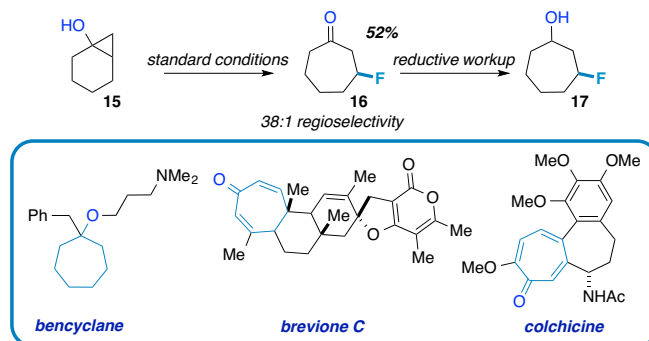
Upon isolation, we observed a propensity for some of the molecules to undergo elimination to form enones when chromatographed on silica or alumina under neutral, acidic, or basic conditions. It is important to note that elimination can be minimized using flash chromatography on acidic Florisil, which allowed us to isolate most  $\beta$ -fluorinated products with typically  $\leq 5\%$  eliminated byproducts. In particularly sensitive cases, we found that a reductive workup using LiAlH<sub>4</sub> allows effective isolation of the corresponding  $\gamma$ -fluoro alcohols after purification by chromatography on silica gel in  $\sim 1:1$  diastereomeric ratio (**8-11**).

In order to probe the selectivity of the reaction in situations where indiscriminate fluorination could be especially problematic, we turned our attention to cyclopropanols possessing linear aliphatic side chains. These compounds could conceivably serve as precursors to  $\beta$ -fluorinated fatty acids, whose proteo-counterparts are frequently metabolized by oxidative cleavage of a  $\beta$ -C-H bond.<sup>14</sup> The selective inclusion of a single fluorine atom at the  $\beta$ -position could therefore prove particularly useful in deterring this pathway.<sup>15</sup> Furthermore, monofluorinated lipids have found considerable use as probes for studying the interaction between drugs or peptides and lipid membranes.<sup>16</sup> Toward this effort, we found that 10-, 14-,

and 20-carbon  $\beta$ -fluorinated ketones **11-13** could be prepared from the respective cyclopropanols. Polyfluorination and direct aliphatic fluorination were not competitive with  $\beta$ -fluorination, as compounds **11-13** were isolated in 65-85% yield.

In another example, ring opening/fluorination of a non-natural steroid, a methylthiocholate derivative,<sup>17</sup> was found to yield the primary fluoride **14** in 28% yield. As expected, yields for primary  $\beta$ -fluorides were often lower than secondary, a possible result of the diminished stability of primary radicals as compared to secondary, but they are still accessible via this method. In an effort to improve upon these results, we found that replacement of TCB by xanthone as the active photocatalyst provided moderate increases in yields. Terminal alkyl fluorides have been shown to be effective reagents for inexpensive nickel or copper-catalyzed cross coupling reactions,<sup>18</sup> but direct syntheses through  $sp^3$  C-C or C-H activation are extremely limited due to preparative difficulty.

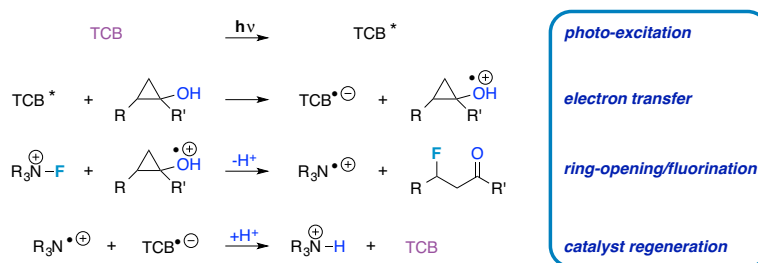
At this point, we considered alternative applications for this method. We explored the use of a tertiary cyclopropanol that could undergo oxidative ring-opening/fluorination to afford a ring-expanded  $\beta$ -fluoride. For a representative example, we selected cyclopropanol **15**, as tandem ring expansion/fluorination should lead to  $\beta$ -fluorocycloheptanone. Cycloheptanone cores are present in pharmaceuticals such as bencyclane, a spasmolytic agent and vasodilator, as well as a vital constituent in many fragrances and polymers (Scheme 6.2).<sup>19</sup> In this instance, photochemical fluorination proceeded smoothly to afford  $\beta$ -fluorocycloheptanone **16** in 52% yield by <sup>19</sup>F NMR regioselectively (38:1). This product was isolated more effectively after purification by chromatography on silica gel as the corresponding  $\gamma$ -fluoro alcohol.



**Scheme 6.2** Tandem ring expansion/ $\beta$ -fluorination to access cycloheptanone or cycloheptanol core.

#### 6.4 Preliminary Mechanistic Investigation.

Finally, a general mechanistic proposal for the reaction is shown in Scheme 6.3. Photoexcitation of TCB is known to yield a powerful oxidant that, in this instance, putatively abstracts an electron from the substrate.<sup>20</sup> The resultant cyclopropanol radical cation prompts C-C bond elongation while relieving ring strain (Figure 6.1); this is accompanied by proton loss to selectively afford a  $\beta$ -carbonyl radical. As precedented, Selectfluor can then act as an atomic source of fluorine to directly fluorinate the radical.<sup>1e,4</sup> Lastly, the Selectfluor radical cation retrieves the electron from the TCB radical anion, as well as the excess proton from the reaction medium, thus generating an ammonium salt by-product and regenerating the TCB catalyst.



**Scheme 6.3** Proposed mechanism for photocatalyzed site-selective  $\beta$ -fluorination.

#### 6.5 Conclusion.

In conclusion, a photocatalyzed protocol for the selective ring-opening/ $\beta$ -fluorination of cyclopropanols is reported. This system is synthetically mild, operationally simple, and can be employed to afford a number of electronically and sterically diverse  $\beta$ -fluorinated carbonyl-containing compounds and  $\gamma$ -fluorinated alcohols. Furthermore, various fluorinated products with medicinal and agrochemical values can be prepared by employing this method. Continued work will seek to elucidate the precise mechanism of the photochemical fluorination system along with the application of this method to the synthesis of complex fluorinated molecules.

## 6.6 References.

- <sup>1</sup> a) S. Bloom, C. R. Pitts, D. Miller, N. Haselton, M. G. Holl, E. Urheim, T. Lectka, *Angew. Chem. Int. Ed.* **2012**, *51*, 10580-10583. b) S. Bloom, C. R. Pitts, R. Woltornist, A. Griswold, M. G. Holl, T. Lectka, *Org. Lett.* **2013**, *15*, 1722-1724. c) S. Bloom, S. A. Sharber, M. G. Holl, J. L. Knippel, T. Lectka, *J. Org. Chem.* **2013**, *78*, 11082-11086. d) S. Bloom, J. L. Knippel, T. Lectka, *Chem. Sci.* **2014**, *5*, 1175-1178. e) C. R. Pitts, S. Bloom, R. Woltornist, D. J. Auvenshine, L. R. Ryzhkov, M. A. Siegler, T. Lectka, *J. Am. Chem. Soc.* **2014**, *136*, 9780-9791. f) C. R. Pitts, B. Ling, R. Woltornist, R. Liu, T. Lectka, *J. Org. Chem.* **2014**, *79*, 8895-8899. g) S. Bloom, M. McCann, T. Lectka, *Org. Lett.* **2014**, *16*, 6338-6341.
- <sup>2</sup> a) W. Liu, X. Huang, M. Cheng, R. J. Nielson, W. A. Goddard III, J. T. Groves, *Science*, **2012**, *337*, 1322. b) W. Liu, J. T. Groves, *Angew. Chem. Int. Ed.* **2013**, *52*, 6024-6027. c) Y. Amaoka, M. Nagamoto, M. Inoue, *Org. Lett.* **2013**, *15*, 2160-2163. d) J-B. Xia, C. Zhu, C. Chen, *J. Am. Chem. Soc.* **2013**, *135*, 17494-17500. e) M-G. Braun, A. Doyle, *J. Am. Chem. Soc.* **2013**, *135*, 12990-12993. f) J-B. Xia, C. Zhu, C. Chen, *Chem. Commun.* **2014**, *50*, 11701-11704. g) J-B. Xia, Y. Ma, C. Chen, *Org. Chem. Front.* **2014**, *1*, 468-472. h) C. W. Kee, K. F. Chin, M. W. Wong, C-H. Tan, *Chem. Commun.* **2014**, *50*, 8211-8214. i) M. Rueda-Becerril, O. Mahe, M. Drouin, M. B. Majewski, J. G. West, M. O. Wolf, G. M. Sammis, J-F. Paquin, *J. Am. Chem. Soc.* **2014**, *136*, 2637-2641. j) D. Cantillo, O. de Frutos, J. A. Rincon, C. Mateos, O. C. Kappe, *J. Org. Chem.*, **2014**, *79*, 8486-8490. k) S. D. Halperin, H. Fan, S. Chang, R. E. Martin, R. Britton, *Angew. Chem. Int. Ed.* **2014**, *53*, 4690-4693.
- <sup>3</sup> For recent reviews on C-C activation, see: a) I. Marek, A. Masarwa, P.-O. Delaye, M. Leibelng, *Angew. Chem. Int. Ed.* **2015**, *54*, 414-429. b) M. A. Drahl, M. Manpadi, L. J. Williams, *Angew. Chem. Int. Ed.* **2013**, *52*, 11222-11251. c) T. F. Schneider, J. Kaschel, D. B. Werz, *Angew. Chem. Int. Ed.* **2014**, *53*, 5504-5523.
- <sup>4</sup> For an initial report on the use of N-F reagents as sources of atomic fluorine, see: M. Rueda-Becerril, C. C. Sazepin, J. C. T. Leung, T. Okbinoglu, P. Kennepohl, J-F. Paquin, G. M. Sammis, *J. Am. Chem. Soc.* **2012**, *134*, 4026-4029.
- <sup>5</sup> a) T. E. Shubina, A. A. Fokin, *WIREs Comput. Mol. Sci.* **2011**, *1*, 661-679. b) H. Rinderhagen, J. Mattay, R. Nussbaum, T. Bally, *Chem. Eur. J.* **2010**, *16*, 7121-7124. c) A. L. Cooksy, H. F. King, W. H. Richardson, *J. Org. Chem.* **2003**, *68*, 9441-9462.
- <sup>6</sup> For examples: a) Y. Ito, S. Fujii, T. Saegusa, *J. Org. Chem.* **1976**, *41*, 2073-2074. b) J. Sun U, J. Lee, J. K. Cha, *Tetrahedron Lett.* **1997**, *38*, 5233-5236. c) S-B. Park, J. K. Cha, *Org. Lett.* **2000**, *2*, 147-149. d) H. B. Lee, M. J. Sung, S. C. Blackstock, J. K. Cha, *J. Am. Chem. Soc.* **2001**, *123*, 11322-11324. e) J. Jiao, L. X. Nguyen, D. R. Patterson, R. A. Flowers II, *Org. Lett.* **2007**, *9*, 1323-1326.
- <sup>7</sup> a) H. E. Simmons, T. L. Cairns, S. A. Vladuchick, C. M. Hoiness, *Org. React.* **1973**, *20*, 1. b) H. E. Simmons, R. D. Smith, *J. Am. Chem. Soc.* **1958**, *80*, 5323-5324.
- <sup>8</sup> a) O. G. Kulinkovich, *Chem. Rev.* **2003**, *103*, 2597-2632. b) O. G. Kulinkovich, S. V. Sviridov, D. A. Vasilevski, *Synthesis*, **1991**, *3*, 234.
- <sup>9</sup> a) N. H. Campbell, D. L. Smith, A. P. Reszka, S. Neidle, D. O'Hagan, *Org. Biomol. Chem.* **2011**, *9*, 1328-1331. b) O. O. Fadeyi, C. W. Lindsley, *Org. Lett.* **2009**, *11*, 943-946. c) S. Venkatraman, A. D. Lebsack, K. Alves, M. F. Gardner, J. James, R. B. Lingham, S. Maniar, R. A. Mumford, Q. Si, N. Stock, K. M. Treonze, B. Wang, J. Zunic, B. Munoz, *Biorg. Med. Chem. Lett.* **2009**, *19*, 5803-5806. d) L. A. Black, D. L. Nersesian, P. Sharma, Y-Y. Ku, Y. L. Bennani, K. C. Marsh, T. R. Miller, T. A. Esbenshade, A. A. Hancock, M. Cowart, *Bioorg. Med. Chem.* **2007**, *17*, 1443-1446.

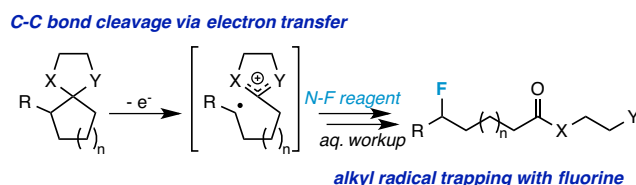
- 
- <sup>10</sup> a) H-J. Bohm, D. Banner, S. Bendels, M. Kansy, B. Kuhn, K. Müller, U. Obst-Sander, M. Stahl, *ChemBioChem*. **2004**, *5*, 637-643.  
b) W. Tang, A. G. Borel, T. Fujimiya, F. S. Abbott, *Chem. Res. Toxicol.* **1995**, *8*, 671-682.
- <sup>11</sup> a) M. M. Alauddin, *Am. J. Nucl. Med. Mol. Imaging* **2012**, *2*, 55-76. b) E. J. Knust, C. Kupfernagel, G. J. Stockiln, *Nucl. Med.* **1979**, *20*, 1170-1173.
- <sup>12</sup> a) K. Shokat, T. Uno, P. G. Schultz, *J. Am. Chem. Soc.* **1994**, *116*, 2261-2270. b.) P. Ryberg, O. Matsson, *J. Am. Chem. Soc.* **2001**, *123*, 2712-2718. c.) Z. Li, Z. Wang, L. Zhu, X. Tan, C. Li, *J. Am. Chem. Soc.* **2014**, *136*, 16439-16443. d.) H. Wang, L-N. Guo, X-H. Duan, *Chem. Commun.* **2014**, *50*, 7382-7384.
- <sup>13</sup> While this manuscript was under review, a similar access to  $\beta$ -fluoroketones was published using a silver-catalyzed ring-opening reaction: H. Zhao, X. Fan, J. Yu, C. Zhu *J. Am. Chem. Soc.* **2015**, *137*, 3490-3493.
- <sup>14</sup> a) L. Zhang, W. Keung, V. Samokvalov, W. Wang, G. D. Lopaschuk, *Biochimica et Biophysica Acta*, **2010**, *1801*, 1-22. b) E. Freneaux, B. Fromenty, A. Berson, G. Labbe, C. Degott, P. Letteron, D. Larrey, D. Pessayre, *J. Pharm. Exp. Ther.* **1990**, *2*, 529-535;  
c) W. Stoffel, A. Caesar, *Hoppe-Seyler's Z. Physiol. Chem.* **1965**, *341*, 76-83.
- <sup>15</sup> a) L. Ojima, *Fluorine in Medicinal Chemistry and Chemical Biology*, Wiley-Blackwell, Chichester, **2009**. b) P. Liu, A. Sharon, C. K. Chu, *J. Fluorine. Chem.* **2008**, *129*, 743-766. c) H. J. Böhm, D. Banner, S. Bendels, M. Kansy, B. Khun, K. Müller, U. Obst-Sander, M. Stahl, *ChemBioChem*. **2004**, *5*, 637-643.
- <sup>16</sup> a) M. P. Krafft, *Adv. Drug. Deliv. Rev.* **2001**, *47*, 209-228. b) D. J. Hirsh, N. Lazaro, L. R. Wright, J. M. Boggs, T. J. McIntosh, J. Schaefer, J. Blazyk, *Biophysical J.* **1998**, *4*, 1858-1868. c) J. F. M. Post, E. E. J. De Ruiter, H. J. C. Brendsen, *FEBS Lett.* **1981**, *132*, 257-260.
- <sup>17</sup> A. Enhsen, W. Kramer, G. Wess, *Drug. Disc. Today*, **1998**, *9*, 409-418.
- <sup>18</sup> a) J. Terao, H. Watabe, N. Kambe, *J. Am. Chem. Soc.* **2005**, *11*, 3656-3657. b) J. Terao, A. Ikumi, H. Kuniyasu, N. Kambe, *J. Am. Chem. Soc.* **2003**, *19*, 5646-564.
- <sup>19</sup> a) H. Yokoe, C. Mitsuhashi, Y. Matsuoka, T. Yoshimura, M. Yoshida, K. Shishido, *J. Am. Chem. Soc.* **2011**, *23*, 8854-857. b) K. Bieroñ, E. Kostk-Trabka, D. Starzyk, A. Goszcz, L. Grodzińska, R. Korbut, *Acta Anglo.* **2005**, *3*, 157-172. c) B. Cornils, P. Lappe, *Ullmann's Encyclopedia of Industrial Chemistry*. Wiley-VCH, Weinheim, **2005**. d) H-G. Schmalz, T. Graening, *Angew. Chem. Int. Ed.* **2004**, *43*, 3230-3256. e) G. Kishore, K. Kishore, *Polymer*, **1995**, *9*, 1903-1910.
- <sup>20</sup> a) M. Christl, M. Braun, O. Deeg, *Org. Biomol. Chem.*, **2013**, *11*, 2811-2817. b) S. Protti, M. Fagnoni, S. Monti, J. Rehaut, O. Poizat, A. Albini, *RSC Adv.* **2012**, *2*, 1897-1904. c) A. A. Fokin, P. A. Gunchenko, S. A. Peleshanko, P. von Ragué Schleyer, P. R. Schreiner, *Eur. J. Org. Chem.* **1999**, 855-860. d) M. Mella, M. Fagnoni, M. Freccero, E. Fasani, A. Albini, *Chem. Soc. Rev.* **1998**, *27*, 81-89. e) M. Mella, M. Freccero, A. Albini, *Tetrahedron*, **1996**, *52*, 5549-5562. f) M. Mella, M. Freccero, A. Albini, *J. Chem. Soc., Chem. Commun.* **1995**, *1*, 41-42.

## Chapter 7

### Unstrained C-C Bond Activation and Directed Fluorination through Photocatalytically-generated Radical Cations

#### 7.1 Introduction.

The foundation of organic chemistry lies on C-C bond formation; it is the spirit of total synthesis, the valued ability to create intricate molecules from simple, cheap starting materials. Alternatively, selective C-C bond *cleavage* (C-C bond activation, in modern parlance) is more seldom discussed, as it is ostensibly a difficult undertaking and its importance is less immediately intuitive to students of organic chemistry. Yet, the field of C-C bond activation<sup>1</sup> is beginning to receive a considerable amount of attention in the contemporary world as chemists are finding unique opportunities to construct complex molecules via C-C fragmentation that are not easily accessible by other means. For instance, our laboratory,<sup>2</sup> among others,<sup>3</sup> has recently become interested in using cyclopropane ring-opening chemistry to, in turn, achieve site-selective fluorination. In any event, it would seem that the application of this chemistry to larger ring systems (5, 6, etc.) that are more readily accessible, but experience relatively little angle strain, is more ambitious. However, the ability to use substituted *cyclopentane* and *cyclohexane* rings (or perhaps larger rings) as synthons en route to more complex molecules would prove handy and fundamentally interesting to synthetic chemists, especially with respect to fluorine chemistry. Given the mechanistic insight provided by our laboratory and others on the fluorination of alkyl radicals vis-à-vis C-H activation<sup>4</sup> (or other approaches<sup>5</sup>), we postulated that site-selective fluorination via unstrained C-C fragmentation might be achieved through the photochemical generation of radical cations with the appropriate substituents.



**Scheme 7.1** Concept for selective C-C fragmentation/C-F formation.

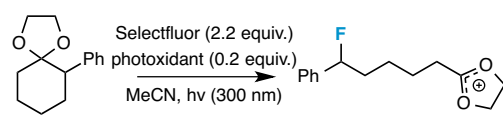


In fact, there is literature precedent (albeit with limited examples) for selective formation of 1,5- and 1,6-radical cations from 5- and 6-membered rings, respectively, employing a putative one-electron photooxidant and proper placement of either acetal or methoxy moieties on the rings.<sup>6</sup> The concept is simple - if the substrate undergoes a one-electron oxidation, the die is cast and the C-C bond productively elongates to form a stable radical (e.g., benzylic or tertiary) and resonance stabilized cation. Both the Albini<sup>7</sup> and Perrott<sup>8</sup> laboratories have shown photosensitized opening of rings followed by hydrogenation. Considering these precedents, we imagined that fluorination of a radical cation should be possible instead, thus allowing highly selective  $sp^3$  C-F formation (Scheme 7.1).

## 7.2 Screening for Reaction Conditions.

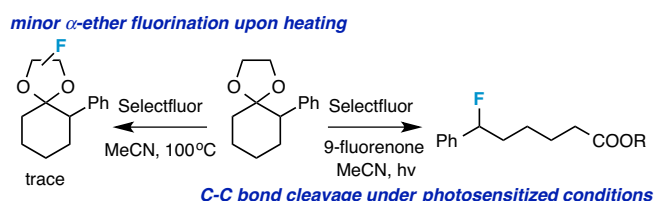
Our initial screen for reaction conditions began with 6-phenyl-1,4-dioxaspiro[4.5]decane. We examined a variety of putative photooxidants in MeCN (300 nm light provided by a Rayonet reactor) in the presence of Selectfluor. Upon assessing the viability of such conventional photooxidants as 1,4-dicyanobenzene,<sup>8</sup> 1,2,4,5-tetracyanobenzene,<sup>9</sup> xanthone,<sup>10</sup> anthraquinone,<sup>11</sup> acetophenone,<sup>12</sup> and 9-fluorenone,<sup>13</sup> we quickly found the most success with 2.2 equiv. of Selectfluor and 0.2 equiv. of 9-fluorenone in producing the desired ring-opened, fluorinated product by  $^{19}\text{F}$  NMR (Table 7.1).

**Table 7.1** Screening for photooxidants.



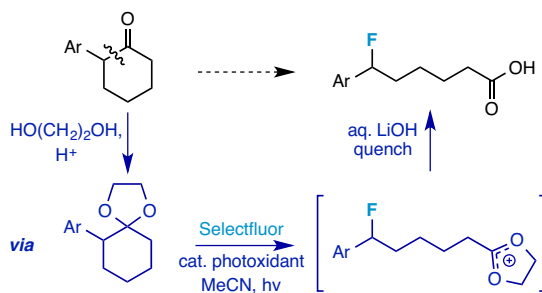
Entry	Photooxidant	$^{19}\text{F}$ NMR Yield (%)
1	--	0
2	1,2,4,5-tetracyanobenzene	30
3	1,4-dicyanobenzene	31
4	acetophenone	28
5	anthraquinone	23
6	xanthone	33
7	<b>9-fluorenone</b>	<b>60</b>

It is important to point out that similar conditions used by our laboratory in the C-C cleavage/fluorination of cyclopropane compounds resulted in a significantly lower yield when applied to this unstrained substrate (Table 7.1, Entry 2). Remarkably, the  $^{19}\text{F}$  NMR yield was *comparable* when a 14-Watt compact fluorescent light bulb was used as the light source instead, denoting the use of visible light as a more accessible alternative. Also note that none of the desired fluorinated product formed in the absence of light or 9-fluorenone, and heating the substrate with Selectfluor in MeCN to 100 °C only resulted in minor  $\alpha$ -fluoro ether products (Scheme 7.2).<sup>14</sup>



**Scheme 7.2** Control reaction.

Upon aqueous workup, we found that the resultant ethylene glycol ester was susceptible to varying degrees of oxidation in the presence of Selectfluor and thus proved difficult to isolate. Consequently, we altered the workup procedure to conduct a mild saponification with 5.0 equiv. aq. LiOH,<sup>15</sup> in order to form the more easily isolable (and more synthetically useful) carboxylic acid **1** in 60% yield (Scheme 7.3).<sup>16</sup>



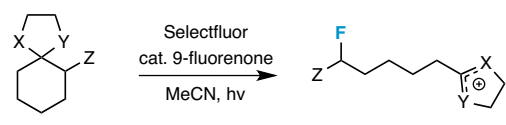
**Scheme 7.3** Standard reaction conditions.

### 7.3 Evaluation of Substrate Scope.

We then surveyed a variety of substrates to probe the stereoelectronic dependence on each substituent (Table 7.2). Interestingly, there was no evidence of C-C fragmentation/fluorination of 1,4-dioxaspiro[4.5]decane or 6-methyl-1,4-dioxaspiro[4.5]decane, suggesting that the aryl group may be essential to stabilize a putative radical cation enough for productive cleavage. In support of this claim, the extent of C-C bond elongation calculated for each radical cation at B3PW91/6-311++G\*\* (MeCN) follows the trend in radical stability ( $2^\circ$  benzylic (2.94 Å)  $\gg$   $2^\circ$  (1.94 Å)  $>$   $1^\circ$  (1.64 Å)).

On the other hand, we found that traditional non-aryl resonance stabilizers in the  $\alpha$ -position (i.e. -OMe, -NPhth, and -COOEt) proved ineffective for C-C bond fragmentation/fluorination. The corresponding *N,O*-acetal also failed to produce any of the desired product under reaction conditions unless the nitrogen atom was substituted with an electron-withdrawing group (e.g. an acetyl group). Still, the acylated *N,O*-acetal performed less well than the *O,O*-acetal. The ideal substituents for C-C fragmentation/fluorination are therefore an aryl moiety and the easily accessible *O,O*-acetal.<sup>17</sup>

**Table 7.2** Screening for substituents.



X	Y	Z	<sup>19</sup> F NMR Yield (%)
O	O	H	0
O	O	Me	0
O	O	Ph	60
O	O	OMe	0
O	O	NPhth	0
O	O	COOEt	0
O	NH	Ph	0
O	NAc	Ph	50

Preceding our evaluation of substrate scope, the success of the aq. LiOH quench for the isolation of the  $\omega$ -fluoro carboxylic acid from 6-phenyl-1,4-dioxaspiro[4.5]decane also prompted a brief investigation of other quenching reagents as means to isolate molecules with diverse functional groups directly from the

same reaction. To our satisfaction, quenching with either 5.0 equiv. aq. LiOMe or 6.0 equiv. LiAlH<sub>4</sub> (with the crude reaction mixture redissolved in anhydrous THF) affords the ω-fluoro ester **2** or ω-fluoro alcohol **3** and in comparable yields (Table 7.3).

**Table 7.3** Substrate scope.

Substrate	Product	Yield (%)	Substrate	Product	Yield (%)
		60 (52) 54 <b>gram scale</b>			51
		59 <sup>a</sup>			28 <sup>c</sup>
		55 <sup>b</sup>			40
		42 (40)			58 <sup>d</sup> (60)
		64 (58)			56 <sup>d</sup>
		70 (68)			30
		54 (49)			28 <sup>e</sup>
		63			
		47			

Unless otherwise stated, all reactions were conducted using Selectfluor (2.2 equiv.) and 9-fluorenone (0.2 equiv.) in anhydrous MeCN under UV-irradiation (300 nm, Rayonet reactor) and inert N<sub>2</sub> atmosphere for 12 h, followed by dilution with H<sub>2</sub>O and 25 min. of stirring with LiOH (5.0 equiv.) to yield carboxylic acids. Isolated yields reported. Yields in parentheses are from reactions using a visible light source (14-Watt CFL). (a) Quenched with LiOMe (5.0 equiv.). (b) Upon reaction completion, reaction mixture was concentrated, redissolved in anhydrous THF, and stirred with LiAlH<sub>4</sub> (6.0 equiv.) for an additional 1 h. (c) Acetal removed during workup/isolation. (d) Isolated as a 1:1 mixture of diastereomers. (e) <sup>19</sup>F NMR yield.

Further assessment of the scope of the reaction revealed several interesting features. For one, conditions are easily amenable to gram scale synthesis with no major sacrifice in yield, as highlighted in Table 7.3, demonstrating the practicality of this method. In terms of electronic effects, the aryl substituent may be adorned with mildly electron donating (**4-5**), mildly electron withdrawing (**6-8**), or electron neutral groups (the extremes typically perform less favorably, e.g. –OMe and –CF<sub>3</sub>); the system is also tolerant of polyaromatic substituents such as naphthalene (**9**). Regarding the chemoselectivity of the reaction, only the

desired C-C bond fragments in the presence of other aliphatic and aryl-substituted acetal functional groups (**10-11**). Even more exceptionally, if other secondary benzylic positions are present on the substrate, barely any direct  $\text{sp}^3$  C-H benzylic fluorination is observed, as C-C fragmentation dominates.<sup>18</sup> This is exemplified in the  $\beta$ -phenyl-substituted  $\alpha$ -tetralone derivative **12**, which, along with the *cis*-decalin derivative **13**, additionally exemplifies the utility of this method in forming complex, substituted rings (e.g. benzene and cyclohexane) from commercially available polycyclic substrates. Lastly, to our knowledge, none of the products we present have been synthesized using direct  $\text{sp}^3$  C-H benzylic fluorination methods to date.

We also provide an example where C-C fragmentation/fluorination can be accomplished from an aryl substituted tertiary alcohol, in lieu of the acetal (**15**). Although the yield is slightly lower in this instance, it exhibits the ability of this method to access  $\omega$ -fluoro- $\omega$ -aryl ketones in addition to  $\omega$ -fluoro- $\omega$ -aryl carboxylic acids, esters, and alcohols. On another note, the acetal functional group can act as an unconventional "leaving group" concomitant with fluorine installation (**16**), if the desired reaction does not call for the opening of a ring.

**Table 7.4** Application to 5-, 7-, 8-, and 12-membered rings.

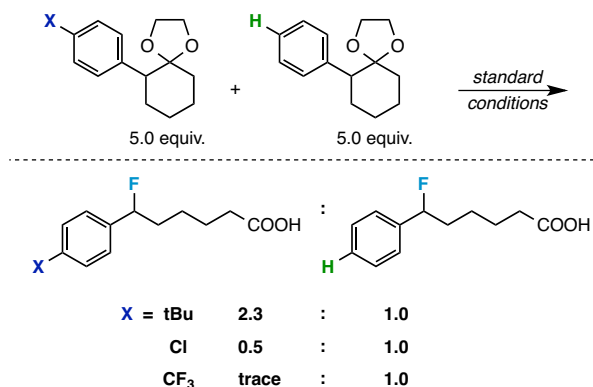
Entry	Substrate	Product	Yield (%)
1			58 (62)
2			57 (53)
3			46
4			30

Isolated yields reported. Yields in parentheses are from reactions using a visible light source (14-Watt CFL).

Although our initial efforts focused primarily on cleavage of ever-pervasive 6-membered rings, we subsequently examined the application to both smaller and larger rings (Table 7.4). Both 5- and 7-membered rings (also common in natural products) underwent ring-opening/fluorination with very similar efficacy to the 6-membered rings *vide supra* (**17** and **18**). Remarkably, the reaction also proved amenable to 8- and 12-membered rings (**19** and **20**). Conceivably, the accessibility of a variety of linear  $\omega$ -fluoro- $\omega$ -aryl carbonyl derivatives as a function of initial ring size using this method may prove particularly useful in the synthesis of fatty acid derivatives (possibly of pharmaceutical or cosmetic interest).<sup>19</sup> In our experience, C-C cleavage/fluorination of the larger rings may also offer a distinct advantage over existing  $sp^3$  C-H benzylic fluorination methods, as these substrates are not prone to competitive  $sp^3$  C-H fluorination along the chain under our specified conditions.

#### 7.4 Preliminary Mechanistic Investigation.

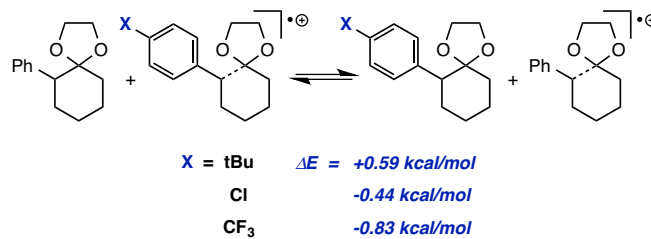
Finally, as a preliminary mechanistic probe, we conducted a few competition experiments to obtain relative rate data, as the effect of structural modifications on reaction rate should provide information about reactive intermediates,<sup>20</sup> *viz.* the postulated radical cation.



**Scheme 7.4** Intermolecular competition experiments.

In support of our hypothesis, the competition experiments (Scheme 7.4) resulted in a larger ratio of the product substituted with a mildly electron donating group (tBu) relative to the electron neutral product, as well as smaller relative ratios of the products substituted with electron withdrawing groups (Cl and CF<sub>3</sub>).

In the most extreme case, hardly any CF<sub>3</sub>-substituted product was formed in the presence of the electron neutral species. This suggests a better ability of electron donating groups to stabilize an electron deficient intermediate.<sup>21</sup> To further investigate the substituent effects on the postulated radical cation, we calculated a series of isodesmic equations.<sup>22</sup> In each case, we consistently found a more stable radical cation with the more electron rich substitution at B3PW91/6-311++G\*\* (Scheme 7.5).<sup>23</sup>



**Scheme 7.5** Isodesmic analyses at B3PW91/6-311++G\*\* (MeCN).

## 7.5 Conclusion.

All in all, this photosensitized C-C bond cleavage reaction provides a mild, unique opportunity for the monofluorination of complex substrates, effortlessly opening classically stable rings in the presence of light. While initial mechanistic studies support the idea of a radical cation intermediate (based on substituent effects and DFT calculations), extensive studies are currently underway to provide a full Hammett analysis, KIE studies, computations, and spectroscopic data.

## 7.6 References.

<sup>1</sup> a) I. Marek, A. Masarwa, P.-O. Delaye, and M. Leibeling, *Angew. Chem. Int. Ed.*, 2015, **54**, 414-429. b) M. A. Drahl, M. Manpadi, and L. J. Williams, *Angew. Chem. Int. Ed.*, 2013, **52**, 11222-11251. c) T. F. Schneider, J. Kaschel, and D. B. Werz, *Angew. Chem. Int. Ed.*, 2014, **53**, 5504-5523.

<sup>2</sup> S. Bloom, D. D. Bume, C. R. Pitts, and T. Lectka, *Chem. Eur. J.*, 2015, **21**, 8060-8063.

<sup>3</sup> a) H. Zhao, X. Fan, J. Yu, and C. Zhu, *J. Am. Chem. Soc.*, 2015, **137**, 3490-3493. b) S. Ren, C. Feng, and T.-P. Loh, *Org. Biomol. Chem.*, 2015, **13**, 5105-5109.

<sup>4</sup> a) S. Bloom, C. R. Pitts, D. Miller, N. Haselton, M. G. Holl, E. Urheim, and T. Lectka, *Angew. Chem. Int. Ed.*, 2012, **51**, 10580-10583. b) S. Bloom, C. R. Pitts, R. Woltrornist, A. Griswold, M. G. Holl, and T. Lectka, *Org. Lett.*, 2013, **15**, 1722-1724. c) S. Bloom, S. A. Sharber, M. G. Holl, J. L. Knippel, and T. Lectka, *J. Org. Chem.*, 2013, **78**, 11082-11086. d) C. R. Pitts, S. Bloom, R.

Woltornist, D. J. Auvenshine, L. R. Ryzhkov, M. A. Siegler, and T. Lectka, *J. Am. Chem. Soc.*, 2014, **136**, 9780-9791. e) C. R. Pitts, B. Ling, R. Woltornist, R. Liu, and T. Lectka, *J. Org. Chem.*, 2014, **79**, 8895-8899. f) W. Liu, X. Huang, M. Cheng, R. J. Nielson, W. A. Goddard III, and J. T. Groves, *Science*, 2012, **337**, 1322. g) W. Liu and J. T. Groves, *Angew. Chem. Int. Ed.*, 2013, **52**, 6024-6027. h) Y. Amaoka, M. Nagamoto, and M. Inoue, *Org. Lett.*, 2013, **15**, 2160-2163. i) M-G. Braun and A. Doyle, *J. Am. Chem. Soc.*, 2013, **135**, 12990-12993. j) J-B. Xia, Y. Ma, and C. Chen, *Org. Chem. Front.*, 2014, **1**, 468-472. k) M. Rueda-Becerril, O. Mahe, M. Drouin, M. B. Majewski, J. G. West, M. O. Wolf, G. M. Sammis, and J-F. Paquin, *J. Am. Chem. Soc.*, 2014, **136**, 2637-2641. l) S. D. Halperin, H. Fan, S. Chang, R. E. Martin, and R. Britton, *Angew. Chem. Int. Ed.*, 2014, **53**, 4690-4693. m) Z. Li, L. Song, and C. Li., *J. Am. Chem. Soc.*, 2013, **135**, 4640-4643.

<sup>5</sup> a) M. Rueda-Becerril, C. C. Sazepin, J. C. T. Leung, T. Okbinoglu, P. Kennepohl, J-F. Paquin, and G. M. Sammis, *J. Am. Chem. Soc.*, 2012, **134**, 4026-4029. b) F. Yin, Z. Wang, Z. Li, and C. Li, *J. Am. Chem. Soc.*, 2012, **134**, 10401-10404. c) Z. Li, Z. Wang, L. Zhu, X. Tan, and C. Li, *J. Am. Chem. Soc.*, 2014, **136**, 16439-16443. d) S. Phae-nok, D. Soorukram, C. Kuhakarn, V. Reutrakul, and M. Pohmakotr, *Eur. J. Org. Chem.*, 2015, **2015**, 2879-2888. e) S. Ventre, F. P. Petronijevic, and D. W. C. MacMillan, *J. Am. Chem. Soc.*, 2015, **137**, 5654-5657. f) N. R. Patel and R. A. Flowers, II, *J. Org. Chem.*, 2015, **80**, 5834-5841.

<sup>6</sup> For a review, see: A. Albini, M. Mella, and M. Freccero, *Tetrahedron*, 1994, **50**, 575-607.

<sup>7</sup> M. Mella, E. Fasani, and A. Albini, *J. Org. Chem.*, 1992, **57**, 3051-3057.

<sup>8</sup> D. R. Arnold, L. J. Lamont, and A. L. Perrott, *Can. J. Chem.*, 1991, **69**, 225-233.

<sup>9</sup> a) S. Bloom, J. L. Knippel, and T. Lectka, *Chem. Sci.*, 2014, **5**, 1175-1178. b) S. Bloom, M. McCann, and T. Lectka, *Org. Lett.*, 2014, **16**, 6338-6341.

<sup>10</sup> D. Cantillo, O. de Frutos, J. A. Rincon, C. Mateos, and O. C. Kappe, *J. Org. Chem.*, 2014, **79**, 8486-8490.

<sup>11</sup> C. W. Kee, K. F. Chin, M. W. Wong, and C-H. Tan, *Chem. Commun.*, 2014, **50**, 8211-8214.

<sup>12</sup> J-B. Xia, C. Zhu, and C. Chen, *Chem. Commun.*, 2014, **50**, 11701-11704.

<sup>13</sup> J-B. Xia, C. Zhu, and C. Chen, *J. Am. Chem. Soc.*, 2013, **135**, 17494-17500.

<sup>14</sup> R. D. Chambers, T. Okazoe, G. Sanford, E. Thomas, and J. Trmccic, *J. Fluorine Chem.*, 2010, **131**, 933-936.

<sup>15</sup> D. A. Evans, *Aldrichimica Acta*, 1982, **15**, 23-32.

<sup>16</sup> In this instance, and with most other products in Table 7.3, the starting material was completely consumed by <sup>1</sup>H NMR analysis of the crude reaction mixture. The remainder of the mass was accounted for in a small amount of unidentified ring-opened byproducts (some detected by <sup>19</sup>F NMR) and/or was lost during workup/isolation.

<sup>17</sup> Note that the penultimate 2-aryl ketone is straightforward to obtain either directly through a variety of Pd-catalyzed  $\alpha$ -arylation reactions or through epoxide opening via arylmagnesium halides, followed by oxidation de choix. See supporting information for details.

<sup>18</sup> This is particularly exceptional given the plethora of direct sp<sup>3</sup> C-H photosensitized benzylic fluorination reactions under similar conditions. See references 9a and 10-13 for some examples. On the other hand, minor direct benzylic fluorination at the primary position of compound **4** (post C-C bond cleavage/fluorination) was observed in the crude <sup>19</sup>F NMR (~10% yield).

<sup>19</sup> A. M. R. Alvarez and M. L. G. Rodríguez, *Grasas Aceites*, 2000, **51**, 74-96.



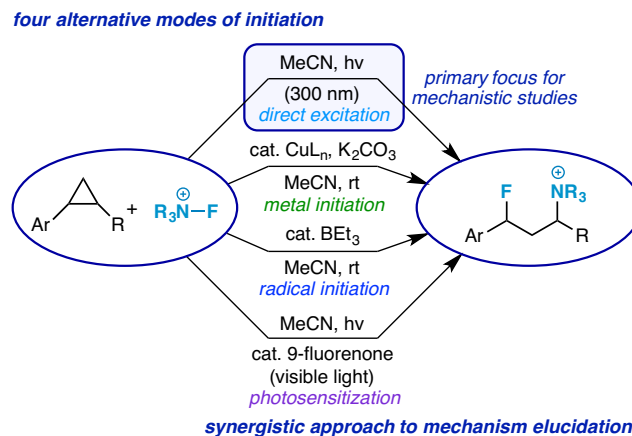
- 
- <sup>20</sup> E. V. Anslyn and D. A. Dougherty, *Modern Physical Organic Chemistry*, University Science Books, Sausalito, CA, 2006.
- <sup>21</sup> L. P. Hammett, *J. Am. Chem. Soc.*, 1937, **59**, 96-103.
- <sup>22</sup> S. E. Wheeler, K. N. Houk, P. v. R. Schleyer, and W. D. Allen, *J. Am. Chem. Soc.*, 2009, **131**, 2547-2560, and cited references therein.
- <sup>23</sup> J. P. Perdew, J. A. Chevary, S. H. Vosko, K. A. Jackson, M. R. Pederson, D. J. Singh, and C. Fiolhais, *Phys. Rev. B*, 1992, **46**, 6671-6687.

## Chapter 8

### Aminofluorination of Cyclopropanes: A Multifold Approach through a Common, Catalytically Generated Intermediate

#### 8.1 Introduction.

Organic methods are rarely *universal* - functional group and reagent compatibility can differ immensely from substrate to substrate, changing "the ideal synthetic method" from case to case. Accordingly, one of the greatest advantages a synthetic chemist can possess is a set of different methods to try - the ability to carry out a transformation under a variety of conditions. Along these lines, we have simultaneously discovered a cluster of reaction conditions – two photochemical, two purely chemical – for the direct, highly regioselective aminofluorination of cyclopropanes. In particular, we report the formation of 1,3-aminofluorinated products from arylcyclopropanes and N-F reagents through 1) direct photoexcitation, 2) metal initiation, 3) radical initiation, and 4) photosensitization (Scheme 8.1). Moreover, the multifold manner in which the reaction can be initiated allows us to propose a "unifying" chain propagation mechanism.



**Scheme 8.1** Four unique aminofluorination tactics provide a synergistic approach to mechanism elucidation.

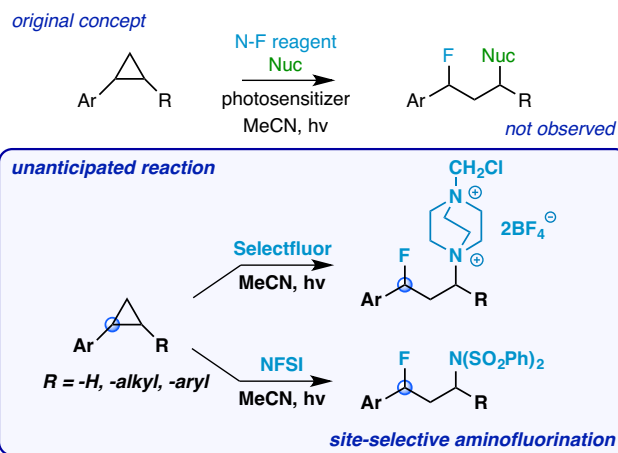
From a synthetic perspective, the development of diverse, direct aminofluorination reactions is of particular interest, given that nitrogen and fluorine represent two of the most important atoms in modern

medicine<sup>1</sup> and agrochemistry.<sup>2</sup> Recently, geminal aminofluorination of diazo compounds<sup>3</sup> and direct 1,2-aminofluorination reactions of alkenes have emerged;<sup>4</sup> however, the 1,3-substitution of cyclopropanes reported herein accesses an entirely unique class of aminofluorinated adducts to serve as synthetic building blocks. From a mechanistic viewpoint, transition metal-promoted  $sp^3$  C-H fluorination<sup>5</sup> and decarboxylative fluorination<sup>6</sup> methods have been studied in depth. Yet, *photochemical fluorination* tactics, despite their synthetic utility, are only ephemerally understood. Though discrete among existing fluorination reactions, the aminofluorination mechanism reported herein confirms the involvement of radical ions through direct spectroscopic observation, but also demonstrates that photochemical fluorination methods are more intricate than previously proposed in the literature. It is our hope that this study will promote further mechanistic investigation in the field to usher in new "photochemical fluorination" reaction development, optimization, and application.

## 8.2 Reaction Discovery.

Our aim was to merge photosensitized "three-electron" nucleophilic substitution reactions on arylcyclopropane compounds<sup>7</sup> with our longstanding interest in the fluorination of catalytically generated  $sp^3$ -carbon radicals.<sup>8,9</sup> Accordingly, we screened several combinations of photosensitizers, nucleophiles, and N-F reagents with 1,2-diphenylcyclopropane under irradiation in MeCN. The *same* signals were observed in the crude <sup>19</sup>F NMR spectra in nearly all instances – except with respect to the use of Selectfluor versus *N*-fluorobenzenesulfonimide (NFSI). Control reactions revealed that although irradiation proved essential, both the putative photosensitizers and external nucleophiles were unnecessary for product formation. Upon closer inspection, we determined that the irradiation of 1,2-diphenylcyclopropane in the presence of Selectfluor or NFSI in MeCN at 300 nm produces the ring-opened aminofluorinated adducts shown in Scheme 8.2 regioselectively.

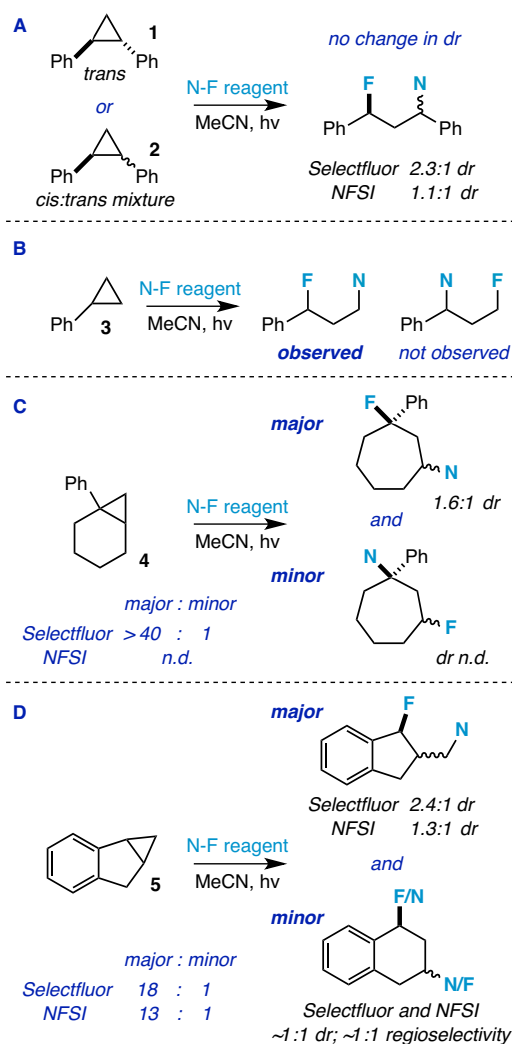
We sought to understand the mechanism of this unusual aminofluorination reaction and, to our surprise, discovered three alternative modes of initiation along the way - using copper(I) salts, triethylborane, or a visible light photosensitizer. What is more, our data suggest that all four methods generate a common intermediate - a Selectfluor-derived radical dication (previously postulated by our laboratory)<sup>5</sup> - allowing us a synergistic approach to mechanism elucidation.



**Scheme 8.2** Discovered aminofluorination reaction.

### 8.3 Product Distribution Studies.

Initial mechanistic study involved probing the selectivity of the reaction with both Selectfluor and NFSI on a variety of substrate types (primarily accessed by a modified Simmons-Smith cyclopropanation).<sup>10</sup> Depending on the nature of the substrate, the resultant regio- and diastereoselectivity of a reaction can provide some valuable insight. For example, one may be able to ascertain whether functionalization occurs in a stepwise or concerted manner, obtain information about steric/electronic influence, and also monitor trends in the stabilities of putative intermediates.<sup>11</sup> Following up on our initial investigation of 1,2-diphenylcyclopropane, we studied the effect of the starting geometry on diastereoselectivity (as this reaction affords two spectroscopically distinct diastereomers by <sup>19</sup>F NMR). Although Selectfluor (2.3:1) and NFSI (1.1:1) provided products in slightly different diastereomeric ratios, an identical result is obtained when either pure *trans*-1,2-diphenylcyclopropane **1** or a *cis:trans* mixture **2** is employed (Scheme 8.3, A). This result, in tandem with the overall low diastereomeric ratios, suggests a stepwise mechanism over a concerted one; however, this alone may be insufficient evidence. The stereochemical integrity of the substrate is potentially compromised by photochemical isomerization (via formation of a biradical intermediate).<sup>12</sup> With this in mind, could the N-F reagent be fluorinating the biradical?



**Scheme 8.3** Diastereoselectivity and regioselectivity probes.

The notion of a radical fluorination followed by radical combination (to form the C-N bond) of a biradical intermediate prompted an investigation of a substrate that is not susceptible to isomerization – phenylcyclopropane **3** (Scheme 8.3, B). In all likelihood, if the biradical were fluorinated in this fashion, then the major product (or at least some product) would be the primary fluoride, as opposed to the benzylic fluoride, following conventional trends in radical reactivity. Yet, the primary fluoride was not observed under any circumstance. Thus, fluorination appears to occur at the most substituted/resonance-stabilized position. To investigate this claim further, the regioselectivity of the reactions with 1-phenylbicyclo[4.1.0]heptane **4** displays an overwhelming preference for fluorination in the tertiary benzylic position (Scheme 8.3, C). Note that aminofunctionalization also occurs in the more substituted

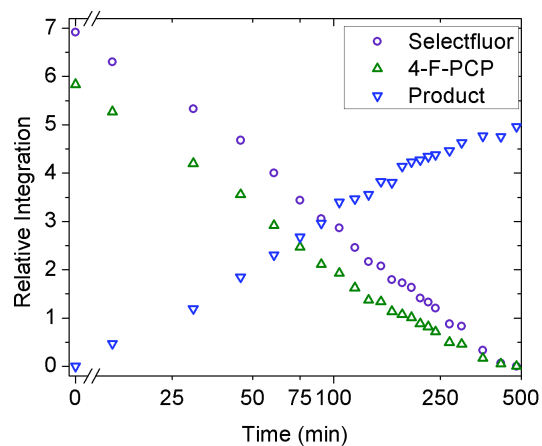
position, affording only the ring-expanded products shown in low diastereomeric ratios (e.g. 1.6:1). These observations argue against the aforementioned biradical fluorination/combination pathway. On the other hand, they may be consistent with the ring opening of a radical cation intermediate (see below).<sup>13</sup>

A seemingly anomalous result surfaced when we employed the rigid arylcyclopropane **5** derived from indene (Scheme 8.3, D). Consistent with previous substrates, fluorination occurred most favorably in the secondary benzylic position of the major product, and low diastereomeric ratios were obtained. Conversely, instead of favoring ring-expansion to form the tetralin derivative, the cyclopropane ring opened to provide the primary aminofunctionalized adduct. Such regioselectivity may be explained by involvement of a radical cation intermediate. In fact, this less-substituted ring-opening behavior has been previously observed from the indene-derived cyclopropane radical cation; literature precedent suggests that the ring-opening step of this particular intermediate may be largely influenced by orbital overlap with the  $\pi$ -system (consistent with our observed regioselectivity).<sup>14,15</sup> Notably, the authors segregate the behavior of this compound from the "less rigid" arylcyclopropane radical cations that are often functionalized in the "more substituted" positions (consistent with all selectivity observed in Scheme 8.3).

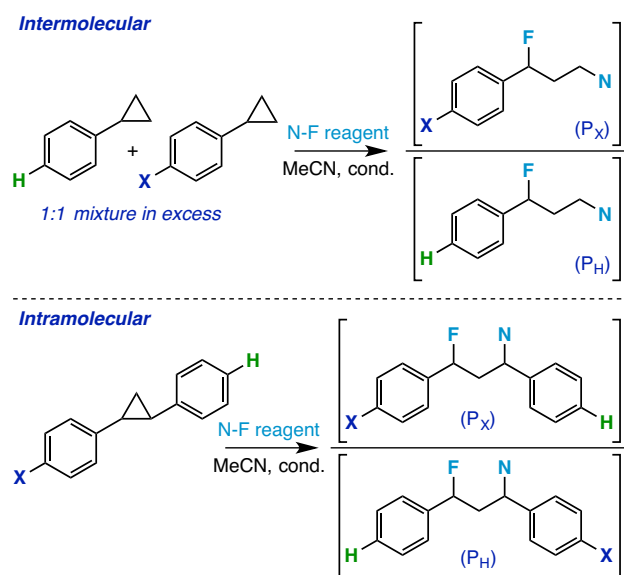
In summation, for both Selectfluor and NFSI, these initial product distribution studies 1) hint at a stepwise mechanism, 2) reveal a preference for fluorination in the most substituted/resonance-stabilized position in all major products, and 3) prompt a search for evidence of arylcyclopropane radical cation intermediates.

#### **8.4 Linear Free Energy Relationships.**

After these selectivity studies, a preliminary kinetic analysis was conducted. We monitored a reaction by <sup>1</sup>H and <sup>19</sup>F NMR and observed a kinetic profile characterized by a concomitant decrease of 4-fluorophenylcyclopropane and Selectfluor (Figure 8.1). Both display an apparent first-order decay, but note that the concept of "reaction order" becomes less straightforward in photochemical systems where the rate of light absorption may be a controlling factor.<sup>16</sup> Without knowing much about the mechanism at this juncture, we believed competition experiments would provide more useful information. Turning to linear free energy relationships, we uncovered additional support for radical cation intermediates.



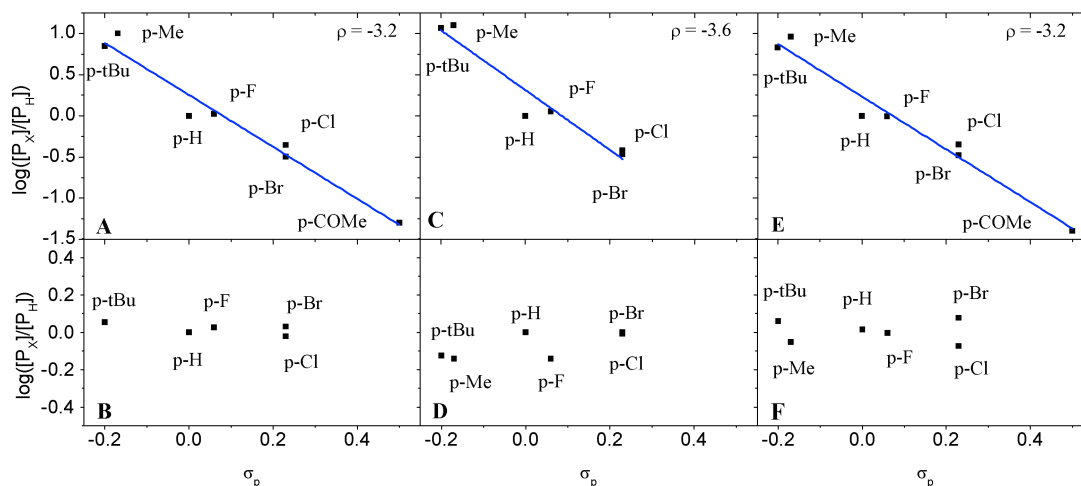
**Figure 8.1** Kinetic profile of 4-fluorophenyl cyclopropane, Selectfluor, and aminofluorination product.



**Scheme 8.4** Hammett plot competition experiments.

The study of *para*- and *meta*-substituent effects on relative reaction rates can reveal potent information regarding charge development over the course of the rate-determining step.<sup>17</sup> As phenylcyclopropane and 1,2-diphenylcyclopropane provide rich opportunities for Hammett analyses, we prepared a variety of substituted phenyl- and 1,2-diphenylcyclopropanes. Analysis of the substituted 1,2-diphenylcyclopropanes was straightforward as a series of intramolecular comparisons (Scheme 8.4). Alternatively, the relative rates of reactions of substituted phenylcyclopropanes were obtained by

assessment of relative product distributions in intermolecular competition experiments, whereby both substrates were run in the same reaction vessel in excess of the N-F reagents ( $[P_X]/[P_H]$ ).



**Figure 8.2** Intermolecular (top row) and intramolecular (bottom row) Hammett plots. Conditions: **A, B** = Selectfluor and 300 nm irradiation, **C, D** = NFSI and 300 nm irradiation, **E, F** = Selectfluor and catalytic  $BEt_3$ .

In the instance of *para*-substituted phenylcyclopropanes, fairly large, negative  $\rho$  values were measured for both Selectfluor (-3.2) and NFSI (-3.6) with good correlation using Hammett  $\sigma_p$  values (Figure 8.2, **A** and **C**).<sup>18</sup> Additionally, *meta*-substituent plots provided  $\rho$  values of -4.2 and -4.6, respectively (see Supporting Information). This denotes 1) a buildup of a positive charge during the rate-determining step and 2) reaction sensitivity to both resonance and inductive effects. Although  $\rho$  values for formal cationic intermediates are typically greater in magnitude,<sup>19</sup> these values could suggest the involvement of arylcyclopropane radical cation intermediates.<sup>20</sup>

For another perspective, we examined the results of intramolecular competition experiments with *para*-substituted 1,2-diphenylcyclopropanes. The structures of an array of arylcyclopropane radical cations have been studied extensively both computationally<sup>21</sup> and spectroscopically;<sup>22,26</sup> although some arylcyclopropanes exhibit closed radical cation geometries, diarylcyclopropanes have been determined to be *open*.<sup>28</sup> Our idea was that substituted diarylcyclopropanes, with the possibility of open geometries, could display divergent behavior in a Hammett plot. In fact, whereas the intermolecular competitions



showed good correlation, these intramolecular competitions provided little to no correlation with Hammett  $\sigma_p$  or  $\sigma^+$  values (Figure 8.2, **B** and **D**).<sup>23</sup>

This largely diminished substituent effect in the intramolecular competitions now opens up possible interpretations of either rate-determining oxidation or ring opening. The former scenario seems more likely *prima facie*, but equilibrium isotope effect (EIE) calculations on arylcyclopropane oxidation suggest upper bounds for kinetic isotope effects (KIE's) that are well below the observed KIE's in Table 8.3 (1.05 for phenylcyclopropane and 1.18 for 1,2-diphenylcyclopropane at wB97XD/6-311++G\*\* [MeCN]). Therefore, oxidation is unlikely rate-determining; on the other hand, additional KIE calculations (below) suggest that rate-determining ring opening of the radical cation intermediate is plausible. In this light, there is evidently minimal impact of the substituents on the ring opening transition states of the two competing sites, each of which is part radical and part cation being attacked by a weak solvent nucleophile.

Together, the results of the Hammett plots begin to build a strong case for arylcyclopropane radical cation intermediates, leading to another important question: how are these radical ions being generated?

### 8.5 On Photoinduced Electron Transfer.

Arylcyclopropane radical cation intermediates have been accessed and studied by electron transfer quenching of the excited states of various singlet or triplet acceptors (e.g. 1,4-dicyanonaphthalene,<sup>13</sup> 1-cyanonaphthalene,<sup>24</sup> 1,4-dicyanobenzene,<sup>25</sup> 1,2,4,5-tetra-cyanobenzene,<sup>26</sup> 9-cyanophenanthrene,<sup>27</sup> chloranil,<sup>28</sup> and 3,3',4,4'-benzophenonetetracarboxylic anhydride<sup>26</sup>).<sup>29</sup> The formation of radical ion pairs between arylcyclopropanes and these photosensitizers by photoinduced electron transfer (PET) is typically guided by the excited state of the electron acceptor, which makes this aminofluorination reaction unique. In a reaction with Selectfluor, the arylcyclopropane is the only chromophore present using 300 nm irradiation.<sup>30</sup> Thus, if a radical ion pair is being formed from PET, the *excited* arylcyclopropane, as opposed to the ground state, must be acting as the electron donor.

The energetics of PET reactions can be studied using the Rehm-Weller relationship (Table 8.1).<sup>31</sup> The free energy of electron transfer ( $\Delta G^0_{ET}$ ) is estimated from consideration of both donor and acceptor one-electron redox potentials ( $E^0_{(D+/D)}$  and  $E^0_{(A/A-)}$ ), the excited state energy of the molecule of interest ( $E^*_{(0,0)}$ ), and a solvent-dependent work function ( $w$ ) accounting for ion pairing.<sup>32</sup> Assessing the excited states of

both phenyl- and 1,2-diphenylcyclopropane in a reaction with Selectfluor, we calculate a thermodynamic preference for electron transfer quenching to form the radical ion pair (-35 and -13 kcal/mol, respectively). Using NFSI, we calculate favorable radical ion formation with phenylcyclopropane at -18 kcal/mol and a small barrier with 1,2-diphenylcyclopropane at +3.7 kcal/mol.

**Table 8.1** Rehm-Weller estimation of PET free energies.<sup>33</sup>

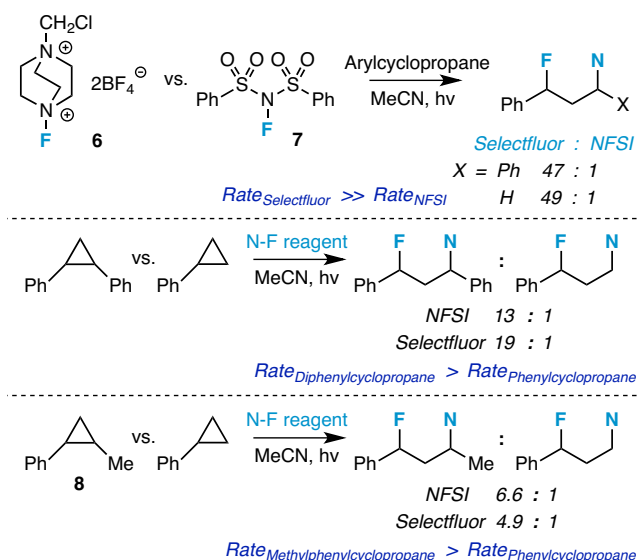
$$\Delta G_{ET}^0 = E_{(D+/D)}^0 - E_{(A/A-)}^0 - E_{0,0} + w^a$$

Donor	Acceptor	$E_{(D+/D)}^0$	$E_{(A/A-)}^0$	$E_{0,0}$	$\Delta G_{ET}^0$
1,2-diphenylcyclopropane*	Selectfluor	1.62 <sup>b</sup>	-0.04 <sup>d</sup>	2.3 <sup>f</sup>	-13
1,2-diphenylcyclopropane*	NFSI	1.62 <sup>b</sup>	-0.78 <sup>d</sup>	2.3 <sup>f</sup>	+3.7
1,2-diphenylcyclopropane	9-fluorenone*	1.62 <sup>b</sup>	-1.29 <sup>e</sup>	2.4 <sup>g</sup>	+13
1,2-diphenylcyclopropane*	9-fluorenone	1.62 <sup>b</sup>	-1.29 <sup>e</sup>	2.3 <sup>f</sup>	+15
phenylcyclopropane*	Selectfluor	1.87 <sup>c</sup>	-0.04 <sup>d</sup>	3.5 <sup>h</sup>	-35
phenylcyclopropane*	NFSI	1.87 <sup>c</sup>	-0.78 <sup>d</sup>	3.5 <sup>h</sup>	-18
phenylcyclopropane	9-fluorenone*	1.87 <sup>c</sup>	-1.29 <sup>e</sup>	2.4 <sup>g</sup>	+19
phenylcyclopropane*	9-fluorenone	1.87 <sup>c</sup>	-1.29 <sup>e</sup>	3.5 <sup>h</sup>	-6.0

<sup>a</sup> $\Delta G_{ET}^0$  = free energy of electron transfer (kcal/mol);  $E_{(D+/D)}^0$  = oxidation potential of electron donor (V vs. SCE);  $E_{(A/A-)}^0$  = reduction potential of electron acceptor (V vs. SCE);  $E_{0,0}$  = excitation energy (eV);  $w$  = Coulomb term (estimated 0.06 eV in MeCN). <sup>b</sup>Ref. 31a. <sup>c</sup>Ref. 31b. <sup>d</sup>Ref. 31c. <sup>e</sup>Ref. 31d. <sup>f</sup>Ref. 31e. <sup>g</sup>Ref. 31f. <sup>h</sup>Ref. 31g.

The higher oxidation potential of Selectfluor lends itself to more thermodynamically favorable electron transfer than NFSI in both instances. Unsurprisingly, competition experiments between Selectfluor **6** and NFSI **7** display an overwhelming preference for the Selectfluor-substituted product (Scheme 8.5). On the other hand, PET is predicted to be more thermodynamically favorable for phenylcyclopropane over 1,2-diphenylcyclopropane (and presumably 1-methyl-2-phenylcyclopropane **8**, as well), yet competition experiments reveal a preference for the disubstituted cyclopropanes in both instances (Scheme 8.5). These discrepancies may suggest that photoinduced electron transfer is not a rate-determining step.

### Competition Experiments



**Scheme 8.5** Relative rates via competition experiments.

### 8.6 Fluorescence and Time-Resolved Spectroscopy.

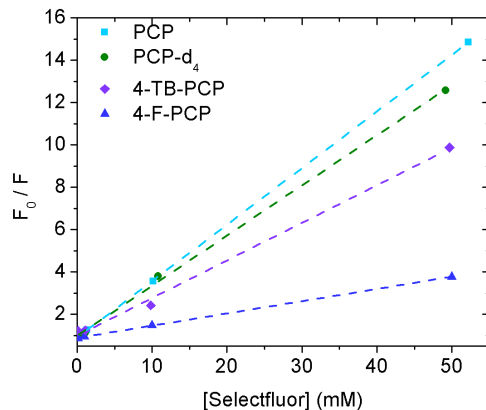
To confirm whether the excited state of the arylcyclopropane is quenched by the N-F reagent via PET, we turned to steady-state fluorescence and transient-absorption spectroscopies. All spectroscopic measurements were conducted with Selectfluor rather than NFSI in order to eliminate overlap in absorption of phenylcyclopropane and the N-F reagent at accessible excitation wavelengths; however, the photochemistry of NFSI and phenylcyclopropane mixtures were examined under identical conditions.<sup>34</sup>

If the excited state of the arylcyclopropane reacts with Selectfluor by PET one would expect quenching of its fluorescence according to the Stern-Volmer relationship (Eq. 8.1).<sup>35</sup>

$$\frac{F_0}{F} = 1 + k_q \tau_0 [Q] \quad (1)$$

Here,  $F_0$  is the fluorescence intensity measured in the absence of quencher Q, F is the fluorescence intensity in the presence of quencher Q,  $k_q$  is the quenching rate constant, and  $\tau_0$  is the innate lifetime of the excited state. Figure 8.3 shows that the fluorescence ratios ( $F_0/F$ ) of several arylcyclopropanes increase linearly with concentration of Selectfluor (Q) with excellent coefficients of determination ( $R^2 \approx 1$ ). The excited-state lifetimes ( $\tau_0$ ) of various arylcyclopropanes were measured by nanosecond transient absorption

spectroscopy in order to explore isotope and substituent effects on quenching rates; values obtained for  $\tau_0$  and  $k_q$  are given in Table 8.2.



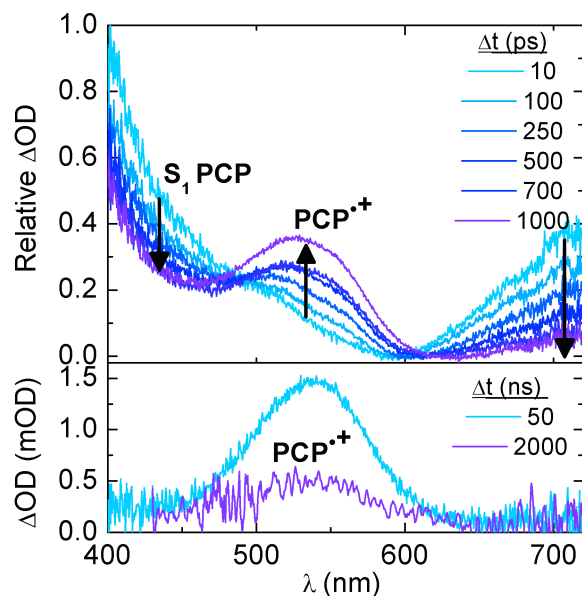
**Figure 8.3** Stern-Volmer plots for fluorescence quenching of arylcyclopropanes by Selectfluor.

**Table 8.2** Excited-state lifetimes ( $\tau_0$ ) measured by nanosecond transient absorption spectroscopy and quenching constants ( $k_q$ ) from Stern-Volmer analysis.

<i>Arylcyclopropane</i>	$\tau_0$ (ns)	$k_q$ (ns M) <sup>-1</sup>
phenylcyclopropane (PCP)	13.8	19.3
phenylcyclopropane- <i>d</i> <sub>4</sub> (PCP- <i>d</i> <sub>4</sub> )	9.9	23.9
4-fluorophenylcyclopropane (4-F-PCP)	5.9	30.0
4- <i>tert</i> -butylphenylcyclopropane (4-TB-PCP)	13.8	4.1

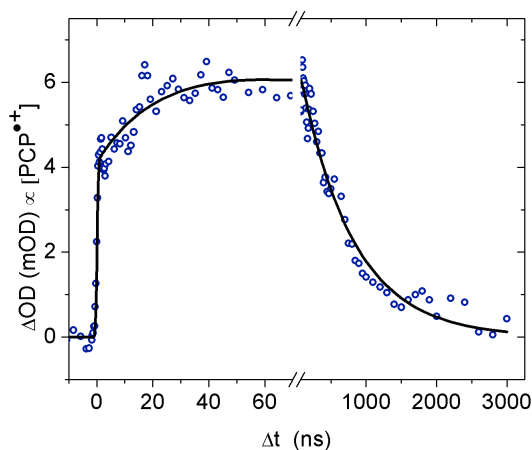
Although these observations verify quenching of excited arylcyclopropanes by Selectfluor, fluorescence spectroscopy alone does not provide conclusive details about the quenching mechanism. If our hypothesis regarding quenching through PET is correct, then transient-absorption spectroscopy could help identify one or more of the putative radical ion intermediates. For instance, arylcyclopropane radical cation transients are reported to have a strong, distinct absorption feature in the visible range.<sup>36</sup> Figure 8.4 presents transient absorption spectra obtained over delays ranging 10 ps to 2 ms after 266-nm excitation of phenylcyclopropane in the presence of Selectfluor, 5:50 mM respectively. Under these conditions the spectrum of the radical cation (PCP<sup>•+</sup>,  $\lambda_{\max} = 545 \text{ nm}$ <sup>37</sup>) is observed to appear with the decay of excited state

absorption of phenylcyclopropane. The radical cation spectrum is consistent with literature precedent and was reproduced under similar experimental conditions for comparison.<sup>7,37,38</sup> In contrast, no signature of the radical cation appears in absence of Selectfluor; ultrafast transient spectroscopy of the excited state in absence of Selectfluor is shown in the Supporting Information. Hence, transient spectroscopy provides direct evidence for the proposed PET quenching mechanism.



**Figure 8.4** Time-resolved transient absorption spectroscopy of phenylcyclopropane following 266-nm excitation; radical cation ( $\text{PCP}^{\bullet+}$ ,  $\lambda_{\text{max}} = 545 \text{ nm}$ <sup>37</sup>) is generated in the presence of Selectfluor. The upper panel has been referenced to a  $\Delta\text{OD}$  of 0 to highlight the spectral evolution.

The kinetics of the phenylcyclopropane radical cation were monitored by transient absorption at 520 nm following 266-nm excitation and is characterized by an exponential rise and decay of 47.2 ns and 816 ns, respectively (Figure 8.5). While a lifetime of  $\sim 1 \mu\text{s}$  has been reported for the decay of phenylcyclopropane radical cation under sensitized reaction conditions, the exponential rise was not reported previously, most likely due to lower instrument time resolution.<sup>24</sup> The broadband transient absorption spectrum recorded at 2 ms (Figure 8.4) indicates that the phenylcyclopropane radical cation does not result in any other spectroscopically detectable reaction products in the range of 430-750 nm.



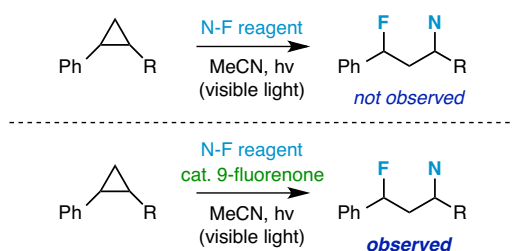
**Figure 8.5** Kinetics of the phenylcyclopropane radical cation ( $\text{PCP}^{\bullet+}$ ) generated in presence of Selectfluor according to nanosecond-resolved transient absorption at 520 nm.

A small, inverse isotope effect is observed in the quenching rate constants of phenylcyclopropane (PCP) and phenylcyclopropane- $d_4$  (PCP- $d_4$ ); this differs from the competitive KIE (below). Additionally, quencher rate constants of different *para*-substituted phenylcyclopropanes (4-*tert*-butyl- and 4-fluorophenylcyclopropane; 4-TB-PCP and 4-F-PCP) do not follow the exact same trend observed in the competition experiments used to generate the Hammett plots. This is not particularly alarming; on the contrary, it supports the claim that the photoinduced electron transfer event has minimal impact on the overall rate equation.

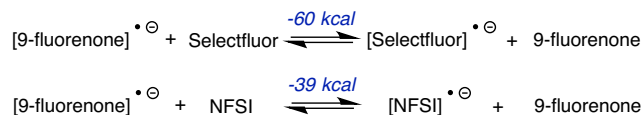
### 8.7 Alternative Photosensitized Initiation.

The spectroscopic observations *vide supra* inspired us to seek out the result of generating an arylcyclopropane radical cation with a visible light photosensitizer. Although we observed no aminofluorination using visible light (14-Watt CFL) with phenylcyclopropane and the N-F reagents alone, we did observe product formation in the presence of 9-fluorenone – an established visible light photosensitizer<sup>39</sup> – albeit in consistently lower yields (Scheme 8.6). Considering that only the excited state of 9-fluorenone is accessible under visible light conditions, electron transfer quenching events by ground state phenyl- and 1,2-diphenylcyclopropane are predicted to be more endergonic at +19 and +13 kcal/mol (Table 8.1). Perhaps lower product yields are a reflection of inefficient PET in these particular cases.

However, this newly discovered mode of initiation prompts us to entertain the probability of a reaction between arylcyclopropane radical cations and N-F reagents directly (unlikely, due to charge repulsion) and also the possibility of an electron relay from the 9-fluorenone radical anion to the N-F reagent (thereafter, providing the same intermediates as direct photoexcitation). Calculations at B3PW91/6-311++G\*\* employing the default MeCN continuum (Scheme 8.7) suggest very favorable electron transfer from the 9-fluorenone radical anion to both Selectfluor ( $\Delta G_{\text{calc}} = -60$  kcal/mol) and NFSI ( $\Delta G_{\text{calc}} = -39$  kcal/mol).<sup>40</sup> As such, the consequences of one-electron reduction of the N-F reagents were explored in more detail.



**Scheme 8.6** Alternative photochemical initiation.



**Scheme 8.7** Electron relay at B3PW91/6-311++G\*\* (MeCN).

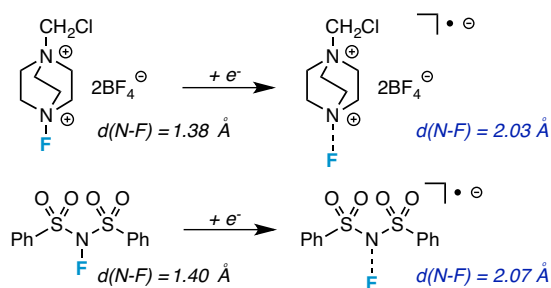
### 8.8 Alternative Chemical Initiation.

From studying the copper(I)/Selectfluor aliphatic fluorination system,<sup>5</sup> we determined that an inner-sphere electron transfer event also results in one-electron reduction of Selectfluor, concomitant with loss of fluoride. This process generates the elusive Selectfluor "radical dication" that is responsible for H-atom abstraction in the copper system<sup>5</sup> (and likely the triethylborane variant<sup>41</sup>). The calculated geometry of the one-electron reduced structure of Selectfluor (and NFSI) that would result from PET shows significant elongation of the N-F bond (Scheme 8.8). It is likely that this structure would rapidly expel fluoride to give the same radical dication species, but the question is whether or not this species is responsible for any of the observed chemistry in this aminofluorination system. In an effort to probe the role of the Selectfluor

radical dication intermediate, we submitted phenylcyclopropane and 1,2-diphenylcyclopropane to the copper(I) and triethylborane reactions *vide infra* in the absence of light and obtained a surprising result – the same aminofluorination reaction (Scheme 8.9).

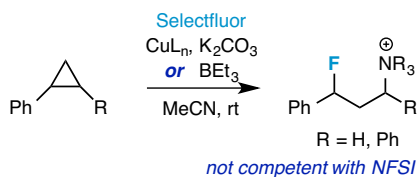
The ability to reproduce the reaction in the absence of light offers a crucial new perspective to understanding the reaction mechanism beyond photoexcitation. However, one must first rule out the possibility of the non-photochemical systems operating by an entirely different mechanism. By repeating the product distribution studies, Hammett analyses, and kinetic isotope effects (see below), we discovered very similar behavior of the triethylborane and copper(I) systems<sup>42</sup> to the direct photoexcitation of arylcyclopropanes and Selectfluor (note that these methods are incompatible with NFSI).

The involvement of an arylcyclopropane radical cation intermediate in the non-photochemical systems is still supported by the negative  $\rho$  values in the intermolecular competition experiments (-3.2 for triethylborane shown; -2.9 for copper(I) in Chapter 12) and similar distributions in the intramolecular experiments (Figure 8.2, **E** and **F**). In this light, another proposal for the formation of arylcyclopropane radical cations that applies to all systems is chemical oxidation by the Selectfluor-derived radical dication. Through this pathway, the arylcyclopropane radical cation could be generated along with a neutral Selectfluor-derived amine that can conceivably participate in a three-electron nucleophilic substitution reaction. The result would be a ring-opened intermediate containing a benzylic radical; we have shown that such radicals are readily fluorinated in the presence of Selectfluor, yielding the fluorinated product and regenerating the radical dication.<sup>5</sup>



**Scheme 8.8** Elongation/cleavage of N-F bond upon reduction at B3PW91/6-311++G\*\* (MeCN).





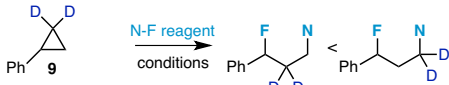
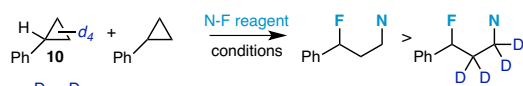

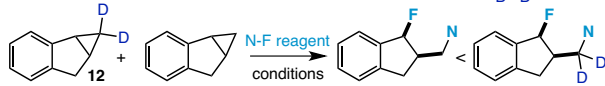
**Scheme 8.9** Alternative chemical initiation.

Qualitatively, a radical chain mechanism after photoexcitation presents an explanation for anomalous behavior of the phenylcyclopropane radical cation kinetics observed during time-resolved experiments (Figure 8.5). After photoexcitation, the single-wavelength trace at 520 nm, which is proportional to the phenylcyclopropane radical cation concentration, exhibits approximately a 50 ns rise. Given the experimental conditions (50 mM Selectfluor) and the determined  $k_q$  from the Stern-Volmer analysis, the phenylcyclopropane excited-state should be quenched on a timescale of  $\sim 0.8$  ns; indeed, ultrafast measurements reflect such a quenching rate under these conditions. Therefore, the observed absorption must be *solely due to the radical cation*. In light of the proposed mechanism, this increase in concentration reflects propagated chemical oxidation of phenylcyclopropane by the Selectfluor-derived radical dication. Furthermore, it is important to note that the lifetimes of radical chain propagations are typically less than one second<sup>43</sup> and require a continuous source of initiation.<sup>44</sup>

### 8.9 Kinetic Isotope Effects.

We further assessed the viability of this pathway with competitive kinetic isotope effect experiments (Table 8.3). Phenylcyclopropane- $d_2$  **9** was synthesized by standard Wittig chemistry with benzaldehyde and iodomethane- $d_3$ ,<sup>45</sup> followed by a modified Simmons-Smith cyclopropanation, to be used as an intramolecular KIE probe. The observed intramolecular KIE's for Selectfluor (0.88) and NFSI (0.87) represent inverse secondary effects. Following the notion that the ring-opening step is rate determining, the inverse secondary effect is consistent with 1) less-hindered nucleophilic attack on the cyclopropane ring<sup>7</sup> and 2) the change in geometry accompanied with ring opening. That is, a consequence of ring strain in cyclopropane compounds is the virtual  $sp^2$  hybridization of the C-H(D) bonds; nucleophilic ring opening thus resembles a change in hybridization from  $sp^2$  to  $sp^3$ .

**Table 8.3** Intramolecular and intermolecular competitive KIE's.

Entry	Competition Experiment	$KIE_{\text{Selectfluor}}(300\text{ nm})$	$KIE_{\text{NFSI}}(300\text{ nm})$	$KIE_{\text{Selectfluor}}(\text{cat. } BEt_3)$
1		0.88	0.89	n.d.
2		1.4(3)	1.4(5)	1.4(3)
3		1.4(9) <sup>a</sup>	1.4(6) <sup>a</sup>	1.4(7) <sup>a</sup>
4		0.89 <sup>b</sup>	0.86 <sup>b</sup>	0.94 <sup>b</sup>

<sup>a</sup>Average KIE (considering both diastereomers). <sup>b</sup>KIE only determined for cis diastereomer.

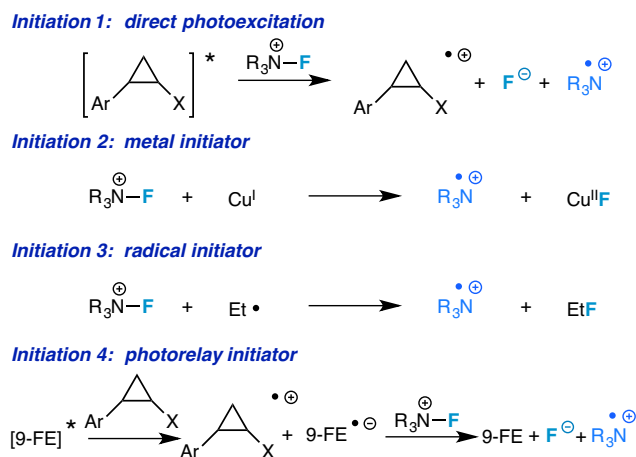
For another vantage point, phenylcyclopropane- $d_4$  **10** and 1,2-diphenylcyclopropane- $d_2$  **11** were synthesized in a similar fashion (using diiodomethane- $d_2$  in the cyclopropanation step) as intermolecular KIE probes. The observed intermolecular KIE's for Selectfluor and NFSI are ca. 1.4 in all instances. These fairly large, normal secondary effects are consistent with rate-determining cyclopropane ring opening if one considers  $\beta$ -H-stabilization (over  $\beta$ -D-stabilization) of the charges in the transition state. To support this claim, a dideuterated indene-derived arylcyclopropane **12** was synthesized as an intermolecular KIE probe lacking  $\beta$ -isotopic substitution. As anticipated, the normal secondary effect that may result from  $\beta$ -H(D)-stabilization was not observed. Instead, an inverse secondary effect was observed that is consistent with nucleophilic ring opening.

### 8.10 Drawing a Unified Mechanism.

At this point, reasonable mechanisms can be drawn for the four methods of initiation and the common chain propagation. Given that the non-photochemical reactions are not competent with NFSI, we focus the discussion in this section to reactions with Selectfluor.

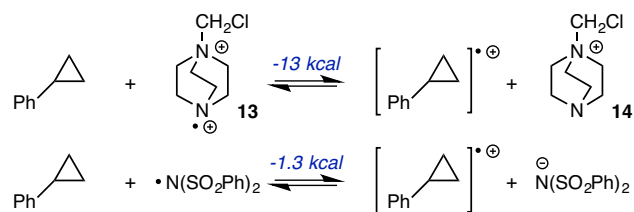
The nearly identical behavior of all photochemical and non-photochemical systems in our mechanistic studies strongly suggests a common mechanism beyond initiation. From precedent, we conclude that the key player is a Selectfluor-derived radical dication.<sup>5</sup> This putative intermediate may be generated in several ways: 1) direct photoexcitation of an arylcyclopropane, followed by photoinduced electron transfer to an N-F reagent that, in its reduced form, is predicted to lose fluoride, 2) inner-sphere electron transfer with

copper(I) concomitant with loss of fluoride, 3) direct F-atom abstraction with an ethyl radical generated from  $\text{BEt}_3$ , and 4) photosensitized oxidation of the arylcyclopropane, followed by a "relay" of the electron to the N-F reagent, which decomposes to the radical dication as mentioned (Scheme 8.10).

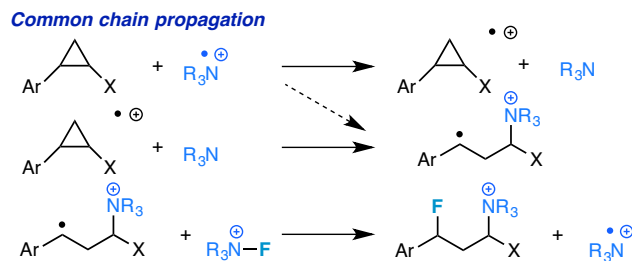


**Scheme 8.10** Proposed initiation mechanisms.

Upon formation, the Selectfluor-derived radical dication **13** is predicted to oxidize arylcyclopropanes very efficiently (Scheme 8.11).<sup>46</sup> This oxidation step could 1) result in an arylcyclopropane radical cation and amine **14** that subsequently undergo three-electron nucleophilic substitution (stepwise) or 2) occur simultaneously with ring opening (concerted). In either case, a radical is generated on the newly aminofunctionalized substrate that is fluorinated in the presence of Selectfluor. Thus, the Selectfluor-derived radical dication is regenerated and the chain propagates (Scheme 8.12).

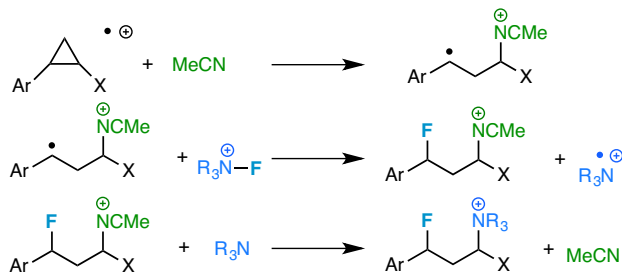


**Scheme 8.11** Calculated phenylcyclopropane oxidations ( $\Delta G_{\text{calc}}$ ) at B3PW91/6-311++G\*\* (MeCN).



**Scheme 8.12** Oxidation, aminofunctionalization, fluorination, and propagation.

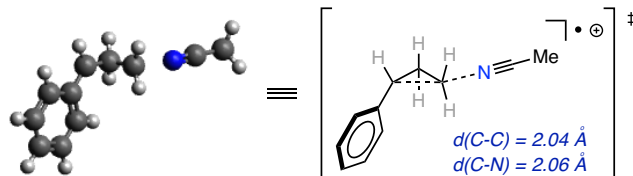
Though NFSI was not studied as thoroughly as Selectfluor in this work, many observations and computations suggest it is operating by a similar mechanism under photochemical conditions. It is surprising how alike the LFER's and KIE's are for reactions with Selectfluor and NFSI. These parallels prompted us to entertain the possibility of a common solvent-assisted ring-opening mechanism (Scheme 8.13).



**Scheme 8.13** Acetonitrile-assisted ring opening.

We argue the plausibility of ring opening by acetonitrile for the following reasons: 1) if ring opening is rate-determining, one might expect the amine nucleophiles derived from Selectfluor and NFSI to have different transition state structures (thus having an impact on isotope effect magnitudes), 2) arylcyclopropanes are known to have irreversible one-electron oxidation potentials in MeCN due to irreversible ring opening,<sup>36,47</sup> and 3) transition state structures have been calculated that are in accord with some of the observed isotope effects above. For instance, using the Bigeleisen-Mayer method of calculating KIE's,<sup>48</sup> we have determined an isotope effect of 0.95 for phenylcyclopropane-*d*<sub>2</sub>

(intramolecular KIE) and 1.30 for phenylcyclopropane- $d_4$  (intermolecular KIE) using the transition state structure in Figure 8.6 (consider aforementioned EIE's and Table 8.3, Entry 1 and 2).



**Figure 8.6** Solvent-assisted ring opening transition state at wB97XD/6-311++G\*\* (MeCN).<sup>49</sup>

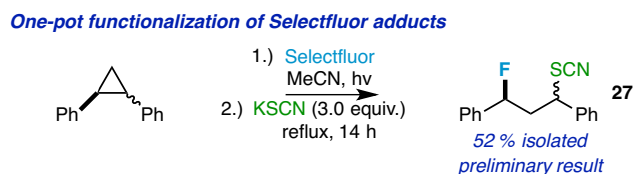
One might expect to obtain a small amount of the 1,3-fluoroacetamide upon workup if this solvent-assisted mechanism is at play, but none was observed. However, we have made a noteworthy observation. While monitoring the kinetic profile of a reaction with 4-fluorophenylcyclopropane and Selectfluor, we noticed a trace amount of another fluorinated product appear and disappear in the  $^{19}\text{F}$  NMR spectra over the course of the reaction that is an apparent ddd with the correct shift/coupling constants to be a benzylic fluoride. This signal was never observed in any NMR spectra of completed reactions, but unveils another benzylic fluoride intermediate - possibly the fluorinated acetonitrile adduct.<sup>50</sup> The acetonitrile molecule is conceivably displaced from the fluorinated product by the more nucleophilic amine derived from either Selectfluor or NFSI, thus accounting for a lack of substantial 1,3-fluoroacetamide in the final product mixture. To provide additional support for solvent involvement, we conducted a few reactions in 1:1 acetonitrile:pivalonitrile and found that new benzylic fluoride peaks evolve in each instance that we have assigned as the pivalonitrile-trapped nitrilium adducts. Likely, the pivalonitrile adducts are less easily displaced than the corresponding acetonitrile adducts; thus, small amounts ( $\leq 3\%$ ) persist upon reaction completion. Although solvent-assisted ring opening cannot be unequivocally determined as the *sole* ring opening mechanism at play, the above observations provide evidence for its viability.

### 8.11 As a Synthetic Method.

Thus far, the primary focus of this article has been elucidation of reaction mechanism. As synthetic methods, our findings also add a very efficient and regioselective aminofluorination reaction to the toolbox

of the synthetic chemist. The reactions with Selectfluor, in many instances, approach quantitative yields; but note that the products are difficult to separate from the chloromethyl DABCO byproduct via chromatography, extraction, or crystallization techniques (thus, spectra of the crude reaction mixtures are reported in the Supporting Information). However, the products (even with the quaternary ammonium substitution) are quite stable and may be separated from other non-ionic byproducts by column chromatography on C18 or diol media, eluting with MeCN/H<sub>2</sub>O.

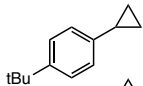
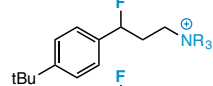
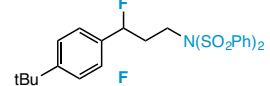
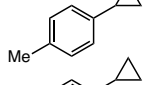
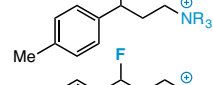
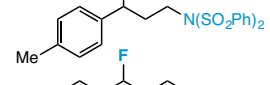
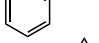
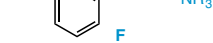

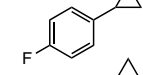
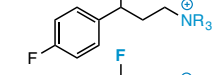
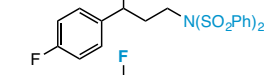
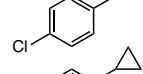
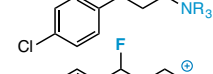
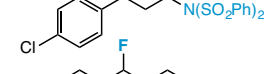
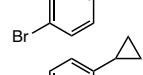
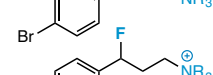
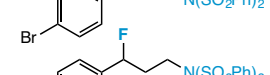
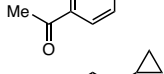
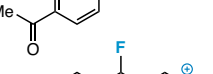
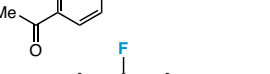
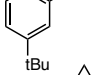
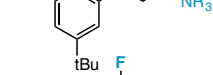
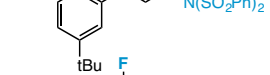
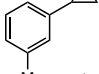
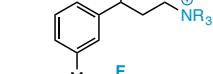
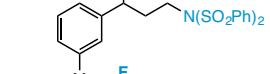
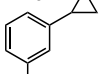
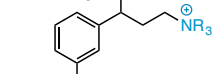
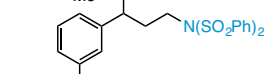
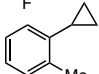
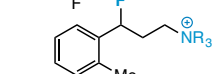
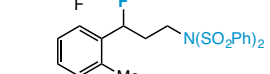
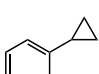
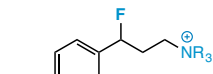
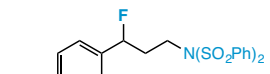
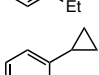
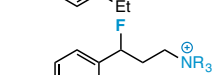
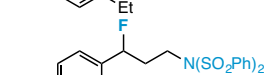
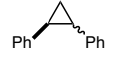
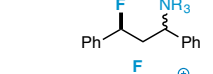
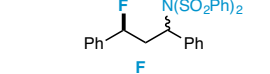
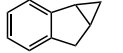
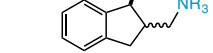
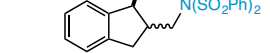
From a more practical standpoint, we found that the 1,3-aminofluorinated products from reactions with NFSI are easily isolated by column chromatography on silica gel or Florisil (more extensive characterization data is reported for these compounds in the Supporting Information). To access more synthetically useful, isolable compounds from the Selectfluor adducts, we imagined the ammonium substituent could be displaced by a nucleophile under proper reaction conditions. Accordingly, we discovered that, following irradiation, the addition of potassium thiocyanate to the reaction mixture under reflux for 14 h provides the 1,3-fluorothiocyanate **27** from 1,2-diphenylcyclopropane in a 52 % isolated yield (Scheme 8.14). Although reaction optimization/examination of the competency of various nucleophiles is beyond the scope of this study, this showcases potential synthetic utility of this method as a one-pot aminofluorination/nucleophilic displacement reaction.<sup>51</sup>



**Scheme 8.14** Potential synthetic utility of Selectfluor adducts.

Over the course of our studies, we have noted several features about the substrate scope (Table 8.4). First of all, reactions with Selectfluor tend to be higher yielding than reactions with NFSI. This is consistent with our studies thus far that highlight several ways in which Selectfluor was determined to be more reactive. Note that the majority (if not entirety) of the remaining mass balance from reactions with NFSI can be assigned to unreacted starting material; longer reaction times and larger quantities of NFSI did not result in higher yields.

**Table 8.4** Scope of aminofluorination reaction for Selectfluor and NFSI under 300 nm irradiation.

Entry	Substrate	Selectfluor Adduct	% Yield	NFSI Adduct	% Yield
1			96		67 (67)
2			90 <sup>a</sup>		41 (43)
3			85		43 (42)
4			95		n.d.
5			87		n.d.
6			92		n.d.
7			54		n.d.
8			72		50 (48)
9			83 <sup>a</sup>		41 (38)
10			74		n.d.
11			93 <sup>a</sup>		60
12			96 <sup>a</sup>		57 (53)
13			93		66 (60)
14			97 <sup>b</sup>		60 (54) <sup>b</sup>
15			78 <sup>b</sup>		66 <sup>b</sup>

Unless otherwise specified, substrates were stirred with 2.2 equiv. N-F reagent in MeCN and irradiated at 300 nm in Pyrex microwave vials for 14 h. <sup>19</sup>F NMR yields are reported; isolated yields for NFSI adducts appear in parentheses. *N*-chloromethyl-DABCO substituents on Selectfluor-arylcyclopropane adducts are abbreviated as NR<sub>3</sub>. <sup>a</sup>Only 1.0 equiv. of N-F reagent used (to minimize additional methyl fluorination). <sup>b</sup>Mixture of diastereomers.

When employing either N-F reagent, substrates adorned with electron donating groups (e.g. Me, Et, *i*Pr, *t*Bu) tend to provide higher product yields than those with electron withdrawing groups (e.g. F, Cl, Br, OAc). Note that stronger donating groups suffer from competitive aryl ring fluorination and more extreme

withdrawing groups (for instance, NO<sub>2</sub>) are not competent in the reaction. Additionally, aryl rings substituted in the *ortho*, *meta*, or *para* positions are competent in the reaction; steric bulk in the *ortho* position has minimal impact on reactivity,<sup>52</sup> though the reaction is sensitive to electronic effects (as demonstrated in the Hammett analyses of *meta* and *para* substitutions). Beyond ring-substituted phenylcyclopropanes, other substituents on the ring (i.e. Me and Ph) guide regioselective aminofunctionalization (in addition to selective benzylic fluorination). More rigid cyclopropanes, e.g. the indene-derived cyclopropane, undergo regioselective substitution, as well. Lastly, primary, secondary, and secondary benzylic amination is shown to be viable, as is secondary and tertiary benzylic fluorination. Note that our example of a tertiary benzylic fluoride was excluded from the table due to its strong tendency to dehydrofluorinate upon workup (presumably to make the allylic or homoallylic amine).

### 8.12 Conclusion.

In exhibition of a "multifold approach" to method development and mechanistic studies, we report four sets of reaction conditions – linked by a common intermediate – that effect a unique, regioselective fluorination of arylcyclopropanes with N-F reagents. We propose a detailed mechanism based on extensive experimental and computational studies; specifically, we propose photochemical initiation (by PET, in the direct excitation method) of a radical chain mechanism that is corroborated by three alternative initiation methods, two of which are non-photochemical. Linear free energy relationships, estimations of free energies of electron transfer (via Rehm-Weller relationships), competition experiments, fluorescence, and transient-absorption spectroscopy all support direct photoexcitation of the arylcyclopropane and subsequent quenching of the excited state via PET in the presence of an N-F reagent. This is solidified by direct observation of the arylcyclopropane radical cation intermediate under reaction conditions. Alternative methods that we have shown to effect the same reaction (using Selectfluor) suggest that the observed PET only initiates the reaction, and it is followed by a radical chain mechanism propagated by a previously postulated Selectfluor-derived radical dication. Further evidence for this radical chain mechanism, characterized by rate-determining cyclopropane ring opening and subsequent radical fluorination, is provided through product distribution studies, kinetic analyses, a table of kinetic isotope effects, literature precedent, and DFT calculations. Additionally, we examined the plausibility of a solvent-assisted



cyclopropane ring opening mechanism instead of/in addition to the amine that ultimately functionalizes the molecule. Lastly, as a synthetic method, the reaction cleanly and regioselectively produces unusual aminofluorinated products in good to excellent yields that may serve as building blocks toward the synthesis of both fluoro- and aminofunctionalized complex molecules.

### 8.13 References.

- 
- <sup>1</sup> Fluorine has been referred to as the "second-favorite heteroatom" in drug design, behind only nitrogen: Ojima, I. *J. Org. Chem.* **2013**, *78*, 6358-6383.
- <sup>2</sup> For some recent literature, see: a) Böhm, H.-J.; Banner, D.; Bendels, S.; Kansy, M.; Kuhn, B.; Müller, K.; Obst-Sander, U.; Stahl, M. *ChemBioChem* **2004**, *5*, 637-643. b) Purser, S.; Moore, P. R.; Swallow, S.; Gouverneur, V. *Chem. Soc. Rev.* **2008**, *37*, 320-330. c) Patrick, G. L. *An Introduction to Medicinal Chemistry*, 5<sup>th</sup> ed.; Oxford University Press: Oxford, UK, 2013. d) Gillis, E. P.; Eastman, K. J.; Hill, M. D.; Donnelly, D. J.; Meanwell, N. A. *J. Med. Chem.* **2015**, *58*, 8315-8359.
- <sup>3</sup> Chen, G.; Song, J.; Yu, Y.; Luo, X.; Li, C.; Huang, X. *Chem. Sci.* **2016**, *7*, 1786-1790.
- <sup>4</sup> a) Qiu, S.; Xu, T.; Zhou, J.; Guo, Y.; Liu, G. *J. Am. Chem. Soc.* **2010**, *132*, 2856-2857. b) Haitao, Z.; Liu, G. *Acta Chim. Sin.* **2012**, *70*, 2404-2407. c) Zhang, H.; Song, Y.; Zhao, J.; Zhang, J.; Zhang, Q. *Angew. Chem. Int. Ed.* **2014**, *53*, 11079-11083. d) Saavedra-Olavarría, J.; Arteaga, G. C.; López, J. J.; Pérez, E. G. *Chem. Commun.* **2015**, *51*, 3379-3382.
- <sup>5</sup> Pitts, C. R.; Bloom, S.; Woltornist, R.; Auvenshine, D. J.; Ryzhkov, L. R.; Siegler, M. A.; Lectka, T. *J. Am. Chem. Soc.* **2014**, *136*, 9780-9791.
- <sup>6</sup> Patel; N. R.; Flowers II, R. A. *J. Org. Chem.* **2015**, *80*, 5834-5841.
- <sup>7</sup> Dinnocenzo, J. P.; Zuilhof, H.; Lieberman, D. R.; Simpson, T. R.; McKechney, M. W. *J. Am. Chem. Soc.* **1997**, *119*, 994-1004.
- <sup>8</sup> For some examples from our laboratory, see: a) Bloom, S.; Pitts, C. R.; Miller, D.; Haselton, N.; Holl, M. G.; Urheim, E.; Lectka, T. *Angew. Chem. Int. Ed.* **2012**, *51*, 10580-10583. b) Bloom, S.; Pitts, C. R.; Woltornist, R.; Griswold, A.; Holl, M. G.; Lectka, T. *Org. Lett.* **2013**, *15*, 1722-1724. c) Bloom, S.; Sharber, S. A.; Holl, M. G.; Knippel, J. L.; Lectka, T. *J. Org. Chem.* **2013**, *78*, 11082-11086. d) Bloom, S.; Knippel, J. L.; Lectka, T. *Chem. Sci.* **2014**, *5*, 1175-1178. e) Bloom, S.; McCann, M.; Lectka, T. *Org. Lett.* **2014**, *16*, 6338-6341. f) Bloom, S.; Bume, D. D.; Pitts, C. R.; Lectka, T. *Chem. Eur. J.* **2015**, *21*, 8060-8063.
- <sup>9</sup> For other recent advances in this research area, see: a) Rueda-Becerril, M.; Sazepin, C. C.; Leung, J. C. T.; Okbinoglu, T.; Kennepohl, P.; Paquin, J.-F.; Sammis, G. M. *J. Am. Chem. Soc.* **2012**, *134*, 4026-4029. b) Liu, W.; Huang, X.; Cheng, M.; Nielson, R. J.; Goddard III, W. A.; Groves, J. T. *Science* **2012**, *337*, 1322-1325. c) Yin, F.; Wang, Z.; Li, Z.; Li, C. *J. Am. Chem. Soc.* **2012**, *134*, 10401-10404. d) Liu, W.; Groves, J. T. *Angew. Chem. Int. Ed.* **2013**, *52*, 6024-6027. e) Amaoka, Y.; Nagamoto, M.; Inoue, M. *Org. Lett.* **2013**, *15*, 2160-2163. f) Braun, M.-G.; Doyle, A. *J. Am. Chem. Soc.* **2013**, *135*, 12990-12993. g) Xia, J.-B.; Ma, Y.; Chen, C. *Org. Chem. Front.* **2014**, *1*, 468-472. h) Rueda-Becerril, M.; Mahe, O.; Drouin, M.; Majewski, M. B.; West, J. G.; Wolf, M. O.; Sammis, G. M.; Paquin, J.-F. *J. Am. Chem. Soc.* **2014**, *136*, 2637-2641. i) Halperin, S. D.; Fan, H.; Chang, S.; Martin, R. E.; Britton, R. *Angew. Chem. Int. Ed.* **2014**, *53*, 4690-4693. j) Li, Z.; Wang, Z.; Zhu, L.; Tan, X.; Li, C. *J. Am. Chem. Soc.* **2014**, *136*, 16439-

- 
16443. k) Phae-nok, S.; Soorukram, D.; Kuhakarn, C.; Reutrakul, V.; Pohmakotr, M. *Eur. J. Org. Chem.* **2015**, *2015*, 2879-2888. l) Ventre, S.; Petronijevic, F. P.; MacMillan, D. W. C. *J. Am. Chem. Soc.* **2015**, *137*, 5654-5657.
- <sup>10</sup> Adapted from: Lorenz, J. C.; Long, J.; Yang, Z.; Xue, S.; Xie, Y.; Shi, Y. *J. Org. Chem.* **2004**, *69*, 327-334.
- <sup>11</sup> Anslyn, E. V.; Dougherty, D. A. *Modern Physical Organic Chemistry*; University Science Books: Sausalito, CA, 2006.
- <sup>12</sup> a) Johnston, L. J.; Scaiano, J. C. *Chem. Rev.* **1989**, *89*, 521-547. b) Ichinose, N.; Mizuno, K.; Otsuji, Y.; Caldwell, R. A.; Helms, A. *M. J. Org. Chem.* **1998**, *63*, 3176-3184.
- <sup>13</sup> Regarding 1,2-diphenylcyclopropane electron-transfer isomerization, see: Wong, P. C.; Arnold, D. R. *Tetrahedron Lett.* **1979**, *23*, 2101-2104.
- <sup>14</sup> Hixson, S. S.; Xing, Y. *Tetrahedron Lett.* **1991**, *23*, 173-174.
- <sup>15</sup> Note that charge stabilization may also be an important factor in determining regioselectivity in less rigid systems.
- <sup>16</sup> Logan, S. R. *J. Chem. Ed.* **1997**, *74*, 1303.
- <sup>17</sup> a) Hammett, L. P. *J. Am. Chem. Soc.* **1937**, *59*, 96-103. b) Hansch, C.; Leo, A.; Taft, R. W. *Chem. Rev.* **1991**, *91*, 165-195.
- <sup>18</sup> Good correlation is also noted with  $\sigma^+$  values, with no change in slope (Selectfluor,  $\rho = -3.2$ ,  $R^2 = 0.98$ ; NFSI,  $\rho = -3.6$ ,  $R^2 = 0.97$ ).
- <sup>19</sup> Electrophilic aromatic substitutions, for instance, tend to have more negative  $\rho$  values attributed to formally cationic Wheland intermediates (e.g. nitration = -6). See: a) Brown, H. C.; Okamoto, Y. *J. Am. Chem. Soc.* **1957**, *79*, 1913-1917. b) Johnson, C. D. *The Hammett Equation*; Cambridge University Press: Cambridge, UK, 1973.
- <sup>20</sup> We have found that Hammett analyses for reactions with carbon-based radical cation intermediates are quite scarce. For examples of "less negative"  $\rho$  values attributed to positive charge buildup (not necessarily formal cations), see: a) Citek, C.; Lyons, C. T.; Wasinger, E. C.; Stack, T. D. P. *Nature Chemistry* **2012**, *4*, 317-322. b) Fristrup, P.; Tursky, M.; Madsen, R. *Org. Biomol. Chem.* **2012**, *10*, 2569-2577. c) Blencowe, C. A.; Thornthwaite, D. W.; Hayes, W.; Russell, A. T. *Org. Biomol. Chem.* **2015**, *13*, 8703-8707.
- <sup>21</sup> For examples: a) Nicholas, A. M. de P.; Boyd, R. J.; Arnold, D. R. *Can. J. Chem.* **1982**, *60*, 3011-3018. b) Wayner, D. D. M.; Boyd, R. J.; Arnold, D. R. *Can. J. Chem.* **1983**, *61*, 2310-2315. c) Wayner, D. D. M.; Boyd, R. J.; Arnold, D. R. *Can. J. Chem.* **1985**, *63*, 3283-3289. d) Dinnocenzo, J. P.; Merchán, M.; Roos, B. O.; Shaik, S.; Zuilhof, H. *J. Phys. Chem. A* **1998**, *102*, 8979-8987.
- <sup>22</sup> CIDNP and EPR have been utilized, for examples: a) Roth, H. D.; Herberitz, T.; Lakkaraju, P. S.; Sluggett, G.; Turro, N. J. *J. Phys. Chem. A* **1999**, *103*, 11350-11354. b) Roth, H. D.; Schilling, M. L. M. *Can. J. Chem.* **1983**, *61*, 1027-1035.
- <sup>23</sup> In a more extreme case, intramolecular competition experiments with an electron-donating group (tBu) on one aryl ring vs. an electron-withdrawing group (Cl) on the other (namely, 1-(*tert*-butyl)-4-(2-(4-chlorophenyl)cyclopropyl)benzene) also did not display drastic ratios in favor of one substituent (Selectfluor, *p*-tBu:*p*-Cl 1.0:1.16; NFSI, *p*-tBu:*p*-Cl 1.0:1.36).
- <sup>24</sup> Dinnocenzo, J. P.; Todd, W. P.; Simpson, T. R.; Gould, I. R. *J. Am. Chem. Soc.* **1990**, *112*, 2462-2464.
- <sup>25</sup> Rao, V. R.; Hixson, S. S. *J. Am. Chem. Soc.* **1979**, *101*, 6458-6459.
- <sup>26</sup> Roth, H. D. *J. Phys. Chem. A* **2003**, *107*, 3432-3437.
- <sup>27</sup> Roth, H. D.; Schilling, M. L. M. *J. Am. Chem. Soc.* **1981**, *103*, 7210-7217.
- <sup>28</sup> Roth, H. D.; Schilling, M. L. M. *J. Am. Chem. Soc.* **1980**, *102*, 7956-7958.

- 
- <sup>29</sup> For a review on the photochemistry of cyclopropanes, see: Mizuno, K.; Ichinose, N.; Yoshimi, Y. *J. Photochem. Photobiol. C* **2000**, *1*, 167-193.
- <sup>30</sup> Absorbance for Selectfluor is almost entirely under 200 nm, see: Rueda-Becerril, M.; Mahé, O.; Drouin, M.; Majewski, M. B.; West, J. G.; Wolf, M. O.; Sammis, G. M.; Paquin, J-F. *J. Am. Chem. Soc.* **2014**, *136*, 2637-2641.
- <sup>31</sup> a) Rehm, D.; Weller, A. *Ber. Bunsen-Ges. Phys. Chem.* **1969**, *73*, 834-839. b) Rehm, D.; Weller, A. *Isr. J. Chem.* **1970**, *8*, 259-271.
- <sup>32</sup> In MeCN, the so-called work function is estimated to be +0.06 eV. See: Farid, S.; Dinnocenzo, J. P.; Merkel, P. B.; Young, R. H.; Shukla, D.; Guirado, G. *J. Am. Chem. Soc.* **2011**, *133*, 11580-11587.
- <sup>33</sup> a) Karki, S. B.; Dinnocenzo, J. P.; Farid, S.; Goodman, J. L.; Gould, I. R.; Zona, T. A. *J. Am. Chem. Soc.* **1997**, *119*, 431-432. b) Shono, T.; Matsumura, Y. *J. Org. Chem.* **1970**, *35*, 4157-4160. c) Furuya, T.; Kuttruff, C. A.; Ritter, T. *Curr. Opin. Drug Disc. Dev.* **2008**, *11*, 803-819. d) Meites, L.; Zuman, P. *CRC Handbook Series in Organic Electrochemistry*; CRC Press: Boca Raton, FL (USA), 1977-1982, volumes I-V. e) Becker, R. S.; Edwards, L.; Bost, R.; Elam, M.; Griffin, G. *J. Am. Chem. Soc.* **1972**, *94*, 6584-6592. f) Valentine, D., Jr.; Hammond, G. S. *J. Am. Chem. Soc.* **1972**, *94*, 3449-3454. g) Evans, D. F. *J. Chem. Soc.* **1959**, 2753-2757.
- <sup>34</sup> NFSI will outcompete phenylcyclopropane for the absorption of incident radiation, complicating fluorescence data and making it extremely difficult to observe the phenylcyclopropane radical cation under transient-absorption experimental conditions. The comparison of molar extinction coefficients for NFSI, phenylcyclopropane, and Selectfluor is given in the Supporting Information.
- <sup>35</sup> a) Stern, O.; Volmer, M. *Z. Phys.* **1919**, *20*, 183-188. b) Calvert, J. G.; Pitts, J. N. *Photochemistry*; John Wiley & Sons: New York, 1966; pp 663-670. c) Lakowicz, J. R. *Principles of Fluorescence Spectroscopy*, 3<sup>rd</sup> ed.; Springer: New York, 2006.
- <sup>36</sup> Guirado, G.; Fleming, C. N.; Lingenfelter, T. G.; Williams, M. L.; Zuilhof, H.; Dinnocenzo, J. P. *J. Am. Chem. Soc.* **2004**, *126*, 14086-14094.
- <sup>37</sup> Godbout, J. T.; Zuilhof, H.; Heim, G.; Gould, I. R.; Goodman, J. L.; Dinnocenzo, J. P.; Kelley, A. M. *J. Raman Spectrosc.* **2000**, *31*, 233-241.
- <sup>38</sup> Takahashi, Y.; Nishioka, N.; Endoh, F.; Ikeda, H.; Miyashi, T. *Tetrahedron Lett.* **1996**, *37*, 1841-1844.
- <sup>39</sup> For some recent examples of 9-fluorenone used as a visible light sensitizer in fluorination chemistry, see: a) Xia, J-B.; Zhu, C.; Chen, C. *J. Am. Chem. Soc.* **2013**, *135*, 17494-17500. b) Pitts, C. R.; Bloom, M. S.; Bume, D. D.; Zhang, Q. A.; Lectka, T. *Chem. Sci.* **2015**, *6*, 5225-5229.
- <sup>40</sup> Perdew, J. P.; Chevary, J. A.; Vosko, S. H.; Jackson, K. A.; Pederson, M. R.; Singh, D. J.; Fiolhais, C. *Phys. Rev. B*, **1992**, *46*, 6671-6687.
- <sup>41</sup> Pitts, C. R.; Ling, B.; Woltornist, R.; Liu, R.; Lectka, T. *J. Org. Chem.* **2014**, *79*, 8895-8899.
- <sup>42</sup> Additionally, we report initial rate studies with the copper(I) system in the Supporting Information identical to those reported in ref. 4. Neglecting the induction period, we have found a similar rate dependence of the reaction on both the substrate and Selectfluor (substrate ~1, Selectfluor <1) to the results in ref. 4.
- <sup>43</sup> Walling, C. *Tetrahedron* **1985**, *41*, 3887-3900.

---

<sup>44</sup> Therefore, the fact that product yield does not appear to increase by NMR after periods of turning the light off provides no evidence for or against the possibility of a chain propagation mechanism.

<sup>45</sup> Hirano, M.; Ueda, T.; Komine, N.; Komiya, S.; Nakamura, S.; Deguchi, H.; Kawauchi, S. *J. Organomet. Chem.* **2015**, *797*, 174-184.

<sup>46</sup> As shown in Scheme 8.11, the putative *N*-centered radical generated from one-electron reduction of NFSI/loss of fluoride is also predicted to oxidize phenylcyclopropane, though much less efficiently than the Selectfluor-derived radical dication.

<sup>47</sup> a) Wayner, D. D. M.; Arnold, D. R. *J. Chem. Soc., Chem. Commun.* **1982**, 1087-1088. b) Wayner, D. D. M.; Arnold, D. R. *Can. J. Chem.* **1985**, *63*, 871-881. c) Dinnocenzo, J. P.; Conlon, D. A. *J. Am. Chem. Soc.* **1988**, *110*, 2324-2326. d) Dinnocenzo, J. P.; Lieberman, D. R.; Simpson, T. R. *J. Am. Chem. Soc.* **1993**, *115*, 366-367. e) Dinnocenzo, J. P.; Conlon, D. A. *Tetrahedron Lett.* **1995**, *36*, 7415-7418. f) Dinnocenzo, J. P.; Simpson, T. R.; Zuilhof, H.; Todd, W. P.; Heinrich, T. *J. Am. Chem. Soc.*, **1997**, *119*, 987-993.

<sup>48</sup> Bigeleisen, J.; Mayer, M. G. *J. Chem. Phys.* **1947**, *15*, 261-267.

<sup>49</sup> Chai, J-D.; Head-Gordon, M. *Phys. Chem. Chem. Phys.* **2008**, *10*, 6615-6620.

<sup>50</sup> Considering that the putative acetonitrile-trapped intermediate is present in only trace amounts, it is difficult to accurately measure differences in rate/quantity. In an attempt to either suppress this signal or observe changes in diastereoselectivity, we synthesized the chloromethyl DABCO salt (**14**) and ran reactions with 1.0 equiv. and 5.0 equiv. **14** (greater equiv. lends way to solubility issues). The signal for the putative intermediate is still present over the course of the reaction. Additionally, we observed only marginal changes in diastereoselectivity - within error of our reported selectivity. These results are likely due to the fact that the solvent (acetonitrile) is still present in great excess of **14**; they do not militate against solvent assistance.

<sup>51</sup> For recent advances in the chemistry of organic thiocyanates, see: Castanheiro, T.; Suffert, J.; Donnard, M.; Gulea, M. *Chem. Soc. Rev.* **2016**, *45*, 494-505.

<sup>52</sup> Both inter- and intramolecular competition experiments with *ortho*-substituted aryl- and diarylcyclopropanes showed no linear trend with steric substituent constants.

## Chapter 9

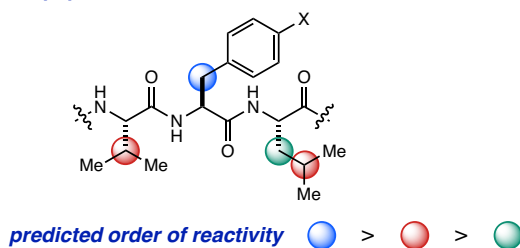
### Direct, Visible Light-sensitized Benzylic C-H Fluorination of Peptides Using Dibenzosuberenone: Selectivity for Phenylalanine-like Residues

#### 9.1 Introduction.

The typical procession of *synthetic method development* passes through three arenas: 1) reaction discovery, 2) optimization and mechanistic understanding, and 3) application. In the world of modern fluorine chemistry, our laboratory<sup>1</sup> and others<sup>2</sup> have discovered some of the first mild ways to effect "radical fluorination" of  $sp^3$  C-H bonds – transformations of high interest in the fields of medicine and agrochemistry (*arena 1*).<sup>3</sup> Significant strides have been made in producing and beginning to understand these reactions; however, greater selectivity and more tangible applications to the synthesis of biologically relevant molecules remain promising goals (*arenas 2 and 3*). Toward these efforts, we report a discrete photochemical method optimized for the site-selective fluorination of peptides.<sup>4</sup>

Historically, chemists have gone to great lengths to access  $\beta$ -fluorinated amino acids.<sup>5</sup> Recently, a few examples regarding direct C-H fluorination of individual amino acids have materialized in the chemical literature. For instance, palladium catalysis has proven valuable in ligand-directed syntheses of  $\beta$ -fluoro- $\alpha$ -amino acids.<sup>6</sup> To a much lesser extent, photochemical benzylic fluorination tactics have also emerged that include a single derivative of  $\beta$ -fluoro-phenylalanine in the substrate scope.<sup>7</sup> Given our interest in the latter approach, we asked: does the innate benzylic selectivity drop off when phenylalanine is incorporated into peptide chains (Figure 9.1)? Would we observe competitive fluorination on the tertiary sites of valine<sup>8</sup> and leucine,<sup>9</sup> for example? To our satisfaction, we found that our newly-developed photochemical approach using Selectfluor, catalytic dibenzosuberenone, and visible light (14-Watt CFL) is remarkably selective for the benzylic sites of phenylalanine- and tyrosine-like residues in short chain peptides that incorporate a variety of aliphatic and protected basic or acidic side chains.

*demonstration peptide for site-selective C-H fluorination*



**Figure 9.1** Benzylic selectivity strategy toward "directed" fluorination within peptide natural products.

## 9.2 Screening for Reaction Conditions.

Our initial screen included an evaluation of existing photochemical fluorination methods (developed in our laboratory<sup>7b,10</sup> and by others<sup>11</sup>) on a simple dipeptide – NPhth-Ala-Phe-OEt (**1**). Immediately, we found the methods that performed suitably in the fluorination of a single amino acid experienced a decline in product yield when applied to this dipeptide (Table 9.1). In some instances, increased loadings of the photosensitizers improved yields, but never above 50%. Accordingly, we expanded our survey to other potential ultraviolet and visible light photosensitizers. To our satisfaction, dibenzosuberenone<sup>12</sup> (5 mol %) and visible light from a 14-Watt CFL proved competent in the selective benzylic fluorination of NPhth-Ala-Phe-OEt using Selectfluor (2.0 equiv.) to provide **2** in 73% yield. We also noted that the diastereomeric ratio of the fluorinated product was ca. 2.1:1, regardless of photosensitizer.

Control experiments revealed that 1) the reaction does not proceed in the absence of either light or dibenzosuberenone, 2) increasing the amount of Selectfluor or dibenzosuberenone begins to have a negative impact on yield (though Selectfluor may be decreased to 1.5 equiv. in some cases with only a 5-10% decrease in yield), and 3) some benzylic fluorination is observed by heating the reaction mixture to reflux in the dark, albeit in poor yield (25%).<sup>13</sup> Furthermore, most photochemical fluorination methods require inert atmosphere, but this approach performs equally well in ambient air. Although anhydrous MeCN was used, rigorous exclusion of air and moisture (e.g. by degasification and Schlenk techniques) proved unnecessary - a testament to the robustness of the protocol.

**Table 9.1** Photochemical fluorination optimized for dipeptides.

Entry	Photosensitizer	(mol %)	Light source	Yield (%) <sup>a</sup>
1	1,2,4,5-Tetracyanobenzene	5	300 nm	21
2		10	300 nm	33
3	Anthraquinone	10	300 nm	38
4		20	300 nm	42
5	1,4-Dicyanobenzene	10	300 nm	18
6		20	300 nm	42
7	1-Cyanonaphthalene	20	300 nm	trace
8	9,10-Phenanthrenequinone	10	300 nm	22
9		20	300 nm	21
10	Xanthone	10	300 nm	39
11		5	14-Watt CFL	39
12	2,7-Dichloro-9-fluorenone	10	300 nm	28
13		5	14-Watt CFL	29
14	9-Fluorenone	20	300 nm	10
15		5	14-Watt CFL	31
16	Benzophenone	20	300 nm	40
17		5	14-Watt CFL	46
18	2-Bromo-9-fluorenone	5	14-Watt CFL	22
19	2-Chlorothioxanthone	5	14-Watt CFL	28
<b>20</b>	<b>5-Dibenzosuberone</b>	<b>5</b>	<b>14-Watt CFL</b>	<b>73<sup>b</sup></b>

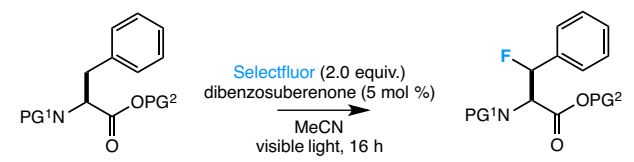
All reactions were irradiated in Pyrex microwave vials for 16 h while stirring, using either a 14-Watt CFL (visible light) or a Rayonet reactor (300 nm). In all cases, a 2.1:1 *dr* was observed. <sup>a</sup>Unless otherwise specified, <sup>19</sup>F NMR yields reported. <sup>b</sup>Isolated yield reported.

### 9.3 Evaluation of Substrate Scope.

Subsequently, we turned our attention to the scope of *N*- and *C*-termini protecting groups using phenylalanine derivatives (Table 9.2). Protecting group strategies are invaluable in peptide synthesis and may also be necessary to maintain compatibility with photochemical fluorination.<sup>14</sup> For instance, basic nitrogen sites have been particularly problematic in *sp*<sup>3</sup> C-H fluorination methods;<sup>15</sup> however, this may be circumvented through the installation of electron-withdrawing groups. Along these lines, phthalimido<sup>16</sup> (NPhth) and trifluoroacetate<sup>17</sup> (TFA) substituents at the *N*-terminus provided the best results (80% and 67%), and acetate groups were also competent (57%). On the other hand, Boc, Fmoc, and Cbz groups were not compatible with fluorination (0-10% yield). At the *C*-terminus, methyl and ethyl esters perform equally well,<sup>18</sup> but *tert*-butyl, trityl, and adamantyl esters decompose or undergo additional fluorination under the reaction conditions (accompanied with a decrease in yield). Moreover, we found that the *C*-terminus does

not require a protecting group – photochemical benzylic fluorination can be achieved in good yields in the presence of carboxylic acids without competitive decarboxylative fluorination.<sup>19</sup>

**Table 9.2** Protecting group compatibility.



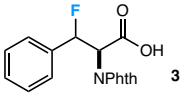
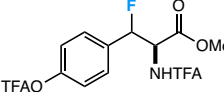
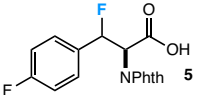
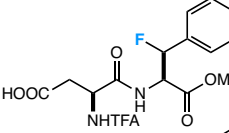
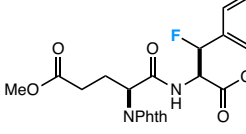
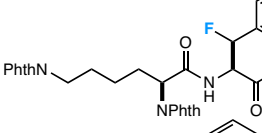
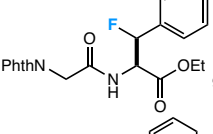
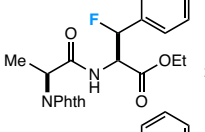
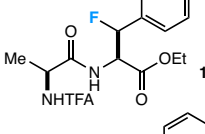
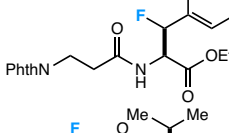
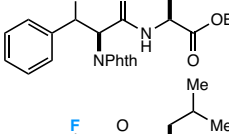
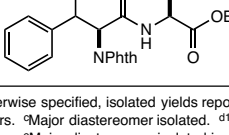
Entry	PG <sup>1</sup>	PG <sup>2</sup>	Yield (%) <sup>a</sup>
1	<i>tert</i> -butyloxycarbonyl (Boc)	-	10
2	fluorenylmethyloxycarbonyl (Fmoc)	-	0
3	carboxybenzyl (Cbz)	-	8
4	acetyl (Ac)	-	57
5	<b>trifluoroacetyl (TFA)</b>	-	<b>67</b>
6	<b>trifluoroacetyl (TFA)</b>	<b>methyl (Me)</b>	<b>74</b>
7	<b>trifluoroacetyl (TFA)</b>	<b>ethyl (Et)</b>	<b>60</b>
8	<b>phthalimide (Phth)</b>	-	<b>80<sup>b</sup></b>
9	-	-	0
10	<b>phthalimide (Phth)</b>	<b>methyl (Me)</b>	<b>78</b>
11	<b>phthalimide (Phth)</b>	<b>ethyl (Et)</b>	<b>80</b>
12	phthalimide (Phth)	<i>tert</i> -butyl ( <i>t</i> -Bu)	31
13	phthalimide (Phth)	trityl (Trt)	28
14	phthalimide (Phth)	1-adamantane (Ada)	20

<sup>a</sup>Unless otherwise specified, <sup>19</sup>F NMR yields reported. <sup>b</sup>Isolated yield reported.

In addition to phenylalanine, we envisioned that other benzylic residues could be targeted, such as tyrosine or other non-natural amino acids. The hydroxy substituent on tyrosine activates the aromatic ring toward background EAS with Selectfluor, which substantially diminishes selectivity and the extent of benzylic fluorination.<sup>20</sup> Acetylation reduces ring fluorination, but still results in poor desired product yields. However, transformation of the hydroxy substituent to a trifluoroacetyl group makes tyrosine residues viable candidates for direct benzylic fluorination (71% yield).<sup>21</sup> What is more, the phthalimide-protected *p*-fluoro-phenylalanine, an isoelectronic and isosteric replacement for tyrosine, underwent benzylic fluorination in 84% yield (Table 9.3).



**Table 9.3** Substrate scope: phenylalanine-like residues targeted for fluorination in amino acids and dipeptides.

Entry	Product	dr	Yield (%) <sup>a</sup>
1		1.2:1	80 <sup>b</sup>
2		1.4:1	71 <sup>c,d</sup>
3		1.2:1	84 <sup>b</sup>
4		1.8:1	78 <sup>b</sup>
5		2.1:1	71 <sup>c,d</sup>
6		2.2:1	61 <sup>c,d</sup>
7		3:1	69 <sup>c,d</sup> 52 <sup>d,e</sup> gram scale
8		2.1:1	73 <sup>c,d</sup>
9		2.1:1	67 <sup>b</sup>
10		2:1	47 <sup>b</sup>
11		1.4:1	62 <sup>d</sup>
12		1.2:1	65 <sup>d</sup>

<sup>a</sup>Unless otherwise specified, isolated yields reported. <sup>b</sup>Isolated as a mixture of diastereomers. <sup>c</sup>Major diastereomer isolated. <sup>d</sup><sup>19</sup>F NMR yield reported for both diastereomers. <sup>e</sup>Major diastereomer isolated in 40% yield.

At this juncture, we had established a visible light protocol on a prototypical dipeptide, determined the compatibility of an array of protecting groups, and investigated the viability of other phenylalanine-like residues as targets for benzylic fluorination (**3**, **4**, and **5**). The next step was to examine the regioselectivity and reaction efficiency in the presence of other amino acids. Thus, we explored a number of dipeptides incorporating one phenylalanine-like residue (Table 9.3).<sup>22</sup> Consistent with our protecting group screen, dipeptides with carboxylic acid side chains (i.e. aspartic acid in TFA-Aspartame and glutamic acid methyl ester in NPhth-Glu-(OMe)-Phe-OEt) were competent in regioselective fluorination (**6** and **7**). Likewise, dipeptides with basic amine side chains were amenable to fluorination (**8**) after applying the same protecting group strategy discussed above (e.g. NPhth-Lys-(NPhth)-Phe-OEt). In both instances (acidic and basic side chain derivatives), benzylic fluorination was nearly site-specific; that is, only trace secondary aliphatic or  $\alpha$ -fluorination was observed, if at all.

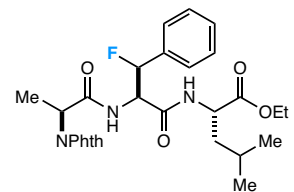
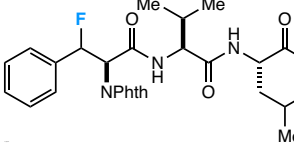
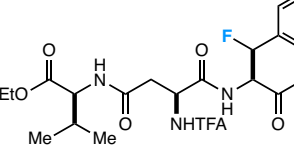
When it comes to nonpolar amino acids, glycine, alanine, and  $\beta$ -alanine derivatives intuitively are not susceptible to regioselectivity issues (**2**, **9-11**). Yet, valine, leucine, and isoleucine all contain tertiary sites that could conceivably compete with benzylic fluorination, assuming a radical-based mechanism.<sup>23</sup> (In fact, photochemical fluorination of the tertiary C-H site in valine has been reported in the literature.<sup>8</sup>) Fortuitously, benzylic fluorination is preferred over tertiary fluorination by more than an order of magnitude (**12** and **13**), with only 4% and trace yield of the tertiary fluoride on **12** and **13**, respectively. This is particularly exciting as NPhth-Val-OH undergoes tertiary fluorination in up to 73% yield under identical reaction conditions when not associated with phenylalanine.

We also extended our scope to a few phenylalanine-containing tripeptides (Table 9.4). For instance, NPhth-Ala-Phe-Leu-OEt displayed similar propensity toward benzylic fluorination as the dipeptides, providing the desired product **14** in 63% yield and high regioselectivity. Also, in the presence of both valine and leucine in NPhth-Phe-Val-Leu-OEt, the benzylic site of phenylalanine is still highly favored for C-H fluorination (**15**).

In general, the diastereoselectivity of the fluorination reactions on amino acids and dipeptides was low ( $\leq 3:1$  dr), but diastereomers were often separable by column chromatography. Regarding the tripeptides, individual fluorinated diastereomers were particularly difficult to isolate from starting material by standard column chromatography. This can be remedied, to some extent, by resubmitting the crude reaction mixture

(after workup) to the same reaction conditions by driving the reaction near complete conversion. However, difluorination of valine-containing peptides (i.e. at the benzylic and tertiary sites) becomes prevalent upon resubmission.

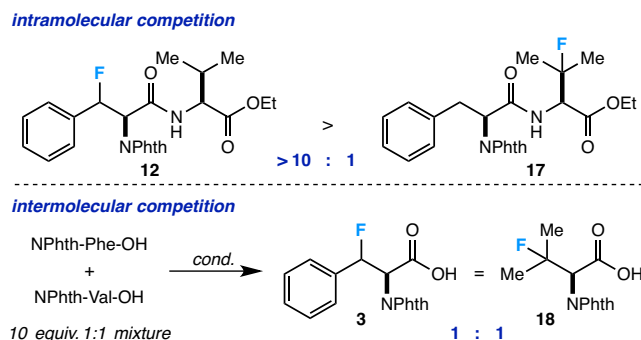
**Table 9.4** Regioselective fluorination showcased in tripeptides.

Entry	Product	dr	Yield (%)
1		1.3:1	63 <sup>a,b</sup>
2		1.4:1	34 <sup>c</sup>
3		1.8:1	42 <sup>c</sup>

<sup>a</sup>Isolated yield reported. <sup>b</sup>Isolated as a mixture of diastereomers. <sup>c</sup><sup>19</sup>F NMR yield reported.

#### 9.4 Preliminary Mechanistic Investigation.

To explore the benzylic selectivity over tertiary sites further, we conducted intra- and intermolecular competition experiments between phenylalanine and valine residues (Scheme 9.1).<sup>24</sup> Under the reaction conditions, the valine- and phenylalanine-containing dipeptide, in an intramolecular competition, underwent fluorination at the benzylic position (**12**) in a ratio > 10:1 over the tertiary site (**17**) by <sup>19</sup>F NMR analysis of the crude reaction mixture. On the other hand, a 1:1 mixture of phenylalanine and valine in an intermolecular competition experiment provided a somewhat unexpected result - a 1:1 mixture of benzylic:tertiary fluorinated products (**3:18**). Likely, there is a product-determining step that ensues the rate-determining step in the dipeptide.<sup>25</sup> This feature would be the culprit for our ability to target benzylic residues in small peptides, even in the presence of "equally reactive" tertiary sites.



**Scheme 9.1** Competition experiments.

## 9.5 Conclusion.

In all, we have found that Selectfluor (2.0 equiv.), catalytic dibenzosuberone (5 mol %), and visible light (14-Watt CFL) provide suitable photochemical conditions for the direct,  $sp^3$  benzylic C-H fluorination of phenylalanine-like residues in amino acids and short chain peptides. Protecting group compatibility was explored at both the *C*- and *N*-termini, and the propensity for benzylic fluorination was studied in the presence of amino acids with protected basic, acidic, and nonpolar side chains (including those with tertiary sites). Despite the near equal reactivity of benzylic and tertiary sites, as shown in an intermolecular competition experiment, the benzylic sites in dipeptides and tripeptides were observed to favor C-H fluorination by over an order of magnitude.

## 9.6 References.

<sup>1</sup> For some examples from our laboratory, see: a) Bloom, S.; Pitts, C. R.; Miller, D.; Haselton, N.; Holl, M. G.; Urheim, E.; Lectka, T. *Angew. Chem. Int. Ed.* **2012**, *51*, 10580-10583. b) Bloom, S.; Pitts, C. R.; Woltornist, R.; Griswold, A.; Holl, M. G.; Lectka, T. *Org. Lett.* **2013**, *15*, 1722-1724. c) Bloom, S.; Sharber, S. A.; Holl, M. G.; Knippel, J. L.; Lectka, T. *J. Org. Chem.* **2013**, *78*, 11082-11086. d) Pitts, C. R.; Ling, B.; Woltornist, R.; Liu, R.; Lectka, T. *J. Org. Chem.* **2014**, *79*, 8895-8899. e) Bloom, S.; Bume, D. D.; Pitts, C. R.; Lectka, T. *Chem. Eur. J.* **2015**, *21*, 8060-8063.

<sup>2</sup> For other recent advances in this research area, see: a) Rueda-Becerril, M.; Sazepin, C. C.; Leung, J. C. T.; Okbinoglu, T.; Kennepohl, P.; Paquin, J.-F.; Sammis, G. M. *J. Am. Chem. Soc.* **2012**, *134*, 4026-4029. b) Liu, W.; Huang, X.; Cheng, M.; Nielson, R. J.; Goddard III, W. A.; Groves, J. T. *Science* **2012**, *337*, 1322-1325. c) Yin, F.; Wang, Z.; Li, Z.; Li, C. *J. Am. Chem. Soc.* **2012**, *134*, 10401-10404. d) Liu, W.; Groves, J. T. *Angew. Chem. Int. Ed.* **2013**, *52*, 6024-6027. e) Amaoka, Y.; Nagamoto, M.; Inoue, M. *Org. Lett.* **2013**, *15*, 2160-2163. f) Braun, M.-G.; Doyle, A. *J. Am. Chem. Soc.* **2013**, *135*, 12990-12993. g) Xia, J.-B.; Ma, Y.; Chen, C.

*Org. Chem. Front.* **2014**, *1*, 468-472. h) Rueda-Becerril, M.; Mahe, O.; Drouin, M.; Majewski, M. B.; West, J. G.; Wolf, M. O.; Sammis, G. M.; Paquin, J.-F. *J. Am. Chem. Soc.* **2014**, *136*, 2637-2641. i) Li, Z.; Wang, Z.; Zhu, L.; Tan, X.; Li, C. *J. Am. Chem. Soc.* **2014**, *136*, 16439-16443. j) Phae-nok, S.; Soorukram, D.; Kuhakarn, C.; Reutrakul, V.; Pohmakotr, M. *Eur. J. Org. Chem.* **2015**, *2015*, 2879-2888.

<sup>3</sup> a) Böhm, H.-J.; Banner, D.; Bendels, S.; Kansy, M.; Kuhn, B.; Müller, K.; Obst-Sander, U.; Stahl, M. *ChemBioChem* **2004**, *5*, 637-643. b) Purser, S.; Moore, P. R.; Swallow, S.; Gouverneur, V. *Chem. Soc. Rev.* **2008**, *37*, 320-330. c) Patrick, G. L. *An Introduction to Medicinal Chemistry*, 5<sup>th</sup> ed.; Oxford University Press: Oxford, UK, 2013. d) Ojima, I. *J. Org. Chem.* **2013**, *78*, 6358-6383. e) Gillis, E. P.; Eastman, K. J.; Hill, M. D.; Donnelly, D. J.; Meanwell, N. A. *J. Med. Chem.* **2015**, *58*, 8315-8359.

<sup>4</sup> Applications of fluorinated peptides are numerous, diverse, and well presented. For some recent reviews and other literature, see: a) Okarvi, S. *Eur. J. Nucl. Med.* **2001**, *28*, 929-938. b) Yoder, N. C.; Kumar, K. *Chem. Soc. Rev.* **2002**, *31*, 335-341. c) Salwiczek, M.; Nyakatura, E. K.; Gerling, U. I. M.; Ye, S.; Kokschi, B. *Chem. Soc. Rev.* **2012**, *41*, 2135-2171. d) Kumar, D. N. T.; Mehdi, N.; Huang, F.; Zhang, M.; Wei, Q. *Int. J. Eng. Res. Appl.* **2012**, *2*, 77-84.

<sup>5</sup> For some examples, see: a) Hart, B. P.; Coward, J. K. *Tetrahedron Lett.* **1993**, *34*, 4917-4920. b) DeJesus, O. T.; Murali, D.; Kitchen, R.; Oakes, T. R.; Nickles, R. J. *J. Fluorine Chem.* **1993**, *65*, 73-77. c) Shi, G.-Q.; Cao, Z.-Y.; Zhang, X.-B. *J. Org. Chem.* **1995**, *60*, 6608-6611. d) Li, K.; Leriche, C.; Liu, H.-W. *Bioorg. Med. Chem. Lett.* **1998**, *8*, 1097-1100. e) Qiu, X.-L.; Meng, W.-D.; Qing, F.-L. *Tetrahedron* **2004**, *60*, 6711-6745. f) Okuda, K.; Hirota, T.; Kingery, D. A.; Nagasawa, H. *J. Org. Chem.* **2009**, *74*, 2609-2612.

<sup>6</sup> a) Zhu, R.-Y.; Tanaka, K.; Li, G.-C.; He, J.; Fu, H.-Y.; Li, S.-H.; Yu, J.-Q. *J. Am. Chem. Soc.* **2015**, *137*, 7067-7070. b) Zhang, Q.; Yin, X.-S.; Chen, K.; Zhang, S.-Q.; Shi, B.-F. *J. Am. Chem. Soc.* **2015**, *137*, 8219-8226. c) Miao, J.; Yang, K.; Kurek, M.; Ge, H. *Org. Lett.* **2015**, *17*, 3738-3741. d) Lu, X.; Xiao, B.; Shang, R.; Liu, L. *Chin. Chem. Lett.* **2016**, *27*, 305-311.

<sup>7</sup> a) Xia, J.-B.; Zhu, C.; Chen, C. *J. Am. Chem. Soc.* **2013**, *135*, 17494-17500. b) Bloom, S.; McCann, M.; Lectka, T. *Org. Lett.* **2014**, *16*, 6338-6341.

<sup>8</sup> a) Xia, J.-B.; Zhu, C.; Chen, C. *Chem. Commun.* **2014**, *50*, 11701-11704. b) Halperin, S. D.; Fan, H.; Chang, S.; Martin, R. E.; Britton, R. *Angew. Chem. Int. Ed.* **2014**, *53*, 4690-4693.

<sup>9</sup> Halperin, S. D.; Kwon, D.; Holmes, M.; Regalado, E. L.; Campeau, L.-C.; DiRocco, D. A.; Britton, R. *Org. Lett.* **2015**, *17*, 5200-5203.

<sup>10</sup> a) Bloom, S.; Knippel, J. L.; Lectka, T. *Chem. Sci.* **2014**, *5*, 1175-1178. b) Pitts, C. R.; Bloom, M. S.; Bume, D. D.; Zhang, Q. A.; Lectka, T. *Chem. Sci.* **2015**, *6*, 5225-5229.

<sup>11</sup> Chatalova-Sazepin, C.; Hemelaere, R.; Paquin, J.-F.; Sammis, G. M. *Synthesis* **2015**, *47*, 2554-2569, and references cited therein.

<sup>12</sup> For a theoretical study on the excitation dynamics of dibenzo-suberone, see: Nakai, H.; Baba, T. *J. Mol. Struct.* **2005**, *735*-736, 211-216.

<sup>13</sup> Chambers, R. D.; Kenwright, A. M.; Parsons, M.; Sandford, G.; Moilliet, J. S. *J. Chem. Soc., Perkin Trans. 1* **2002**, 2190-2197.

<sup>14</sup> Sureshbabu, V. V.; Narendra, N. Protection Reactions. In *Amino Acids, Peptides and Proteins in Organic Chemistry*; Hughes, A. B., Ed.; Wiley-VCH Verlag GmbH & Co. KGaA: Weinheim, 2011.

- 
- <sup>15</sup> In our experience, basic nitrogen sites are typically either oxidized or fluorinated (followed by a Stevens-like rearrangement) in the presence of N-F reagents.
- <sup>16</sup> For standard phthalimide *N*-protection procedure, see: Satzinger, G. *Arzneim-Forsch. Drug Res.* **1994**, *44*, 261-266.
- <sup>17</sup> For a trifluoroacetate *N*-protection procedure, see: Curphey, T. J. *J. Org. Chem.* **1979**, *44*, 2805-2807.
- <sup>18</sup> For a sample esterification procedure for amino acids, see: Armstrong, A.; Edmonds, I. D.; Swarbrick, M. E.; Treweeke, N. R. *Tetrahedron* **2005**, *61*, 8423-8442.
- <sup>19</sup> For examples of decarboxylative fluorination applied to a phenyl-alanine derivative, see: a) Wu, X.; Meng, C.; Yuan, X.; Jia, X.; Qian, X.; Ye, J. *J. Chem. Commun.* **2015**, *51*, 11864-11867. b) Ventre, S.; Petronijevic, F. R.; MacMillan, D. W. C. *J. Am. Chem. Soc.* **2015**, *137*, 5654-5657. c) Huang, X.; Liu, W.; Hooker, J. M.; Groves, J. T. *Angew. Chem. Int. Ed.* **2015**, *54*, 5241-5245.
- <sup>20</sup> Banks, R. E.; Besheesh, M. K.; Mohialdin-Khaffaf, S. N.; Sharif, I. *J. Chem. Soc., Perkin Trans. 1* **1996**, 2069-2076.
- <sup>21</sup> Lugemwa, F. N.; Shaikh, K.; Hochstedt, E. *Catalysts* **2013**, *3*, 954-965.
- <sup>22</sup> Dipeptides were synthesized using a standard DCC coupling protocol. See: Rich, D. H.; Singh, J. The carbodiimide method. In *The Peptides: Analysis, Synthesis, Biology*; Gross, E., Meienhofer, J., Eds.; Academic: New York, 1979; pp 241-261.
- <sup>23</sup> Although photochemical C-H fluorination methods have not yet been studied extensively, a few detailed mechanistic studies on "radical fluorination" using Selectfluor have appeared in recent literature. See: a) Pitts, C. R.; Bloom, S.; Woltornist, R.; Auvenshine, D. J.; Ryzhkov, L. R.; Siegler, M. A.; Lectka, T. *J. Am. Chem. Soc.* **2014**, *136*, 9780-9791. b) Patel; N. R.; Flowers II, R. A. *J. Org. Chem.* **2015**, *80*, 5834-5841. c) Pitts, C. R.; Ling, B.; Snyder, J. A.; Bragg, A. E.; Lectka, T. *J. Am. Chem. Soc.* **2016**, *138*, 6598-6609.
- <sup>24</sup> Anslyn, E. V.; Dougherty, D. A. *Modern Physical Organic Chemistry*; University Science Books: Sausalito, CA, 2006.
- <sup>25</sup> For a discussion on rate- and product-determining steps in competition experiments (with respect to KIEs), see: Simmons, E. M.; Hartwig, J. F. *Angew. Chem. Int. Ed.* **2012**, *51*, 3066-3072.

## Chapter 10

### Multiple Enone-directed Reactivity Modes Lead to the Selective Photochemical Fluorination of Polycyclic Terpenoid Derivatives

#### 10.1 Introduction.

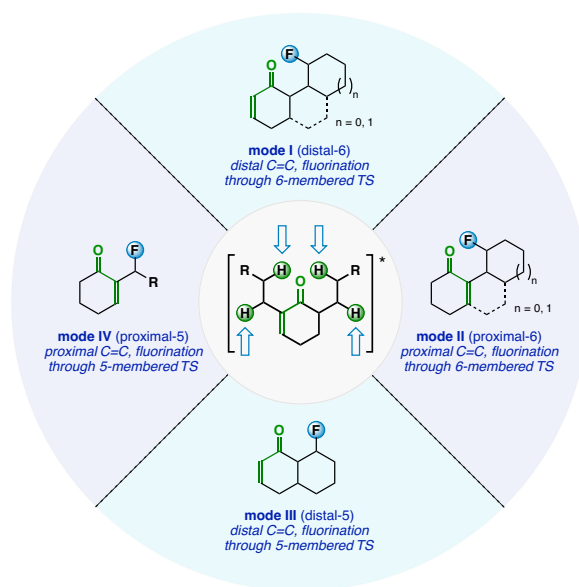
*Reactivity* and *selectivity* define two central challenges in aliphatic C–H bond functionalization. In the domain of aliphatic fluorination, recent advances in *reactivity* beyond the reliance on harsh reagents such as fluorine gas are notable.<sup>1</sup> Since the advent of metal-catalyzed  $sp^3$  C–H fluorination in 2012,<sup>2</sup> we, and others, have developed several user-friendly examples of aliphatic fluorination reactions using transition metal catalysts,<sup>3</sup> organocatalysts,<sup>4</sup> radical initiators,<sup>5</sup> and photosensitizers,<sup>6</sup> putting controllable "radical fluorination" within arm's reach. However, using these methods, *selectivity* is still quite limited to smaller molecules of high symmetry and to those with more acidic C–H bonds adjacent to aromatic rings or activated by chelating auxiliaries.<sup>7,8</sup> In a few cases, selective fluorination has been observed on more intricate substrates, but it is usually in a serendipitous and unpredictable fashion. More often, the subsection of molecules with large numbers of dissimilar C–H bonds to these procedures results in a large number of fluorinated products. Given the growing importance of fluorinated molecules in medicine,<sup>9</sup> among areas of biology, agrochemistry, and materials science, the leap toward *predictable, site-selective  $sp^3$  C–H fluorination on complex molecules* is both timely and necessary.

Accordingly, we show that the enone functional group, upon photoexcitation, can direct  $sp^3$  C–H fluorination with a high degree of predictability in less than 4 hours. By the placement of the enone oxygen at various positions in steroids and other bioactive polycycles, different sites can be fluorinated selectively that otherwise would be inaccessible on substrates with as many as 65  $sp^3$  C–H bonds. Notably, steroidal and other terpenoidal enones constitute a number of drugs on the market and in clinical trials (in part, due to improved physicochemical and pharmacokinetic properties over non-oxidized counterparts<sup>10</sup>), asserting them as desirable targets for fluorine installation. In addition, we have found that the enone group can direct either  $\gamma$ - or  $\beta$ -fluorination through a number of modes that involve different transition state conformations, ring sizes, and C=C bond positioning. Here, the strict proclivity for  $\gamma$ - or  $\beta$ -hydrogen atom abstraction is surprising, given the ability of enone photoexcitation to promote  $\alpha$ -cleavage (Norrish I),  $\beta$ -

cleavage (Norrish II), cyclization (Norrish-Yang), geometric isomerization, dimerization, and electron transfer chemistry, among other reactions.<sup>11</sup> Furthermore, we demonstrate the ability to predict <sup>19</sup>F NMR shifts using DFT calculations to assist in product characterization prior to isolation. Finally, we offer preliminary insight on the putative enone-assisted hydrogen atom transfer mechanism.

## 10.2 Classification of Reactivity Modes.

As this method can be used to access a variety of C–H sites through well-defined reactivity modes, we offer a classification system for the anticipated products of an enone-directed photochemical fluorination based on proximity of the C=C bond to the reaction site and the conformation of the transition state (Figure 10.1).



**Figure 10.1** Classification of reactivity modes (I-IV) that lead to selective  $\gamma$ -,  $\beta$ -, homoallylic, and allylic photochemical fluorination.

*Mode I* and *mode II* represent reactions that proceed through 6-membered transition states with the placement of the enone C=C bond distal and proximal, respectively, to the fluorination site. Interestingly, *mode III* and *mode IV* represent reactions that proceed through 5-membered transition states and are also compatible with distal and proximal C=C bond placement. Note that the proximal *mode II* and *mode IV* are



distinguished from distal modes because the products represent chemically distinct homoallylic and allylic fluorides. In all, we have found these four reactivity modes to be predictable and directly applicable to targeting previously inaccessible fluorination sites on biologically relevant terpenoids and derivatives thereof.<sup>12</sup> What is more, the reaction is operationally simple and mindful of principles of green chemistry, requiring only the enone, Selectfluor, and mid- to near-ultraviolet light (see conditions in Table 10.1).

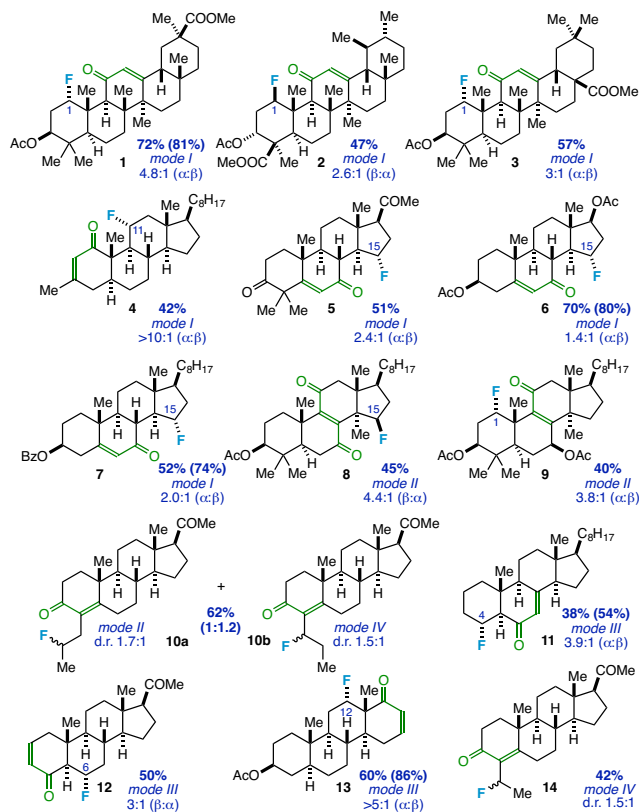
### 10.3 Evaluation of Substrate Scope.

The most abundant or easily accessible enones on polycycles are those primed for C–H fluorination through the 6-membered transition state (*modes I and II*); thus, the corresponding  $\gamma$ -fluorination products comprise the majority of Table 10.1. The starting materials for compounds **1-3** represent derivatives of the pentacyclic triterpenoids 18- $\beta$ -glycyrrhetic acid, boswellic acid, and oleanolic acid, with the enone located on the C-ring poised for *mode I* fluorination on the A-ring (analogues of these molecules have been shown to exhibit numerous pharmacological properties, including anti-inflammatory,<sup>13</sup> anticancer,<sup>14</sup> anti-HIV,<sup>15</sup> and anti-HCV<sup>16</sup>). The predicted fluorinated products at the C1 position were obtained in good yields (up to 72%) with a preference for the  $\alpha$ -isomer in **1** and **3** and the  $\beta$ -isomer in **2**. Upon isolation, the site of fluorination for each product was confirmed by 1) relocation of the distinct equatorial C1 hydrogen atom in the <sup>1</sup>H NMR spectrum (dt at ~ 2.8 ppm) of the starting material to the appropriate chemical shift and splitting of a hydrogen atom geminal to fluorine, 2) <sup>2</sup>J<sub>CF</sub>- and <sup>3</sup>J<sub>CF</sub>-coupling to distinguishable peaks in the <sup>13</sup>C NMR spectrum (see Chapter 12 for details), and 3) comparison to the calculated <sup>19</sup>F NMR shifts using an empirical equation developed in our laboratory.<sup>17</sup> If the enone is placed instead on the A-ring, poised for *mode I* fluorination on the C-ring (compound **4**), selective fluorination at the C11 position can be achieved. In this instance, we determined the  $\alpha$ -isomer to be the major diastereomer and have identified the fluorination site as stated above.

We also investigated *mode I* fluorination of the D-ring at the C15 position by placing the enone group on the B-ring of derivatives of bioactive steroids such as progesterone, testosterone acetate, and cholesterol (compounds **5-7**). In fact, fluorination on the five-membered ring occurs in up to 70% yield ( $\alpha$ -isomer favored), as confirmed by chemical shift and <sup>2</sup>J<sub>HF</sub>-coupling in the <sup>19</sup>F NMR spectra (> 50 Hz is typical for cyclopentane ring fluorination) followed by <sup>13</sup>C NMR analysis of the products. Furthermore, crystals were

grown of compound **5** through solvent evaporation that proved suitable for X-ray structure determination. To the best of our knowledge, the C15 position is an unprecedented site of fluorination, and thus, products of this reaction could be interesting candidates for studying structure-activity relationships and pharmacological properties.<sup>18</sup>

**Table 10.1** Directed photochemical sp<sup>3</sup> C–H fluorination of bioactive polycyclic terpenoid derivatives.



The substrates and 2.2 equiv. of Selectfluor were stirred in MeCN solvent under N<sub>2</sub> for 4 h in a Rayonet reactor (300 or 350 nm bulbs). Yields include both diastereomers and were determined by integration of <sup>19</sup>F NMR signals using 3-chlorobenzotrifluoride as an internal standard and confirmed by isolation of products via column chromatography. Yields in parentheses are based on recovered starting materials. Diastereomeric ratios are reported; major diastereomers with respect to C–F bond are depicted in known cases. Reactivity modes are indicated.

In lanosterol derivatives **8** and **9**, enones were shown to direct homoallylic (*mode II*) fluorination at the C15 and C1 positions, respectively, through similar transition states. Interestingly, enedione **8** can undergo fluorination at either position, yet favors functionalization of the C15 position (here, the  $\beta$ -isomer is preferred, likely due to the vicinal methyl group on the bottom face). We attribute the observed selectivity to the "polar effect;" that is, the inductive effect from the electron-withdrawing group at the C3 position

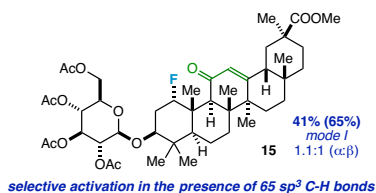
(acetate) decreases the reactivity of the C1 hydrogen atoms relative to those at the C15 position toward abstraction. This phenomenon is well preceded in radical-based hydrogen atom abstractions.<sup>19</sup> Notably, if the option to fluorinate the C15 position is removed, fluorination will still occur three bonds away at C1 (**9**). However, if an electron-withdrawing group (for instance, an acetate or a carbonyl) is present two bonds from the fluorination site, we have found that reactivity is suppressed.

In addition to 5- and 6-membered ring fluorination on polycyclic cores, we discovered that the reaction is amenable to *mode II* side-chain fluorination. Running the reaction on a progesterone derivative with an n-propyl group in the C4 position, we discovered the anticipated homoallylic fluoride along with the unexpected allylic fluoride in near equal ratios (~1:1.2 **10a:10b**) by <sup>19</sup>F NMR analysis. This result prompted an investigation of fluorination through less common 5-membered transition states to, at the very least, double the number of accessible fluorination sites on steroids (and other polycycles) using this method.

The starting enones for **11**, **12**, and **13** were synthesized in order to determine the viability of fluorination through 5-membered transition states with the C=C bond distal to the reaction site (*mode III*). In fact, *mode III* fluorination in up to 60% yield was achieved on the decalin-like substructures that permit selective  $\beta$ -functionalization on the C4 (**11**, A-ring,  $\alpha$ -isomer favored), C6 (**12**, B-ring,  $\alpha$ -isomer favored), and C12 (**13**, C-ring,  $\alpha$ -isomer favored) positions by <sup>19</sup>F, <sup>1</sup>H, and <sup>13</sup>C NMR analyses. Finally, the aforementioned result of the n-propylated progesterone suggested one more reactivity mode, *mode IV*, which would allow access to allylic fluorides. An ethylated analog was synthesized that underwent *mode IV* fluorination exclusively in the allylic position (**14**), with no primary fluoride observed from a *mode II* reaction. Allylic fluorination on the secondary position was also favored over homoallylic fluorination on the tertiary position of an isobutyl-substituted progesterone (not shown in Table 10.1), albeit the reaction proceeded in poor yield. Nevertheless, this result is significant in establishing basic reactivity trends such that secondary > tertiary and primary carbon fluorination sites.

As a testament to the selectivity of the reaction, we subjected triterpenoid saponin derivative **15** to photochemical fluorination. Even in the presence of 65 distinct sp<sup>3</sup> C–H bonds, the enone functional group very effectively directs fluorination to the C1 position in 41% yield (Figure 10.2). Here, and in most cases (*modes I-IV*), it is important to note that the majority of the mass balance can be accounted for with

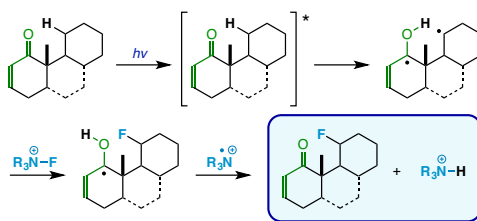
recovered starting material and very minor fluorinated byproducts through NMR analyses of the crude reaction mixture. Though, in some cases, we have identified slight, competitive fluorination directed by ketones (for example, compounds **5**, **10**, **12**, and **14**). From another vantage point, we have found preliminary success in the fluorination of simpler enone substrates, e.g. 2-butylcyclohexa-2-en-1-one (predominately mode IV) and piperitone (mode III), albeit in lower yields. In general, we note that the method is better primed for rigid structures, regardless of complexity.



**Figure 10.2** Fluorination of triterpenoid saponin derivative **15** in an extreme illustration of selectivity.

#### 10.4 Preliminary Mechanistic Investigation.

Finally, we present a preliminary mechanistic hypothesis (Figure 10.3). Regarding reaction initiation, we addressed the role of photochemistry with a number of control experiments. To rule out thermal processes, reactions were performed at the operating temperature of the Rayonet reactor (~40 °C), but they provided no fluorinated products (although, at reflux, note that a large distribution of different fluorinated products is observed<sup>20</sup>). The UV-vis spectra of Selectfluor and the enone-containing substrates reveal that Selectfluor has no absorbance above the Pyrex cut-off (ca. 275 nm)<sup>21</sup> and the substrates typically absorb between 275 and 380 nm; therefore, the substrates contain the only possible chromophores under our reaction conditions. Literature precedent suggests that excited enones experience rapid intersystem crossing from the singlet ( $S_1$ ) state to the triplet state ( $T_1$ ), and that enones with  $n \rightarrow \pi^*$  lowest-energy  $T_1$  states can undergo hydrogen atom abstraction.<sup>11</sup> If a triplet mechanism is at play, we should be able to effect the reaction with a triplet sensitizer. Accordingly, if the reaction is run using cool white LED's (cut-off at ca. 400 nm), no fluorinated products are observed. Yet if the same reaction is performed in the presence of 9-fluorenone, a known triplet sensitizer with absorbance above 400 nm,<sup>22</sup> *the desired fluorinated products are observed*. Thus, we can conclude that enone photochemistry plays a crucial role in the mechanism and reactivity likely occurs from  $T_1$ .



**Figure 10.3** Preliminary mechanistic hypothesis for enone-directed photochemical  $sp^3$  C–H fluorination using Selectfluor.

An intramolecular hydrogen atom abstraction directed by the  $T_1$  excited enone would explain the observed selectivity.<sup>23</sup> In fact, we have calculated transition states for intramolecular 1,4- and 1,5-hydrogen atom transfer at B3LYP/6-311++G\*\* (activation energies ( $E_a$ ) of 9.1 and 9.8 kcal/mol, respectively) that suggest these are reasonable processes. Beyond this step, the translocated, carbon-centered radical is susceptible to fluorination in the presence of Selectfluor, which is known to react with free radicals very rapidly.<sup>24</sup> The Selectfluor-derived byproduct of this step – the  $N$ -centered radical – could conceivably undergo hydrogen atom transfer from the oxygen atom to regenerate the carbonyl carbon and terminate the  $N$ -centered radical. In order to probe the role of the  $N$ -centered radical, we generated it in the dark using the established triethylborane method<sup>5</sup> and examined the  $^{19}\text{F}$  NMR spectrum of the reaction mixture. Note that we have previously shown that this intermediate is responsible for C–H cleavage,<sup>25</sup> as well as oxidation,<sup>21</sup> in radical chain fluorination reactions, but its role as a chain propagator seems unlikely here. As anticipated, a triethylborane-initiated reaction resulted in minor  $sp^3$  C–H fluorination, but did not provide similar fluorinated products, yields, or selectivity. Thus, if the  $N$ -centered radical is formed under photochemical conditions, it is necessarily playing a different role, that is, likely, hydrogen atom transfer from the oxygen to restore the enone in the final step. In all, this appears to be a reasonable mechanism; however, enone photochemistry is generally complicated. Thus, at this time it is difficult to rule out the possibility of electron transfer chemistry playing a role.

## 10.5 Conclusion.

Considering the complexity of enone photochemistry, the ability to direct  $sp^3$  C–H fluorination on such intricate molecules is a surprising and notable result. The reaction is relatively fast, simple, and predictable, thus paving clear paths to new late-stage fluorination products. In addition, this method has effectively quadrupled the number of accessible C–H sites for aliphatic fluorination on steroids. Accordingly, we anticipate near-term adoption of this method in a medicinal chemistry setting, and we hope it will encourage the exploration of additional enone-directed functionalization and corresponding mechanistic elucidation.

## 10.6 References.

- 
- <sup>1</sup> Champagne, P. A.; Desroches, J.; Hamel, J.-D.; Vandamme, M.; Paquin, J.-F. *Chem. Rev.* **2015**, *115*, 9073-9174.
- <sup>2</sup> (a) Liu, W.; Huang, X.; Cheng, M.-J.; Nielsen, R. J.; Goddard III, W. A.; Groves, J. T. *Science* **2012**, *337*, 1322-1325. (b) Bloom, S.; Pitts, C. R.; Miller, D. C.; Haselton, N.; Holl, M. G.; Urheim, E.; Lectka, T. *Angew. Chem. Int. Ed.* **2012**, *51*, 10580-10583.
- <sup>3</sup> (a) Bloom, S.; Pitts, C. R.; Woltornist, R.; Griswold, A.; Holl, M. G.; Lectka, T. *Org. Lett.* **2013**, *15*, 1722-1724. (b) Liu, W.; Groves, J. T. *Angew. Chem. Int. Ed.* **2013**, *52*, 6024-6027. (c) Xia, J.-B.; Ma, Y.; Chen, C. *Org. Chem. Front.* **2014**, *1*, 468-472.
- <sup>4</sup> Amaoka, Y.; Nagatomo, M.; Inoue, M. *Org. Lett.* **2013**, *15*, 2160-2163.
- <sup>5</sup> Pitts, C. R.; Ling, B.; Woltornist, R.; Liu, R.; Lectka, T. *J. Org. Chem.* **2014**, *79*, 8895-8899.
- <sup>6</sup> (a) Xia, J.-B.; Zhu, C.; Chen, C. *J. Am. Chem. Soc.* **2013**, *135*, 17494-17500. (b) Bloom, S.; Knippel, J. L.; Lectka, T. *Chem. Sci.* **2014**, *5*, 1175-1178. (c) Kee, C. W.; Chin, K. F.; Wong, M. W.; Tan, C.-H. *Chem. Commun.* **2014**, *50*, 8211-8214. (d) Xia, J.-B.; Zhu, C.; Chen, C. *Chem. Commun.* **2014**, *50*, 11701-11704. (e) Halperin, S. D.; Fan, H.; Chang, S.; Martin, R. E.; Britton, R. *Angew. Chem. Int. Ed.* **2014**, *53*, 4690-4693. (f) Rueda-Becerril, M.; Mahe, O.; Drouin, M.; Majewski, M. B.; West, J. G.; Wolf, M. O.; Sammis, G. M.; Paquin, J.-F. *J. Am. Chem. Soc.* **2014**, *136*, 2637-2641. (g) West, J. G.; Bedell, T. A.; Sorensen, E. J. *Angew. Chem. Int. Ed.* **2016**, *55*, 8923-8927. (h) Bume, D. D.; Pitts, C. R.; Jokhai, R. T.; Lectka, T. *Tetrahedron* **2016**, *72*, 6031-6036.
- <sup>7</sup> (a) Zhu, R.-Y.; Tanaka, K.; Li, G.-C.; He, J.; Fu, H.-Y.; Li, S.-H.; Yu, J.-Q. *J. Am. Chem. Soc.* **2015**, *137*, 7067-7070. (b) Zhang, Q.; Yin, X.-S.; Chen, K.; Zhang, S.-Q.; Shi, B.-F. *J. Am. Chem. Soc.* **2015**, *137*, 8219-8226. (c) Miao, J.; Yang, K.; Kurek, M.; Ge, H. *Org. Lett.* **2015**, *17*, 3738-3741. (d) Lu, X.; Xiao, B.; Shang, R.; Liu, L. *Chin. Chem. Lett.* **2016**, *27*, 305-311.
- <sup>8</sup> Amidyl radical-based remote C–H fluorination reactions have also been reported, but with limited scope: (a) Li, Z.; Song, L.; Li, C. *J. Am. Chem. Soc.* **2013**, *135*, 4640-4643. (b) Groendyke, B. J.; AbuSalim, D. I.; Cook, S. P. *J. Am. Chem. Soc.* **2016**, *138*, 12771-12774.
- <sup>9</sup> Purser, S.; Moore, P. R.; Swallow, S.; Gouverneur, V. *Chem. Soc. Rev.* **2008**, *37*, 320-330.
- <sup>10</sup> Michaudel, Q.; Journot, G.; Regueiro-Ren, A.; Goswami, A.; Guo, Z.; Tully, T. P.; Zou, L.; Ramabhadran, R. O.; Houk, K. N.; Baran, P. S. *Angew. Chem. Int. Ed.* **2014**, *53*, 12091-12096.

- 
- <sup>11</sup> Turro, N. J.; Scaiano, J. C.; Ramamurthy, V. *Modern Molecular Photochemistry of Organic Molecules*; University Science Books: Sausalito, CA, 2010.
- <sup>12</sup> Predictability and selectivity are aided by structural rigidity of the substrates.
- <sup>13</sup> Han, N.; Bakovic, M. *J. Bioanal. Biomed.* **2015**, *S12*, 1-11.
- <sup>14</sup> Petronelli, A.; Pannitteri, G.; Testa, U. *Anti-Cancer Drugs* **2009**, *20*, 880-892.
- <sup>15</sup> Cassels, B. K.; Asencio, M. *Phytochem. Rev.* **2011**, *10*, 545-564.
- <sup>16</sup> Yu, F.; Wang, Q.; Zhang, Z.; Peng, Y.; Qiu, Y.; Shi, Y.; Zheng, Y.; Xiao, S.; Wang, H.; Huang, X.; Zhu, L.; Chen, K.; Zhao, C.; Zhang, C.; Yu, M.; Sun, D.; Zhang, L.; Zhou, D. *J. Med. Chem.* **2013**, *56*, 4300-4319.
- <sup>17</sup> At B3LYP/6-311++G\*\*, we performed geometry optimizations on a number of fluorinated products in Gaussian, followed by NMR calculations using the CSGT method. After compiling the calculated isotropic shifts for the fluorine atoms, we performed a simple linear regression analysis between these isotropic shifts ( $\delta_{\text{iso}}$ ) and experimentally observed chemical shifts in the <sup>19</sup>F NMR spectra ( $\delta_{\text{obs}}$ ). In doing so, we established an empirical equation that was used to predict the <sup>19</sup>F NMR shift ( $\delta_{\text{calc}}$ ) of a desired polycyclic product within an average of  $0.6 \pm 0.5$  ppm ( $|\delta_{\text{obs}} - \delta_{\text{calc}}|$ ), which is significant in light of the large <sup>19</sup>F NMR chemical shift range. The equation was also helpful in assigning stereochemistry of the diastereomers prior to isolation and full characterization.
- <sup>18</sup> Kumagai, G.; Takano, M.; Shindo, K.; Sawada, D.; Saito, N.; Saito, H.; Kakuda, S.; Takagi, K.-I.; Takimoto-Kamimura, M.; Takenouchi, K.; Chen, T. C.; Kittaka, A. *Anticancer Res.* **2012**, *32*, 311-317.
- <sup>19</sup> (a) Walling, C. *Free Radicals in Solution*; Wiley: New York, NY, 1957. (b) Zavitsas, A. A.; Pinto, J. A. *J. Am. Chem. Soc.* **1972**, *94*, 7390-7396. (c) Newhouse, T.; Baran, P. S. *Angew. Chem. Int. Ed.* **2011**, *50*, 3362-3374.
- <sup>20</sup> Chambers, R. D.; Parsons, M.; Sandford, G.; Bowden, R. *Chem. Commun.* **2000**, 959-960.
- <sup>21</sup> Pitts, C. R.; Ling, B.; Snyder, J. A.; Bragg, A. E.; Lectka, T. *J. Am. Chem. Soc.* **2016**, *138*, 6598-6609.
- <sup>22</sup> Valentine, Jr., D.; Hammond, G. S. *J. Am. Chem. Soc.* **1972**, *94*, 3449-3454.
- <sup>23</sup> For examples of selective C-H functionalization achieved through stepwise Norrish-Yang cyclization and oxidation/iodination, see: (a) Wehrli, H.; Heller, M. S.; Schaffner, K.; Jeger, O. *Helv. Chim. Acta* **1961**, *44*, 2162-2173. (b) Renata, H.; Zhou, Q.; Baran, P. S. *Science* **2013**, *339*, 59-63.
- <sup>24</sup> Rueda-Becerril, M.; Sazepin, C. C.; Leung, J. C. T.; Okbinoglu, T.; Kennepohl, P.; Paquin, J.-F.; Sammis, G. M. *J. Am. Chem. Soc.* **2012**, *134*, 4026-4029.
- <sup>25</sup> Pitts, C. R.; Bloom, S.; Woltornist, R.; Auvenshine, D. J.; Ryzhkov, L. R.; Siegler, M. A.; Lectka, T. *J. Am. Chem. Soc.* **2014**, *136*, 9780-9791.

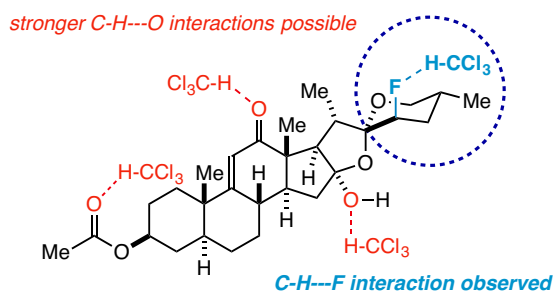
## Chapter 11

### An Intermolecular Aliphatic C-F---H-C Interaction in the Presence of "Stronger" Hydrogen Bond

#### Acceptors: Crystallographic, Computational, and IR Studies

#### 11.1 Introduction.

The definition of "hydrogen bond" in X-H---Y interactions has evolved from the traditional (X and Y being strictly electronegative elements, for example O and N)<sup>1,2,3</sup> to the incorporation of such "nonclassical" interactions as C-H--- $\pi$ ,<sup>4,5,6</sup> C-H---Y,<sup>7,8,9</sup> and O-H--- $\pi$ .<sup>10,11</sup> Today, it is widely accepted that there is a large continuum of hydrogen bonds whereby seemingly weaker or atypical interactions are encompassed as well. Many of these nonclassical (weak) interactions are known to exert notable impacts on biological systems, catalysis, and crystal formation.<sup>12</sup> One of the more controversial nonclassical interactions has been the C-F---H-C hydrogen bond.<sup>13,14,15,16</sup> Until recently, the role of fluorine as a hydrogen bond acceptor was debatable at best, yet well-documented intermolecular  $sp^2$  C-F---H-C systems,<sup>17</sup> fluoroform dimers,<sup>18</sup> and intramolecular  $sp^3$  C-F---H-C interactions<sup>19</sup> have all emerged in the literature as special cases. In any event, these interactions are presumed to be weak, such that in the presence of stronger, classical acceptors such as O and N they would be most likely disrupted.<sup>20</sup>



**Figure 11.1** A C-F---H-C interaction observed in the presence of traditionally stronger oxygen-based hydrogen bond acceptors.

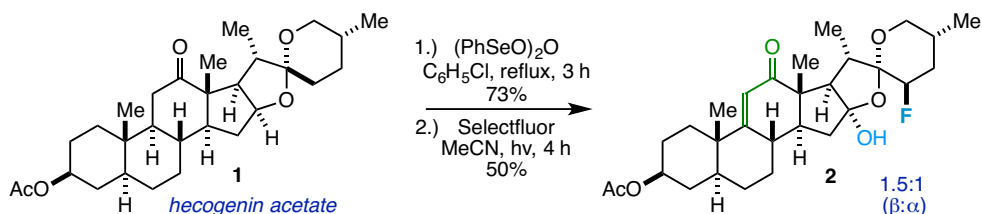
In this chapter, we present a surprising occurrence whereby the fluorine atom in an aliphatic C-F bond acts as the preferred hydrogen bond acceptor in the presence of traditionally *stronger* oxygen-based acceptors (Figure 11.1). This C-F---H-C intermolecular interaction was discovered serendipitously in an



X-ray crystal structure, then studied with DFT and AIM calculations and further characterized through IR spectroscopy as a blue-shifted weak-moderate hydrogen bond.

### 11.2 Synthesis of Parent Molecule.

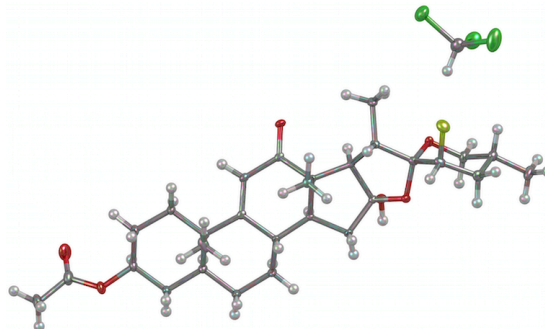
The parent molecule was synthesized from hecogenin acetate<sup>21,22</sup> (**1**) in two steps: dehydrogenation using benzeneseleninic anhydride<sup>23</sup> followed by photochemical aliphatic C-H fluorination (Scheme 11.1).<sup>24</sup> The fluorination step exhibited unanticipated site-selectivity and simultaneous incorporation of a hydroxy group. Based on our previous report on enone-directed photochemical fluorination and molecular modeling, 9,11-dehydrohecogenin acetate does not appear to be poised for so-called mode I, II, III, or IV fluorination.<sup>24</sup> Instead, we imagine that this "frustrated" excited-state enone participates in intermolecular hydrogen atom abstraction. However, the mechanism for this transformation and rationale for site-selectivity/oxygen incorporation are not yet understood and beyond the scope of this study.



**Scheme 11.1** Synthesis of the parent molecule **2** (major diastereomer depicted with respect to C-F bond).

### 11.3 Discovery and Computational Investigation of C-F---H-C Interaction.

In any case, the major diastereomer **2** was isolated, crystallized from a mixture of chloroform and hexanes using a solvent evaporation technique, and subjected to single-crystal X-ray diffraction. We found that the composition of the crystal was 1:1 parent molecule **2**: $\text{CHCl}_3$  with a well-ordered solvent molecule located in proximity to the C-F bond (Figure 11.2). Surprisingly, the spatial orientation of chloroform and the experimental  $\text{F}-\text{C}^2$  distance of 3.14 Å in the crystal structure indicated a significant C-F---H-C interaction (Table 11.1).



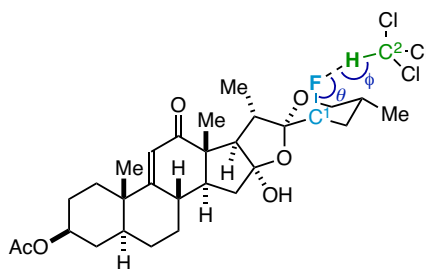
**Figure 11.2** Crystal structure determined from single-crystal X-ray diffraction (displacement ellipsoids given at 50% probability level) with hydrogen atoms refined using a riding model.

Through DFT calculations, an average F---H distance of 2.13 Å was determined with four different functionals using fixed heavy atom coordinates from the crystal structure (Table 11.1). Although this distance is greater than previously reported forced intramolecular aliphatic C-F---H-C interactions (e.g. 1.83-1.91 Å),<sup>19</sup> to our knowledge, it is among the shortest *intermolecular* contacts of this type to date.<sup>25</sup> Additionally, this interaction is less frequently observed with aliphatic C-F bonds than sp<sup>2</sup> C-F, sp C-F, or perfluorinated acceptors.<sup>26,27,28,29,30</sup> One might argue that chloroform and the alkyl fluoride are forced into close proximity unfavorably due to crystal packing. However, we also performed full geometry optimizations on the parent molecule **2**:CHCl<sub>3</sub> complex (unfixed CHCl<sub>3</sub>) with the same functionals/basis sets and found average F---H distances of 2.14 Å (ranging 2.09-2.20 Å) and F-C<sup>2</sup> distances of 3.21 Å (ranging 3.15-3.28 Å). The fact that the free chloroform molecule was not repelled from the parent compound, but instead maintained similar atomic distances and angles to that of the crystal structure, implies an energetic minimum whereby an attractive F---H interaction does exist.

Can we consider this a hydrogen bond? The basic criterion of a covalently bound hydrogen atom being at the center of the two species is in place, but by the most prudent definition we must consider 1) the stabilization of the complex relative to the individual species and 2) the nature of charge transfer from the acceptor to the donor.<sup>31</sup> For one, straightforward DFT calculations of the interaction energy predict the complex to be 4.50-4.84 kcal/mol more stable than the individual non-hydrogen-bound entities (Table 11.1). On the vast energy continuum of hydrogen bonding, this could be indicative of a weak-moderate hydrogen bonding interaction.<sup>32</sup> Regarding the nature of the *bond* in this attractive interaction, electron

density ( $\rho$ ) calculations using the atoms-in-molecules (AIM) program provide more insight.<sup>33</sup> One of the criteria used to assess bonding is the presence of a bond critical point (BCP).<sup>34</sup> According to the AIM calculations, a BCP between the fluorine and hydrogen atom exists with  $\rho = 0.016$  with the proper Laplacian of electron density to be consistent with a weak-moderate hydrogen bond.<sup>32,35</sup> With respect to the nature of charge transfer, a natural bond orbital (NBO) analysis is informative. As anticipated, we found an increase in net charge of the hydrogen atom in the calculated complex versus free chloroform (positive  $\Delta q_H$ ); this is at the expense of the net charge of the fluorine acceptor (negative  $\Delta q_F$ ).<sup>36</sup>

**Table 11.1** DFT and AIM computational analyses.



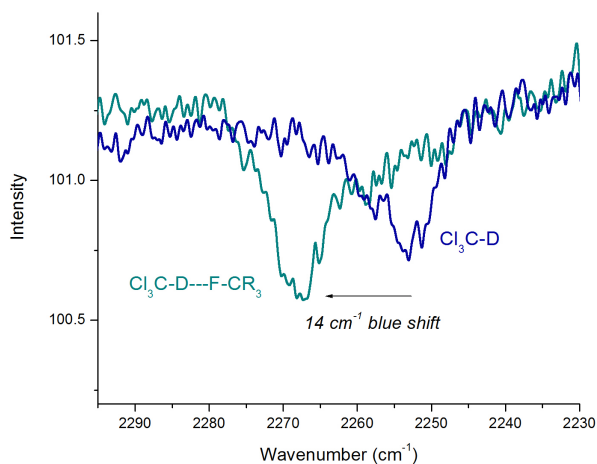
functional/basis set	$d(F-H)$ (Å) <sup>a</sup>	$d(F-C^2)$ (Å)	$\theta_{C1-F-H}$	$\phi_{F-H-C2}$	$\rho$ ( $10^{-2}$ ) <sup>b</sup>	$\Delta E_{int}$ (kcal/mol) <sup>c</sup>	$\Delta q_H$ <sup>d</sup>	$\Delta q_F$ <sup>d</sup>
B3LYP/6-311++G**	2.13	3.20	140.4	170.4	-	-4.84	0.028	-0.018
B3PW91/6-311++G**	2.20	3.28	160.2	174.7	-	-4.52	0.026	-0.016
PBEPBE/6-311++G**	2.13	3.21	137.5	171.8	-	-4.63	0.026	-0.018
CAM-B3LYP/6-311++G**	2.09	3.15	142.1	166.1	1.6	-4.50	0.029	-0.018

<sup>a</sup>Hydrogen atom on chloroform is in a calculated position based on a fully optimized structure (no bond constraints). <sup>b</sup>Refers to electron density at BCP (bond critical point). <sup>c</sup>Interaction energy, calculated as  $\Delta E_{int} = E(2:CHCl_3) - [E(2) + E(CHCl_3)]$ . <sup>d</sup>Change in natural charge of the specified atom in the hydrogen bound complex relative to the individual species by NBO (natural bond orbital) analysis.

#### 11.4 Characterization as Blue-shifted H-bond by IR Spectroscopy.

Beyond the above quantum mechanical analyses, the complex was studied using solid-state IR spectroscopy, as frequency shifts are often correlated with the strength of a hydrogen bonding interaction. IR data were obtained on the crystal using an ATR-IR instrument, as solution-phase analyses do not discriminate C-F---H-C interactions among other possible hydrogen bonds in this system. The weak  $Cl_3C-H$  stretch was difficult to analyze in the presence of a broad O-H stretch; consequently, another crystal was grown from a mixture of deuterated chloroform ( $CDCl_3$ ) and hexanes to study a more distinguishable  $Cl_3C-$

D stretch in the complex.<sup>37</sup> An IR spectrum revealed the incorporation of  $\text{CDCl}_3$  in the crystal and furthermore exhibited an *increase* in C-D stretch vibration frequency (relative to  $\text{CDCl}_3$ ) by  $14\text{ cm}^{-1}$  (Figure 11.3). Single-crystal X-ray crystallography confirmed that this sample is, in fact, the same polymorph with 1:1 parent molecule **2**: $\text{CDCl}_3$  incorporation. Thus, this frequency shift is attributed to the corresponding C-F---D-C interaction. Conventionally, an X-H---Y interaction manifests in a weakening of the X-H bond, and thus bond elongation and a decrease (or red shift) in the X-H stretch vibration frequency.<sup>38</sup> Yet, this particular C-H---F interaction experiences a less common *blue shift*.<sup>39</sup> Such an interaction has been noted in many instances as an "improper" hydrogen bond, as it harbors the appropriate stabilizing features but manifests in X-H bond compression.<sup>31</sup>

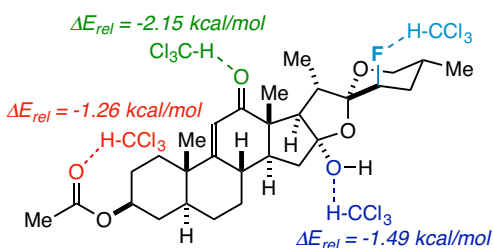


**Figure 11.3** Zoomed in overlay of the IR spectra of the 1:1 parent molecule **2**: $\text{CDCl}_3$  crystal and pure  $\text{CDCl}_3$ , highlighting the blue shift in the C-D stretch vibration frequency.

What is more, this blue shift is predicted by DFT calculations. Vibrational analyses of the isotopomers using the CAM-B3LYP/6-311++G\*\* method suggest an  $11\text{ cm}^{-1}$  shift in the fully optimized structure of the complex and a  $13\text{ cm}^{-1}$  shift in the calculated structure with fixed chloroform coordinates. The calculations were also conducted using the various functionals in Table 11.1; in each case, a blue shift was determined.

### 11.5 C-F---H-C Interaction in the Presence of Potentially Stronger H-bonding Interactions.

Perhaps the most intriguing aspect is not only that this C-F---H-C blue-shifted hydrogen bonding interaction exists, rather that it exists in the presence of stronger oxygen-based hydrogen bonding acceptors. Upon placing chloroform near a number of available oxygen atoms on the parent molecule, several structures were optimized at B3LYP/6-311++G\*\* that also suggest potential hydrogen bonding interactions. Naturally, when the energies of these systems are compared to the energy of the F-bound chloroform, the calculated O-bound chloroform structures are consistently lower in energy by 1.26-2.15 kcal/mol (Figure 11.4).<sup>20,40</sup> So why is the C-F---H-C interaction occurring instead? In short, the crystal packing arrangement with the C-F---H-C interaction is the most favorable.<sup>41</sup> It is extremely difficult to model alternative packing scenarios, but we can note some important features from the packing diagram at hand. For one, the chlorine atoms do not have any significant short contacts with other atoms in the lattice; therefore, the presence and orientation of chloroform must be influenced primarily by the C-F---H-C interaction. Additionally, if we consider other interactions, the diagram contains an intermolecular O-H---O=C interaction ( $d(\text{H-O}) = 1.98 \text{ \AA}$ ) between the hydroxy group and the enone oxygen that is certainly influencing the arrangement. It is possible that this conventionally stronger O-H---O hydrogen bonding interaction precludes a C-H---O interaction at this site, but in any case, the C-H---F interaction evidently plays an important role in crystal packing.



**Figure 11.4** Relative energies of O-bound chloroform complexes to the observed F-bound chloroform complex, calculated at B3LYP/6-311++G\*\*.

## 11.6 Conclusion.

In all, we find the intermolecular aliphatic C-F---H-C hydrogen bonding interaction to be a surprising and notable result. By probing this phenomenon with DFT and AIM calculations, we have found that the interaction meets the basic criteria for a hydrogen bond. Additionally, the X-ray crystal structure and computational data are substantiated through spectroscopic (IR) evaluation of the complex that determines a blue shift of ca.  $14\text{ cm}^{-1}$ , indicative of a rarer hydrogen bond characterized by C-H bond compression. While other features of the crystal packing undoubtedly influence its occurrence, the fact that the C-H---F interaction is preferred over a packing arrangement with a more favorable C-H---O interaction (or no chloroform incorporation) is significant. Given the biological relevance of similar triterpenoids, this result may prompt investigation of aliphatic fluorine interactions, for instance, in enzyme active sites.

## 11.7 References.

- 
- <sup>1</sup> Pauling, L. *The Nature of the Chemical Bond*, 3<sup>rd</sup> ed.; Cornell University Press: New York, 1960.
- <sup>2</sup> Jeffrey, G. A. *An Introduction to Hydrogen Bonding*; Oxford University Press: New York, 1997.
- <sup>3</sup> Arunan, E.; Desiraju, G. R.; Klein, R. A.; Sadlej, J.; Scheiner, S.; Alkorta, I.; Clary, D. C.; Crabtree, R. H.; Dannenberg, J. J.; Hobza, P.; Kjaergaard, H. G.; Legon, A. C.; Mennucci, B.; Nesbitt, D. *J. Pure Appl. Chem.* **2011**, *83*, 1637-1641.
- <sup>4</sup> Steiner, T.; Starikov, E. B.; Amado, A. M.; Teixeira-Dias, J. J. C. *J. Chem. Soc., Perkin 2* **1995**, 1321-1326.
- <sup>5</sup> Steiner, T.; Tamm, M.; Grzegorzewski, A.; Schulte, M.; Veldman, N.; Schreurs, A. M. M.; Kanters, J. A.; Kroon, J.; van der Maas, J. *J. Chem. Soc., Perkin Trans. 2* **1996**, 2441-2446.
- <sup>6</sup> Sodupe, M.; Rios, R.; Branchadell, V.; Nicholas, T.; Oliva, A.; Dannenberg, J. J. *J. Am. Chem. Soc.* **1997**, *119*, 4232-4238.
- <sup>7</sup> Legon, A. C.; Roberts, B. P.; Wallwork, A. L. *Chem. Phys. Lett.* **1990**, *173*, 107-114.
- <sup>8</sup> Legon, A. C.; Wallwork, A. L.; Warner, H. E. *Chem. Phys. Lett.* **1992**, *191*, 97-101.
- <sup>9</sup> Steiner, T.; Desiraju, G. R. *Chem. Commun.* **1998**, 891-892.
- <sup>10</sup> Tarakeshwar, P.; Kim, K. S.; Brutschy, B. *J. Chem. Phys.* **2000**, *112*, 1769-1781.
- <sup>11</sup> Struble, M. D.; Holl, M. G.; Coombs, G.; Siegler, M. A.; Lectka, T. *J. Org. Chem.* **2015**, *80*, 4803-4807.
- <sup>12</sup> Takahashi, O.; Kohno, Y.; Nishio, M. *Chem. Rev.* **2010**, *110*, 6049-6076.
- <sup>13</sup> Desiraju, G. R.; Steiner, T. *The Weak Hydrogen Bond in Structural Chemistry and Biology*; Oxford University Press: Oxford, UK, 1999; pp 205-209.
- <sup>14</sup> Howard, J. A. K.; Hoy, V. J.; O'Hagan, D.; Smith, G. T. *Tetrahedron* **1996**, *52*, 12613-12622.
- <sup>15</sup> Schneider, H.-J. *Chem. Sci.* **2012**, *3*, 1381-1394.
- <sup>16</sup> Champagne, P. A.; Desroches, J.; Paquin, J.-F. *Synthesis* **2015**, *47*, 306-322.

- 
- <sup>17</sup> Thakur, T. S.; Kirchner, M. T.; Bläser, D.; Boese, R.; Desiraju, G. R. *Cryst. Eng. Commun.* **2010**, *12*, 2079-2085.
- <sup>18</sup> Kryachko, E.; Scheiner, S. *J. Phys. Chem. A* **2004**, *108*, 2527-2535.
- <sup>19</sup> Struble, M. D.; Strull, J.; Patel, K.; Siegler, M. A.; Lectka, T. *J. Org. Chem.* **2014**, *79*, 1-6.
- <sup>20</sup> Shimoni, L.; Glusker, J. P. *Struct. Chem.* **1994**, *5*, 383-397.
- <sup>21</sup> Corbiere, C.; Liagre, B.; Bianchi, A.; Bordji, K.; Dauça, M.; Netter, P.; Beneytout, J. L. *Int. J. Oncol.* **2003**, *22*, 899-905.
- <sup>22</sup> Santos Cerqueira, G.; dos Santos e Silva, G.; Rios Vasconcelos, E.; Fragoso de Freitas, A. P.; Arcanjo Moura, B.; Silveira Macedo, D.; Lopes Souto, A.; Barbosa Filho, J. M.; de Almeida Leal, L. K.; de Castro Brito, G. A.; Souccar, C.; de Barros Viana, G. S. *Eur. J. Pharmacol.* **2012**, *683*, 260-269.
- <sup>23</sup> Barton, D. H. R.; Lester, D. J.; Ley, S. V. *J. Chem. Soc., Perkin Trans. 1*, **1980**, 2209-2212.
- <sup>24</sup> Pitts, C. R.; Bume, D. D.; Harry, S. A.; Siegler, M. A.; Lectka, T. *J. Am. Chem. Soc.* **2017**, *139*, 2208-2211.
- <sup>25</sup> A CSD search (CSD version 5.37 + 1 update Feb 2016) was performed to check for C-F---H-CCl<sub>3</sub> intermolecular interactions. Here, 109 hits were found, and the H---F distances were ranging from 2.25 to 2.67 Å. Most of the C-F bonds are from aryl fluorides and trifluoromethyl groups.
- <sup>26</sup> Dikundwar, A. G.; Sathishkumar, R.; Guru Row, T. N. *Z. Kristallogr.* **2014**, *229*, 609-624.
- <sup>27</sup> Shukla, R.; Chopra, D. *CrystEngComm* **2015**, *17*, 3596-3609.
- <sup>28</sup> Omorodion, H.; Twamley, B.; Platts, J. A.; Baker, R. J. *Cryst. Growth Des.* **2015**, *15*, 2835-2841.
- <sup>29</sup> Taylor, R. *Cryst. Growth Des.* **2016**, *16*, 4165-4168.
- <sup>30</sup> Panini, P.; Gonnade, R. G.; Chopra, D. *New J. Chem.* **2016**, *40*, 4981-5001.
- <sup>31</sup> Hobza, P.; Havlas, Z. *Chem. Rev.* **2000**, *100*, 4253-4264.
- <sup>32</sup> Parthasarathi, R.; Subramanian, V.; Sathyamurthy, N. *J. Phys. Chem. A* **2006**, *110*, 3349-3351.
- <sup>33</sup> AIMAll (Version 13.05.06): Keith, T. A. TK Gristmill Software, Overland Park KS, 2013 (aim.tkgristmill.com).
- <sup>34</sup> Bader, R. F. W. *Acc. Chem. Res.* **1985**, *18*, 9-15.
- <sup>35</sup> Grabowski, S. J. *J. Phys. Chem. A* **2011**, *115*, 12789-12799.
- <sup>36</sup> Charge transfer from the proton acceptor to the proton donor is a common feature in nearly all hydrogen bonding definitions. For example: Popelier, P. L. A. *J. Phys. Chem. A* **1998**, *102*, 1873-1878.
- <sup>37</sup> Anslyn, E. V.; Dougherty, D. A. *Modern Physical Organic Chemistry*; University Science Books: Sausalito, CA, 2006.
- <sup>38</sup> Scheiner, S. *Hydrogen Bonding*; Oxford University Press: New York, 1997.
- <sup>39</sup> For another example of blue-shifted hydrogen bonding in a haloform complex, see: Van den Kerkhof, T.; Bouwen, A.; Goovaerts, E.; Herrebout, W. A.; van der Veken, B. *J. Phys. Chem. Chem. Phys.* **2004**, *6*, 358-362.
- <sup>40</sup> For examples of C-H---O hydrogen bonding in crystals, see: Desiraju, G. R. *Acc. Chem. Res.* **1991**, *24*, 290-296.
- <sup>41</sup> Dauber, P.; Hagler, A. T. *Acc. Chem. Res.* **1980**, *13*, 105-112.

## Chapter 12

### Experimental Section

#### 12.1 General Methods.

Unless otherwise stated, all reactions were carried out under strictly anhydrous, air-free conditions under nitrogen. All solvents and reagents were dried and distilled or recrystallized by standard methods. All  $^{19}\text{F}$  NMR spectra were acquired on a Bruker Avance 300 MHz instrument. All  $^1\text{H}$  and  $^{13}\text{C}$  NMR spectra were acquired on a Bruker Avance 400 MHz instrument. The  $^{19}\text{F}$ ,  $^1\text{H}$ , and  $^{13}\text{C}$  chemical shifts ( $\delta$ ) are given in parts per million (ppm) with respect to an internal standard, i.e. 3-chlorobenzotrifluoride ( $\delta = -64.2$ )<sup>1</sup> or tetramethylsilane (TMS,  $\delta = 0.00$  ppm). NMR data are reported in the following format: chemical shift (integration, multiplicity, coupling constants [Hz]). Spectral data were processed with Bruker software and ACD/NMR Processor Academic Edition.<sup>2</sup> Electrochemistry experiments were carried out on a BAS CV-50W potentiostat. UV-vis spectra were acquired on a Varian Cary-50 spectrophotometer. EPR spectra were acquired on a Bruker EMX spectrometer controlled with a Bruker ER 041 X G microwave bridge operating at X-band (~9.4 GHz), equipped with a liquid helium cryostat. IR data were obtained using an ATR-IR instrument or FT-IR with a flat  $\text{CaF}_2$  cell. Photochemical reactions were run in a Rayonet reactor (for ultraviolet light) or in front of either a 14-Watt compact fluorescent light bulb or cool white LED setup (for visible light). HPLC purification was conducted on a Teledyne Isco CombiFlash EZ Prep system using a Dynamax-60A  $\text{SiO}_2$  column and HPLC grade EtOAc and hexanes. X-ray crystal structures were obtained using a SuperNova diffractometer (equipped with Atlas detector) with Mo  $K\alpha$  radiation ( $\lambda = 0.71073 \text{ \AA}$ ) under the program CrysAlisPro (Version 1.171.36.24 Agilent Technologies, 2012). MS analyses were completed using positive ion mode electrospray ionization (Apollo II ion source) on a Bruker 12.0 Tesla APEX -Qe FTICR-MS. The Gaussian '09 package<sup>3</sup> and Spartan '06 were used for all calculations. All computational files and spectra omitted from this chapter are available upon request or can otherwise be located in the Supporting Information of the published bodies of work.



## 12.2 Experimental Details for Chapter 2.

**Representative Fluorination Procedure.** An oven-dried, 10 mL round bottom flask equipped with a stir bar was placed under an atmosphere of N<sub>2</sub>. Subsequently, KB(C<sub>6</sub>F<sub>5</sub>)<sub>4</sub> (22.0 mg, 0.025 mmol, 0.1 equiv), Selectfluor (195 mg, 0.55 mmol, 2.2 equiv), copper(I) iodide (5.0 mg, 0.025 mmol, 0.1 equiv), *N,N*-bis(phenylmethylene)-1,2-ethanediamine (6.0 mg, 0.025 mmol, 0.1 equiv), *N*-hydroxyphthalimide (4.0 mg, 0.025 mmol, 0.1 equiv) and potassium iodide (50.0 mg, 0.3 mmol, 1.2 equiv) were added, followed by degassed MeCN (3.0 mL), and the mixture was allowed to stir for 10 min. Under a stream of N<sub>2</sub>, cyclododecane **8** (42.0 mg, 0.25 mmol, 1.0 equiv) was added neat, and the mixture was heated to reflux for 2 h. The reaction was monitored by <sup>19</sup>F NMR at 30 min intervals. Final yields were determined either by <sup>19</sup>F NMR using 3-chlorobenzotrifluoride as an internal standard or else column chromatography on silica (either method was in good agreement). Note that this procedure (omitting the addition of KI) also applies to the allylic and benzylic substrates.

**Computational Methods.** Chemical shifts were computed using Gaussian at the B3LYP/6-311++G\*\* level of theory and scaled by 0.9614.<sup>4</sup> The <sup>19</sup>F NMR calculated chemical shifts were fitted to the empirical equation (at B3LYP/6-311++G\*\*)  $\delta_{\text{calc}} = -0.914\delta + 142.63$ . The isotropic values ( $\delta$ ) employed were obtained from the CS UT calculation parameter found in the results menu. Geometry optimizations were likewise determined using the B3LYP/6-311++G\*\* level.

**Characterization Data.** Characterization of 1-fluoroadamantane<sup>5</sup> (**2**), 2-fluoroadamantane<sup>6</sup> (**3**), 1-fluorocyclododecane<sup>7</sup> (**9**), 1-fluorocycloheptane<sup>3</sup> (**11**), 1-fluorocyclooctane<sup>3</sup> (**13**), 1-fluorocyclodecane<sup>8</sup> (**15**), monofluorodecalin<sup>9</sup> (**17**), 1-fluorocycloundecane<sup>4</sup> (**19**) 1-fluorododecane<sup>10</sup> (**21**), (3-fluoroprop-1-en-2-yl)benzene<sup>11</sup> (**23**), 1-[1-(fluoromethyl)ethenyl]-4-methylbenzene<sup>12</sup> (**25**), and 1-(1-fluoroethyl)benzene<sup>13</sup> (**27**) were consistent with literature precedent. Compounds **29**, **33** and **35** are reported as inseparable mixtures.

Fluorohexyl acetate (**28**). Clear oil. <sup>1</sup>H NMR (CDCl<sub>3</sub>):  $\delta$  4.14-4.02 (m, 2H), 2.03 (s, 3H), 1.72-1.50 (m, 2H), 1.34-1.24 (br m, 6H), 1.20-1.01 (m, 1H), 0.90-0.81 (m, 7H); <sup>13</sup>C NMR (CDCl<sub>3</sub>):  $\delta$  171.2, 171.0,

64.6, 64.0, 60.3, 41.4, 36.1, 34.1, 31.4, 28.6, 25.6, 22.5, 21.0, 20.9, 19.4, 18.7, 13.9, 11.4;  $^{19}\text{F}$  NMR ( $\text{CDCl}_3$ ):  $\delta$  -128.8 (m, 1F), -173.0 (m, 1F), -182.3 (m, 1F), -183.5 (m, 1F), -187.1 (m, 1F) consistent with calcd values -175.3 (5-fluorohexylacetate), -182.0 (3-fluorohexylacetate); IR ( $\text{CDCl}_3$ ): 1727  $\text{cm}^{-1}$ , 1251  $\text{cm}^{-1}$ ; HRMS-(ESI $^+$ ) calcd for  $\text{C}_8\text{H}_{15}\text{FO}_2\text{Na}^+$  : 185.0954, found 185.0943.

Fluoro-dihydrocoumarin (**31**). Colorless oil.  $^1\text{H}$  NMR ( $\text{CDCl}_3$ ):  $\delta$  7.4-7.0 (m, 4H), 5.70 (dt, 1H,  $J = 50.9$  Hz, 3.7 Hz), 3.34-2.95 (m, 2H);  $^{19}\text{F}$  NMR ( $\text{CDCl}_3$ ):  $\delta$  -158.5 (m, 1F); HRMS-(ESI $^+$ ) calcd for  $\text{C}_9\text{H}_7\text{FO}_2\text{Na}^+$  : 189.0328, found 189.0321. Prone to dehydrofluorination over time.

Fluoroundecanoic  $\delta$ -lactone (**33**). Colorless oil.  $^1\text{H}$  NMR ( $\text{CDCl}_3$ ):  $\delta$  4.9-4.0 (m, 1H), 2.7-2.2 (m, 1H), 2.0-1.2 (m, 8H), 1.1-0.8 (m, 1H);  $^{13}\text{C}$  NMR ( $\text{CDCl}_3$ ):  $\delta$  171.85, 171.82, 171.76, 171.64, 171.55, 91.55, 80.50, 80.45, 80.33, 79.74, 42.71, 37.47, 37.27, 37.06, 36.86, 36.83, 36.65, 36.62, 35.76, 35.74, 34.91, 34.70, 34.58, 34.37, 34.16, 32.05, 31.73, 31.14, 31.09, 30.93, 30.28, 29.45, 29.43, 29.31, 29.16, 28.05, 27.95, 27.84, 27.83, 27.80, 27.75, 27.44, 27.11, 27.07, 24.93, 24.90, 24.85, 24.78, 24.75, 22.58, 22.46, 21.13, 21.11, 20.90, 20.89, 20.87, 20.82, 18.56, 18.50, 18.45, 18.41, 18.36, 18.29, 14.06, 13.94, 13.90, 9.41, 9.40;  $^{19}\text{F}$  NMR ( $\text{CDCl}_3$ ):  $\delta$  -172.2 (m, 1F), -173.5 (m, 1F), -181.0 (m, 1F), -181.6 (m, 1F), -184.2 (m, 1F); HRMS-(ESI $^+$ ) calcd for  $\text{C}_{11}\text{H}_{19}\text{FO}_2\text{Na}^+$  : 225.1268, found 225.1276.

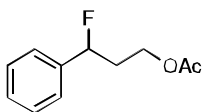
Fluoro-1,8-dibromooctane (**35**). Colorless oil.  $^1\text{H}$  NMR ( $\text{CDCl}_3$ ): 4.8-3.9 (m, 1H), 3.7-3.1 (m, 5H), 2.4-1.2 (m, 14H);  $^{13}\text{C}$  NMR ( $\text{CDCl}_3$ ):  $\delta$  94.1, 92.4, 38.7, 38.3, 38.2, 37.3, 34.3, 34.1, 33.9, 33.7, 33.6, 33.5, 33.4, 33.2, 32.4, 32.1, 28.6, 28.4, 28.0, 27.9, 24.2, 23.08, 23.8;  $^{19}\text{F}$  NMR ( $\text{CDCl}_3$ ):  $\delta$  -182.1 (m, 1F), -185.5 (m, 2F); HRMS-(ESI $^+$ ) calcd for  $\text{C}_8\text{H}_{15}\text{Br}_2\text{FNa}^+$  : 310.9418, found 310.9424.

### 12.3 Experimental Details for Chapter 3.

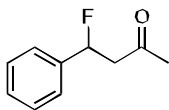
**Representative Fluorination Procedure.** An oven-dried, 10 mL round bottom flask equipped with a stir bar was placed under an atmosphere of  $\text{N}_2$ . Selectfluor (195.0 mg, 0.55 mmol, 2.2 equiv) and  $\text{Fe}(\text{acac})_2$  (6.0 mg, 0.025 mmol, 0.1 equiv) were added followed by MeCN (3.0 mL). 3-phenylpropylacetate (45.0 mg, 0.25 mmol, 1 equiv) was then added, and the mixture was allowed to stir overnight. The product was

extracted into CH<sub>2</sub>Cl<sub>2</sub> and washed with water. The combined organic layers were dried with MgSO<sub>4</sub> and filtered through Celite. The solvents were removed by rotary evaporation, and the residue was subjected to column chromatography on Florisil eluting with ethyl acetate/hexanes.

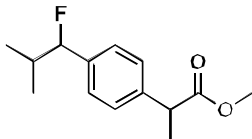
**Characterization Data.** Characterization of 1-(fluoromethyl)-4-isopropylbenzene (**2b**),<sup>14</sup> 4-fluorochroman-2-one (**2f**),<sup>15</sup> (1-fluoro-2-methylpropyl)benzene (**2j**),<sup>16</sup> 4-(fluoromethyl)biphenyl (**2k**),<sup>17</sup> and (1-fluoroethyl)benzene (**2l**)<sup>18</sup> were consistent with the literature precedents. Crude spectra of **2i** were collected with a 1 s presaturation pulse on the residual solvent. Compounds **2d**, **2h**, and **2m** are reported as mixtures of major benzylic fluorinated products and minor fluorinated isomers.



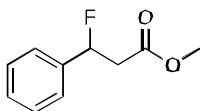
**3-phenylpropylacetate (2a).** <sup>1</sup>H NMR (CDCl<sub>3</sub>): δ 7.43-7.36 (m, 5H), 5.6 (ddd, 1H, *J* = 47.8, 8.7, 4.3 Hz), 4.33-4.18 (m, 2H), 2.39-2.11 (m, 2H), 2.08 (s, 3H); <sup>13</sup>C NMR (CDCl<sub>3</sub>): δ 170.8 (s), 139.6 (s), 139.4 (s), 128.5 (s), 125.5 (s), 91.4 (d, *J* = 171 Hz), 60.4 (s), 36.4 (s), 36.1 (s), 20.9 (s); <sup>19</sup>F NMR (CDCl<sub>3</sub>): δ -176.9 (ddd, 1F, *J* = 46.4, 29.9, 15.5 Hz); HRMS-(ESI<sup>+</sup>) calcd for C<sub>11</sub>H<sub>13</sub>FO<sub>2</sub>Na<sup>+</sup>: 219.0798, found 219.0783.



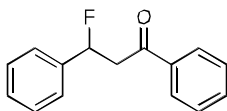
**4-fluoro-4-phenylbutan-2-one (2c).** <sup>1</sup>H NMR (CDCl<sub>3</sub>): δ 7.57-7.34 (m, 5H), 5.97 (ddd, 1H, *J* = 46.9, 8.9, 4.1 Hz), 3.21 (ddd, 1H, *J* = 16.8, 14.7, 8.7 Hz), 2.82 (ddd, 1H, *J* = 32.0, 16.8, 4.1 Hz), 2.24 (s, 3H); <sup>13</sup>C NMR (CDCl<sub>3</sub>): δ 198.4 (s), 143.4 (s), 139.2 (s), 139.0 (s), 134.4 (s), 130.5 (s), 129.0 (s), 128.7 (s), 125.5 (s), 125.4 (s), 90.2 (d, *J* = 171 Hz), 50.8 (s), 50.6 (s), 27.5 (s); <sup>19</sup>F NMR (CDCl<sub>3</sub>): δ -173.6 (ddd, 1F, *J* = 47.4, 32.0, 15.5 Hz); HRMS-(ESI<sup>+</sup>) calcd for C<sub>10</sub>H<sub>11</sub>FONa<sup>+</sup>: 189.0692, found 189.0686.



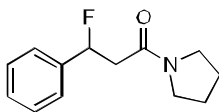
**methyl-2-(4-(1-fluoro-2-methylpropyl)phenyl)propanoate (2d).**  $^1\text{H}$  NMR ( $\text{CDCl}_3$ ):  $\delta$  7.31-7.18 (m, 5H), 5.10 (dd, 1H,  $J = 47.1, 6.8$  Hz), 3.73 (q, 1H,  $J = 7.0$  Hz), 3.66 (s, 3H), 2.18-1.99 (m, 1H), 1.50 (d, 3H,  $J = 7.2$  Hz), 1.02 (dd, 3H,  $J = 6.6, 0.9$  Hz), 0.87 (d, 3H,  $J = 6.8$  Hz);  $^{13}\text{C}$  NMR ( $\text{CDCl}_3$ ):  $\delta$  175.0 (s), 174.9 (s), 140.4 (s), 138.4 (s), 138.2 (s), 130.6 (s), 127.3 (s), 126.5 (s), 99.0 (d,  $J = 175$  Hz), 96.3 (s), 52.0 (s), 47.3 (s), 45.2 (s), 45.1 (s), 34.4 (s), 34.1 (s), 26.8 (s), 26.5 (s), 18.6 (s), 18.4 (s), 18.3 (s), 17.6 (s), 17.5 (s);  $^{19}\text{F}$  NMR ( $\text{CDCl}_3$ ):  $\delta$  -179.8 (ddd, 1F,  $J = 47.4, 16.5, 6.2$  Hz); HRMS-(ESI $^+$ ) calcd for  $\text{C}_{14}\text{H}_{19}\text{FO}_2\text{Na}^+$ : 261.1267, found 261.1273.



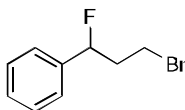
**methyl-3-fluoro-3-phenylpropanoate (2e).**  $^1\text{H}$  NMR ( $\text{CDCl}_3$ ):  $\delta$  7.40-7.34 (m, 5H), 5.90 (ddd, 1H,  $J = 46.7, 9.0, 4.1$  Hz), 3.74 (s, 3H), 3.04 (ddd, 1H,  $J = 16.0, 13.6, 9.0$  Hz), 2.80 (ddd, 1H,  $J = 32.4, 16.0, 4.1$  Hz);  $^{13}\text{C}$  NMR ( $\text{CDCl}_3$ ):  $\delta$  170.0 (s), 138.9 (s), 128.9 (s), 128.7 (s), 125.6 (s), 125.5 (s), 90.6 (d,  $J = 172$  Hz), 52.0 (s), 42.4 (s), 42.2 (s);  $^{19}\text{F}$  NMR ( $\text{CDCl}_3$ ):  $\delta$  -172.9 (ddd, 1F,  $J = 46.4, 32.0, 13.4$  Hz); HRMS-(ESI $^+$ ) calcd for  $\text{C}_{10}\text{H}_{11}\text{FO}_2\text{Na}^+$ : 205.0641, found 205.0635.



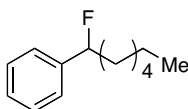
**3-fluoro-1,3-diphenylpropan-1-one (2g).**  $^1\text{H}$  NMR ( $\text{CDCl}_3$ ):  $\delta$  8.10-7.30 (m, 10H), 6.21 (ddd, 1H,  $J = 46.5, 8.3, 4.1$  Hz), 3.83 (ddd, 1H,  $J = 17.0, 14.9, 8.3$ ), 3.35 (ddd, 1H,  $J = 29.6, 17.0, 4.1$ );  $^{13}\text{C}$  NMR ( $\text{CDCl}_3$ ):  $\delta$  190.6 (s), 144.8 (s), 139.7 (s), 139.4 (s), 136.7 (s), 133.5 (s), 132.8 (s), 130.5 (s), 129.0 (s), 128.7 (s), 128.2 (s), 125.7 (s), 125.6 (s), 122.2 (s), 90.3 (d,  $J = 170$  Hz), 46.2 (s), 45.8 (s);  $^{19}\text{F}$  NMR ( $\text{CDCl}_3$ ):  $\delta$  -173.0 (ddd, 1F,  $J = 46.4, 29.9, 15.5$  Hz); HRMS-(ESI $^+$ ) calcd for  $\text{C}_{15}\text{H}_{13}\text{FONa}^+$ : 251.0848, found 251.0853.



**3-fluoro-3-phenyl-1-(pyrrolidin-1-yl)propanoate (2h).**  $^1\text{H}$  NMR ( $\text{CDCl}_3$ ):  $\delta$  7.42-7.20 (m, 5H), 6.03 (ddd, 1H,  $J = 47.1, 9.0, 3.6$  Hz), 4.13-4.04 (m, 1H), 3.73-3.56 (m, 1H), 3.23-3.11 (m, 1H), 3.01-2.96 (m, 1H), 2.86-2.67 (m, 1H), 1.81-1.60 (m, 6H), 1.44-1.06 (m, 11H);  $^{13}\text{C}$  NMR ( $\text{CDCl}_3$ ):  $\delta$  206.9 (s), 153.9 (s), 153.5 (s), 140.9 (s), 139.0 (s), 138.8 (s), 128.7 (s), 128.6 (s), 125.5 (s), 125.4 (s), 91.9 (d,  $J = 172$  Hz), 55.2 (s), 50.1 (s), 49.8 (s), 43.5 (s), 43.2 (s), 37.5 (s), 32.8 (s), 32.6 (s), 32.5 (s), 30.9 (s), 29.7 (s), 26.3 (s), 26.1 (s), 25.3 (s), 24.7 (s);  $^{19}\text{F}$  NMR ( $\text{CDCl}_3$ ):  $\delta$  -172.8 (ddd, 1F,  $J = 46.4, 34.0, 12.4$  Hz); HRMS-(ESI $^+$ ) calcd for  $\text{C}_{13}\text{H}_{16}\text{FNONa}^+$ : 244.1114, found 244.1109.



**(3-bromo-1-fluoropropyl)benzene (2i).**  $^1\text{H}$  NMR ( $\text{CDCl}_3$ ):  $\delta$  7.41-7.24 (m, 5H), 5.60 (ddd, 1H,  $J = 47.9, 8.9, 3.4$  Hz), 3.59-3.51 (m, 1H), 3.45-3.38 (m, 1H), 2.75 (t, 2H,  $J = 7.3$  Hz),  $^{13}\text{C}$  NMR ( $\text{CDCl}_3$ ):  $\delta$  140.3 (s), 139.0 (s), 138.7 (s), 128.6 (s), 128.4 (s), 128.3 (s), 126.4 (s), 125.9 (s), 125.3 (s), 125.2 (s), 116.2 (s), 91.9 (d,  $J = 172$  Hz), 40.1 (s), 39.7 (s), 33.9 (s), 33.7 (s), 32.9 (s), 28.3 (s), 28.2 (s);  $^{19}\text{F}$  NMR ( $\text{CDCl}_3$ ):  $\delta$  -178.6 (ddd, 1F,  $J = 48.5, 30.9, 14.4$  Hz); HRMS-(ESI $^+$ ) calcd for  $\text{C}_9\text{H}_{10}\text{BrFNa}^+$ : 238.9848, found 238.9854.



**(1-fluoroheptyl)benzene (2m).**  $^1\text{H}$  NMR ( $\text{CDCl}_3$ ):  $\delta$  7.42-7.19 (m, 13H), 6.42-6.22 (m, 1H), 5.44 (ddd, 1H,  $J = 48.0, 8.1, 5.1$  Hz), 2.98-2.65 (m, 1H), 2.26-2.20 (m, 1H), 2.07-1.92 (m, 1H), 1.92-1.75 (m, 1H), 1.74-1.59 (m, 1H), 1.54-1.45 (m, 3H), 1.42-1.29 (m, 12H), 0.95-0.89 (m, 6H);  $^{13}\text{C}$  NMR ( $\text{CDCl}_3$ ):  $\delta$  140.7 (s), 131.3 (s), 128.5 (s), 128.4 (s), 126.8 (s), 125.9 (s), 125.6 (s), 125.5 (s), 94.7 (d,  $J = 170$  Hz), 45.1 (s), 33.0 (s), 31.7 (s), 31.4 (s), 29.0 (s), 25.1 (s), 22.6 (s), 14.1 (s);  $^{19}\text{F}$  NMR ( $\text{CDCl}_3$ ):  $\delta$  -173.6 (ddd, 1F,  $J = 46.4, 27.8, 16.5$  Hz); HRMS-(ESI $^+$ ) calcd for  $\text{C}_{13}\text{H}_{19}\text{FNa}^+$ : 217.1369, found 217.1364.

## 12.4 Experimental Details for Chapter 4.

**Simplified sp<sup>3</sup> C-H fluorination procedure.** Selectfluor (390 mg, 1.1 mmol), cuprous iodide (10 mg, 0.05 mmol), *N,N'*-bis(2,6-dichloro-benzylidene)ethane-1,2-diamine (19 mg, 0.05 mmol), and potassium carbonate (7 mg, 0.05 mmol) were added to a flame-dried 10 mL round bottom flask equipped with a stir bar under N<sub>2</sub>. Degassed (with N<sub>2</sub>) acetonitrile (6 mL) was added to the reaction flask, and the solution was stirred vigorously at room temperature. After 15 minutes, starting material (0.50 mmol) was added to the reaction flask, and the reaction stirred overnight. Products (previously characterized) were determined by <sup>19</sup>F NMR. Product yields were also determined by <sup>19</sup>F NMR, upon making a sample tube composed of a 0.3 mL aliquot from the reaction flask and 0.2 mL of a solution of 3-chlorobenzotrifluoride (internal standard) dissolved in CD<sub>3</sub>CN. Note that non-volatile products can typically be isolated by diluting the reaction mixture with Et<sub>2</sub>O, filtering through Celite, extracting into Et<sub>2</sub>O, drying with MgSO<sub>4</sub>, filtering, concentrating, and carefully columning on Florisil with a non-polar solvent.

**Gram-scale synthesis of 1-fluorocyclododecane.** Selectfluor (4.676 g, 13.2 mmol), cuprous iodide (114 mg, 0.6 mmol), *N,N'*-bis(2,6-dichloro-benzylidene)ethane-1,2-diamine (223 mg, 0.6 mmol), potassium carbonate (83 mg, 0.6 mmol), and cyclododecane (1.008 g, 6.0 mmol) were added to a flame-dried 10 mL round bottom flask equipped with a stir bar under N<sub>2</sub>. Degassed acetonitrile (72 mL) - better accomplished via several *free-pump-thaw* cycles on a large scale - was added to the reaction flask, and the solution was stirred vigorously at room temperature for 8 h. The desired product – 1-fluorocyclododecane – was obtained in 50% yield, as determined by <sup>19</sup>F NMR.

**Liquid-phase EPR general procedure.** Selectfluor (390 mg, 1.1 mmol), cuprous iodide (10 mg, 0.05 mmol), *N,N'*-bis(2,6-dichloro-benzylidene)ethane-1,2-diamine (19 mg, 0.05 mmol), and potassium carbonate (7 mg, 0.05 mmol) were added to a flame-dried 10 mL round bottom flask equipped with a stir bar under N<sub>2</sub>. Degassed (with N<sub>2</sub>) acetonitrile (6 mL) was added to the reaction flask, and the solution was stirred vigorously at room temperature. After 15 minutes, starting material (0.50 mmol) was added to the reaction flask (where specified), the reaction stirred for the specified time, 2,4,6-tri-tert-butyl nitrosobenzene (14 mg, 0.05 mmol) was added to the reaction flask (if/when specified in text), then an

aliquot was transferred via syringe (fit with a disposable syringe filter) to an oven-dried quartz flat cell Bruker ER 160FC-Q immediately prior to collecting an EPR spectrum at room temperature. An additional aliquot was taken simultaneously for  $^{19}\text{F}$  NMR analysis of product formation.

**Solid-state EPR general procedure.** Selectfluor (390 mg, 1.1 mmol),  $^{63}\text{CuI}$  (10 mg, 0.05 mmol),  $^{15}\text{N}$ -labelled *N,N'*-bis(2,6-dichloro-benzylidene)ethane-1,2-diamine (19 mg, 0.05 mmol), and potassium carbonate (7 mg, 0.05 mmol) were added to a flame-dried 10 mL round bottom flask equipped with a stir bar under  $\text{N}_2$ . Degassed (with  $\text{N}_2$ ) acetonitrile (6 mL) was added to the reaction flask, and the solution was stirred vigorously at room temperature. After 15 minutes, starting material (0.50 mmol) was added to the reaction flask (where specified), the reaction stirred for the specified time, then an aliquot was transferred via syringe to a 4 mm quartz EPR tube under  $\text{N}_2$  and immediately submerged in liquid nitrogen for transport to the EPR spectrometer. Unless otherwise stated, solid-state EPR spectra were collected at 4 K using a temperature-controlled liquid helium cryostat. An additional aliquot was taken concomitantly for  $^{19}\text{F}$  NMR analysis of product formation.

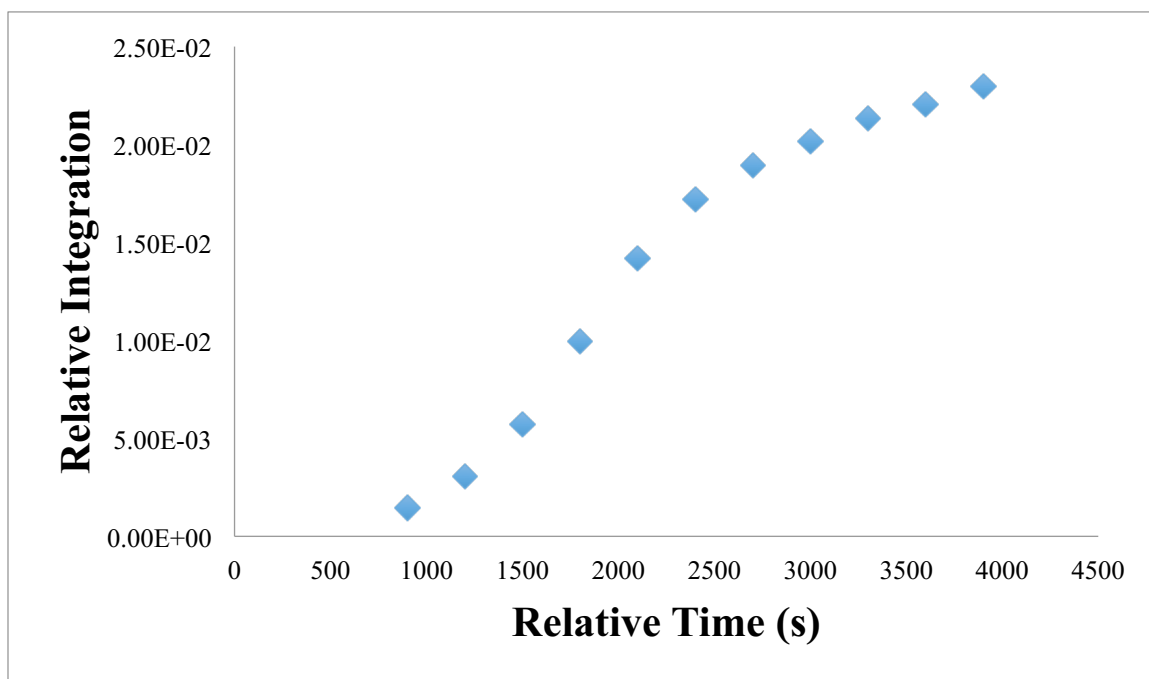
**Preparation of  $^{63}\text{CuI}$ .**  $^{63}\text{CuI}$  was prepared from  $^{63}\text{Cu}$  metal (86.2 mg, 1.4 mmol) and a slight excess of iodine chips (195.2 mg, 0.77 mmol). The reactants were sealed in an evacuated fused-silica tube, and then the reaction vessel was placed in a furnace. The furnace temperature was ramped at 30 °C per hour to a final temperature of 325 °C, held at 325 °C for 24 hours, and then cooled to room temperature. A powder X-ray diffraction pattern of the resulting product was collected using Cu K $\alpha$  radiation (1.5418 Å) on a Bruker D8 Focus diffractometer with a LynxEye detector, showing  $^{63}\text{CuI}$  as the only phase present.

**Voltammetry general procedure.** Differential pulse voltammograms were measured using an Epsilon electrochemical analyzer (Bioanalytical Systems, Inc.) for solutions of the copper(I) compounds in 0.1 M TBAClO $_4$  in acetonitrile with an effective scan rate of 20 mV/s (step potential of 4 mV, pulse width of 50 ms, pulse period of 200 ms, pulse amplitude of 50 mV). Solutions were degassed with Ar for 15 minutes immediately prior to acquisition and maintained in an Ar atmosphere at room temperature. The

three-electrode setup [platinum disk (working electrode), platinum wire (counter electrode), Ag/AgCl (sat. KCl(aq)) (reference electrode)] was calibrated versus ferrocene ( $\text{Fe}^{+/0}$ ) before and after all measurements.

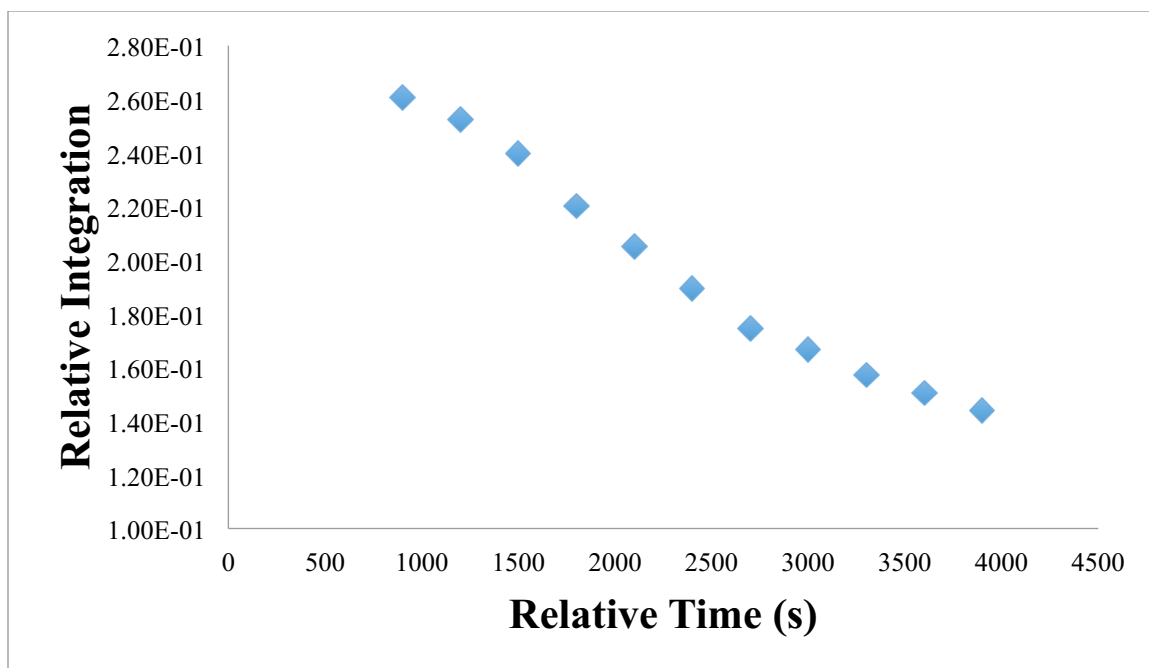
**Spectroelectrochemistry procedure.** Spectroelectrochemistry was conducted on a solution of 1-(chloromethyl)-4-aza-1-azoniabicyclo[2.2.2]octane tetrafluoroborate in 0.1 M TBABF<sub>4</sub> in acetonitrile (degassed with Ar) at room temperature. Controlled potential electrolysis was conducted at +2.5 V and +3.0 V (vs. Ag/AgCl) for ~1 h in an Ar atmosphere at room temperature. UV-Vis spectra were acquired periodically on a Varian Cary-50 spectrophotometer.

**UV-vis kinetic parameters.** UV-vis samples were prepared in a flame-dried round bottom flask under N<sub>2</sub>, as per the general procedure. The specified solution was passed through a syringe filter after 3 min. of stirring, and the first spectrum was collected at t = 5 min. Up until t = 14.5 min., spectra were collected every 0.5 min. From t = 14.5 min. to t = 20 min., spectra were collected every 1.5 min. From t = 20 min. on, spectra were collected every 5 min. The first 19 spectra are reported in the text.

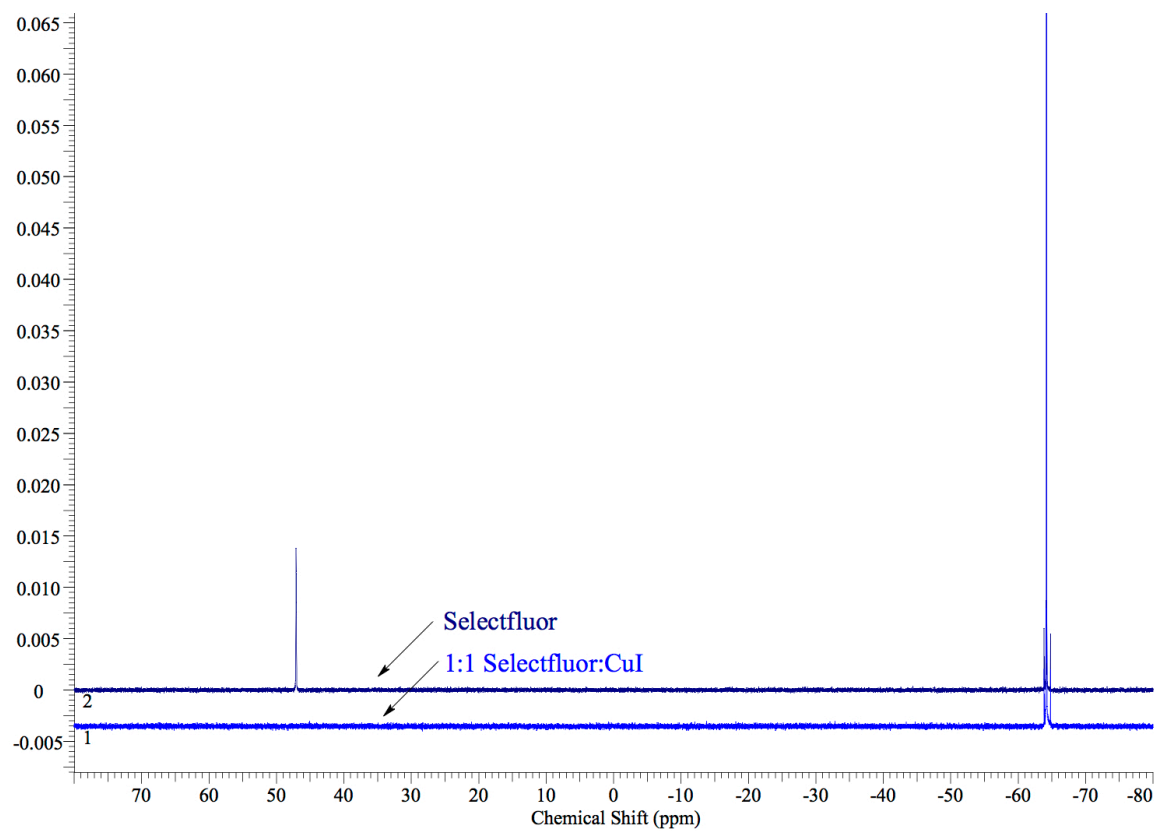


**Figure 12.1** Plot of formation of fluorocyclodecane over time by <sup>19</sup>F NMR.



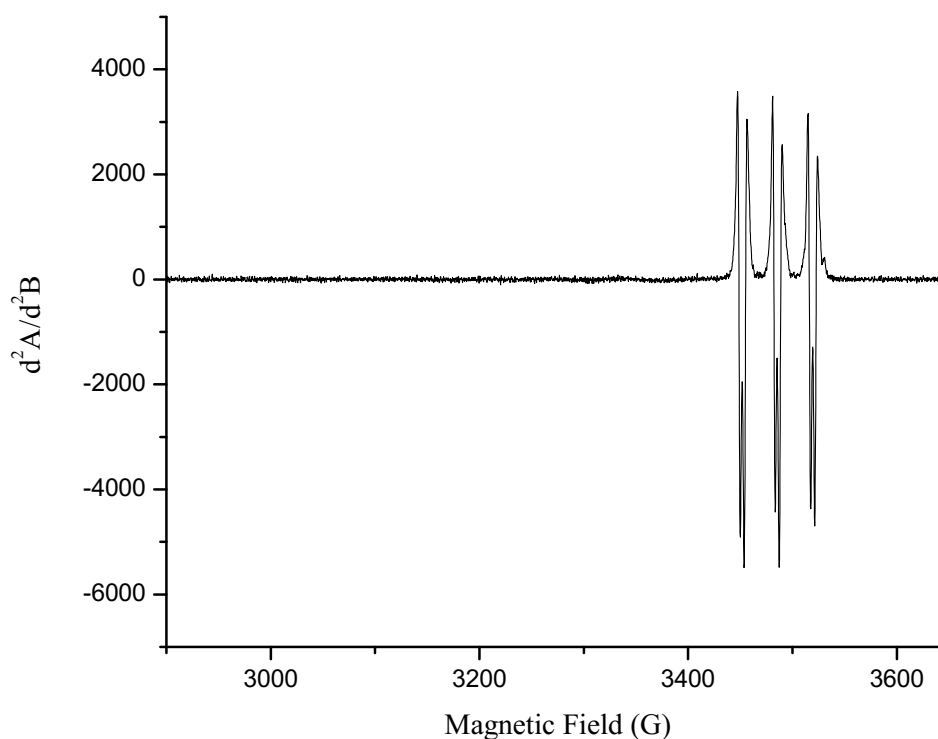


**Figure 12.2** Plot of disappearance of Selectfluor N-F signal over time by  $^{19}\text{F}$  NMR.



**Figure 12.3** Overlay of Selectfluor and 1:1 Selectfluor:CuI  $^{19}\text{F}$  NMR spectra.

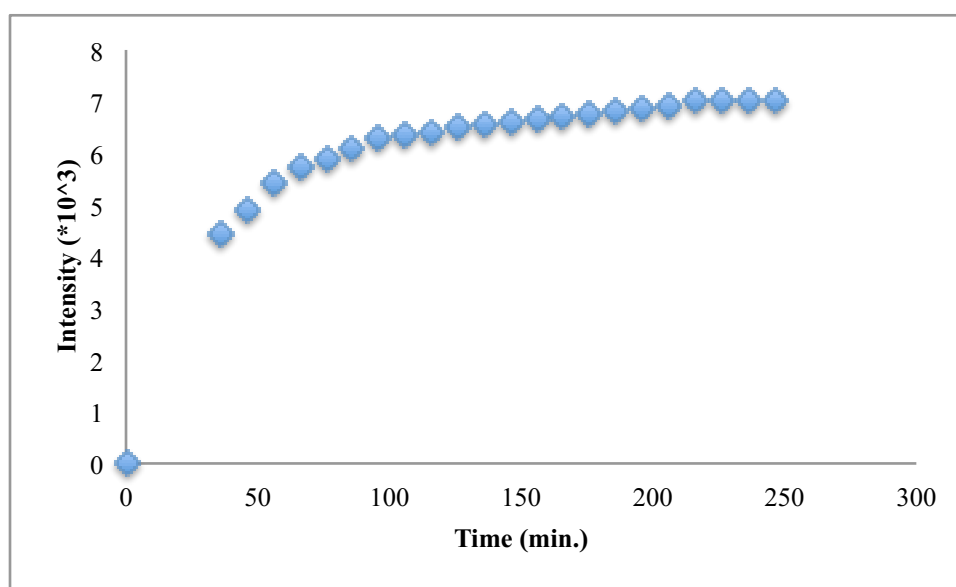
**Copper fluoride control experiments.**  $\text{CuF}_2$  or  $(\text{PPh}_3)_3\text{CuF}_2 \cdot \text{MeOH}$  (0.50 mmol), *N,N*-bis(2,6-dichlorobenzylidene)-ethane-1,2-diamine (190 mg, 0.50 mmol), and potassium carbonate (7 mg, 0.05 mmol) were added to a flame-dried 10 mL round bottom flask equipped with a stir bar under  $\text{N}_2$ . Degassed (with  $\text{N}_2$ ) acetonitrile (6 mL) was added to the reaction flask, and the solution was stirred vigorously at room temperature. After 15 minutes, starting material (0.50 mmol) was added to the reaction flask, and the reaction stirred overnight. The reaction was conducted with adamantane, cyclododecane, 3-phenylpropyl acetate, and hexyl acetate with each copper fluoride species, with and without ligand added. In each instance, no fluorinated products were observed without Selectfluor present. Also, no fluorinated products were detected using Selectfluor in the absence of copper.



**Figure 12.4** Second derivative graph of spin trapped copper(II) post-induction period.

**EPR spin trapping.** The presence of two copper(II) species was also confirmed during an attempt to detect and identify any short-lived organic radicals in solution that was made using 2,4,6-tri-*tert*-butyl

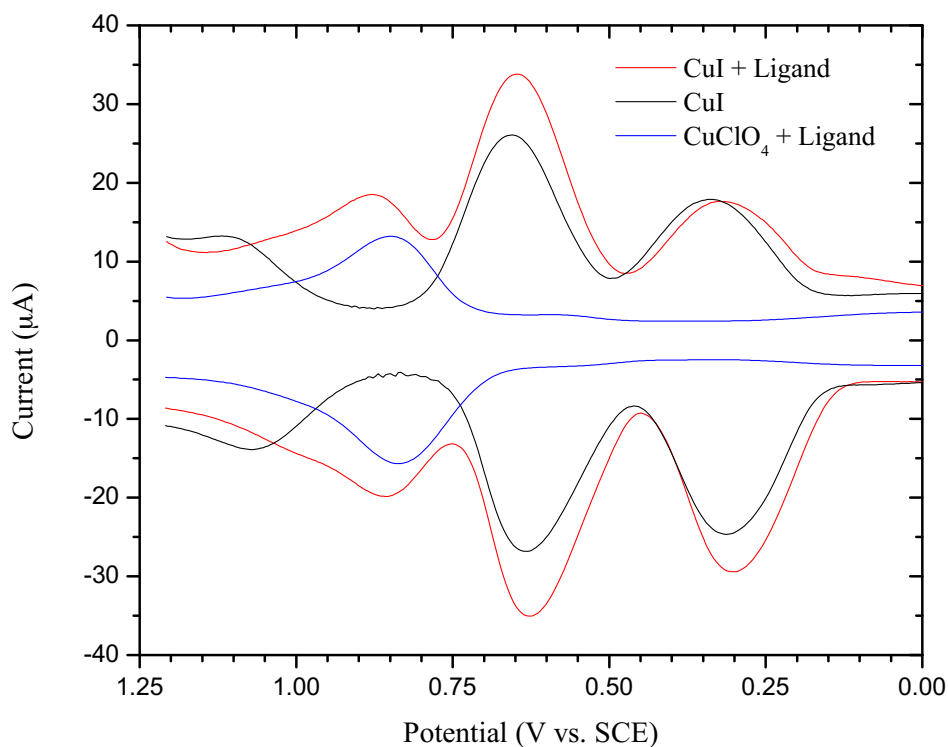
nitrosobenzene (TTBNB), a known spin trap.<sup>19</sup> As anticipated, the reagent only trapped copper (regardless of when it was introduced to the reaction), replacing the four-line pattern with a distinct three-line pattern of the nitroso radical. In the second derivative graph, two minima were detected, corresponding to two inflection points in the first derivative graph. A difference of 3.7 G between the two minima is notably greater than previously reported *meta*-proton hyperfine coupling constants, which range from 0.8-1.9 G.<sup>20</sup> Thus, this is less likely observed "splitting" as it is the trapping of two copper(II) species, which is consistent with the solid-state EPR conclusions.



**Figure 12.5** Plot of intensity vs. time of a standard reaction in a flat-cell monitored at room temperature by EPR.

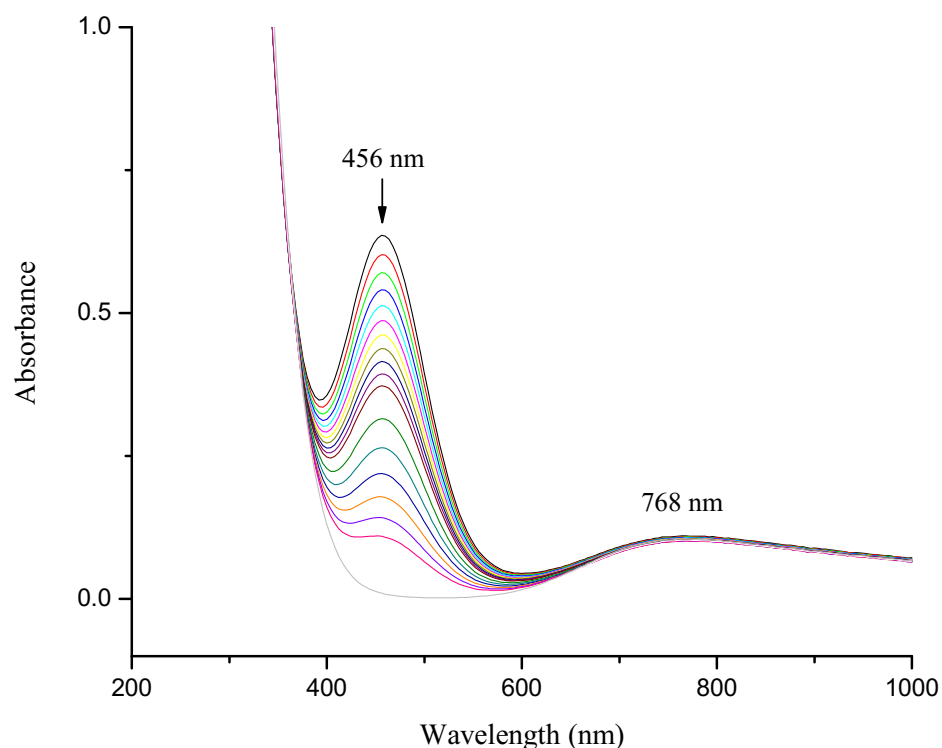
**Differential pulse voltammogram control experiments.** The differential pulse voltammogram of a 1:1 mixture of cuprous iodide to the *N,N*-bis(2,6-dichlorobenzylidene)ethane-1,2-diamine ligand in 0.1 M tetrabutylammonium perchlorate (TBAClO<sub>4</sub>) acetonitrile revealed three quasi-reversible transitions. An additional voltammogram of cuprous iodide and a 1:1 mixture of tetrakis(acetonitrile)copper(I) perchlorate to ligand proved amenable in assigning these waves more accurately. The DPV of cuprous iodide accounted for the two waves at +0.64 V and +0.31 V vs. SCE, which can be respectively assigned as copper(II/I) and I<sub>2</sub>/I<sup>-</sup> couples.<sup>21</sup> The DPV of 1:1 tetrakis(acetonitrile)copper(I) perchlorate to ligand mixture

matched up with the third  $1e^-$  process at a higher oxidation potential of +0.87 V, a slightly tuned copper(II/I) transition. This suggests that our copper species is more easily oxidized in the presence of the ligand.



**Figure 12.6** Overlay of differential pulse voltammograms.

**UV-vis spectra of CuI and Selectfluor.** We observe visible bands at 456 nm and 768 nm upon the addition of cuprous iodide to Selectfluor in MeCN under  $N_2$ . The broad band at 768 nm is conceivably a new copper(II) absorbance, consistent with our EPR findings. The decreasing absorbance at 456 nm completely replaces the band observed from cuprous iodide alone in MeCN at 424 nm<sup>22</sup> and was later determined to result from an interaction between iodide and Selectfluor. This absorbance was duplicated when taking a UV-vis spectrum upon mixing Selectfluor with tetrabutylammonium iodide (the interaction between iodide and Selectfluor alone will not effect the fluorination reaction – copper is necessary).



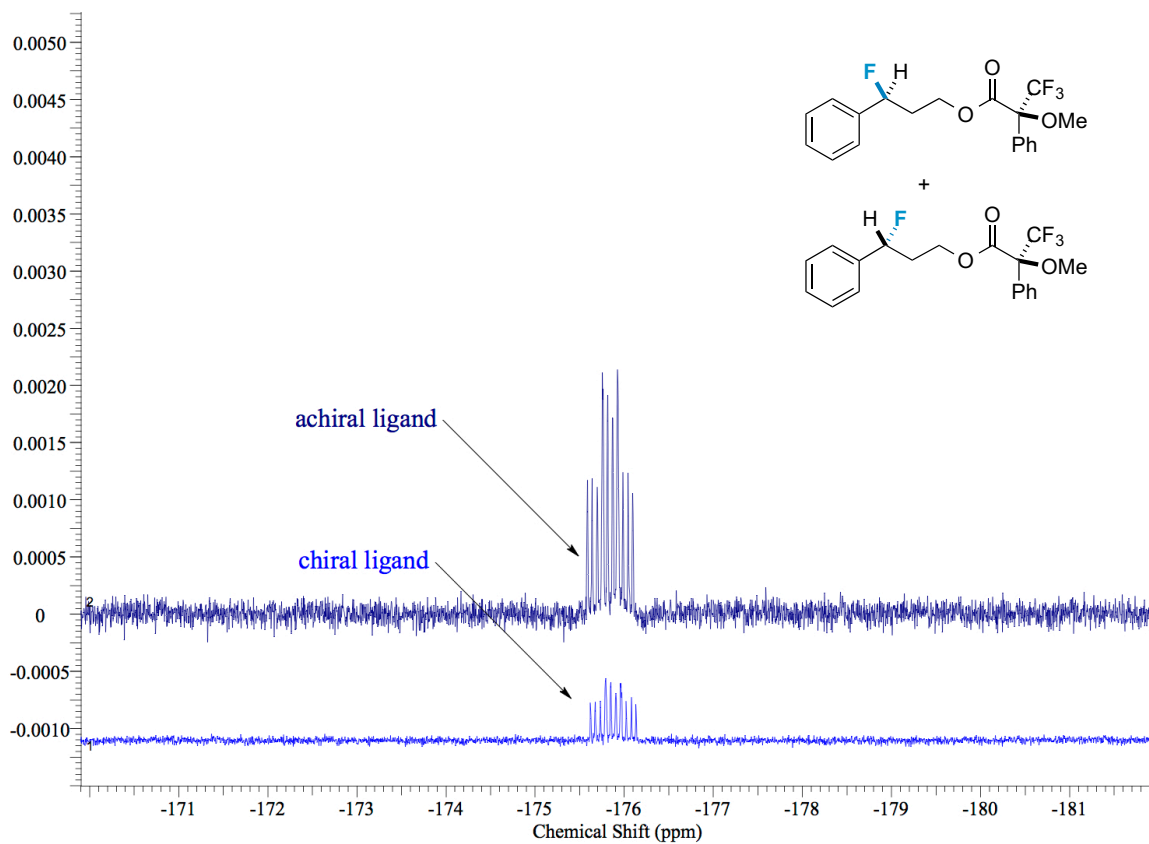
**Figure 12.7** UV-vis spectra of CuI and Selectfluor over time.

**Discussion of copper removal/sequestration experiments.** Additional efforts were made to probe the role of copper as either an initiator or a catalyst by attempting to remove or sequester copper during the course of the reaction. First, we considered using a solid-supported copper(I) species in place of cuprous iodide – a silica or resin bound reagent can be filtered out of the reaction (under  $N_2$ ) at any time. Silica- and resin-supported pyridylmethanimine copper(I) catalysts<sup>23</sup> were suitable replacements for cuprous iodide in effecting the fluorination reaction, and we found that the reaction did proceed in both instances upon filtering off the solid-support. However, firm conclusions cannot be drawn from these experiments, as there was visibly some degree of copper leaching.

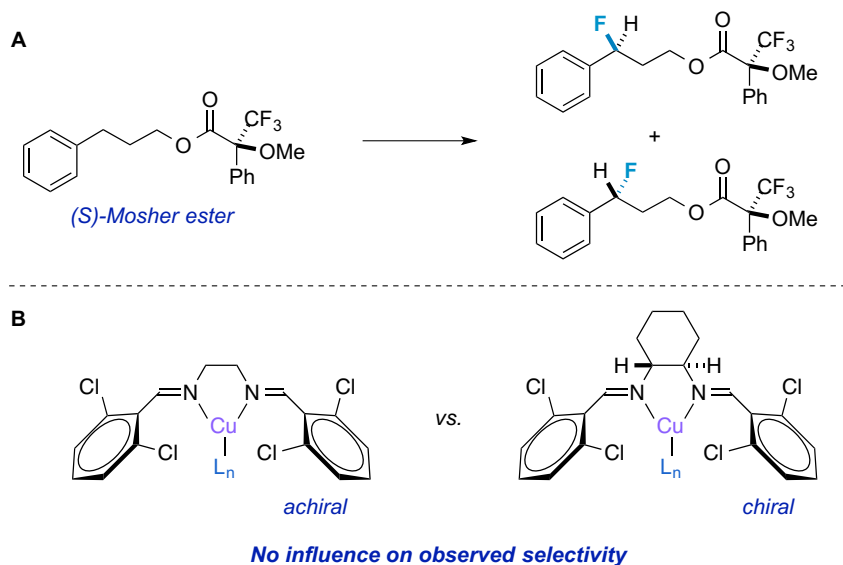
Removing copper from the reaction altogether proved difficult, so we attempted to sequester it using excess ligand. The reaction proceeded with a similar product yield using 0.2 equiv. of ligand (2:1 ligand:copper) from the start of the reaction, as well as when the extra 0.1 equiv. of ligand was introduced after 15 minutes of stirring. Assuming the copper(II) species is bound by both bis(imine)

ligands, the atom center would be very hindered.<sup>24</sup> If copper has dynamic redox-activity as a catalyst beyond initiating the reaction, the sequestration using 2:1 ligand:copper during the reaction should slow down the reaction, shut it down altogether, or have an effect on yield, and none of the above seemed to be the case.

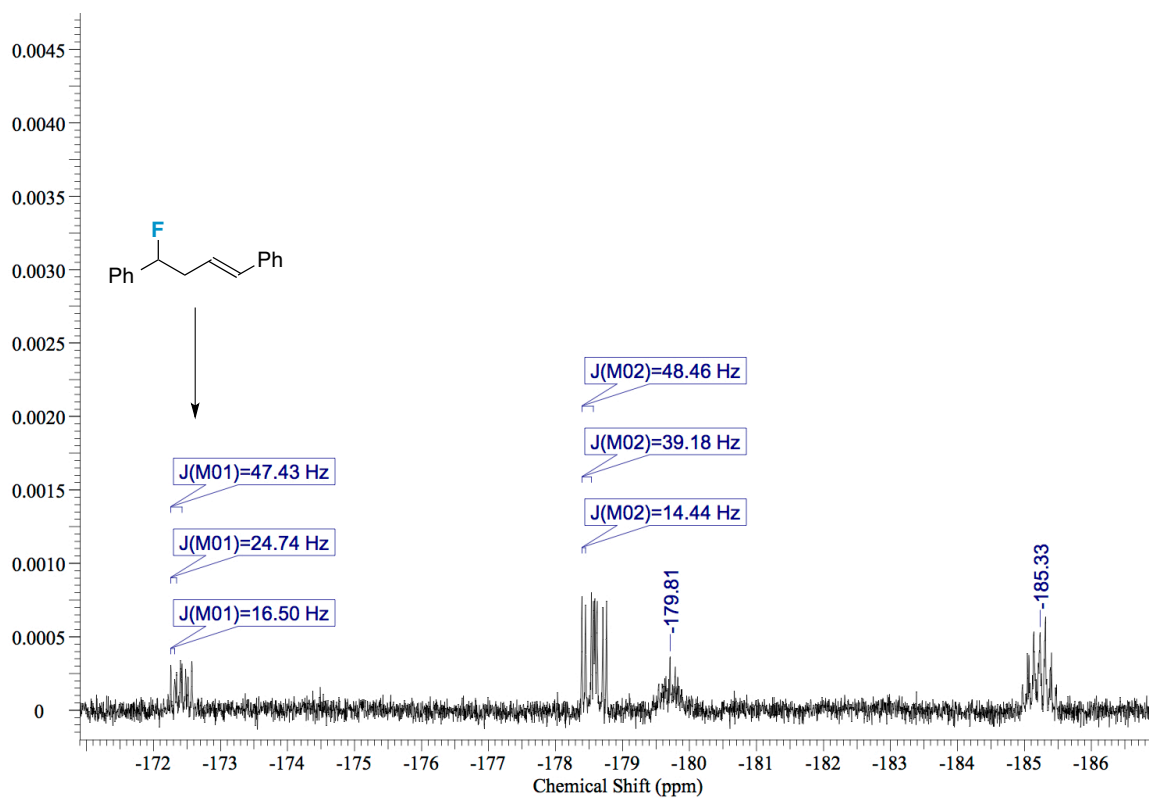
On the other hand, we were able to shut down the reaction immediately using 0.4 equiv. ligand (4 times the amount of copper), that is, by adding 0.3 extra equiv. of ligand any time over the course of the reaction. However, it is very plausible that this is entirely unrelated to the matter of copper sequestration. More likely, the putative radical dication **3** is preferentially oxidizing the bis(imine) ligand instead of the alkane substrate if the imine is present in higher concentrations, which also shuts down the reaction. This is further supported by the fact that the reaction can also be immediately shut down upon addition of 0.1 equiv. of tertiary amines, e.g. triethylamine or Hünig's base, that are certainly more easily oxidized than an alkane.



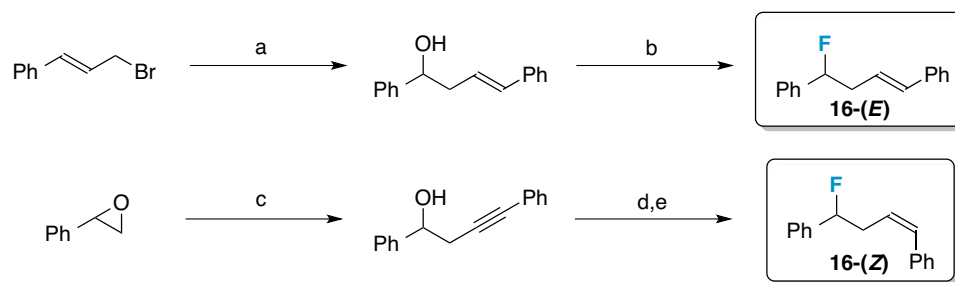
**Figure 12.8** Overlay of <sup>19</sup>F NMR spectra for reactions using a Mosher ester substrate.



**Scheme 12.1** (A) Products of reaction on a Mosher ester substrate. (B) Achiral and chiral ligands employed.



**Figure 12.9**  $^{19}\text{F}$  NMR spectrum of crude reaction mixture from 2-phenylbenzylcyclopropane fluorination.



a) PhCOH, Sn, H<sub>2</sub>O, rt, 4 days;<sup>25</sup> b) DAST, CH<sub>2</sub>Cl<sub>2</sub>, -78°C to rt, 16 h;<sup>26</sup> c) PhCClLi, LiClO<sub>4</sub>, THF, 0°C, 24 h;<sup>27</sup> d) Lindlar's catalyst, H<sub>2</sub>, 1 atm, rt, EtOAc, 2 h;<sup>28</sup> e) DAST, CH<sub>2</sub>Cl<sub>2</sub>, -78°C to rt, 12 h.<sup>26</sup>

**Scheme 12.2** Syntheses of (4-fluorobut-1-ene-1,4-diyl)dibenzene isomers.

### Characterization Data.

**(E)-(4-fluorobut-1-ene-1,4-diyl)dibenzene.** <sup>19</sup>F NMR (CD<sub>3</sub>CN): -172.45 (1 F, ddd, *J* = 47.4, 26.8, 17.5 Hz); <sup>1</sup>H NMR (CD<sub>3</sub>CN): 7.34-7.11 (10 H, m), 6.41 (1 H, d, *J* = 15.8 Hz), 6.16 (1 H, dt, *J* = 16.0, 7.0 Hz), 5.52 (1 H, ddd, *J* = 47.5, 7.5, 5.3 Hz), 2.88-2.60 (2 H, m); <sup>13</sup>C NMR (CD<sub>3</sub>CN): 139.9, 137.3, 132.9, 128.6, 128.5, 128.4, 128.4, 127.4, 126.0, 125.8, 125.7, 124.7, 124.6, 93.8 (d, *J* = 170.5 Hz), 40.4, 40.1.

**(Z)-(4-fluorobut-1-ene-1,4-diyl)dibenzene.** <sup>19</sup>F NMR (CD<sub>3</sub>CN): -173.78 (1 F, ddd, *J* = 47.4, 27.8, 18.6 Hz); <sup>1</sup>H NMR (CD<sub>3</sub>CN): 7.45-7.27 (10 H, m), 6.60 (1 H, d, *J* = 11.7 Hz), 5.77 (1 H, dt, *J* = 11.7, 7.0 Hz), 5.64 (1 H, ddd, *J* = 47.7, 7.7, 5.1 Hz), 3.12-2.80 (2 H, m); <sup>13</sup>C NMR (CD<sub>3</sub>CN): 140.0, 139.8, 137.0, 131.4, 128.6, 128.5, 128.3, 127.0, 125.8, 125.7, 93.8 (d, *J* = 169.6 Hz), 36.1, 35.8.

**Table 12.1** Intrinsic relative hexyl acetate radical stabilities.

Radical Species	Relative Selectivity of Product by <sup>19</sup> F NMR	<i>E</i> <sub>relative</sub> in kcal/mol	
		B3LYP/6-311++G**	RI-MP2/6-311++G**
Me-	1.00	0.000	0.000
Me-	0.39	+ 0.117	+ 0.311
Me-	0.14	+ 0.181	+ 0.324
Me-	0.05	+ 1.112	+ 1.529



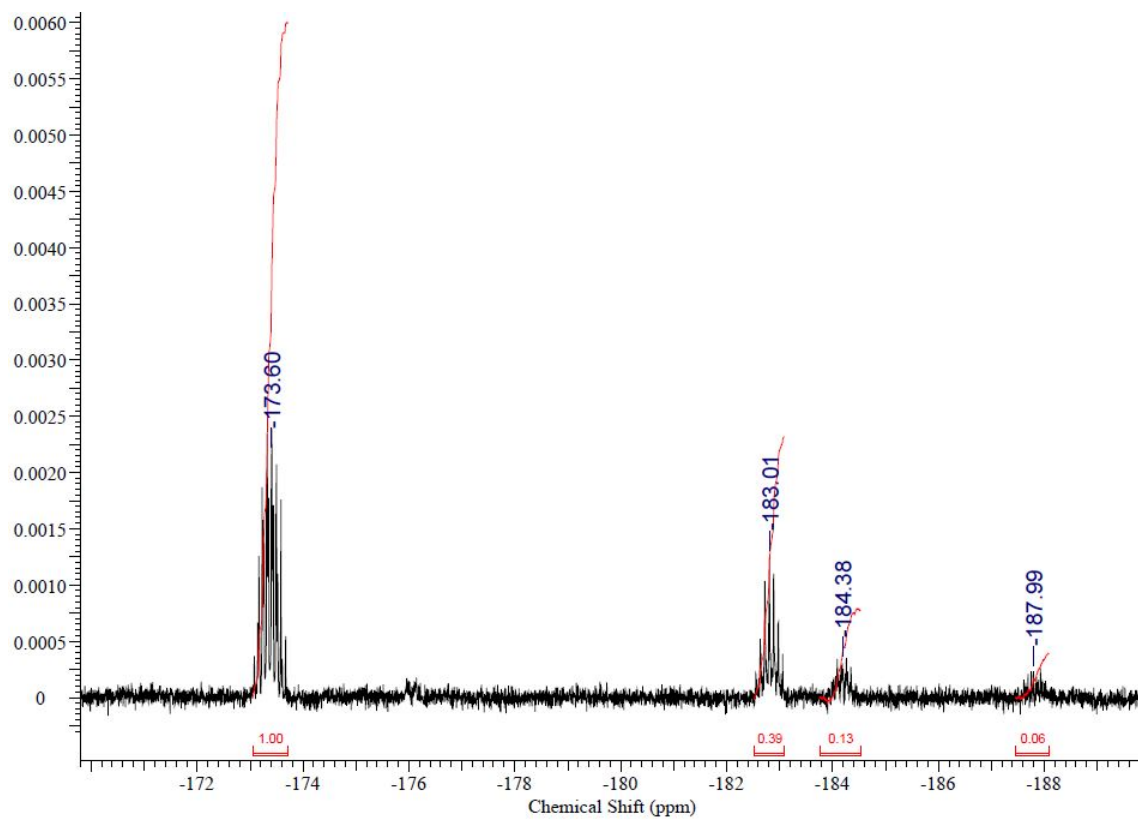


Figure 12.10 Relative n-fluoro-hexyl acetate  $^{19}\text{F}$  NMR integrations.

**Table 12.2** Isodesmic reactions: predictive properties of radical cations.

Isodesmic Reaction		$\Delta E$ (kcal/mol)
		-3.0*
		-14.6**
		0.8
		5.4
		0.2
		-1.5
		18
		-13
		-2.3
		-52
		6.0

All geometry optimizations were performed at B3PW91/6-311+G\*\*(MeCN), unless otherwise stated.  
 \*Geometry optimizations performed at B3PW91/DGDZVP(MeCN). \*\*Geometry optimizations performed at B3LYP/6-311++G\*\*(MeCN).

**Table 12.3** Compiled initial rate data.

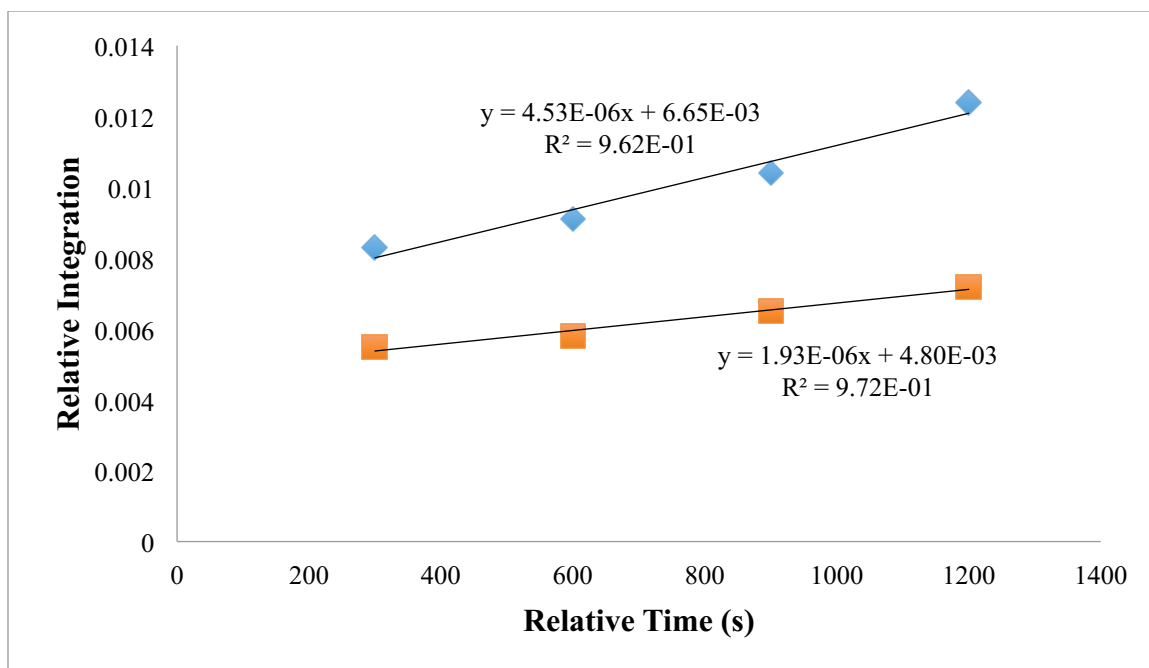
<b>Rate (Int./sec)</b>	<b>[3-phenylpropyl acetate]</b>	<b>[Selectfluor]</b>	<b>[CuI-Ligand]</b>	<b>[K<sub>2</sub>CO<sub>3</sub>]</b>
1.02E-05	0.083	0.183	0.0083	0.017
7.40E-06	0.057	0.183	0.0083	0.017
4.72E-06	0.042	0.183	0.0083	0.017
<b>Rate (M/sec)</b>	<b>[Cyclodecane]</b>	<b>[Selectfluor]</b>	<b>[CuI-Ligand]</b>	<b>[K<sub>2</sub>CO<sub>3</sub>]</b>
7.69E-07	0.083	0.183	0.0083	0.017
5.32E-07	0.062	0.183	0.0083	0.017
<b>Rate (Int./sec)</b>	<b>[3-phenylpropyl acetate]</b>	<b>[Selectfluor]</b>	<b>[CuI-Ligand]</b>	<b>[K<sub>2</sub>CO<sub>3</sub>]</b>
4.72E-06	0.042	0.183	0.0083	0.017
3.87E-06	0.042	0.142	0.0083	0.017
<b>Rate (Int./sec)</b>	<b>[3-phenylpropyl acetate]</b>	<b>[Selectfluor]</b>	<b>[CuI-Ligand]</b>	<b>[K<sub>2</sub>CO<sub>3</sub>]</b>
1.02E-05	0.083	0.183	0.0083	0.017
9.47E-06	0.083	0.183	0.0042	0.017
<b>Rate (Int./sec)</b>	<b>[3-phenylpropyl acetate]</b>	<b>[Selectfluor]</b>	<b>[CuI-Ligand]</b>	<b>[K<sub>2</sub>CO<sub>3</sub>]</b>
1.09E-05	0.083	0.183	0.0083	0.025
1.02E-05	0.083	0.183	0.0083	0.017

\*Reported rates are the average of two runs.

**Procedure for rate studies with 3-phenylpropyl acetate.** Selectfluor (390 mg, 1.1 mmol), cuprous iodide (10 mg, 0.05 mmol), *N,N*-bis(2,6-dichloro-benzylidene)ethane-1,2-diamine (19 mg, 0.05 mmol), and potassium carbonate (7 mg, 0.05 mmol) were added to a flame-dried 10 mL round bottom flask equipped with a stir bar under N<sub>2</sub>. A degassed (with N<sub>2</sub>) mixture of 4:1 CH<sub>3</sub>CN:CD<sub>3</sub>CN (6 mL) was added to the reaction flask, and the solution was stirred vigorously at room temperature. After 10 minutes, 3-chlorobenzotrifluoride (0.02 mL, 0.15 mmol) was added via syringe. After 15 minutes, 3-phenylpropyl acetate (0.09 mL, 0.50 mmol) was added to the reaction flask. The reaction solution stirred for an additional 2 minutes, then 0.5 mL was transferred via syringe from the reaction flask to an NMR tube fit with a septum under N<sub>2</sub>. A <sup>19</sup>F NMR spectrum of the same sample was collected every 300 seconds at room temperature. Product concentrations were determined using 3-chlorobenzotrifluoride as an internal standard.

**Procedure for rate studies with cyclodecane.** Selectfluor (390 mg, 1.1 mmol), cuprous iodide (10 mg, 0.05 mmol), *N,N*-bis(2,6-dichloro-benzylidene)ethane-1,2-diamine (19 mg, 0.05 mmol), and potassium carbonate (7 mg, 0.05 mmol) were added to a flame-dried 10 mL round bottom flask equipped with a stir bar under N<sub>2</sub>. A degassed (with N<sub>2</sub>) mixture of 4:1 CH<sub>3</sub>CN:CD<sub>3</sub>CN (6 mL) was added to the reaction flask; the solution was immediately cooled to 0°C and stirred vigorously. After 10 minutes, 3-chlorobenzotrifluoride (0.02 mL, 0.15 mmol) was added via syringe. After 15 minutes, cyclodecane (0.08 mL, 0.50 mmol) was added to the reaction flask. The reaction solution stirred for an additional 2 minutes, then 0.5 mL was transferred via syringe from the reaction flask to an NMR tube in an ice bath fit with a septum under N<sub>2</sub>. A <sup>19</sup>F NMR spectrum of the same sample was collected every 300 seconds at 10 °C. Product concentrations were determined using 3-chlorobenzotrifluoride as an internal standard. The data points were fitted to the equation of a sigmoidal curve with high coefficients of determination, and this equation was used to extrapolate five points in the initial rate regime (within 600 s of first reported data point, as small peaks were observed 300 s and 600 s prior to the first reported data point, but could not be accurately integrated). All curves were fit/analyzed in the exact same manner.

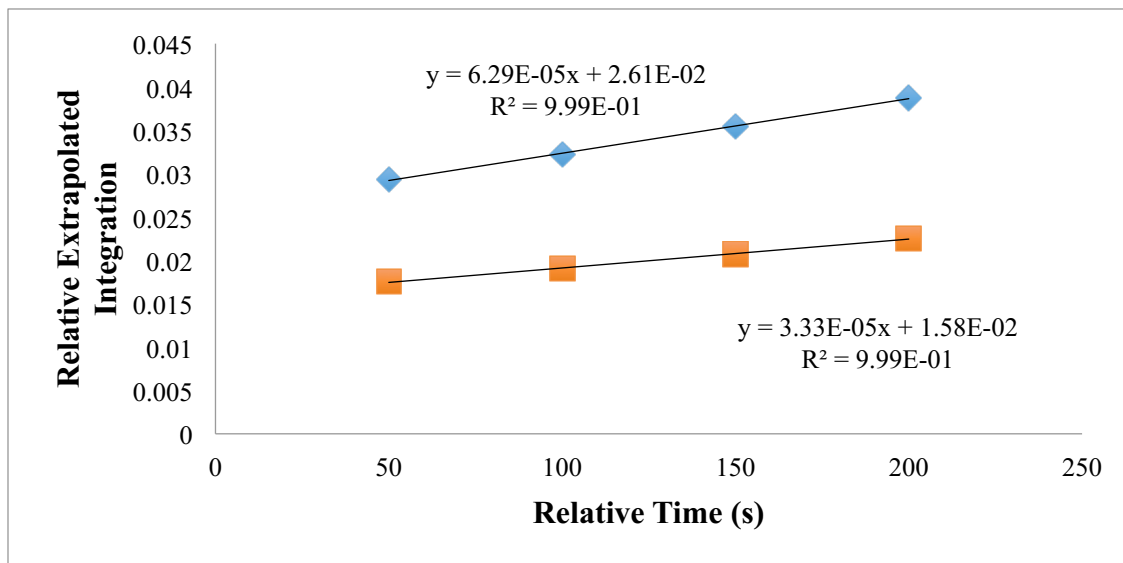
**Competitive KIE: 3-phenylpropyl acetate.** Selectfluor (390 mg, 1.1 mmol), cuprous iodide (10 mg, 0.05 mmol), *N,N*-bis(2,6-dichloro-benzylidene)ethane-1,2-diamine (19 mg, 0.05 mmol), and potassium carbonate (7 mg, 0.05 mmol) were added to a flame-dried 10 mL round bottom flask equipped with a stir bar under N<sub>2</sub>. A degassed (with N<sub>2</sub>) mixture of 4:1 CH<sub>3</sub>CN:CD<sub>3</sub>CN (6 mL) was added to the reaction flask, and the solution was stirred vigorously at room temperature. After 10 minutes, 3-chlorobenzotrifluoride (0.02 mL, 0.15 mmol) was added via syringe. After 15 minutes, a mixture of 3-phenylpropyl acetate, 3-phenylpropyl-3-*d* acetate, and 3-phenylpropyl-3,3-*d*<sub>2</sub> acetate (0.09 mL, 0.50 mmol) was added to the reaction flask (ca. 50% incorporation of deuterium in the benzylic position by <sup>1</sup>H NMR). The reaction solution stirred for an additional 2 minutes, then 0.5 mL was transferred via syringe from the reaction flask to an NMR tube fit with a septum under N<sub>2</sub>. A <sup>19</sup>F NMR spectrum of the same sample was collected every 300 seconds at room temperature. Product concentrations were determined using 3-chlorobenzotrifluoride as an internal standard.  $k_H/k_D \approx 2.3$  (average of two runs: 2.3 + 2.3).



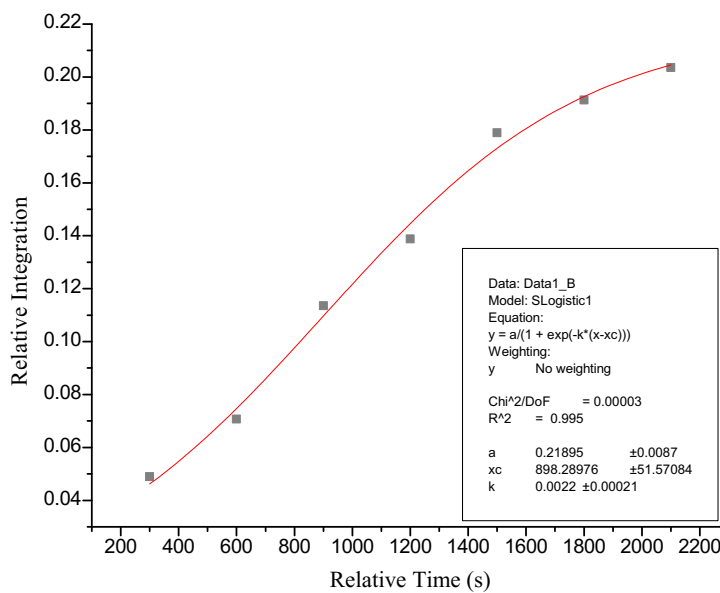
**Figure 12.11** Representative plot for initial rate of formation of 3-fluoro-3-phenylpropyl acetate (*top*) vs. 3-fluoro-3-phenylpropyl-3-*d* acetate (*bottom*) by  $^{19}\text{F}$  NMR.

**Competitive KIE: cyclohexane.** Selectfluor (390 mg, 1.1 mmol), cuprous iodide (10 mg, 0.05 mmol), *N,N*-bis(2,6-dichloro-benzylidene)ethane-1,2-diamine (19 mg, 0.05 mmol), and potassium carbonate (7 mg, 0.05 mmol) were added to a flame-dried 10 mL round bottom flask equipped with a stir bar under  $\text{N}_2$ . A degassed (with  $\text{N}_2$ ) mixture of 4:1  $\text{CH}_3\text{CN}:\text{CD}_3\text{CN}$  (6 mL) was added to the reaction flask, and the solution was immediately cooled to  $0^\circ\text{C}$  and stirred vigorously. After 10 minutes, 3-chlorobenzotrifluoride (0.02 mL, 0.15 mmol) was added via syringe. After 15 minutes, a 1:1 mixture of cyclohexane:cyclohexane- $d_{12}$  (0.06 mL, 0.50 mmol) was added to the reaction flask. The reaction solution stirred for an additional 2 minutes, then 0.5 mL was transferred via syringe from the reaction flask to an NMR tube fit with a septum under  $\text{N}_2$ . A  $^{19}\text{F}$  NMR spectrum of the same sample was collected every 300 seconds at  $25^\circ\text{C}$ . Product concentrations were determined using 3-chlorobenzotrifluoride as an internal standard. The data points were fitted to the equation of a sigmoidal curve (seen below) with high coefficients of determination, and this equation was used to extrapolate five points in the initial rate regime (within 600 s of first reported data point, as small peaks were observed 300 s and 600 s prior to the first

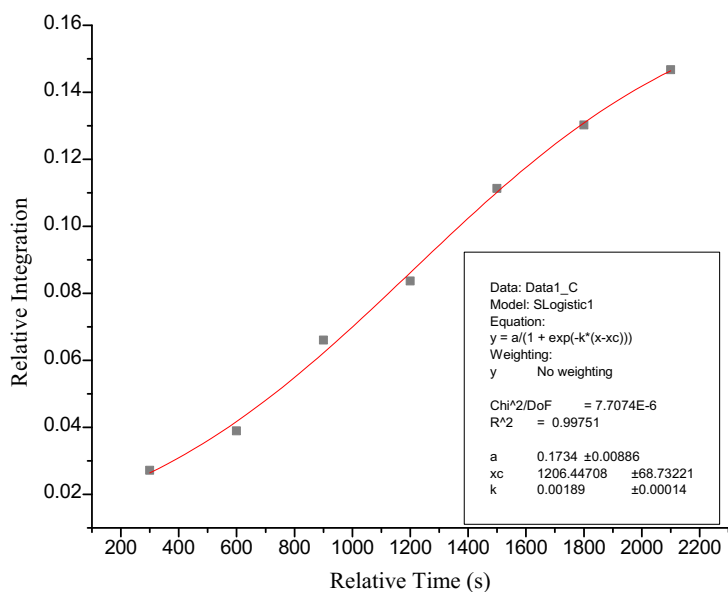
reported data point, but could not be accurately integrated). All curves were fit/analyzed in the exact same manner.  $k_H/k_D \approx 2.0$  (average of two runs: 1.9 + 2.1).



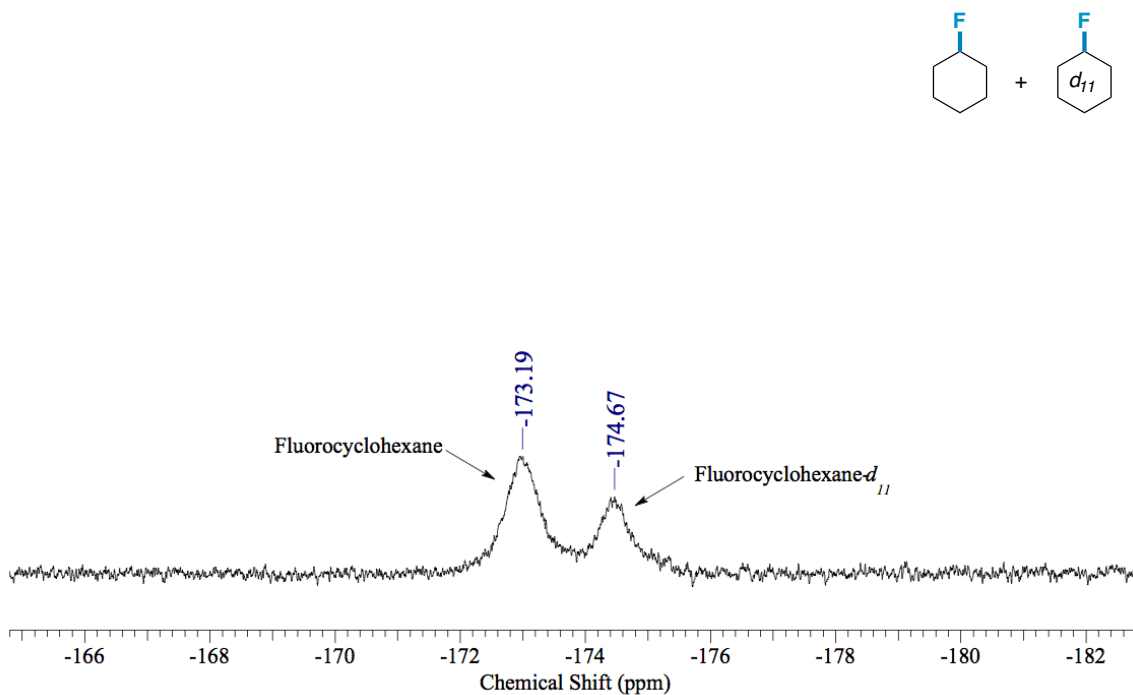
**Figure 12.12** Representative plot for initial rate of formation of fluorocyclohexane (*top*) vs. fluorocyclohexane- $d_{11}$  (*bottom*) by  $^{19}\text{F}$  NMR extrapolated from sigmoidal fit equations.



**Figure 12.13** Sigmoidal fit for appearance of fluorocyclohexane by  $^{19}\text{F}$  NMR.

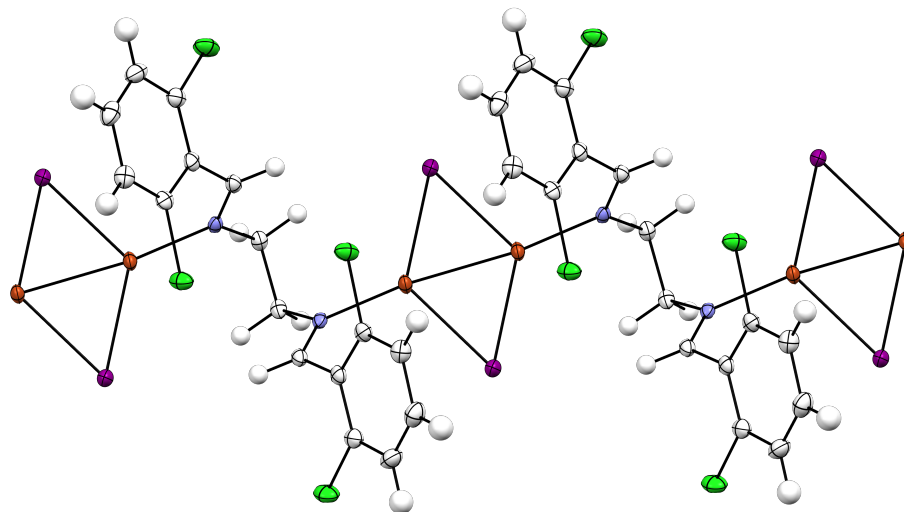


**Figure 12.14** Sigmoidal fit for appearance of fluorocyclohexane- $d_{11}$  by  $^{19}\text{F}$  NMR.



**Figure 12.15** Sample  $^{19}\text{F}$  NMR of competitive KIE experiment following the rate of appearance of fluorocyclohexane vs. fluorocyclohexane- $d_{11}$ .

**Crystallographic Information.** An attempt was made to grow single crystals of the unoxidized copper-ligand complex. A yellow precipitate formed from a 1:1 mixture of cuprous iodide to ligand in MeCN after approximately 2 h of stirring. Upon filtration, dissolution, and solvent evaporation, single yellow crystals were obtained and suitable for X-ray structure determination. The crystal structure showed a polymeric complex exhibiting 2:1 cuprous iodide to ligand stoichiometry, copper atoms linked by bridging iodine atoms, and the nitrogen atoms on the ligand singly bound to two different copper atoms. The same compound was also isolated as more defined yellow microcrystals via the vapor diffusion technique with acetonitrile and diethyl ether.



**Figure 12.16** Displacement ellipsoid plot (50% probability level) of  $2\text{CuI}\cdot\text{bis}(\text{imine})$  complex at 110(2) K.

Despite the tendency for these molecules to crystallize as a polymeric structure, we can quickly gather that this is unlikely playing any active role in solution during the reaction. In fact, the EPR signatures of the copper(II) species observed over the course of the reaction do not resemble those of dimeric or polymeric copper species.<sup>29</sup> This polymeric form is more likely just a thermodynamic sink for a copper-ligand interaction in its unoxidized form. Any attempt to grow crystals of the oxidized copper species (in the presence of Selectfluor) only afforded the ammonium salt -  $\text{H-TEDA-BF}_4$  - previously reported by the Baran group.



All reflection intensities were measured at 110(2) K using a SuperNova diffractometer (equipped with Atlas detector) with Mo  $K\alpha$  radiation ( $\lambda = 0.71073 \text{ \AA}$ ) under the program CrysAlisPro (Version 1.171.36.24 Agilent Technologies, 2012). The program CrysAlisPro (Version 1.171.36.24 Agilent Technologies, 2012) was used to refine the cell dimensions. Data reduction was done using the program CrysAlisPro (Version 1.171.36.24 Agilent Technologies, 2012). The structure was solved with the program SHELXS-2013 (Sheldrick, 2013) and was refined on  $F^2$  with SHELXL-2013 (Sheldrick, 2013). Analytical numeric absorption corrections based on a multifaceted crystal model were applied using CrysAlisPro (Version 1.171.36.24 Agilent Technologies, 2012). The temperature of the data collection was controlled using the system Cryojet (manufactured by Oxford Instruments). The H atoms were placed at calculated positions using the instructions AFIX 23 or AFIX 43 with isotropic displacement parameters having values 1.2 times  $U_{eq}$  of the attached C atoms. The structure is ordered.

**Complex:**  $F_w = 377.48$ , irregular yellow shaped crystals,  $0.25 \times 0.16 \times 0.06 \text{ mm}^3$ , monoclinic,  $P2/c$  (no. 13),  $a = 8.25345(18)$ ,  $b = 7.57776(17)$ ,  $c = 17.1862(3) \text{ \AA}$ ,  $\beta = 94.4721(18)^\circ$ ,  $V = 1071.60(4) \text{ \AA}^3$ ,  $Z = 4$ ,  $D_x = 2.340 \text{ g cm}^{-3}$ ,  $\mu = 5.368 \text{ mm}^{-1}$ , abs. corr. range: 0.420–0.772. 9111 Reflections were measured up to a resolution of  $(\sin \theta/\lambda)_{\max} = 0.65 \text{ \AA}^{-1}$ . 2467 Reflections were unique ( $R_{\text{int}} = 0.0215$ ), of which 2319 were observed [ $I > 2\sigma(I)$ ]. 118 Parameters were refined.  $R1/wR2$  [ $I > 2\sigma(I)$ ]: 0.0167/0.0389.  $R1/wR2$  [all refl.]: 0.0186/0.0398.  $S = 1.051$ . Residual electron density found between  $-0.40$  and  $0.46 \text{ e \AA}^{-3}$ .

**Computational Methods.** All  $^{19}\text{F}$  NMR calculated chemical shifts were fitted to the empirical equation (at B3LYP/6-311++G\*\*)  $\delta_{\text{calc}} = -0.914d + 142.63$ . The isotropic values ( $\delta$ ) employed were obtained from the CSGT calculation parameter found in the results menu. Geometry optimizations were determined at either B3LYP/6-311++G\*\*, RI-MP2/6-311++G\*\*, B3PW91/6-311++G\*\*, or DGDZVP/6-311++G\*\* (employed for Cu and I) using the default acetonitrile solvent continuum. Transition states were determined at the B3LYP/6-311++G\*\* level of theory using the default acetonitrile solvent continuum.

## 12.5 Experimental Details for Chapter 5.

**Representative Fluorination Procedure.** Selectfluor (390.0 mg, 1.1 mmol, 2.2 equiv) was added to a 10 mL flame-dried round bottom flask equipped with a stir bar under N<sub>2</sub>. Acetonitrile (6.0 mL) was added to the reaction flask, and the solution was stirred vigorously at room temperature. 2-Benzylcyclohexanone (94.0 mg, 0.5 mmol, 1.0 equiv) was added, followed by 1.0 M triethylborane solution in hexanes (10.0 mg, 0.1 mmol, 0.2 equiv). The reaction mixture stirred for 4 h. The product was diluted with Et<sub>2</sub>O and filtered through Celite. The solvents were removed by rotary evaporation, and the residue was subjected to preparative TLC on silica with a mixture of ethyl acetate/hexanes as eluent to afford 2-(fluoro(phenyl)methyl)cyclohexanone as a clear oil (43 mg, 41%).

**Characterization Data.** Characterization of fluorocycloheptane (**5**),<sup>30</sup> fluorocyclooctane (**6**),<sup>31</sup> fluorocyclodecane (**7**),<sup>32</sup> fluorocyclododecane (**8**),<sup>33</sup> fluoroadamantane (**9**),<sup>34</sup> 3-fluoroadamantan-1-ol (**10**),<sup>33</sup> (1-fluoroethyl)benzene (**11**),<sup>35</sup> 4-fluoro-4-phenylbutan-2-one (**12**),<sup>36</sup> 3-fluoro-1,3-diphenylpropan-1-one (**13**),<sup>30</sup> methyl-3-fluoro-3-phenylpropanoate (**14**),<sup>30</sup> 2-(fluoro(phenyl)methyl)cyclohexanone (**15**)<sup>37</sup> were consistent with literature precedent.

**Fluorocycloheptane (5).** <sup>1</sup>H NMR (CD<sub>3</sub>CN): 5.26-4.97 (1 H, dm, *J* = 47.7 Hz), 2.46-1.19 (12 H, m); <sup>19</sup>F NMR (CD<sub>3</sub>CN): -164.55 (1 F, m). Yield: (47%).<sup>30</sup>

**Fluorocyclooctane (6).** <sup>1</sup>H NMR (CD<sub>3</sub>CN): 5.25-4.92 (1 H, dm, *J* = 46.3), 2.38-1.19 (14 H, m); <sup>19</sup>F NMR (CD<sub>3</sub>CN): -164.51 (1 F, m). Yield: (41%).<sup>31</sup>

**Fluorocyclodecane (7).** <sup>1</sup>H NMR (CD<sub>3</sub>CN): 5.36-5.06 (1 H, dm, *J* = 46.5 Hz), 2.42-1.16 (18 H, m); <sup>19</sup>F NMR (CD<sub>3</sub>CN): -166.29 (1 F, m). Yield: (40%).<sup>32</sup>

**Fluorocyclododecane (8).** <sup>1</sup>H NMR (CDCl<sub>3</sub>): 4.72 (1 H, dm, *J* = 47.5 Hz), 1.87-1.51 (4 H, m), 1.48-1.26 (18 H, m); <sup>19</sup>F NMR (CDCl<sub>3</sub>): -176.88 (1 F, m). Yield: 47 mg (50%).<sup>33</sup>

**Fluoroadamantane (9).**  $^1\text{H}$  NMR ( $\text{CDCl}_3$ ): 2.27-2.20 (3 H, brs), 1.91-1.86 (6H, m), 1.66-1.60 (6H, m);  $^{19}\text{F}$  NMR ( $\text{CDCl}_3$ ): -128.5 (1 F, m). Yield: (42%).<sup>34</sup>

**3-Fluoroadamantan-1-ol (10).**  $^1\text{H}$  NMR ( $\text{CDCl}_3$ ): 2.41-2.34 (2 H, m), 1.92-1.88 (2 H, d,  $J = 5.7$  Hz), 1.84-1.80 (4 H, dd,  $J = 5.4$  Hz, 3.3 Hz), 1.72-1.61 (4 H, m), 1.52-1.47 (3 H, m);  $^{19}\text{F}$  NMR ( $\text{CDCl}_3$ ): -132.34 (1 F, m), -138.96 (1 F, m). Yield: (37%).<sup>33</sup>

**(1-Fluoroethyl)benzene (11).**  $^{19}\text{F}$  NMR ( $\text{CD}_3\text{CN}$ ): -167.06 (1 F, dq,  $J = 47.4$  Hz, 23.7 Hz). Yield: (30%).<sup>35</sup>

**4-Fluoro-4-phenylbutan-2-one (12).**  $^1\text{H}$  NMR ( $\text{CDCl}_3$ ): 7.46-7.32 (5 H, m), 6.08-5.86 (1 H, ddd,  $J = 46.9$  Hz, 8.7 Hz, 3.8 Hz), 3.31-3.16 (1 H, m), 2.94-2.75 (1H, ddd,  $J = 32.2$  Hz, 16.6 Hz, 4.0 Hz), 2.24 (3 H, s);  $^{19}\text{F}$  NMR ( $\text{CDCl}_3$ ): -173.59 (1 F, ddd,  $J = 47.4$  Hz, 34.0 Hz, 15.5 Hz). Yield: 32 mg (38%).<sup>36</sup>

**3-Fluoro-1,3-diphenylpropan-1-one (13).**  $^1\text{H}$  NMR ( $\text{CDCl}_3$ ): 8.00-7.32 (10 H, m), 6.29-6.08 (1 H, ddd,  $J = 46.9$  Hz, 8.3 Hz, 4.5 Hz), 3.88-3.73 (1 H, ddd,  $J = 17.1$  Hz, 14.8 Hz, 8.2 Hz), 3.42-3.24 (1 H, ddd,  $J = 29.6$  Hz, 17.0 Hz, 4.1 Hz);  $^{19}\text{F}$  NMR ( $\text{CDCl}_3$ ): -172.97 (1 F, ddd,  $J = 46.4$  Hz, 29.9 Hz, 15.5 Hz). Yield: 41 mg (36%).<sup>30</sup>

**Methyl-3-fluoro-3-phenylpropanoate (14).**  $^1\text{H}$  NMR ( $\text{CDCl}_3$ ): 7.41-7.34 (5 H, m), 6.03-5.82 (1 H, ddd,  $J = 46.7$  Hz, 9.0 Hz, 4.1 Hz), 3.74 (3 H, s), 3.11-2.98 (1 H, ddd,  $J = 16.0$  Hz, 13.6 Hz, 9.0 Hz), 2.89-2.71 (1 H, ddd,  $J = 32.6$  Hz, 16.2 Hz, 4.3 Hz);  $^{19}\text{F}$  NMR ( $\text{CDCl}_3$ ): -172.92 (1 F, ddd,  $J = 46.4$  Hz, 32.0 Hz, 13.4 Hz). Yield: 28 mg (31%).<sup>30</sup>

**2-(fluoro(phenyl)methyl)cyclohexanone (15).**  $^1\text{H}$  NMR ( $\text{CDCl}_3$ ): 7.67-7.03 (10 H, m), 6.17-5.96 (dd,  $J = 46.5$  Hz, 4.1 Hz), 5.95-5.74 (1 H, dd,  $J = 45.8$  Hz, 7.5 Hz), 3.03-2.80 (1 H, m), 2.77-2.60 (1 H, m), 2.58-2.22 (4 H, m), 2.18-1.49 (11 H, m), 1.35-1.15 (1 H, m);  $^{19}\text{F}$  NMR ( $\text{CDCl}_3$ ): -191.84 (1 F, dd,  $J = 46.4$  Hz, 21.7 Hz), -172.64 (1 F, dd,  $J = 45.4$  Hz, 14.4 Hz). Yield: 43 mg (41%).<sup>37</sup>

**3b-fluoro-5a-androstan-17-one and 2a-fluoro-5a-androstan-17-one (major products) (16).** <sup>19</sup>F NMR (CD<sub>3</sub>CN): -170.7 (1 F, dm, *J* = 49.5 Hz); -174.9 (1 F, dm, *J* = 47.4 Hz). Yield: (47%).<sup>38</sup>

**2-(fluoro(phenyl)methyl)progesterone (17).** <sup>1</sup>H NMR (CDCl<sub>3</sub>): δ 7.41-7.36 (m, 2 H), 7.34-7.27 (m, 3 H), 6.55-6.42 (dd, 1 H, *J* = 46.2 Hz, 1.8 Hz), 5.84-5.82 (d, 1 H, *J* = 1.2 Hz), 2.72-2.58 (dddd, 1 H, *J* = 30.3 Hz, 13.3 Hz, 5.3 Hz, 2.0 Hz), 2.56-2.50 (t, 1 H, *J* = 9.2 Hz), 2.42-2.32 (m, 2 H), 2.20-2.15 (m, 1 H), 2.11 (s, 3 H), 2.04-1.99 (dt, 1 H, *J* = 12.1 Hz, 2.9 Hz), 1.89-1.61 (m, 5 H), 1.53-1.07 (m, 10 H), 1.06-1.03 (s, 3 H), 1.03-1.00 (m, 1 H), 0.61 (s, 3 H); <sup>13</sup>C NMR (CDCl<sub>3</sub>): δ 209.3 (s), 196.4 (s), 170.9 (s), 139.1 (s), 138.9 (s), 129.9 (s), 128.4 (s), 127.7 (s), 124.7 (s), 124.6 (s), 123.9 (s), 90.2 (d, *J* = 175.6 Hz), 63.5 (s), 55.9 (s), 53.8 (s), 49.4 (s), 48.1 (s), 47.9 (s), 43.8 (s), 38.7 (s), 38.6 (s), 35.4 (s), 33.7 (s), 33.6 (s), 32.5 (s), 31.7 (s), 31.5 (s), 24.3 (s), 22.8 (s), 20.9 (s), 17.6 (s), 13.3 (s); <sup>19</sup>F NMR (CDCl<sub>3</sub>): δ -198.57 (dd, 1 F, *J* = 46.4 Hz, 30.9 Hz); IR (CDCl<sub>3</sub>) 1701 cm<sup>-1</sup>, 1671 cm<sup>-1</sup>. HRMS-(ESI+) calcd for C<sub>28</sub>H<sub>35</sub>FO<sub>2</sub>Na<sup>+</sup>: 445.2513, found 445.2527. Yield: 59 mg (28%).

## 12.6 Experimental Details for Chapter 6.

**Synthesis of 1-substituted cyclopropanols: From alkenes (respective cyclopropanols of compounds 1-13).**<sup>39</sup> To a flame dried round bottom flask, under N<sub>2</sub> was added ethyl acetate (10 mmol, 1.0 equivalent), olefin (15 mmol, 1.5 equivalent) and Ti(i-OPr)<sub>3</sub>Cl (10 mmol, 1.0 equivalent, 1.0 M in hexanes). With stirring, cyclohexylmagnesium bromide (45 mmol, 4.5 equiv., 2.0 M in Et<sub>2</sub>O) was added drop wise to the solution. The reaction mixture was stirred overnight at room temperature. After overnight stirring, the reaction mixture was hydrolyzed with H<sub>2</sub>O and extracted with ether. The combined extracts were washed with brine, dried with MgSO<sub>4</sub>, and filtered through Celite. The crude mixture was concentrated by rotary evaporation and purified by column chromatography on silica gel using ethyl acetate/hexanes as eluent.

**Synthesis of 1-substituted cyclopropanols: From methyl esters (respective cyclopropanol of compound 14).**<sup>40</sup> To a flame dried round bottom flask equipped with a stir bar was added the methyl ester (25 mmol, 1.0 equiv.) in anhydrous diethyl ether. To this solution was added Ti(i-OPr)<sub>3</sub>Cl (5 mmol, 20 mol%) followed by drop wise addition of a 2.0 M solution of EtMgBr in Et<sub>2</sub>O (50 mmol, 2.0 equiv.) at

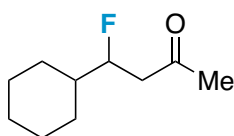
room temperature. The reaction mixture was stirred overnight under nitrogen. After overnight stirring, the reaction was cooled to 0°C and quenched with 10% aqueous H<sub>2</sub>SO<sub>4</sub>. The mixture was extracted into Et<sub>2</sub>O, then the combined extracts were washed with DI water, dried with MgSO<sub>4</sub>, and filtered through Celite. The crude reaction mixture was concentrated by rotary evaporation and purified by column chromatography on silica gel using ethyl acetate/hexanes as eluent.

**Representative fluorination procedure.** To a 10 mL microwave vial equipped with a stir bar were added Selectfluor (195 mg, 0.55 mmol, 2.2. equiv.), photocatalyst - either 1,2,4,5-tetracyanobenzene (4.45 mg, 0.025 mmol, 0.10 equiv.) or xanthone (5.00 mg, 0.025 mmol, 0.10 equiv.), and anhydrous acetonitrile (3 ml) under an atmosphere of N<sub>2</sub>. The respective cyclopropanol (0.25 mmol, 1.0 equiv.) was added to the vial, and the reaction mixture irradiated with a UV Pen Lamp (or a Rayonet reactor) at 302 nm for ~16 h. After 16 h, the reaction mixture was diluted with CH<sub>2</sub>Cl<sub>2</sub>, washed with 1 M HCl, washed with saturated NaHCO<sub>3</sub>, and the combined organic extracts dried with MgSO<sub>4</sub>, filtered through Celite, and concentrated by rotary evaporation. Alternatively, the reaction mixture may be diluted with Et<sub>2</sub>O, filtered through Celite, and concentrated to effectively remove salts. The crude mixture was subjected to column chromatography on Florisil using a slightly acidified mixture of ethyl acetate/hexanes with a few drops of concentrated HCl as eluent. Isolated yields are reported for all fluorinated products except for compound **16** (previously reported in the literature), whose yield was determined by <sup>19</sup>F NMR due to degradation upon isolation.

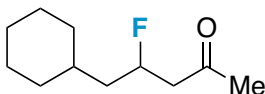
**Reductive workup to form  $\gamma$ -fluorinated alcohols (8-11 and 17).** After overnight stirring, the reaction mixture was diluted with Et<sub>2</sub>O, filtered through Celite, and concentrated by rotary evaporation. The crude reaction mixture was placed under an atmosphere of N<sub>2</sub>, dissolved in anhydrous THF and cooled to 0°C. Solid LiAlH<sub>4</sub> (47 mg, 1.25 mmol, 5.0 equiv.) was added and the reaction stirred vigorously for 2 min. After 2 min, the reaction was quenched by the standard Fieser method and extracted into Et<sub>2</sub>O; the combined organic extracts were washed with H<sub>2</sub>O, dried with MgSO<sub>4</sub>, filtered through Celite, and concentrated by rotary evaporation. A <sup>19</sup>F NMR of the crude reaction mixture indicates ~1:1 dr prior to

isolation of the compound of interest (in all cases). The crude alcohol was isolated as a mixture of diastereomers by column chromatography on silica gel using ethyl acetate/hexanes as eluent.

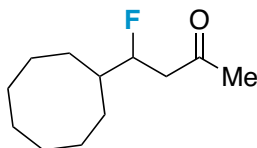
**Characterization Data.** Compounds **6** and **7** are reported as the major  $\beta$ -fluorinated products isolated with minor fluorinated byproducts. Respective cyclopropanols of compounds **5**,<sup>41</sup> **6**,<sup>42</sup> **8**,<sup>41</sup> **10**,<sup>41</sup> **12**,<sup>41</sup> and **15**<sup>43[4]</sup> have been previously reported in the literature. Compounds **5**<sup>44</sup> and **16**<sup>45</sup> have been previously reported in the literature.



**4-cyclohexyl-4-fluorobutan-2-one (1).**  $^1\text{H}$  NMR ( $\text{CDCl}_3$ ):  $\delta$  4.75 (dm,  $J = 47.8$  Hz, 1H), 2.80 (m, 1H), 2.55 (m, 1H), 2.20 (s, 3H), 1.90-0.85 (m, 11H);  $^{13}\text{C}$  NMR ( $\text{CDCl}_3$ ): 206.24 (d,  $J = 2.20$  Hz), 93.61 (d,  $J = 171.3$  Hz), 46.17 (d,  $J = 24.9$  Hz), 41.96 (19.0 Hz), 31.0, 30.95 (d,  $J = 3.7$  Hz), 28.38 (d,  $J = 8.1$  Hz), 27.41, 26.19, 25.79;  $^{19}\text{F}$  NMR ( $\text{CDCl}_3$ ): -184.7 (m,  $J = 47.4$  Hz, 1F).

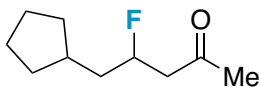


**5-cyclohexyl-4-fluoropentan-2-one (2).**  $^1\text{H}$  NMR ( $\text{CDCl}_3$ ):  $\delta$  5.03 (dm,  $J = 49.5$  Hz, 1H), 2.91-2.74 (m, 1H), 2.64-2.43 (m, 1H), 2.19 (s, 3H), 1.86-0.85 (m, 13H);  $^{13}\text{C}$  NMR ( $\text{CDCl}_3$ ): 205.75 (d,  $J = 3.7$  Hz), 88.29 (d,  $J = 166.86$  Hz), 49.30 (d,  $J = 22.7$  Hz), 42.71 (d,  $J = 20.49$ ), 33.87, 33.80, 32.65, 30.84, 26.39, 26.20, 26.03;  $^{19}\text{F}$  NMR ( $\text{CDCl}_3$ ): -179.4 (m,  $J = 49.5$  Hz).

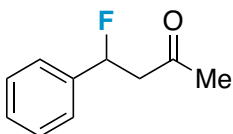


**4-cyclooctyl-4-fluorobutan-2-one (3).**  $^1\text{H}$  NMR ( $\text{CDCl}_3$ ):  $\delta$  4.75 (dm,  $J = 47.8$  Hz, 1H), 2.77 (m, 1H), 2.50 (m, 1H), 2.20 (s, 3H), 1.85-1.20 (m, 15H);  $^{13}\text{C}$  NMR ( $\text{CDCl}_3$ ): 206.23 (d,  $J = 2.2$  Hz), 94.15 (d,  $J = 172.0$

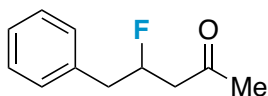
Hz), 46.0 (d,  $J = 23.4$  Hz), 41.32 (d,  $J = 18.3$  Hz), 30.89, 28.69 (d,  $J = 3.7$  Hz), 27.17 (d,  $J = 5.9$  Hz), 26.74, 26.50, 25.81, 25.54;  $^{19}\text{F}$  NMR ( $\text{CDCl}_3$ ): -182.1 (m,  $J = 48.5$  Hz, 1F).



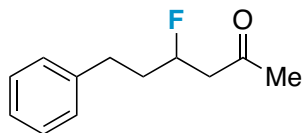
**5-cyclopentyl-4-fluoropentan-2-one (4).**  $^1\text{H}$  NMR ( $\text{CDCl}_3$ ):  $\delta$  4.95 (dm,  $J = 48.4$  Hz, 1H), 2.82 (m, 1H), 2.58 (m, 1H), 2.19 (s, 3H), 1.99-1.04 (m, 11H);  $^{13}\text{C}$  NMR ( $\text{CDCl}_3$ ): 205.83 (d,  $J = 3.7$  Hz), 89.84 (d,  $J = 167.60$  Hz), 49.18 (d,  $J = 22.7$  Hz), 41.30 (s,  $J = 20.5$  Hz), 36.28 (d,  $J = 3.7$  Hz), 33.02, 32.37, 30.90, 25.01, 24.88;  $^{19}\text{F}$  NMR ( $\text{CDCl}_3$ ): -179.7 (m,  $J = 49.5$  Hz, 1F).



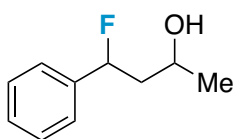
**4-fluoro-4-phenylbutan-2-one (5).**  $^1\text{H}$  NMR ( $\text{CDCl}_3$ ):  $\delta$  7.41-7.32 (m, 5H), 5.95 (ddd,  $J = 47.0, 4.9, 3.9$  Hz, 1H), 3.21 (m, 1H), 2.83 (m, 1H), 2.20 (s, 3H);  $^{19}\text{F}$  NMR ( $\text{CDCl}_3$ ): -173.6 (ddd,  $J = 47.0, 17.2, 14.9$  Hz, 1F).



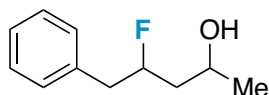
**4-fluoro-5-phenylpentan-2-one (6).**  $^1\text{H}$  NMR ( $\text{CDCl}_3$ ):  $\delta$  7.30-7.07 (m, 5H), 5.11 (dm,  $J = 47.4$  Hz, 1H), 2.99-2.30 (m, 4H), 2.12 (s, 3H);  $^{13}\text{C}$  NMR ( $\text{CDCl}_3$ ): 205.5 (d,  $J = 3.7$  Hz), 136.27, 129.5, 128.6, 126.9, 90.95 (d,  $J = 171.0$  Hz), 47.86 (d,  $J = 22.9$  Hz), 41.08 (d,  $J = 21.4$  Hz), 30.8;  $^{19}\text{F}$  NMR ( $\text{CDCl}_3$ ): -178.0 (m,  $J = 47.1$  Hz).



**4-fluoro-6-phenylhexan-2-one (7).**  $^1\text{H}$  NMR ( $\text{CDCl}_3$ ):  $\delta$  7.46-7.18 (m, 5H), 4.99 (ddt,  $J = 48.5, 12.1, 4.1$  Hz), 3.03-2.48 (m, 4H), 2.18 (s, 3H), 2.08-1.76 (m, 2H);  $^{13}\text{C}$  NMR ( $\text{CDCl}_3$ ): 205.44 (d,  $J = 4.4$  Hz), 140.98, 128.55, 128.53, 128.51, 128.43, 126.13, 89.29 (d,  $J = 168.1$  Hz), 48.73 (d,  $J = 22.1$  Hz), 36.78 (d,  $J = 20.6$  Hz), 31.17, 30.84;  $^{19}\text{F}$  NMR ( $\text{CDCl}_3$ ): -181.4 (m,  $J = 48.2$  Hz, 1F).

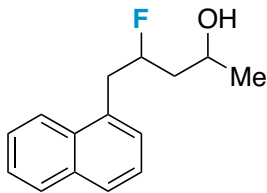


**4-fluoro-4-phenylbutan-2-ol (8).** Isolated as mixture of diastereomers.  $^1\text{H}$  NMR ( $\text{CDCl}_3$ ):  $\delta$  7.42-7.30 (m, 5H), 5.73 (ddd,  $J = 48.3, 7.43, 2.5$  Hz, 1H), 5.62 (ddd,  $J = 48.1, 4.9, 3.7$  Hz, 1H), 4.03 (m, 1H), 2.30-1.75 (m, 3H), 1.68 (s, 1H), 1.28 (d,  $J = 6.3$  Hz, 3H), 1.27 (d,  $J = 6.3$  Hz, 3H);  $^{13}\text{C}$  NMR ( $\text{CDCl}_3$ ): 140.31 (d,  $J = 19.2$  Hz), 139.77 (d,  $J = 19.9$  Hz), 128.6, 128.5, 128.29, 128.25, 125.7, 125.6, 125.4, 125.3, 94.08 (d,  $J = 168.1$  Hz), 91.72 (d,  $J = 168.80$  Hz), 65.91 (d,  $J = 4.4$  Hz), 64.2, 46.6, 46.4, 46.1, 45.9, 24.1, 23.6;  $^{19}\text{F}$  NMR ( $\text{CDCl}_3$ ): -177.8 (ddd,  $J = 49.3, 21.8, 16.1$  Hz, 1F), -173.5 (ddd,  $J = 45.9, 17.2, 13.8$  Hz, 1F).

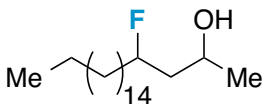


**4-fluoro-5-phenylpentan-2-ol (9).** Isolated as mixture of diastereomers.  $^1\text{H}$  NMR ( $\text{CDCl}_3$ ):  $\delta$  7.38-7.18 (m, 5H), 4.95 (m, 1H), 4.06 (m, 1H), 3.10-2.82 (m, 2H), 1.97-1.52 (m, 3H), 1.22 (d,  $J = 6.14$  Hz, 3H), 1.21 (d,  $J = 6.14$  Hz, 3H);  $^{13}\text{C}$  NMR ( $\text{CDCl}_3$ ): 137.0, 136.9, 136.7, 136.6, 129.4, 128.5, 128.4, 126.7, 126.6, 94.4 (d,  $J = 168.1$  Hz), 91.7 (d,  $J = 169.5$  Hz), 66.3, 66.2, 64.3, 64.2, 43.7, 43.5, 43.3, 42.0, 41.9, 41.8, 41.7, 24.1, 23.3;  $^{19}\text{F}$  NMR ( $\text{CDCl}_3$ ): -180.8 (m, 1F), -178.2 (m, 1F).

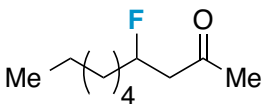




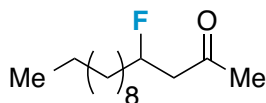
**4-fluoro-5-(naphthalen-1-yl)pentan-2-ol (10).** Isolated as mixture of diastereomers.  $^1\text{H}$  NMR ( $\text{CDCl}_3$ ):  $\delta$  8.03 (dd,  $J = 8.04, 1.46$  Hz, 1H), 7.88 (m, 1H), 7.79 (m, 1H), 7.59-7.37 (m, 4H), 5.09 (m, 1H), 4.07 (m, 1H), 3.42 (m, 2H), 1.84 (m, 2H), 1.22 (d,  $J = 6.0$  Hz, 3H), 1.20 (d,  $J = 6.0$  Hz, 3H);  $^{13}\text{C}$  NMR ( $\text{CDCl}_3$ ): 133.9, 133.2, 133.1, 132.93, 132.86, 132.2, 132.1, 128.94, 128.85, 127.9, 127.8, 127.7, 127.6, 126.2, 126.1, 125.7, 93.9 (d,  $J = 168.0$  Hz), 91.3 (d,  $J = 168.0$  Hz), 66.3 (d,  $J = 3.7$  Hz), 64.3 (d,  $J = 2.9$  Hz), 44.1 (d,  $J = 19.9$  Hz), 43.9 (d,  $J = 19.2$  Hz), 39.1 (d,  $J = 13.3$  Hz), 38.8 (d,  $J = 13.3$  Hz), 24.2, 23.3;  $^{19}\text{F}$  NMR ( $\text{CDCl}_3$ ): -178.4 (m, 1F), -176.1 (m, 1F).



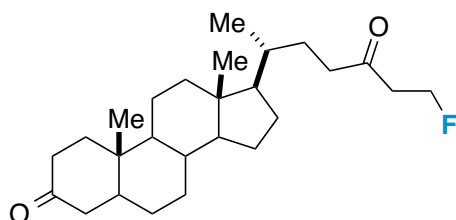
**4-fluoricosan-2-ol (11).** Isolated as mixture of diastereomers.  $^1\text{H}$  NMR ( $\text{CDCl}_3$ ):  $\delta$  4.72 (m, 1H), 4.04 (m, 1H), 2.09-1.08 (m, 36H), 0.88 (t,  $J = 6.8$  Hz, 3H);  $^{13}\text{C}$  NMR ( $\text{CDCl}_3$ ): 94.6 (d,  $J = 164.4$  Hz), 91.8 (d,  $J = 165.12$  Hz), 66.5 (d,  $J = 2.9$  Hz), 64.4 (d,  $J = 2.9$  Hz), 44.3, 44.2, 44.1, 44.0, 35.7, 35.6, 35.5, 35.4, 31.9, 29.7, 29.69, 29.67, 29.64, 29.57, 29.53, 29.51, 29.45, 29.42, 29.37, 25.0, 24.94, 24.91, 24.90, 24.1, 23.4, 22.7, 14.1;  $^{19}\text{F}$  NMR ( $\text{CDCl}_3$ ): -182.1 (m, 1F), -179.9 (m, 1F).



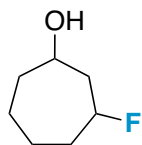
**4-fluorodecan-2-one (12).**  $^1\text{H}$  NMR ( $\text{CDCl}_3$ ):  $\delta$  4.95 (dm,  $J = 48.4$  Hz, 1H), 2.85 (m, 1H), 2.57 (m, 1H), 1.70-1.20 (m, 10H), 0.90 (t,  $J = 7.0$ , 3H);  $^{13}\text{C}$  NMR ( $\text{CDCl}_3$ ): 205.79 (d,  $J = 3.7$  Hz), 90.13 (d,  $J = 168.3$  Hz), 48.78 (d, 23.4 Hz), 35.02 (d,  $J = 20.5$  Hz), 31.64, 30.90, 28.95, 22.81 (d,  $J = 4.4$  Hz), 22.51, 14.01;  $^{19}\text{F}$  NMR ( $\text{CDCl}_3$ ): -179.6 (m,  $J = 47.4$  Hz).



**4-fluorotetradecan-2-one (13).**  $^1\text{H}$  NMR ( $\text{CDCl}_3$ ):  $\delta$  4.96 (dm,  $J = 48.2$  Hz, 1H), 2.86 (m, 1H), 2.58 (m, 1H), 2.22 (s, 3H), 1.60-1.20 (m, 18H), 0.90 (t,  $J = 7.0$  Hz, 3H);  $^{13}\text{C}$  NMR ( $\text{CDCl}_3$ ): 205.79 (d,  $J = 3.7$  Hz), 90.17 (d,  $J = 167.6$  Hz), 48.82 (d,  $J = 22.7$  Hz), 35.05 (d,  $J = 20.5$  Hz), 32.0, 30.88, 29.53, 29.31, 24.85 (d,  $J = 4.4$  Hz), 22.68, 14.10;  $^{19}\text{F}$  NMR ( $\text{CDCl}_3$ ): -180.0 (m,  $J = 47.4$  Hz, 1F).



**(5R,10S,13R)-17-((S)-7-fluoro-5-oxoheptan-2-yl)-10,13-dimethyltetradecahydro-1H-cyclopenta[*a*]-phenanthren-3(2H)-one (14):**  $^1\text{H}$  NMR ( $\text{CDCl}_3$ ):  $\delta$  4.72 (dt,  $J = 46.5, 6.1$  Hz, 2H), 2.83 (m, 2H), 2.65 (m, 2H), 2.42-1.20 (m, 26H), 1.04 (s, 3H), 0.94 (d,  $J =$ , 3H), 0.70 (s, 3H);  $^{13}\text{C}$  NMR ( $\text{CDCl}_3$ ): 213.47, 208.1 (d,  $J = 4.4$  Hz), 79.1 (d,  $J = 165.1$  Hz), 56.44, 56.02, 44.32, 42.96, 42.78, 42.37, 40.73, 40.49, 40.05, 37.12 (d,  $J = 21.18$  Hz), 35.53, 35.24, 34.89, 29.39, 28.19, 26.61, 25.77, 24.16, 22.66, 21.19, 18.43, 12.08, 7.8;  $^{19}\text{F}$  NMR ( $\text{CDCl}_3$ ): -219.8 (m,  $J = 46.5$  Hz, 1F)



**3-fluorocycloheptanol (17):** Isolated as mixture of diastereomers.  $^1\text{H}$  NMR ( $\text{CDCl}_3$ ):  $\delta$  4.87 (m, 1H), 4.08 (m, 1H), 2.43-1.34 (m, 11 H);  $^{13}\text{C}$  NMR ( $\text{CDCl}_3$ ): 91.7, 91.3, 90.8, 89.6, 67.2, 67.1, 43.6, 43.4, 38.1, 37.6, 34.6, 34.4, 23.7, 23.3, 22.6, 22.4;  $^{19}\text{F}$  NMR ( $\text{CDCl}_3$ ): -168.2 (m, 1F), -164.3 (m, 1F).

## 12.7 Experimental Details for Chapter 7.

**Representative Fluorination Procedures.** Selectfluor (195 mg, 0.55 mmol, 2.2 equiv.), 9-fluorenone (9 mg, 0.25 mmol, 0.2 equiv.), and the substrate (0.25 mmol, 1.0 equiv.) were added to an oven-dried microwave vial equipped with a stir bar. The microwave vial was sealed via crimper with a cap w/ septum; it was evacuated and refilled with N<sub>2</sub> multiple times. Anhydrous CH<sub>3</sub>CN (3 mL) was then added to the vial via syringe under N<sub>2</sub> atmosphere. The reaction mixture was stirred in a Rayonet reactor and irradiated at 300 nm for 12 h.

*To obtain carboxylic acid:* The reaction mixture was diluted with approximately equal parts H<sub>2</sub>O. LiOH•H<sub>2</sub>O (63 mg, 1.25 mmol, 5.0 equiv.) was added, and the reaction mixture was stirred for 25 min. open to air. The mixture was acidified with 1 M HCl (pH ~2) and extracted into CH<sub>2</sub>Cl<sub>2</sub>. The combined organic layers were dried with MgSO<sub>4</sub>, filtered through Celite, and concentrated. Products typically columned on Florisil, eluting with 5:94:1 EtOAc:hexanes:AcOH. (Do not column on silica – it promotes dehydrofluorination.) Better results can be achieved by flushing the loaded column with a few column volumes of EtOAc:hexanes before acidifying it. Analytical purity can be obtained via subsequent gradient C18 column chromatography, eluting with MeCN/H<sub>2</sub>O.

*To obtain methyl ester:* The reaction mixture was diluted with approximately equal parts H<sub>2</sub>O. LiOMe (47 mg, 1.25 mmol, 5.0 equiv.) was added, and the reaction mixture was stirred for 25 min. open to air. The mixture was extracted into CH<sub>2</sub>Cl<sub>2</sub>. The combined organic layers were dried with MgSO<sub>4</sub>, filtered through Celite, and concentrated. Products typically columned on Florisil, eluting with 5:95 EtOAc:hexanes. (Do not column on silica – it promotes dehydrofluorination.) Analytical purity can be obtained via subsequent gradient C18 column chromatography, eluting with MeCN/H<sub>2</sub>O, or via flash chromatography on silica gel, eluting with 10:90 EtOAc:toluene.

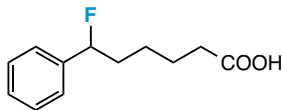
*To obtain alcohol:* The reaction mixture was concentrated and dissolved in 10 mL anhydrous THF under N<sub>2</sub> atmosphere. After cooling to 0 °C, LiAlH<sub>4</sub> (57 mg, 1.50 mmol, 6.0 equiv.) was added to the reaction mixture; the mixture slowly warmed to rt and was stirred vigorously for 1 h. The reaction was quenched

and worked up via the standard Fieser method. Products typically columned on Florisil, eluting with 5:95 EtOAc:hexanes. (Do not column on silica – it promotes dehydrofluorination.) Analytical purity can be obtained via subsequent gradient C18 column chromatography, eluting with MeCN/H<sub>2</sub>O.

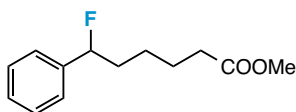
*To obtain ketone/fragmentation product:* The reaction mixture was diluted with approximately equal parts H<sub>2</sub>O and was stirred for 25 min. open to air. The mixture was extracted into CH<sub>2</sub>Cl<sub>2</sub>. The combined organic layers were dried with MgSO<sub>4</sub>, filtered through Celite, and concentrated. Products typically columned on Florisil, eluting with 5:95 EtOAc:hexanes. (Do not column on silica – it promotes dehydrofluorination.) Analytical purity can be obtained via subsequent gradient C18 column chromatography, eluting with MeCN/H<sub>2</sub>O.

**Gram Scale Synthesis.** Selectfluor (3.90 g, 11.0 mmol, 2.2 equiv.), 9-fluorenone (0.180 g, 1.0 mmol, 0.2 equiv.), and 6-phenyl-1,4-dioxaspiro[4.5]decane (1.09 g, 5.0 mmol, 1.0 equiv.) were added to an oven-dried round bottom flask equipped with a stir bar. The flask was evacuated and refilled with N<sub>2</sub> multiple times. Anhydrous CH<sub>3</sub>CN (60 mL) was then added to the flask via syringe under N<sub>2</sub> atmosphere. The reaction mixture was stirred in a Rayonet reactor and irradiated at 300 nm for 12 h. The reaction was worked up to obtain 6-fluoro-6-phenyl-hexanoic acid as outlined above in 54% yield (568 mg).

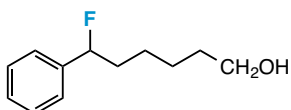
**Characterization Data.** The 2-aryl ketone precursors for compounds **1-6**, **9-14**, and **18-20** were synthesized using the Pd-catalyzed 2-arylation procedure by Kawatsura and Hartwig;<sup>46</sup> the precursors for compounds **7**, **15**, and **17** were synthesized using standard Grignard reactions<sup>47</sup> followed by PCC oxidations;<sup>48</sup> the precursor for compound **8** was synthesized using the Pd-catalyzed 2-arylation procedure by Willis, Taylor, and Gillmore.<sup>49</sup> The ethylene glycol acetals were synthesized according to a general literature procedure.<sup>50</sup> Characterization data for **16** is consistent with literature.<sup>51</sup>



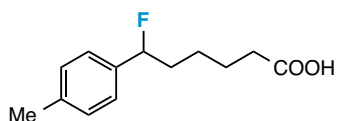
6-fluoro-6-phenylhexanoic acid (**1**). 60% yield. Clear oil.  $\nu_{\max}/\text{cm}^{-1}$  3300-2500 (COOH) and 1708 (CO).  $^1\text{H}$  NMR ( $\text{CDCl}_3$ ): 11.26 (1H, br s), 7.38-7.30 (5H, m), 5.42 (1H, ddd,  $J = 47.9, 8.0, 4.9$  Hz), 2.36 (2H, t,  $J = 7.4$  Hz), 2.05-1.92 (1H, m), 1.91-1.75 (1H, m), 1.68 (2H, quint,  $J = 7.5$  Hz), 1.59-1.48 (1H, m), 1.48-1.37 (1H, m);  $^{13}\text{C}$  NMR ( $\text{CDCl}_3$ ): 180.2, 140.2 (d,  $J = 19.9$  Hz), 128.4, 128.2, 125.5 (d,  $J = 7.4$  Hz), 94.3 (d,  $J = 170.3$  Hz), 36.8 (d,  $J = 23.6$  Hz), 33.9, 24.5 (d,  $J = 4.4$  Hz), 24.3;  $^{19}\text{F}$  NMR ( $\text{CDCl}_3$ ): -174.31 (1F, ddd,  $J = 47.0, 28.7, 17.2$  Hz).



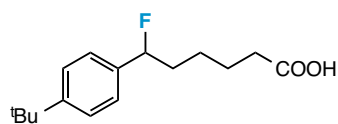
methyl 6-fluoro-6-phenylhexanoate (**2**). 59% yield. Clear oil.  $\nu_{\max}/\text{cm}^{-1}$  1733 (CO).  $^1\text{H}$  NMR ( $\text{CDCl}_3$ ): 7.41-7.29 (5H, m), 5.42 (1H, ddd,  $J = 47.8, 8.0, 4.8$  Hz), 3.66 (3H, s), 2.32 (2H, t,  $J = 7.5$  Hz), 2.09-1.92 (1H, m), 1.76-1.74 (1H, m), 1.72-1.64 (2H, m), 1.56-1.36 (2H, m);  $^{13}\text{C}$  NMR ( $\text{CDCl}_3$ ): 173.9, 140.4, 140.2, 128.4, 128.23, 128.21, 125.51, 125.44, 94.3 (d,  $J = 171$  Hz), 51.5, 37.0, 36.7, 33.9, 24.7, 24.6;  $^{19}\text{F}$  NMR ( $\text{CDCl}_3$ ): -174.24 (1F, ddd,  $J = 47.0, 27.5, 16.1$  Hz).



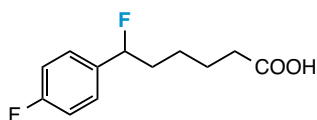
6-fluoro-6-phenylhexan-1-ol (**3**). 55% yield. Clear oil.  $\nu_{\max}/\text{cm}^{-1}$  3381 (OH).  $^1\text{H}$  NMR ( $\text{CDCl}_3$ ): 7.40-7.35 (2H, m), 7.34-7.30 (3H, m), 5.43 (1H, ddd,  $J = 47.7, 8.0, 4.9$  Hz), 3.64 (2H, m), 2.06-1.91 (1H, m), 1.90-1.75 (1H, m), 1.61-1.47 (3H, m), 1.47-1.37 (3H, m);  $^{13}\text{C}$  NMR ( $\text{CDCl}_3$ ): 140.6, 140.4, 128.4, 128.18, 128.17, 125.53, 125.46, 94.5 (d,  $J = 170.3$  Hz), 62.8, 37.3, 37.0, 32.6, 25.5, 24.90, 24.86;  $^{19}\text{F}$  NMR ( $\text{CDCl}_3$ ): -173.96 (1F, ddd,  $J = 45.9, 27.5, 16.1$  Hz).



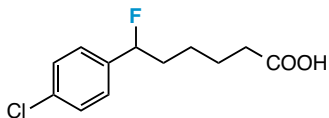
6-fluoro-6-(*p*-tolyl)hexanoic acid (**4**). 42% yield. White solid; m.p. 49-51 °C.  $\nu_{\max}/\text{cm}^{-1}$  3300-2500 (COOH) and 1695 (CO).  $^1\text{H NMR}$  ( $\text{CDCl}_3$ ): 8.77 (1H, br s), 7.23-7.17 (4H, m), 5.39 (1H, ddd,  $J = 47.7$ , 8.2, 4.9 Hz), 2.43-2.33 (5H, m), 2.06-1.93 (1H, m), 1.90-1.76 (1H, m), 1.74-1.66 (2H, m), 1.59-1.50 (1H, m), 1.48-1.39 (1H, m);  $^{13}\text{C NMR}$  ( $\text{CDCl}_3$ ): 138.10, 138.07, 137.3, 137.1, 129.1, 125.6, 125.5, 94.3 (d,  $J = 169.5$  Hz), 36.8, 36.6, 24.69, 24.65, 24.4, 21.2.  $^{19}\text{F NMR}$  ( $\text{CDCl}_3$ ): -172.10 (1F, ddd,  $J = 45.9$ , 27.5, 16.1 Hz).



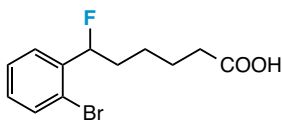
6-(4-(*tert*-butyl)phenyl)-6-fluorohexanoic acid (**5**). 64% yield. Clear oil.  $\nu_{\max}/\text{cm}^{-1}$  3300-2500 (COOH) and 1706 (CO).  $^1\text{H NMR}$  ( $\text{CDCl}_3$ ): 11.47 (1H, br s), 7.40 (2H, dm,  $J = 8.6$  Hz), 7.38 (2H, dm,  $J = 8.2$  Hz), 5.40 (1H, ddd,  $J = 47.7$ , 8.2, 4.7 Hz), 2.36 (2H, t,  $J = 7.4$  Hz), 2.09-1.93 (1H, m), 1.91-1.74 (1H, m), 1.70 (2H, quint,  $J = 7.8$  Hz), 1.61-1.51 (1H, m), 1.50-1.38 (1H, m), 1.32 (9H, s);  $^{13}\text{C NMR}$  ( $\text{CDCl}_3$ ): 180.1, 151.30, 151.28, 137.3, 137.1, 125.38, 125.35, 125.31, 93.4 (d,  $J = 169.5$  Hz), 36.7, 36.5, 34.6, 33.9, 31.31, 31.29, 24.73, 24.68, 24.4;  $^{19}\text{F NMR}$  ( $\text{CDCl}_3$ ): -172.34 (1F, ddd,  $J = 45.9$ , 28.7, 16.1 Hz).



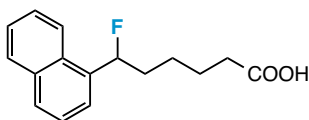
6-fluoro-6-(4-fluorophenyl)hexanoic acid (**6**). 70% yield. Clear oil.  $\nu_{\max}/\text{cm}^{-1}$  3300-2500 (COOH) and 1705 (CO).  $^1\text{H NMR}$  ( $\text{CDCl}_3$ ): 11.27 (1H, br s), 7.31-7.26 (2H, m), 7.06 (2H, t,  $J = 8.4$  Hz), 5.40 (1H, ddd,  $J = 47.9$ , 8.0, 4.9 Hz), 2.37 (2H, t,  $J = 7.4$  Hz), 2.05-1.91 (1H, m), 1.89-1.75 (1H, m), 1.69 (2H, quint,  $J = 7.6$  Hz), 1.58-1.48 (1H, m), 1.48-1.36 (1H, m);  $^{13}\text{C NMR}$  ( $\text{CDCl}_3$ ): 179.7, 162.6 (dd,  $J = 246.2$ , 2.2 Hz), 127.4 (d,  $J = 6.6$  Hz), 127.3 (d,  $J = 6.6$  Hz), 124.0 (d,  $J = 3.7$  Hz), 115.4 (d,  $J = 21.4$  Hz), 93.7 (d,  $J = 171.8$  Hz), 36.8 (d,  $J = 24.3$  Hz), 33.8, 24.6 (d,  $J = 4.4$  Hz), 24.29;  $^{19}\text{F NMR}$  ( $\text{CDCl}_3$ ): -113.2 (1F, m), -172.0 (1F, ddd,  $J = 48.2$ , 28.7, 17.2 Hz).



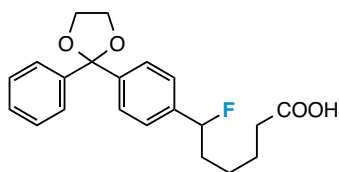
6-(4-chlorophenyl)-6-fluorohexanoic acid (**7**). 54% yield. Clear oil.  $\nu_{\max}/\text{cm}^{-1}$  3300-2500 (COOH) and 1684 (CO).  $^1\text{H}$  NMR ( $\text{CDCl}_3$ ): 8.65 (1H, br s), 7.34 (2H, d,  $J = 7.8$  Hz), 7.24 (2H, d,  $J = 8.6$  Hz), 5.40 (1H, ddd,  $J = 47.3, 8.0, 4.7$  Hz), 2.37 (1H, t,  $J = 7.0$  Hz), 2.03-1.90 (1H, m), 1.89-1.75 (1H, m), 1.69 (2H, quint,  $J = 7.4$  Hz), 1.58-1.48 (1H, m), 1.47-1.37 (1H, m);  $^{13}\text{C}$  NMR ( $\text{CDCl}_3$ ): 179.5, 138.8, 138.6, 134.02, 134.00, 128.6, 126.9, 126.8, 93.3 ( $J = 171.2$  Hz), 36.86, 36.85, 36.63, 36.61, 24.5, 24.4, 24.3;  $^{19}\text{F}$  NMR ( $\text{CDCl}_3$ ): -174.74 (1F, ddd,  $J = 45.9, 27.5, 17.2$  Hz).



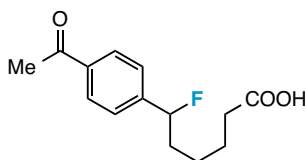
6-(2-bromophenyl)-6-fluorohexanoic acid (**8**). 63% yield. Clear oil.  $\nu_{\max}/\text{cm}^{-1}$  3300-2500 (COOH) and 1685 (CO).  $^1\text{H}$  NMR ( $\text{CDCl}_3$ ): 7.52 (1H, dt,  $J = 8.0, 1.1$  Hz), 7.48 (1H, dd,  $J = 7.8, 1.6$  Hz), 7.36 (1H, td,  $J = 7.5, 1.2$  Hz), 7.18 (1H, td,  $J = 7.8, 1.8$  Hz), 5.76 (1H, ddd,  $J = 47.3, 8.4, 3.5$  Hz), 2.40 (2H, t,  $J = 7.4$  Hz), 2.02-1.82 (2H, m), 1.80-1.67 (2H, m), 1.66-1.54 (2H, m);  $^{13}\text{C}$  NMR ( $\text{CDCl}_3$ ): 178.7, 140.0, 139.8, 132.6, 129.4, 127.7, 126.8, 126.7, 120.64, 120.58, 93.1 (d,  $J = 172.5$  Hz), 35.9, 35.6, 33.7, 24.61, 24.59, 24.3;  $^{19}\text{F}$  NMR ( $\text{CDCl}_3$ ): -181.16 (1F, ddd,  $J = 47.0, 32.1, 20.7$  Hz).



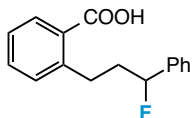
6-fluoro-6-(naphthalen-1-yl)hexanoic acid (**9**). 47% yield. Light brown oil.  $\nu_{\max}/\text{cm}^{-1}$  3300-2500 (COOH) and 1704 (CO).  $^1\text{H}$  NMR ( $\text{CDCl}_3$ ): 11.22 (1H, br s), 7.96-7.93 (1H, m), 7.88-7.86 (1H, m), 7.81 (1H, d,  $J = 8.2$  Hz), 7.57-7.45 (4H, m), 6.14 (1H, ddd,  $J = 47.1, 8.0, 4.3$  Hz), 2.36 (2H, t,  $J = 7.2$  Hz), 2.20-1.97 (2H, m), 1.78-1.51 (4H, m);  $^{13}\text{C}$  NMR ( $\text{CDCl}_3$ ): 179.8, 136.0, 135.8, 133.7, 129.85, 129.81, 128.9, 128.70, 128.68, 126.3, 125.7, 125.2, 123.1, 122.99, 122.94, 92.3 (d,  $J = 171.0$  Hz), 36.4, 36.2, 25.09, 25.06, 24.4;  $^{19}\text{F}$  NMR ( $\text{CDCl}_3$ ): -178.13 (1F, ddd,  $J = 48.2, 29.8, 19.5$  Hz).



6-fluoro-6-(4-(2-phenyl-1,3-dioxolan-2-yl)phenyl)hexanoic acid (**10**). 51% yield. Clear oil.  $\nu_{\max}/\text{cm}^{-1}$  3300-2500 (COOH) and 1706 (OH).  $^1\text{H NMR}$  ( $\text{CD}_3\text{OD}$ ): 7.48-7.45 (4H, m), 7.33-7.24 (5H, m), 5.42 (1H, ddd,  $J = 47.9, 8.2, 4.9$  Hz), 4.02 (4H, s), 2.25 (2H, t,  $J = 7.3$  Hz), 2.00-1.73 (2H, m), 1.63 (2H, quint,  $J = 7.2$  Hz), 1.54-1.44 (1H, m), 1.43-1.33 (1H, m);  $^{13}\text{C NMR}$  ( $\text{CD}_3\text{OD}$ ): 178.5, 143.7, 143.6, 142.0, 141.8, 131.0, 129.1, 127.4, 127.3, 126.4, 126.3, 110.4, 95.2 (d,  $J = 169.5$  Hz), 65.9, 38.2, 37.9, 35.6, 26.1, 25.89, 25.85;  $^{19}\text{F NMR}$  ( $\text{CD}_3\text{OD}$ ): -175.90 (1F, ddd,  $J = 45.9, 28.7, 17.2$  Hz).



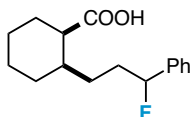
6-(4-acetylphenyl)-6-fluorohexanoic acid (**11**). 28% yield. Clear oil.  $\nu_{\max}/\text{cm}^{-1}$  3300-2500 (COOH) and 1668 (CO).  $^1\text{H NMR}$  ( $\text{CD}_3\text{OD}$ ): 8.00 (2H, d,  $J = 7.8$  Hz), 7.48 (2H, d,  $J = 8.4$  Hz), 5.54 (1H, ddd,  $J = 48.1, 7.8, 5.1$  Hz), 2.61 (3H, s), 2.16 (t,  $J = 7.5$  Hz), 2.02-1.75 (2H, m), 1.64 (2H, quint,  $J = 7.2$  Hz), 1.54-1.36 (2H, m);  $^{13}\text{C NMR}$  ( $\text{CD}_3\text{OD}$ ): 200.1, 182.6, 147.8, 147.6, 138.0, 129.6, 126.72, 126.65, 94.8 (d,  $J = 171.8$  Hz), 39.0, 38.3, 38.1, 27.4, 26.7, 26.10, 26.06;  $^{19}\text{F NMR}$  ( $\text{CD}_3\text{OD}$ ): -178.70 (1F, ddd,  $J = 47.0, 28.7, 18.4$  Hz).



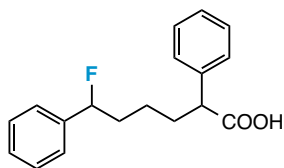
2-(3-fluoro-3-phenylpropyl)benzoic acid (**12**). 40% yield. Clear oil.  $\nu_{\max}/\text{cm}^{-1}$  3300-2500 (COOH) and 1687 (CO).  $^1\text{H NMR}$  ( $\text{CDCl}_3$ ): 11.67 (1H, br s), 8.09 (1H, d,  $J = 7.6$  Hz), 7.50 (1H, m), 7.36-7.28 (7H, m), 5.50 (1H, ddd,  $J = 47.9, 8.2, 3.9$  Hz), 3.28-3.21 (1H, m), 3.18-3.11 (1H, m), 2.38-2.22 (1H, m), 2.20-2.11 (1H, m);  $^{13}\text{C NMR}$  ( $\text{CDCl}_3$ ): 173.0, 144.4, 140.2, 140.0, 133.2, 132.0, 131.6, 128.54, 128.50, 128.4, 128.24,



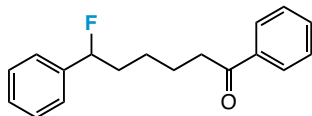
128.22, 126.4, 125.6, 125.5, 94.1 (d,  $J = 171.0$  Hz), 38.9, 38.7, 30.6, 30.5;  $^{19}\text{F}$  NMR ( $\text{CDCl}_3$ ): -175.12 (1F, ddd,  $J = 47.0, 29.8, 16.1$  Hz).



*cis*-2-(3-fluoro-3-phenylpropyl)cyclohexane-1-carboxylic acid (**13**). 58% yield. Clear oil.  $\nu_{\text{max}}/\text{cm}^{-1}$  3300-2500 (COOH), 1702 (CO), and 1699 (CO).  $^1\text{H}$  NMR ( $\text{CDCl}_3$ ): 11.32 (1H, br s), 7.38-7.28 (5H, m), 5.49-5.29 (1H, m), 2.15-2.02 (1H, m), 2.01-1.83 (3H, m), 1.82-1.71 (2H, m), 1.70-1.59 (2H, m), 1.58-1.46 (1H, m), 1.44-1.35 (1H, m), 1.34-1.13 (2H, m), 1.00-0.87 (1H, m);  $^{13}\text{C}$  NMR ( $\text{CDCl}_3$ ): 182.4, 140.5, 140.3, 140.2, 128.39, 128.37, 128.25, 128.23, 128.12, 128.11, 125.7, 125.6, 125.5, 125.4, 95.0 (d,  $J = 170.3$  Hz), 94.4 (d,  $J = 171.8$  Hz), 49.7, 49.5, 38.3, 38.2, 34.3, 34.1, 34.0, 33.8, 30.5, 30.4, 30.18, 30.15, 30.13, 30.00, 29.97, 25.5, 25.30, 25.28;  $^{19}\text{F}$  NMR ( $\text{CDCl}_3$ ): -171.99 (1F, m), -175.23 (1F, ddd,  $J = 48.2, 31.0, 17.2$  Hz).

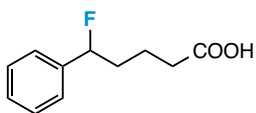


6-fluoro-2,6-diphenylhexanoic acid (**14**). 56% yield. Clear oil.  $\nu_{\text{max}}/\text{cm}^{-1}$  3300-2500 (COOH) and 1704 (CO).  $^1\text{H}$  NMR ( $\text{CDCl}_3$ ): 7.37-7.25 (10H, m), 5.38 (1H, ddd,  $J = 47.7, 8.2, 4.5$  Hz), 3.59 (1H, br s), 2.19-2.07 (1H, m), 2.06-1.91 (1H, m), 1.91-1.72 (2H, m), 1.57-1.28 (3H, m);  $^{13}\text{C}$  NMR ( $\text{CDCl}_3$ ): 140.3, 140.1, 128.7, 128.4, 128.24, 128.23, 128.0, 127.5, 125.5, 125.4, 95.13, 95.08, 93.44, 93.38, 37.0, 36.8, 32.8, 23.3;  $^{19}\text{F}$  NMR ( $\text{CDCl}_3$ ): -174.16 (1F, ddd,  $J = 47.0, 29.8, 17.2$  Hz), -174.39 (1F, ddd,  $J = 47.0, 29.8, 16.1$  Hz).

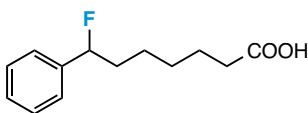


6-fluoro-1,6-diphenylhexanone (**15**). 30% yield. White solid; 30-32 °C.  $\nu_{\text{max}}/\text{cm}^{-1}$  2938 (CH), 2863 (CH), and 1684 (CO).  $^1\text{H}$  NMR ( $\text{CDCl}_3$ ): 7.96-7.93 (2H, m), 7.59-7.53 (1H, m), 7.49-7.43 (2H, m), 7.39-7.30 (5H, m), 5.45 (1H, ddd,  $J = 47.5, 7.8, 5.0$  Hz), 2.99 (1H, t, 7.3 Hz), 2.17-1.87 (2H, m), 1.86-1.74 (2H, m),

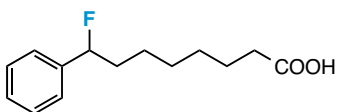
1.65-1.55 (1H, m), 1.53-1.40 (1H, m);  $^{13}\text{C}$  NMR ( $\text{CDCl}_3$ ): 200.1, 133.0, 128.64, 128.60, 128.50, 128.45, 128.2, 128.1, 128.0, 125.6, 125.5, 94.4 (d,  $J = 169.5$  Hz), 38.4, 37.1 (d,  $J = 23.6$  Hz), 24.9, 23.9;  $^{19}\text{F}$  NMR ( $\text{CDCl}_3$ ): -174.1 (1F, ddd,  $J = 47.0, 28.7, 16.1$  Hz).



5-fluoro-5-phenylpentanoic acid (**17**). 58% yield. Clear oil.  $\nu_{\text{max}}/\text{cm}^{-1}$  3300-2500 (COOH) and 1705 (CO).  $^1\text{H}$  NMR ( $\text{CDCl}_3$ ): 11.19 (1H, br s), 7.39-7.35 (2H, m), 7.33-7.31 (3H, m), 5.45 (1H, ddd,  $J = 48.1, 7.8, 4.1$  Hz), 2.44-2.41 (2H, m), 2.09-1.98 (1H, m), 1.96-1.81 (2H, m), 1.79-1.69 (1H, m);  $^{13}\text{C}$  NMR ( $\text{CDCl}_3$ ): 179.5, 140.1, 139.9, 128.5, 128.3, 125.5, 125.4, 94.1 (d,  $J = 171.8$  Hz), 36.5, 36.2, 20.4, 20.3;  $^{19}\text{F}$  NMR ( $\text{CDCl}_3$ ): -174.90 (1F, ddd,  $J = 45.9, 28.7, 18.4$  Hz).

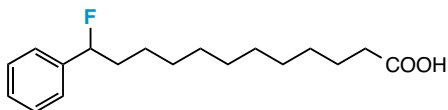


7-fluoro-7-phenylheptanoic acid (**18**). 57% yield. Clear oil.  $\nu_{\text{max}}/\text{cm}^{-1}$  3300-2500 (COOH) and 1706 (CO).  $^1\text{H}$  NMR ( $\text{CDCl}_3$ ): 10.49 (1H, br s), 7.41-7.36 (2H, m), 7.35-7.31 (3H, m), 5.43 (1H, ddd,  $J = 47.7, 8.0, 4.7$  Hz), 2.35 (2H, t,  $J = 7.4$  Hz), 2.06-1.92 (1H, m), 1.91-1.75 (1H, m), 1.65 (2H, quint,  $J = 7.4$  Hz), 1.57-1.47 (1H, m), 1.45-1.38 (3H, m);  $^{13}\text{C}$  NMR ( $\text{CDCl}_3$ ): 180.2, 140.5, 140.3, 128.4, 128.17, 128.16, 125.5, 125.4, 94.5 (d,  $J = 171.0$  Hz), 37.1, 36.8, 34.0, 28.7, 24.72, 24.68, 24.4;  $^{19}\text{F}$  NMR ( $\text{CDCl}_3$ ): -174.05 (1F, ddd,  $J = 47.0, 28.7, 17.2$  Hz).



8-fluoro-8-phenyloctanoic acid (**19**). 46% yield. Clear oil.  $\nu_{\text{max}}/\text{cm}^{-1}$  3300-2500 (COOH) and 1705 (CO).  $^1\text{H}$  NMR ( $\text{CDCl}_3$ ): 9.97 (1H, br s), 7.40-7.35 (2H, m), 7.34-7.29 (3H, m), 5.41 (1H, ddd,  $J = 47.7, 8.0, 4.9$  Hz), 2.34 (2H, t,  $J = 7.4$  Hz), 2.03-1.90 (1H, m), 1.88-1.73 (1H, m), 1.62 (2H, quint,  $J = 7.2$  Hz), 1.54-1.44 (1H, m), 1.43-1.31 (5H, m);  $^{13}\text{C}$  NMR ( $\text{CDCl}_3$ ): 180.1, 140.6, 140.4, 128.4, 128.3, 128.16, 128.14, 125.53,

125.46, 94.6 (d,  $J = 170.3$  Hz), 37.2, 37.0, 34.0, 28.9, 28.8, 24.9, 24.8, 24.5;  $^{19}\text{F}$  NMR ( $\text{CDCl}_3$ ): -173.83 (1F, ddd,  $J = 47.0, 27.5, 17.2$  Hz).



12-fluoro-12-phenyldodecanoic acid (**20**). 30% yield. White solid; m.p. 58-61 °C.  $\nu_{\text{max}}/\text{cm}^{-1}$  3300-2500 (COOH) and 1704 (CO).  $^1\text{H}$  NMR ( $\text{CDCl}_3$ ): 8.01 (1H, br s), 7.39-7.35 (2H, m), 7.33-7.29 (3H, m), 5.41 (1H, ddd,  $J = 47.9, 8.2, 5.1$  Hz), 2.34 (2H, t,  $J = 7.4$  Hz), 2.03-1.90 (1H, m), 1.88-1.72 (1H, m), 1.62 (2H, quint,  $J = 7.2$  Hz), 1.52-1.41 (1H, m), 1.40-1.23 (13H, m);  $^{13}\text{C}$  NMR ( $\text{CDCl}_3$ ): 140.7, 140.5, 128.4, 128.13, 128.11, 125.6, 125.5, 94.7 (d,  $J = 171.0$  Hz), 37.3, 37.1, 29.43, 29.41, 29.35, 29.33, 29.2, 29.0, 25.10, 25.05, 24.7;  $^{19}\text{F}$  NMR ( $\text{CDCl}_3$ ): -173.57 (1F, ddd,  $J = 47.0, 28.7, 17.2$  Hz).

## 12.8 Experimental Details for Chapter 8.

**General Aminofluorination Procedures.** *Direct Photoexcitation Procedure (compatible with Selectfluor or NFSI):* The N-F reagent (1.1 mmol) was added to an oven-dried microwave vial equipped with a stir bar. Then, the vial was sealed via crimper with a cap w/ septum; it was evacuated and refilled with  $\text{N}_2$  multiple times. Anhydrous  $\text{CH}_3\text{CN}$  (6 mL) was added via syringe under  $\text{N}_2$ , followed by the arylcyclopropane substrate (0.5 mmol). The reaction mixture was stirred in a Rayonet reactor and irradiated at 300 nm for 14 h.

*Metal Initiation Procedure (compatible with Selectfluor):* Selectfluor (390 mg, 1.1 mmol), cuprous iodide (10 mg, 0.05 mmol), *N,N*-bis(2,6-dichloro-benzylidene)ethane-1,2-diamine (19 mg, 0.05 mmol), and potassium carbonate (7 mg, 0.05 mmol) were added to a flame-dried 10 mL round bottom flask equipped with a stir bar under  $\text{N}_2$ . Degassed (with  $\text{N}_2$ ) acetonitrile (6 mL) was added to the reaction flask, and the solution was stirred vigorously at room temperature. After 15 minutes, the arylcyclopropane substrate (0.50 mmol) was added to the reaction flask, and the reaction stirred overnight.

*Radical Initiation Procedure (compatible with Selectfluor):* Selectfluor (390.0 mg, 1.1 mmol) was added to a 10 mL flame-dried round-bottom flask equipped with a stir bar under N<sub>2</sub>. Then, anhydrous CH<sub>3</sub>CN (6.0 mL) was added to the reaction flask, and the solution was stirred vigorously at room temperature. The arylcyclopropane substrate (0.5 mmol) was added, followed by 1.0 M triethylborane solution in hexanes (10.0 mg, 0.1 mmol). The reaction mixture was stirred for 8 h.

*Photosensitized Procedure (compatible with Selectfluor or NFSI):* The N-F reagent (1.1 mmol) and 9-fluorenone (18 mg, 0.1 mmol) were added to an oven-dried microwave vial equipped with a stir bar. Then, the vial was sealed via crimper with a cap w/ septum; it was evacuated and refilled with N<sub>2</sub> multiple times. Anhydrous CH<sub>3</sub>CN (6 mL) was added via syringe under N<sub>2</sub>, followed by the arylcyclopropane substrate (0.5 mmol). The reaction mixture was stirred in front of a 14-Watt CFL for 14 h.

*Workup Procedures:* All reactions with NFSI were concentrated and subjected to column chromatography on silica gel or Florisil with gradient elution using hexanes to 10:90 EtOAc:hexanes in all instances. Further purification was obtained for the indene-derived cyclopropane products via column chromatography on C18 media eluting with MeCN/H<sub>2</sub>O. All reactions with Selectfluor were analyzed as crude reaction mixtures, but note that these compounds will survive chromatography on both C18 and diol column media using MeCN/H<sub>2</sub>O as eluent (but will often co-elute with the chloromethyl DABCO byproduct).

**Functionalization of Selectfluor Adduct with Thiocyanate.** Potassium thiocyanate (3.0 equiv.) was added to the crude reaction mixture of 1,2-diphenylcyclopropane and Selectfluor following irradiation. The mixture was stirred and heated to reflux for 14 h. It was then diluted with H<sub>2</sub>O, extracted into DCM, dried with NaSO<sub>4</sub>, filtered through Florisil, and concentrated. Further purification was obtained via column chromatography on Florisil with gradient elution using hexanes to 20:80 EtOAc:hexanes.

**General Competition Experiment Procedures.** *General Intermolecular Competition Procedure (applies to Hammett plots and KIEs):* The N-F reagent (0.55 mmol) was added to an oven-dried microwave vial

equipped with a stir bar. Then, the vial was sealed via crimper with a cap w/ septum; it was evacuated and refilled with N<sub>2</sub> multiple times. Anhydrous CH<sub>3</sub>CN (3 mL) was added via syringe under N<sub>2</sub>, followed by a 1:1 mixture of two arylcyclopropane compounds (5.5 mmol). The reaction mixture was stirred in a Rayonet reactor and irradiated at 300 nm for 14 h. Product ratios (e.g., [P<sub>X</sub>]/[P<sub>H</sub>] or [P<sub>H</sub>]/[P<sub>D</sub>]) were determined by <sup>19</sup>F NMR analysis upon making a sample tube composed of a 0.3 mL aliquot from the reaction flask and 0.2 mL of a dilute solution of 3-chlorobenzotrifluoride (internal standard) dissolved in CD<sub>3</sub>CN.

*General Intramolecular Competition Procedure (applies to Hammett plots and KIEs):* The N-F reagent (0.55 mmol) was added to an oven-dried microwave vial equipped with a stir bar. Then, the vial was sealed via crimper with a cap w/ septum; it was evacuated and refilled with N<sub>2</sub> multiple times. Anhydrous CH<sub>3</sub>CN (3 mL) was added via syringe under N<sub>2</sub>, followed by the arylcyclopropane compound (0.25 mmol). The reaction mixture was stirred in a Rayonet reactor and irradiated at 300 nm for 14 h. Product ratios (e.g., [P<sub>X</sub>]/[P<sub>H</sub>] or [P<sub>H</sub>]/[P<sub>D</sub>]) were determined by <sup>19</sup>F NMR analysis upon making a sample tube composed of a 0.3 mL aliquot from the reaction flask and 0.2 mL of a dilute solution of 3-chlorobenzotrifluoride (internal standard) dissolved in CD<sub>3</sub>CN.

**General Arylcyclopropane Synthesis Procedures.** *Simmons-Smith Procedure:*<sup>52</sup> DCM (20 mL) was added to a flame-dried three-neck flask equipped with a stir bar, reflux condenser, and drop funnel under N<sub>2</sub>. A 1.0 M solution of ZnEt<sub>2</sub> in hexanes (19 mL, 19 mmol) was carefully added via syringe, and the solution was stirred and cooled to 0 °C. A solution of TFA (1.4 mL, 19 mmol) in DCM (10 mL) was added very slowly and carefully via drop funnel; the reaction mixture stirred for 30 min. Next, a solution of CH<sub>2</sub>I<sub>2</sub> (1.5 mL, 19 mmol) in DCM (10 mL) was added via drop funnel; the reaction mixture stirred for 30 min. Finally, a solution of a substituted alkene (19 mmol) in DCM (10 mL) was added via drop funnel; the reaction mixture stirred and gradually warmed to room temperature overnight. (If unreacted alkene is still present, an additional equivalent of ZnEt<sub>2</sub> and CH<sub>2</sub>I<sub>2</sub> may be added to drive the reaction further toward completion.) The reaction mixture was carefully quenched with 1 M HCl. The DCM layer was separated, and the aqueous layer was extracted into hexanes. All organic layers were washed with NaHCO<sub>3</sub>, washed

with H<sub>2</sub>O, dried with MgSO<sub>4</sub>, filtered through Celite, and concentrated. The crude reaction mixture was subjected to column chromatography on silica gel, eluting with pentane. Note: excess CH<sub>2</sub>I<sub>2</sub> in the sample is detrimental to the aminofluorination reaction. If it cannot be removed by initial column chromatography due to poor separation, dissolve the crude sample in Et<sub>2</sub>O, add a three- to five-fold excess of DABCO, and reflux the mixture overnight. Upon cooling, filter the reaction mixture through Celite (washing with Et<sub>2</sub>O), concentrate, and push it through a plug of silica gel, eluting with pentane. This should remove the excess CH<sub>2</sub>I<sub>2</sub> effectively.

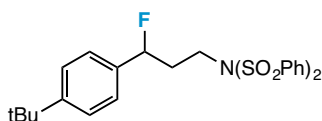
*Suzuki Coupling Procedure:*<sup>53</sup> A substituted bromobenzene (17.9 mmol), cyclopropylboronic acid (2.00 g, 23.2 mmol), and K<sub>3</sub>PO<sub>4</sub> (13.3 g, 62.7 mmol) were added to a flame-dried three-neck flask equipped with a stir bar and a reflux condenser under N<sub>2</sub>. Toluene (80 mL) and H<sub>2</sub>O (4 mL) were added to the reaction flask; the mixture was stirred. A 20 wt. % solution of P(Cy)<sub>3</sub> in toluene (2.5 mL, 1.8 mmol) was then added via syringe, followed by Pd(OAc)<sub>2</sub> (0.202 g, 0.90 mmol). The reaction mixture was heated to 100 °C and left to stir overnight. After removing from heat, the reaction mixture was diluted with H<sub>2</sub>O and extracted into EtOAc. The combined organic layers were washed with brine, dried with MgSO<sub>4</sub>, filtered through Celite, and concentrated. Arylcyclopropane products were often effectively purified via Kugelrohr distillation.

*Heck Coupling Procedure (for p-Cl and p-Br compounds):*<sup>54</sup> Phenylboronic acid (3.33 g, 27 mmol), Pd(OAc)<sub>2</sub> (0.307 g, 1.4 mmol), and NBS (1.46 g, 8.2 mmol) were added to a flame-dried three-neck flask equipped with a stir bar and a reflux condenser under N<sub>2</sub>. Toluene (30 mL) was added to the reaction flask; the mixture was stirred. A substituted styrene (27 mmol) was then added, and the reaction mixture was left to stir overnight. Upon completion, the mixture was concentrated and pushed through a plug of silica gel, eluting with hexanes and ethyl acetate. The substituted stilbene product was recrystallized using DCM and hexanes.

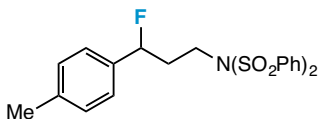
*Heck Coupling Procedure (for p-tBu, p-Me, and p-F compounds):*<sup>55</sup> A substituted bromobenzene (25 mmol), K<sub>3</sub>PO<sub>4</sub> (7.43 g, 35 mmol), and Pd(OAc)<sub>2</sub> (0.056 g, 0.25 mmol) were added to a flame-dried three-

neck flask equipped with a stir bar and a reflux condenser under N<sub>2</sub>. DMF (25 mL) was added to the reaction flask; the mixture was stirred. Styrene (3.4 mL, 30 mmol) was then added, and the reaction mixture was heated to 120 °C and left to stir overnight. Upon cooling, the reaction mixture was poured into H<sub>2</sub>O and extracted into EtOAc. The combined organic layers were washed with brine, dried with MgSO<sub>4</sub>, filtered through Celite, and concentrated. The crude mixture was pushed through a plug of silica, eluting with hexanes. The substituted stilbene product was recrystallized from EtOAc and hexanes.

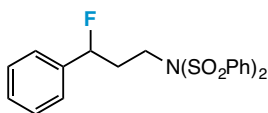
#### Characterization Data.



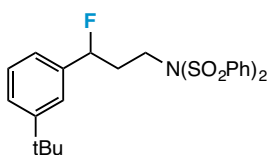
*N*-(3-(4-(*tert*-butyl)phenyl)-3-fluoropropyl)-*N*-(phenylsulfonyl)benzenesulfonamide: 67% yield. Clear oil. <sup>1</sup>H NMR (CD<sub>3</sub>CN): 7.90-7.88 (4 H, m), 7.74 (2 H, t, *J* = 7.5 Hz), 7.60 (4 H, t, *J* = 8.1 Hz), 7.45 (2 H, d, *J* = 8.2 Hz), 7.23 (2 H, d, *J* = 7.8 Hz), 5.47 (1 H, ddd, *J* = 47.7, 8.2, 4.1 Hz), 3.91-3.79 (2 H, m), 2.37-2.11 (2 H, m), 1.32 (9 H, s); <sup>19</sup>F NMR (CD<sub>3</sub>CN): -174.8 (1 F, ddd, *J* = 46.5, 28.7, 17.8 Hz); <sup>13</sup>C NMR (CD<sub>3</sub>CN): 152.83, 152.80, 140.3, 137.5, 137.1, 136.9, 135.4, 130.9, 130.6, 130.4, 129.0, 128.9, 126.5, 126.4, 92.7 (d, *J* = 168.1 Hz), 46.5 (d, *J* = 5.2 Hz), 37.7 (d, *J* = 23.6 Hz), 35.3, 31.5.



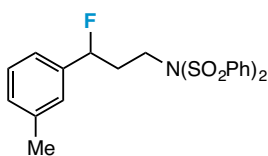
*N*-(3-fluoro-3-(*p*-tolyl)propyl)-*N*-(phenylsulfonyl)benzenesulfonamide: 41% yield. Clear oil. <sup>1</sup>H NMR (CD<sub>3</sub>CN): 7.93-7.89 (4 H, m), 7.79-7.75 (4 H, m), 7.65-7.61 (2 H, m), 7.26-7.19 (4 H, m), 5.49 (1 H, ddd, *J* = 47.7, 8.1, 4.3 Hz), 3.88-3.84 (2 H, m), 2.38 (3 H, s), 2.35-2.12 (2 H, m); <sup>19</sup>F NMR (CD<sub>3</sub>CN): -174.7 (1 F, ddd, *J* = 47.0, 28.7, 17.8 Hz); <sup>13</sup>C NMR (CD<sub>3</sub>CN): 139.3, 138.71, 138.69, 136.1, 136.0, 134.4, 129.5, 129.2, 127.9, 125.7, 125.6, 93.6 (d, *J* = 168.4 Hz), 46.4 (d, *J* = 5.2 Hz), 37.8 (d, *J* = 24 Hz), 20.2.



*N*-(3-fluoro-3-phenylpropyl)-*N*-(phenylsulfonyl)benzenesulfonamide: 43% yield. Clear oil.  $^1\text{H}$  NMR ( $\text{CD}_3\text{CN}$ ): 7.96-7.90 (4 H, m), 7.78-7.73 (2 H, m), 7.65-7.59 (4 H, m), 7.43-7.30 (5 H, m), 5.54 (1 H, ddd,  $J = 47.8, 7.7, 4.5$  Hz), 3.89 (2 H, m), 2.41-2.12 (2 H, m);  $^{19}\text{F}$  NMR ( $\text{CD}_3\text{CN}$ ): -176.8 (1 F, ddd,  $J = 47.6, 28.7, 18.4$  Hz);  $^{13}\text{C}$  NMR ( $\text{CD}_3\text{CN}$ ): 140.3, 140.1, 139.9, 135.4, 130.4, 130.3, 129.7, 129.63, 129.60, 128.9, 126.5, 126.4, 92.7 (d,  $J = 169.2$  Hz), 46.5 (d,  $J = 4.8$  Hz), 38.0 (d,  $J = 23.6$  Hz).

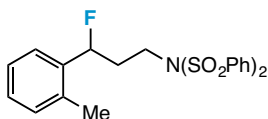


*N*-(3-(3-(*tert*-butyl)phenyl)-3-fluoropropyl)-*N*-(phenylsulfonyl)benzenesulfonamide: 50% yield. Clear oil.  $^1\text{H}$  NMR ( $\text{CD}_3\text{CN}$ ): 7.91-7.88 (4 H, m), 7.75-7.71 (2 H, m), 7.62-7.57 (4 H, m), 7.45-7.42 (1 H, m), 7.35-7.31 (2 H, m), 7.12-7.09 (1 H, m), 5.49 (1 H, ddd,  $J = 47.8, 8.1, 4.4$  Hz), 3.88-3.84 (2 H, m), 2.37-2.12 (2 H, m), 1.31 (9 H, s);  $^{19}\text{F}$  NMR ( $\text{CD}_3\text{CN}$ ): -175.6 (1 F, ddd,  $J = 47.6, 29.3, 18.4$  Hz);  $^{13}\text{C}$  NMR ( $\text{CD}_3\text{CN}$ ): 152.6, 140.30, 140.29, 139.7, 139.6, 135.3, 130.41, 130.40, 130.39, 130.38, 129.4, 128.88, 128.87, 126.67, 126.65, 123.74, 123.67, 123.6, 123.5, 93.1 (d,  $J = 169.5$  Hz), 46.5 (d,  $J = 4.8$  Hz), 37.9 (d,  $J = 24.0$  Hz), 35.4, 31.5.

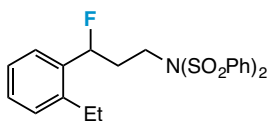


*N*-(3-fluoro-3-(*m*-tolyl)propyl)-*N*-(phenylsulfonyl)benzenesulfonamide: 41% yield. Clear oil.  $^1\text{H}$  NMR ( $\text{CD}_3\text{CN}$ ): 7.91-7.88 (4 H, m), 7.76-7.72 (2 H, m), 7.63-7.58 (4 H, m), 7.30-7.27 (1 H, m), 7.20-7.18 (1 H, m), 7.10-7.07 (2 H, m), 5.47 (1 H, ddd,  $J = 47.9, 8.2, 4.2$  Hz), 3.90-3.82 (2 H, m), 2.35 (3 H, s), 2.33-2.10 (2 H, m);  $^{19}\text{F}$  NMR ( $\text{CD}_3\text{CN}$ ): -176.6 (1 F, ddd,  $J = 47.6, 29.3, 18.4$  Hz);  $^{13}\text{C}$  NMR ( $\text{CD}_3\text{CN}$ ): 139.3, 139.1, 138.9, 138.5, 136.5, 134.4, 129.9, 129.6, 129.5, 129.33, 129.31, 128.6, 127.9, 126.2, 126.1, 122.6, 122.5, 92.8 (d,  $J = 169.2$  Hz), 46.5 (d,  $J = 4.8$  Hz), 38.0 (d,  $J = 23.6$  Hz), 29.9, 20.5.

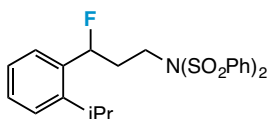




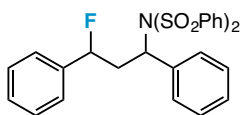
*N*-(3-fluoro-3-(*o*-tolyl)propyl)-*N*-(phenylsulfonyl)benzenesulfonamide: 60% yield. Clear oil.  $^1\text{H}$  NMR ( $\text{CD}_3\text{CN}$ ): 7.90-7.87 (4 H, m), 7.76-7.72 (2 H, m), 7.62-7.57 (4 H, m), 7.33-7.18 (4 H, m), 5.82-5.67 (1 H, m), 3.99-3.86 (2 H, m), 2.27 (3 H, s), 2.24-2.13 (2 H, m);  $^{19}\text{F}$  NMR ( $\text{CD}_3\text{CN}$ ): -180.3 (1 F, m);  $^{13}\text{C}$  NMR ( $\text{CD}_3\text{CN}$ ): 140.3, 138.3, 138.1, 135.70, 135.65, 135.4, 131.6, 130.4, 129.5, 129.4, 128.9, 127.2, 126.0, 125.9, 90.4 (d,  $J = 167.7$  Hz), 46.7 (d,  $J = 3.7$  Hz), 37.1 (d,  $J = 24.7$  Hz), 19.0.



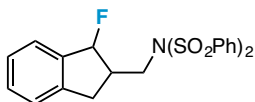
*N*-(3-(2-ethylphenyl)-3-fluoropropyl)-*N*-(phenylsulfonyl)benzenesulfonamide: 57% yield. Clear oil.  $^1\text{H}$  NMR ( $\text{CD}_3\text{CN}$ ): 7.93-7.90 (4 H, m), 7.75-7.71 (2 H, m), 7.62-7.57 (4 H, m), 7.35-7.29 (2 H, m), 7.27-7.22 (2 H, m), 5.78 (1 H, ddd,  $J = 47.2, 8.7, 3.4$  Hz), 3.99-3.94 (2 H, m), 2.63-2.52 (2 H, m), 2.35-2.09 (2 H, m), 1.16 (3 H, t,  $J = 7.3$  Hz);  $^{19}\text{F}$  NMR ( $\text{CD}_3\text{CN}$ ): -177.4 (1 F, ddd,  $J = 48.2, 32.7, 17.2$  Hz);  $^{13}\text{C}$  NMR ( $\text{CD}_3\text{CN}$ ): 142.03, 141.99, 140.3, 137.5, 137.3, 135.4, 130.8, 130.6, 130.4, 129.9, 129.8, 129.7, 128.9, 127.2, 126.4, 126.3, 89.9 (d,  $J = 167.7$  Hz), 46.8 (d,  $J = 3.7$  Hz), 37.9 (d,  $J = 24.3$  Hz), 25.7, 16.1.



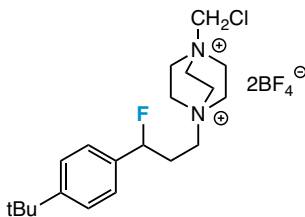
*N*-(3-fluoro-3-(2-isopropylphenyl)propyl)-*N*-(phenylsulfonyl)benzenesulfonamide: 66% yield. Clear oil.  $^1\text{H}$  NMR ( $\text{CD}_3\text{CN}$ ): 7.92-7.90 (4 H, m), 7.75-7.71 (2 H, m), 7.62-7.58 (4 H, m), 7.38-7.31 (3 H), 7.25-7.21 (1 H, m), 5.85 (1 H, ddd,  $J = 47.4, 8.9, 3.4$  Hz), 3.98-3.94 (2 H, m), 3.04 (1 H, spt,  $J = 6.8$  Hz), 2.36-2.11 (2 H, m), 1.21-1.18 (6 H, m);  $^{19}\text{F}$  NMR ( $\text{CD}_3\text{CN}$ ): -178.20 (1 F, ddd,  $J = 49.9, 32.7, 17.8$  Hz);  $^{13}\text{C}$  NMR ( $\text{CD}_3\text{CN}$ ): 146.7, 146.6, 140.2, 136.8, 136.6, 135.4, 130.4, 129.9, 129.8, 128.9, 127.0, 126.7, 126.3, 126.2, 89.9 (d,  $J = 167.7$  Hz), 46.8 (d,  $J = 3.7$  Hz), 38.3 (d,  $J = 23.6$  Hz), 29.1, 24.6, 24.0.



*N*-(3-fluoro-1,3-diphenylpropyl)-*N*-(phenylsulfonyl)benzenesulfonamide: 60% yield. Yellow oil.  $^1\text{H}$  NMR ( $\text{CD}_3\text{CN}$ ): 7.72-7.33 (18 H, m), 7.18-7.13 (1 H, m), 7.09-7.04 (1 H, m), 5.82-5.44 (1 H, m), 5.34-5.12 (1 H, m), 3.40-3.20 (1 H, m), 2.46-1.90 (1 H, m);  $^{19}\text{F}$  NMR ( $\text{CD}_3\text{CN}$ ): -171.3 (1 F, ddd,  $J = 47.0, 26.4, 13.2$  Hz), -177.8 (1 F, ddd,  $J = 49.3, 36.7, 13.2$  Hz);  $^{13}\text{C}$  NMR ( $\text{CD}_3\text{CN}$ ): 140.1, 139.9, 139.8, 139.6, 136.4, 135.2, 130.8, 130.6, 130.1, 130.0, 129.93, 129.91, 129.89, 129.77, 129.75, 129.72, 129.70, 129.60, 129.59, 129.4, 129.0, 128.9, 126.63, 126.57, 126.4, 126.3, 93.0 (d,  $J = 170.6$  Hz), 92.3 (d,  $J = 170.3$  Hz), 62.5 (d,  $J = 6.3$  Hz), 61.7 (d,  $J = 2.9$  Hz), 40.9 (d,  $J = 22.1$  Hz), 40.7 (d,  $J = 25.4$  Hz).

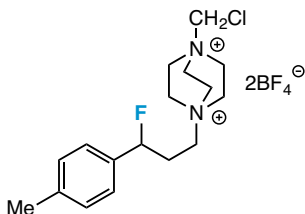


*N*-((1-fluoro-2,3-dihydro-1*H*-inden-2-yl)methyl)-*N*-(phenylsulfonyl)benzenesulfonamide: 66% yield. Yellow oil.  $^1\text{H}$  NMR ( $\text{CD}_3\text{CN}$ ): 8.00-7.89 (4 H, m), 7.80-7.72 (2 H, m), 7.67-7.58 (4 H, m), 7.50-7.15 (4 H, m), 5.97-5.52 (1 H, m), 4.68-3.67 (2 H, m), 3.19-2.65 (3 H, m);  $^{19}\text{F}$  NMR ( $\text{CD}_3\text{CN}$ ): -164.5 (1 F, m), -176.6 (1 F, m);  $^{13}\text{C}$  NMR ( $\text{CD}_3\text{CN}$ ): 145.5, 144.5, 143.8, 143.6, 143.5, 140.7, 140.5, 140.3, 140.2, 140.0, 137.1, 135.4, 135.0, 132.8, 132.6, 132.4, 131.70, 131.67, 131.4, 131.3, 130.92, 130.88, 130.63, 130.59, 130.42, 130.38, 130.3, 130.1, 129.6, 129.4, 129.1, 129.0, 128.9, 128.8, 128.13, 128.10, 127.98, 127.94, 127.91, 127.87, 127.8, 127.3, 126.84, 126.81, 126.47, 126.46, 126.23, 126.21, 126.1, 126.0, 125.9, 124.6, 121.9, 100.4, 98.7, 97.9, 96.2, 91.2, 89.6, 56.3, 51.7, 51.6, 49.3, 49.2, 47.0, 46.7, 45.6, 45.4, 35.18, 35.16, 34.5, 34.4.



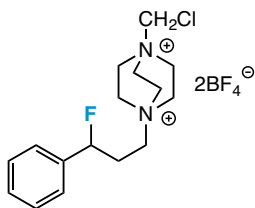
1-(3-(4-(*tert*-butyl)phenyl)-3-fluoropropyl)-4-(chloromethyl)-1,4-diazabicyclo[2.2.2]-octane bis(tetrafluoroborate): 96% yield.  $^1\text{H}$  NMR ( $\text{CD}_3\text{CN}$ ): 7.51 (2 H, d,  $J = 7.5$  Hz), 7.38 (2 H, d,  $J = 7.3$  Hz),

5.57 (1 H, ddd,  $J = 48.2, 9.6, 2.9$  Hz), 5.26 (2 H, s), 3.98-3.91 (12 H, m), 3.77-3.74 (2 H, m), 2.59-2.22 (2 H, m);  $^{19}\text{F}$  NMR ( $\text{CD}_3\text{CN}$ ): -150.3 (8 F, s), -174.5 (1 F, ddd,  $J = 47.0, 32.7, 13.2$  Hz).

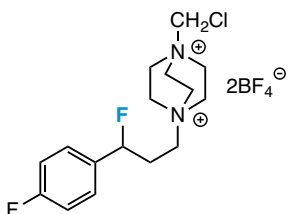


1-(3-(4-methylphenyl)-3-fluoropropyl)-4-(chloromethyl)-1,4-diazabicyclo[2.2.2]octane

bis(tetrafluoroborate): 90% yield.  $^1\text{H}$  NMR ( $\text{CD}_3\text{CN}$ ): 7.33 (2 H, m), 7.27 (2 H, m), 5.56 (1 H, ddd,  $J = 48.1, 9.3, 3.0$  Hz), 5.25 (2 H, s), 3.99-3.89 (12 H, m), 3.79-3.69 (2 H, m), 2.56-2.43 (1 H, m), 2.38-2.20 (1 H, m), 2.36 (3 H, s);  $^{19}\text{F}$  NMR ( $\text{CD}_3\text{CN}$ ): -151.8 (8 F, s), -175.6 (1 F, ddd,  $J = 46.5, 31.6, 13.8$  Hz).



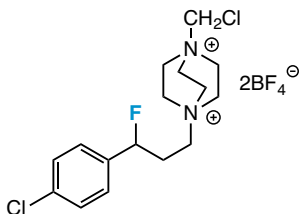
1-(chloromethyl)-4-(3-fluoro-3-phenylpropyl)-1,4-diaza-bicyclo[2.2.2]octane bis(tetra-fluoroborate): 85% yield.  $^1\text{H}$  NMR ( $\text{CD}_3\text{CN}$ ): 7.49-7.42 (5 H, m), 5.63 (1 H, ddd,  $J = 48.0, 9.3, 3.3$  Hz), 5.25 (2 H, s), 3.97-3.90 (12 H, m), 3.76-3.72 (2 H, m), 2.56-2.25 (2 H, m);  $^{19}\text{F}$  NMR ( $\text{CD}_3\text{CN}$ ): -150.54 (8 F, s), -176.4 (1 F, ddd,  $J = 45.9, 31.5, 14.3$  Hz).



1-(3-(4-fluorophenyl)-3-fluoropropyl)-4-(chloromethyl)-1,4-diazabicyclo[2.2.2]octane

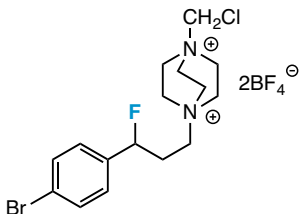
bis(tetrafluoroborate): 95% yield.  $^1\text{H}$  NMR ( $\text{CD}_3\text{CN}$ ): 7.50-7.46 (2 H, m), 7.22-7.18 (2 H, m), 5.62 (1 H,

ddd,  $J = 47.8, 9.3, 3.2$  Hz), 5.25 (2 H, s), 3.98-3.91 (12 H, m), 3.75-3.69 (2 H, m), 2.56-2.24 (2 H, m);  $^{19}\text{F}$  NMR ( $\text{CD}_3\text{CN}$ ): -113.7 (1 F, m), -150.4 (8 F, s), -174.4 (1 F, m).



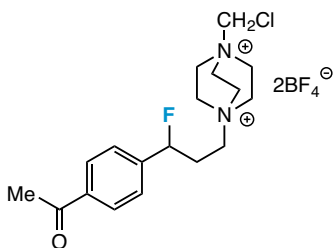
1-(3-(4-chlorophenyl)-3-fluoropropyl)-4-(chloromethyl)-1,4-diazabicyclo[2.2.2]octane

bis(tetrafluoroborate): 87% yield.  $^1\text{H}$  NMR ( $\text{CD}_3\text{CN}$ ): 7.51-7.45 (4 H, m), 5.65 (1 H, ddd,  $J = 47.7, 9.0, 3.3$  Hz), 5.28 (2 H, s), 4.02-3.92 (12 H, m), 3.77-3.72 (2 H, m), 2.56-2.26 (2 H, m);  $^{19}\text{F}$  NMR ( $\text{CD}_3\text{CN}$ ): -150.3 (8 F, s), -177.1 (1 F, ddd,  $J = 47.0, 31.6, 14.9$  Hz).



1-(3-(4-bromophenyl)-3-fluoropropyl)-4-(chloromethyl)-1,4-diazabicyclo[2.2.2]octane

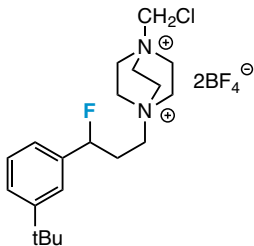
bis(tetrafluoroborate): 92% yield.  $^1\text{H}$  NMR ( $\text{CD}_3\text{CN}$ ): 7.63 (2 H, d,  $J = 8.1$  Hz), 7.37 (2 H, d,  $J = 8.2$  Hz), 5.61 (1 H, ddd,  $J = 47.6, 8.9, 3.2$  Hz), 5.25 (2 H, s), 3.98-3.89 (12 H, m), 3.76-3.69 (2 H, m), 2.53-2.25 (2 H, m);  $^{19}\text{F}$  NMR ( $\text{CD}_3\text{CN}$ ): -150.5, (8 F, s), -177.6 (1 F, ddd,  $J = 46.5, 31.0, 14.9$  Hz).



1-(3-(4-acetylphenyl)-3-fluoropropyl)-4-(chloromethyl)-1,4-diazabicyclo[2.2.2]octane

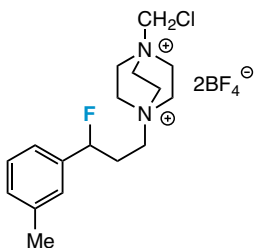
bis(tetrafluoroborate): 54% yield.  $^1\text{H}$  NMR ( $\text{CD}_3\text{CN}$ ): 8.08-8.01 (2 H, m), 7.61-7.52 (2 H, m), 5.82-5.66 (1

H, m), 5.28 (2 H, s), 4.03-3.91 (12 H, m), 2.63 (3 H, s), 2.61-2.30 (4 H, m);  $^{19}\text{F}$  NMR ( $\text{CD}_3\text{CN}$ ): -150.5 (8 F, s), -180.4 (1 F, ddd,  $J = 47.0, 31.6, 14.9$  Hz).



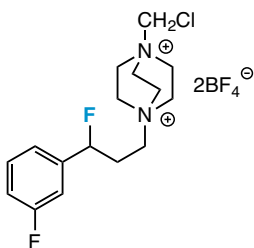
1-(3-(3-(*tert*-butyl)phenyl)-3-fluoropropyl)-4-(chloromethyl)-1,4-diazabicyclo[2.2.2]-octane

bis(tetrafluoroborate): 72% yield.  $^1\text{H}$  NMR  $\text{CD}_3\text{CN}$ : 7.49-7.46 (2 H, m), 7.41-7.36 (1 H, m), 7.26-7.24 (1 H, m), 5.59 (1 H, ddd,  $J = 48.3, 9.6, 3.2$  Hz), 5.26 (2 H, s), 3.98-3.91 (12 H, m), 3.78-3.71 (2 H, m), 2.58-2.45 (1 H, m), 2.40-2.23 (1 H, m), 1.33 (9 H, s);  $^{19}\text{F}$  NMR  $\text{CD}_3\text{CN}$ : -150.45 (8 F, s), -175.2 (1 F, ddd,  $J = 47.0, 32.7, 13.8$  Hz).



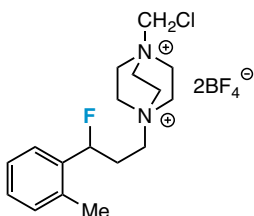
1-(3-(3-methylphenyl)-3-fluoropropyl)-4-(chloromethyl)-1,4-diazabicyclo[2.2.2]octane

bis(tetrafluoroborate): 83% yield.  $^1\text{H}$  NMR ( $\text{CD}_3\text{CN}$ ): 7.39-7.35 (1 H, m), 7.30-7.24 (3 H, m), 5.60 (1 H, ddd,  $J = 48.0, 9.0, 3.2$  Hz), 5.28 (2 H, s), 4.01-3.92 (12 H, m), 3.77-3.72 (2 H, m), 2.58-2.24 (2 H, m), 2.40 (3 H, s);  $^{19}\text{F}$  NMR ( $\text{CD}_3\text{CN}$ ): -150.4 (8 F, s), -175.9 (1 F, ddd,  $J = 47.0, 31.6, 14.3$  Hz).



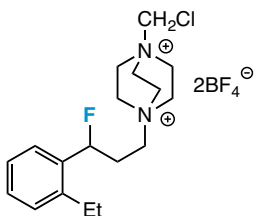
1-(3-(3-fluorophenyl)-3-fluoropropyl)-4-(chloromethyl)-1,4-diazabicyclo[2.2.2]octane

bis(tetrafluoroborate): 74% yield.  $^1\text{H}$  NMR ( $\text{CD}_3\text{CN}$ ): 7.51-7.41 (1 H, m), 7.27-7.14 (3 H, m), 5.64 (1 H, ddd,  $J = 47.5, 8.6, 3.4$  Hz), 5.18 (2 H, s), 4.01-3.90 (12 H, m), 3.75-3.70 (2 H, m), 2.53-2.24 (2 H, m);  $^{19}\text{F}$  NMR ( $\text{CD}_3\text{CN}$ ): -113.3 (1 F, m), -150.6 (8 F, s), -178.4 (1 F, ddd,  $J = 46.5, 31.0, 14.9$  Hz).



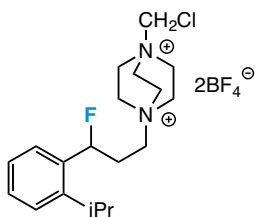
1-(3-(2-methylphenyl)-3-fluoropropyl)-4-(chloromethyl)-1,4-diazabicyclo[2.2.2]octane

bis(tetrafluoroborate): 93% yield.  $^1\text{H}$  NMR ( $\text{CD}_3\text{CN}$ ): 7.48-7.43 (1 H, m), 7.33-7.24 (3 H, m), 5.82 (1 H, ddd,  $J = 47.4, 9.5, 3.0$  Hz), 5.25 (2 H, s), 3.98-3.92 (12 H, m), 3.86-3.78 (2 H, m), 2.55-2.19 (2 H, m), 2.37 (3 H, s);  $^{19}\text{F}$  NMR ( $\text{CD}_3\text{CN}$ ): -150.4 (8 F, s), -177.8 (1 F, ddd,  $J = 46.5, 32.1, 13.8$  Hz).



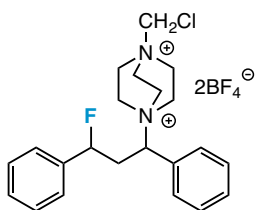
1-(3-(2-ethylphenyl)-3-fluoropropyl)-4-(chloromethyl)-1,4-diazabicyclo[2.2.2]octane

bis(tetrafluoroborate): 96% yield.  $^1\text{H}$  NMR ( $\text{CD}_3\text{CN}$ ): 7.53-7.50 (1 H, m), 7.41-7.32 (3 H, m), 5.88 (1 H, ddd,  $J = 47.5, 9.6, 2.8$  Hz), 5.29 (2 H, s), 4.02-3.89 (14 H, m), 2.82-2.66 (2 H, m), 2.64-2.50 (1 H), 2.38-2.19 (1 H, m), 1.24 (3 H, t,  $J = 7.5$  Hz);  $^{19}\text{F}$  NMR ( $\text{CD}_3\text{CN}$ ): -151.7 (8 F, s), -176.3 (1 F, ddd,  $J = 47.0, 33.3, 13.2$  Hz).

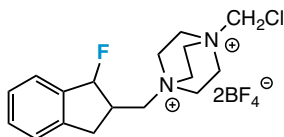


1-(3-(2-isopropylphenyl)-3-fluoropropyl)-4-(chloromethyl)-1,4-diazabicyclo[2.2.2]octane

bis(tetrafluoroborate): 93% yield.  $^1\text{H}$  NMR ( $\text{CD}_3\text{CN}$ ): 7.50-7.39 (3 H, m), 7.34-7.30 (1 H, m), 5.95 (1 H, ddd,  $J = 47.6, 9.7, 2.6$  Hz), 5.29 (2 H, s), 4.03-3.77 (14 H, m), 3.22 (1 H, spt,  $J = 6.8$  Hz), 2.61-2.48 (1 H, m), 2.38-2.19 (1 H, m), 1.27 (6 H, t,  $J = 6.3$  Hz);  $^{19}\text{F}$  NMR ( $\text{CD}_3\text{CN}$ ): -150.3 (8 F, s), -175.7 (1 F, ddd,  $J = 47.0, 33.3, 13.2$  Hz).

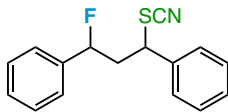


1-(chloromethyl)-4-(3-fluoro-1,3-diphenylpropyl)-1,4-diazabicyclo[2.2.2]octane bis(tetrafluoroborate): 97% yield.  $^1\text{H}$  NMR ( $\text{CD}_3\text{CN}$ ): 7.74-7.48 (5 H, m), 7.46-7.24 (5 H, m), 5.41-4.95 (1 H, m), 5.22 (2 H, m), 4.04-3.83 (12 H, m), 3.74-3.66 (1 H, m), 3.21-2.74 (2 H, m);  $^{19}\text{F}$  NMR ( $\text{CD}_3\text{CN}$ ): -150.5 (8 F, s), -168.7 (1 F, ddd,  $J = 47.2, 20.1, 13.2$  Hz), -177.3 (1 F, ddd,  $J = 47.0, 35.0, 11.5$  Hz).



1-(chloromethyl)-4-((1-fluoro-2,3-dihydro-1*H*-inden-2-yl)methyl)-1,4-diazabicyclo[2.2.2]octane

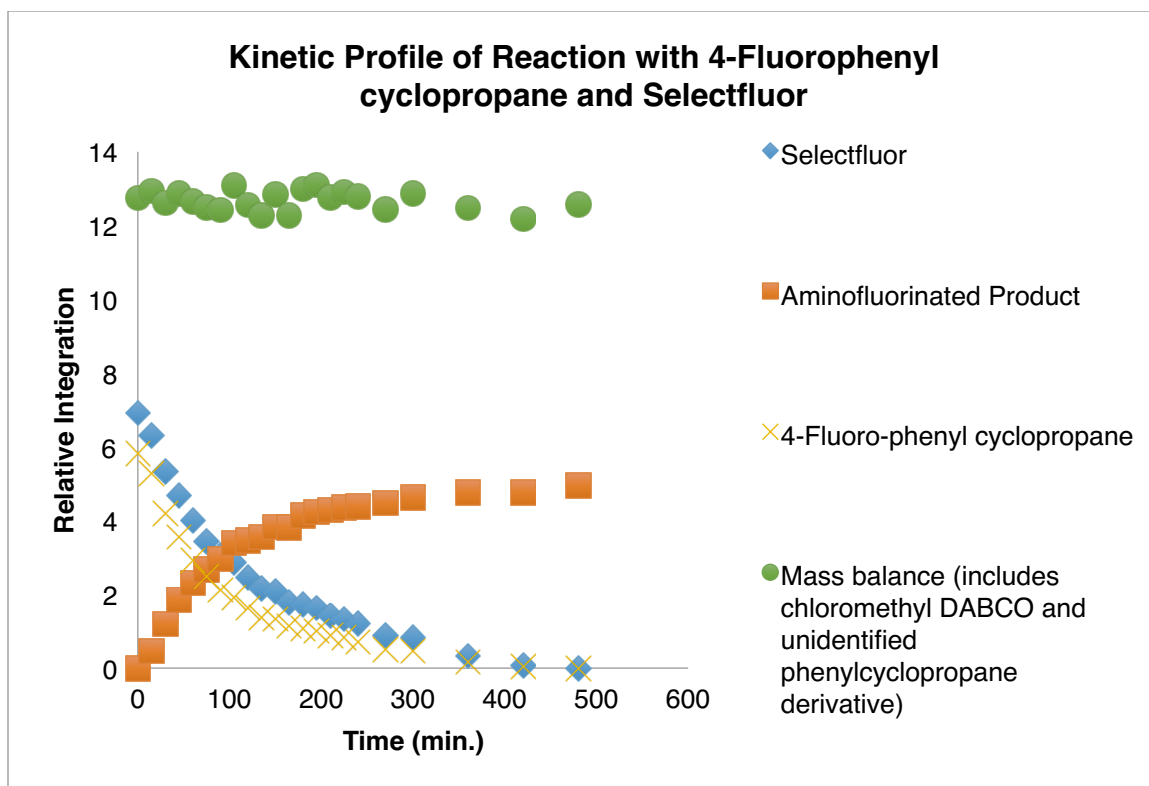
bis(tetrafluoroborate): 78% yield.  $^1\text{H}$  NMR ( $\text{CD}_3\text{CN}$ ): 7.53-7.25 (4 H, m), 6.11-5.91 (1 H, m), 5.33-5.22 (2 H, m), 4.07-3.90 (14 H, m), 3.44-2.71 (3 H, m);  $^{19}\text{F}$  NMR ( $\text{CD}_3\text{CN}$ ): -150.4 (8 F, s), -169.3 (1 F, ddd,  $J = 56.2, 23.5, 5.2$  Hz), -172.6 (1 F, ddm,  $J = 56.2, 31.6$  Hz).



(1-fluoro-3-thiocyanatopropane-1,3-diyl)dibenzene: 52% yield. Yellow oil.  $\nu_{\max}/\text{cm}^{-1}$  2253 (SC $\equiv$ N), 2154 (SC $\equiv$ N).  $^1\text{H}$  NMR ( $\text{CDCl}_3$ ): 7.49-7.34 (9 H, m), 7.29-7.27 (1 H, m), 5.74-5.09 (1 H, m), 4.69-4.45 (1 H, m), 2.90-2.54 (2 H, m);  $^{19}\text{F}$  NMR ( $\text{CDCl}_3$ ): -175.5 (1 F, ddd,  $J = 41.9, 29.3, 13.2$  Hz), -177.6 (1 F, ddd,  $J = 47.6, 35.0, 12.6$  Hz);  $^{13}\text{C}$  NMR ( $\text{CDCl}_3$ ): 138.5, 138.34, 138.32, 138.2, 136.7, 129.43, 129.41, 129.22, 129.21, 129.1, 129.02, 129.00, 128.91, 128.89, 128.8, 128.7, 127.6, 127.2, 125.6, 125.5, 125.4, 125.3, 111.0, 110.7, 91.6 (d,  $J = 173.6$  Hz), 91.1 (d,  $J = 173.2$  Hz), 49.2 (d,  $J = 4.1$  Hz), 49.0 (d,  $J = 2.2$  Hz), 43.5 (d,  $J = 24.7$  Hz), 42.6 (d,  $J = 24.7$  Hz).

**Reaction Kinetics.** Selectfluor (0.283 g, 0.8 mmol) was added to an oven-dried microwave vial equipped with a stir bar. Then, the vial was sealed via crimper with a cap w/ septum; it was evacuated and refilled with  $\text{N}_2$  multiple times. Anhydrous  $\text{CH}_3\text{CN}$  (8 mL) was added via syringe under  $\text{N}_2$ , followed by the arylcyclopropane substrate (0.091 g, 0.67 mmol). The reaction mixture was stirred in a Rayonet reactor and irradiated at 300 nm. At each specified time interval (for 8 h), 0.3 mL aliquots were taken from the vial (under  $\text{N}_2$ ) and combined with dilute 0.1 mL solution of 3-chlorobenzotrifluoride (internal standard) in  $\text{CD}_3\text{CN}$  to make NMR samples. Samples were kept in the dark and ultimately analyzed by  $^1\text{H}$ ,  $^{19}\text{F}$ , and  $^{19}\text{F}\{^1\text{H}\}$  NMR. Prior to the experiment, it was determined that there is no significant increase in yield after removing "light." Also, note that the unidentified phenylcyclopropane derivative byproduct does not contain a fluorine atom.





**Figure 12.17** Kinetic profile (4-fluorophenyl cyclopropane and Selectfluor under 300 nm hv).

**Procedure for Rate Studies with Phenylcyclopropane (Metal Initiation).** Selectfluor (195 mg, 0.55 mmol), cuprous iodide (10 mg, 0.05 mmol), *N,N'*-bis(2,6-dichloro-benzylidene)ethane-1,2-diamine (19 mg, 0.05 mmol), and potassium carbonate (7 mg, 0.05 mmol) were added to a flame-dried 10 mL round bottom flask equipped with a stir bar under  $N_2$ . A degassed (with  $N_2$ ) mixture of 4:1  $CH_3CN:CD_3CN$  (6 mL) was added to the reaction flask, and the solution was stirred vigorously at room temperature. After 10 min., 3-chlorobenzotrifluoride (0.02 mL, 0.15 mmol) was added via syringe. After 15 min., phenylcyclopropane (0.06 mL, 0.50 mmol) was added to the reaction flask. The reaction solution stirred for an additional 2 min., then 0.5 mL was transferred via syringe from the reaction flask to an NMR tube fit with a septum under  $N_2$ . A  $^{19}F$  NMR spectrum of the same sample was collected every 300 seconds at room temperature. Product concentrations were determined using 3-chlorobenzotrifluoride as an internal standard. Initial rates were measured after the appearance of product by  $^{19}F$  NMR; the induction periods were not considered due to variability.

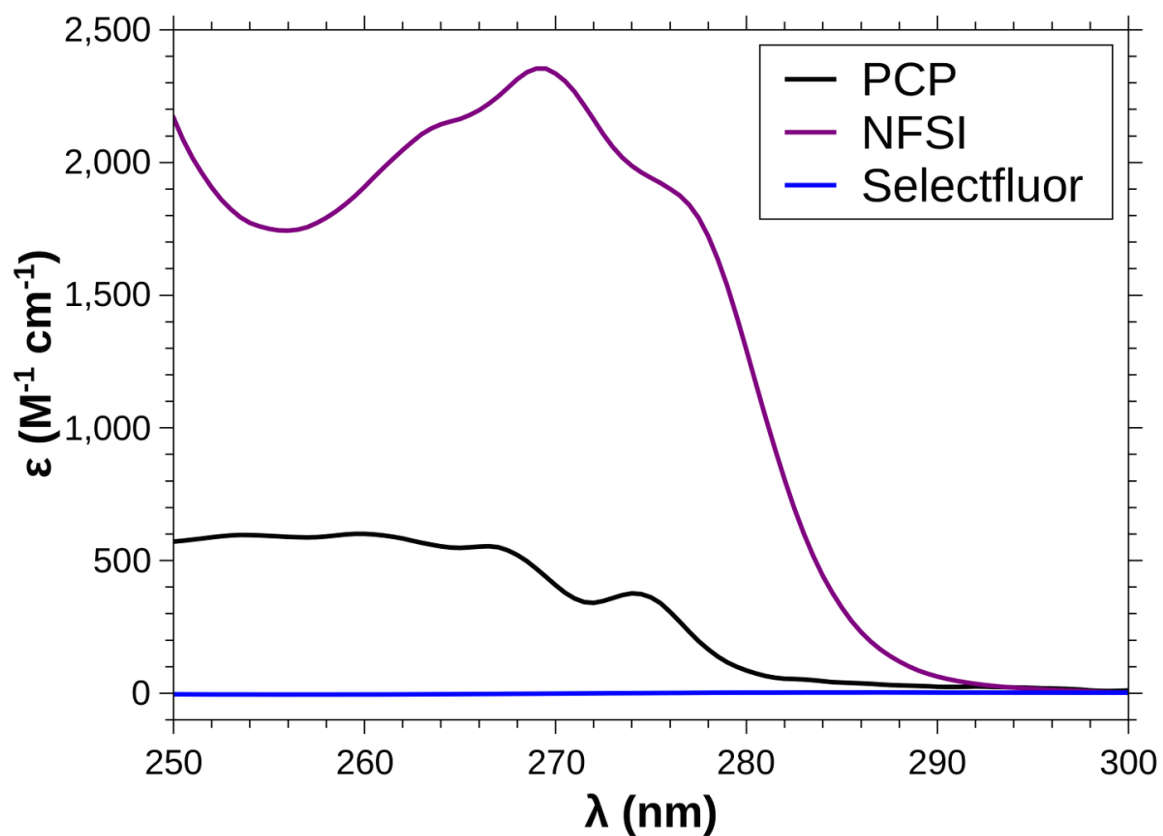
**Table 12.4** Compiled initial rate data (metal initiation procedure).

Rate (int./min.)	[Phenylcyclopropane] (M)	[Selectfluor] (M)
4.90E-03	0.083	0.092
6.00E-03	0.108	0.092

Rate (int./min.)	[Phenylcyclopropane] (M)	[Selectfluor] (M)
4.90E-03	0.083	0.092
5.70E-03	0.083	0.117

\*Reported rates are the average of two runs.



**Figure 12.18** UV-vis spectra of phenylcyclopropane, NFSI, and Selectfluor (in MeCN).

**Raw Hammett Data from Competition Experiments (Determined by  $^{19}\text{F}$  NMR).****Table 12.5** Intermolecular Competition with Selectfluor (para substituent effects);  $\rho = -3.2$ ,  $R^2 = 0.97$ .

Substituent	[PX]/[PH]	$\log([PX]/[PH])$	Hammett $\sigma$
p-tBu	7.1	0.8513	-0.20
p-Me	10.1	1.0043	-0.17
p-H	1.00	0.0000	0.00
p-F	1.06	0.0253	0.06
p-Cl	0.44	-0.3565	0.23
p-Br	0.32	-0.4949	0.23
p-COMe	0.05	-1.3010	0.50

**Table 12.6** Intermolecular Competition with Selectfluor (meta substituent effects);  $\rho = -4.2$ ,  $R^2 = 0.99$ .

Substituent	[PX]/[PH]	$\log([PX]/[PH])$	Hammett $\sigma$
m-tBu	3.37	0.5276	-0.10
m-Me	3.09	0.4900	-0.07
m-H	1.00	0.0000	0.00
m-F	0.05	-1.3010	0.34

**Table 12.7** Intermolecular Competition with NFSI (para substituent effects);  $\rho = -3.6$ ,  $R^2 = 0.94$ .

Substituent	[PX]/[PH]	$\log([PX]/[PH])$	Hammett $\sigma$
p-tBu	11.7	1.0682	-0.20
p-Me	12.6	1.1004	-0.17
p-H	1.00	0.0000	0.00
p-F	1.13	0.0531	0.06
p-Cl	0.38	-0.4202	0.23
p-Br	0.34	-0.4685	0.23

**Table 12.8** Intermolecular Competition with NFSI (meta substituent effects);  $\rho = -4.6$ ,  $R^2 = 0.99$ .

Substituent	[PX]/[PH]	log([PX]/[PH])	Hammett $\sigma$
m-tBu	5.04	0.7024	-0.10
m-Me	3.11	0.4928	-0.07
m-H	1.00	0.0000	0.00
m-F	0.04	-1.3979	0.34

**Table 12.9** Intermolecular Competition with Triethylborane (para substituent effects);  $\rho = -3.2$ ,  $R^2 = 0.97$ .

Substituent	[PX]/[PH]	log([PX]/[PH])	Hammett $\sigma$
p-tBu	6.8	0.8325	-0.20
p-Me	9.1	0.9590	-0.17
p-H	1.00	0.0000	0.00
p-F	0.98	-0.0088	0.06
p-Cl	0.45	-0.3468	0.23
p-Br	0.33	-0.4815	0.23
p-COMe	0.04	-1.3979	0.50

**Table 12.10** Intermolecular Competition with Copper (para substituent effects);  $\rho = -2.9$ ,  $R^2 = 0.92$ .

Substituent	[PX]/[PH]	log([PX]/[PH])	Hammett $\sigma$
p-tBu	7.5	0.8751	-0.20
p-Me	9.8	0.9912	-0.17
p-H	1.00	0.0000	0.00
p-F	1.5	0.1761	0.06
p-Cl	0.53	-0.2757	0.23
p-Br	0.47	-0.3279	0.23

**Table 12.11** Intramolecular Competition with Selectfluor (para substituent effects); poor correlation.

<b>Substituent</b>	<b>[PX]/[PH]</b>	<b>log([PX]/[PH])</b>	<b>Hammett <math>\sigma</math></b>
p-tBu	1.13	0.0531	-0.20
p-F	1.06	0.0253	0.06
p-H	1.00	0.0000	0.00
p-Cl	0.95	-0.0223	0.23
p-Br	1.07	0.0294	0.23

**Table 12.12** Intramolecular Competition with NFSI (para substituent effects); poor correlation.

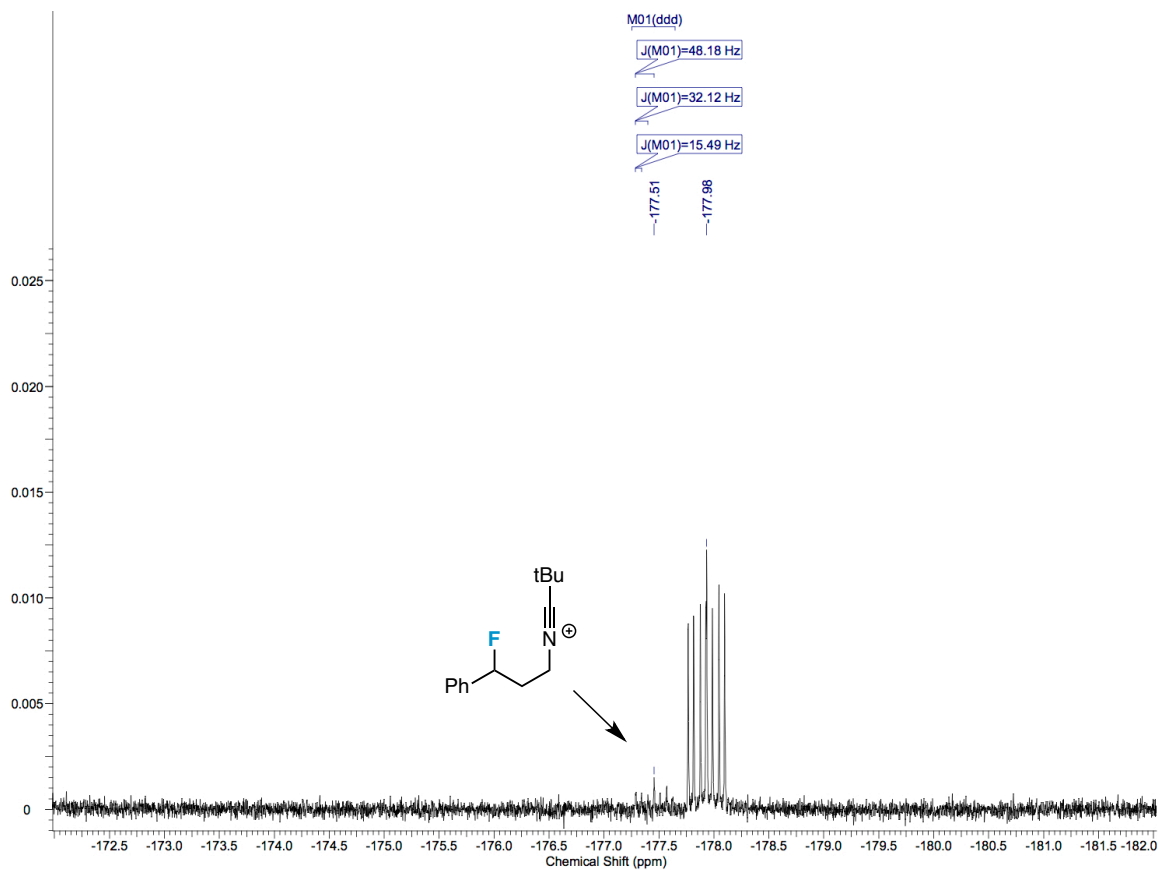
<b>Substituent</b>	<b>[PX]/[PH]</b>	<b>log([PX]/[PH])</b>	<b>Hammett <math>\sigma</math></b>
p-tBu	0.75	-0.1249	-0.20
p-Me	0.72	-0.1427	-0.17
p-F	0.72	-0.1427	0.06
p-H	1.00	0.0000	0.00
p-Cl	0.98	-0.0088	0.23
p-Br	1.00	0.0000	0.23

*Intramolecular Competition with Triethylborane (para substituent effects); poor correlation*

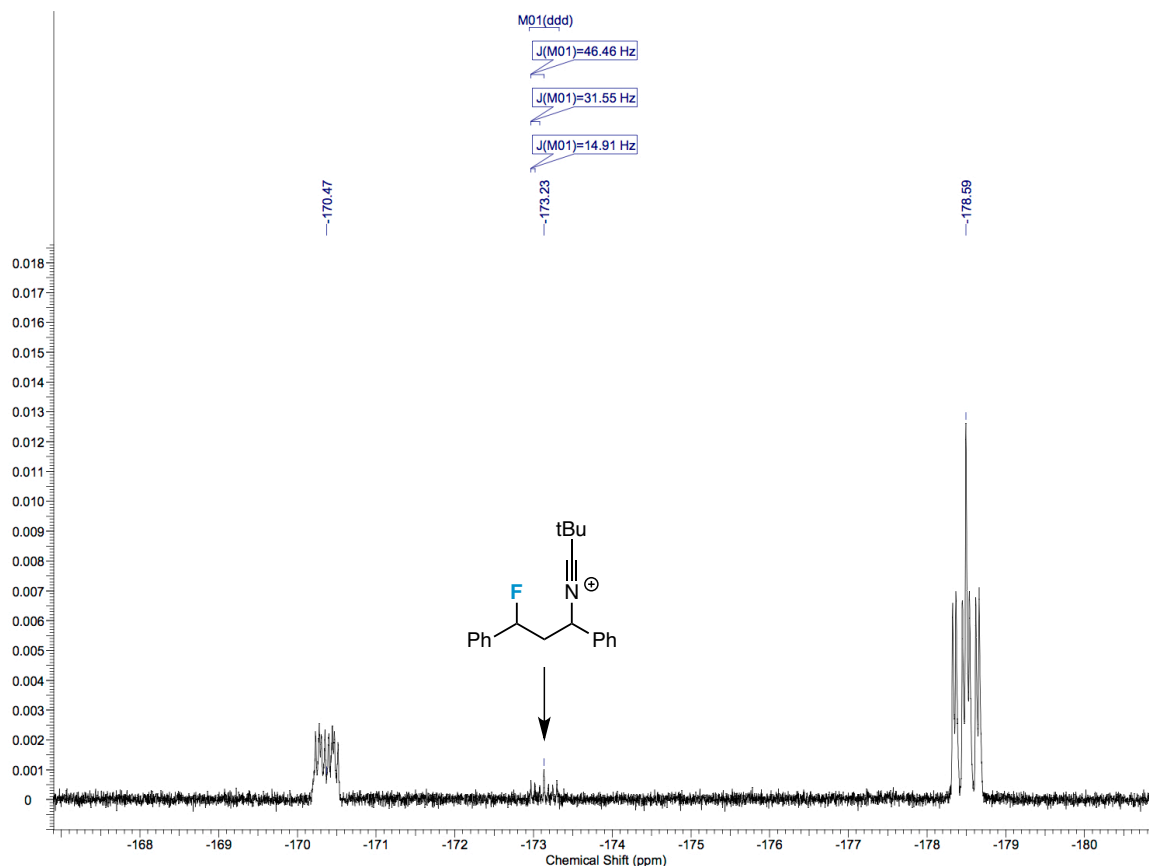
<b>Substituent</b>	<b>[PX]/[PH]</b>	<b>log([PX]/[PH])</b>	<b>Hammett s</b>
p-tBu	1.15	0.0607	-0.20
p-Me	0.89	-0.0506	-0.17
p-F	1.04	0.0170	0.06
p-H	1.00	0.0000	0.00
p-Cl	0.85	-0.0706	0.23
p-Br	1.20	0.0792	0.23

*Intramolecular Competition with Copper (para substituent effects); poor correlation*

<b>Substituent</b>	<b>[PX]/[PH]</b>	<b>log([PX]/[PH])</b>	<b>Hammett s</b>
p-tBu	1.60	0.2041	-0.20
p-Me	1.06	0.0253	-0.17
p-H	1.00	0.0000	0.00
p-Cl	0.79	-0.1024	0.23
p-Br	1.50	0.1761	0.23



**Figure 12.19**  $^{19}\text{F}$  NMR spectrum of reaction with 1:1 acetonitrile:pivalonitrile; putative pivalonitrile-trapped product from phenylcyclopropane observed.

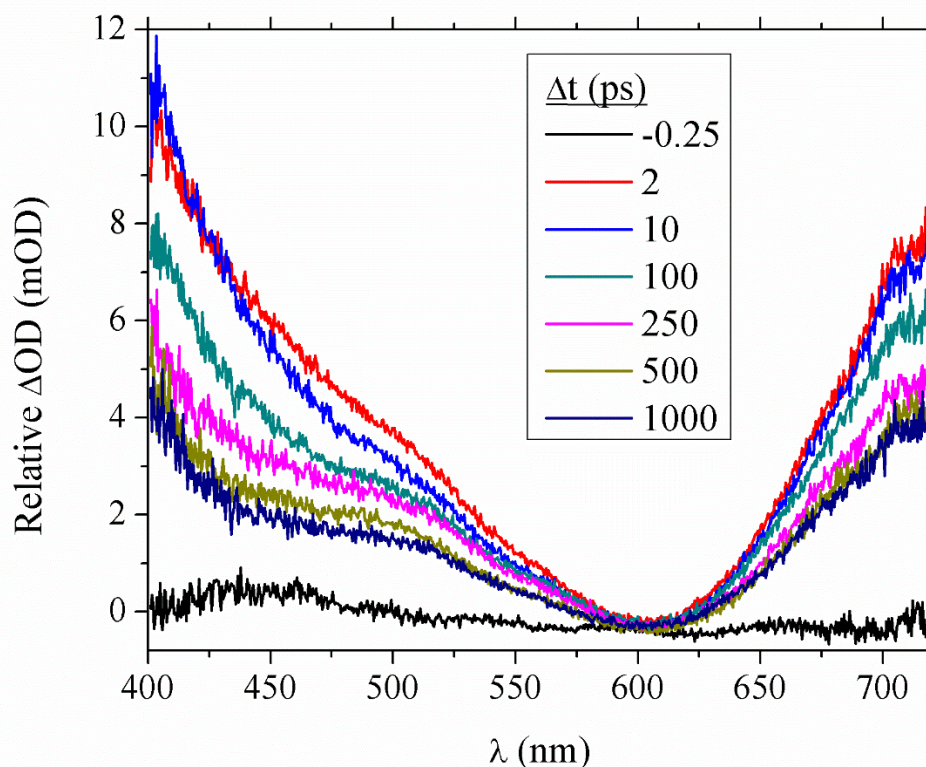


**Figure 12.20**  $^{19}\text{F}$  NMR spectrum of reaction with 1:1 acetonitrile:pivalonitrile; putative pivalonitrile-trapped product from 1,2-diphenylcyclopropane observed.

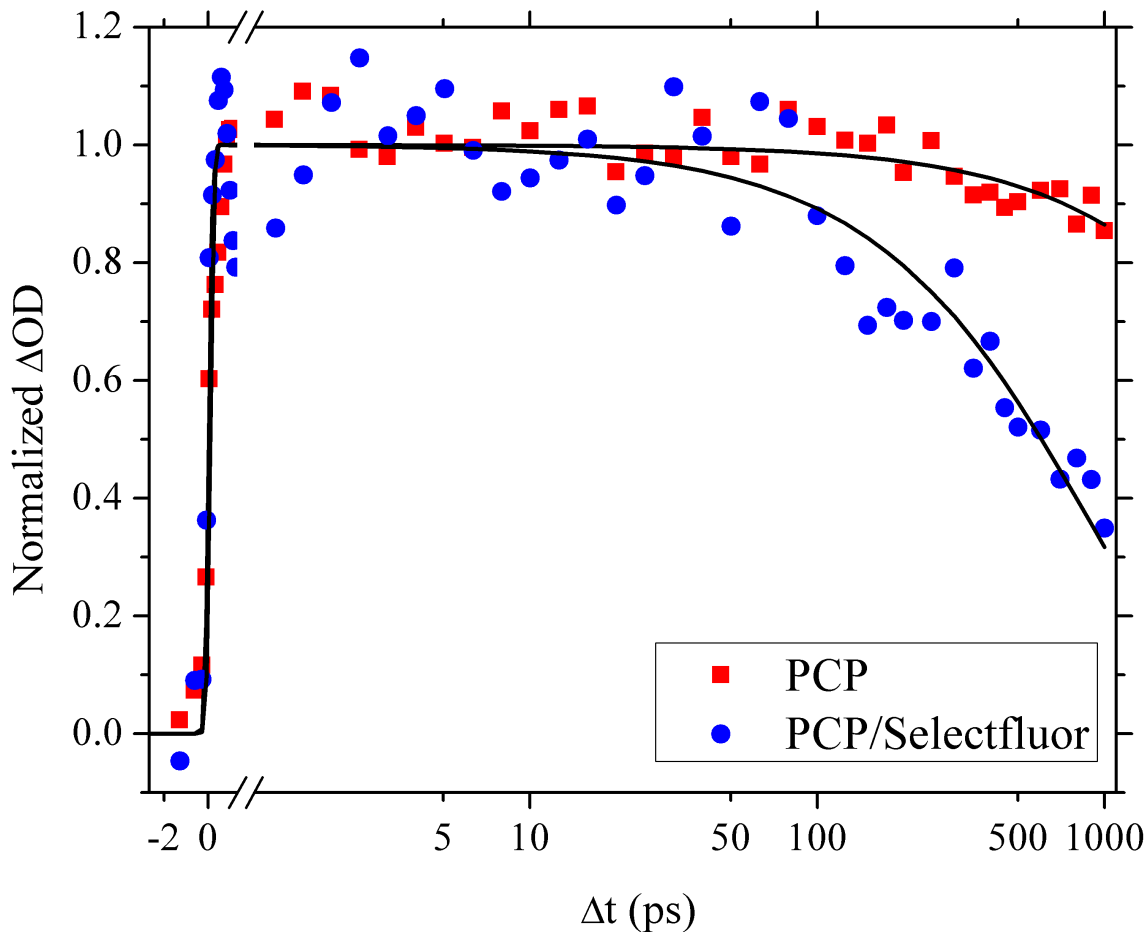
**Transient Absorption Spectroscopy.** Mixtures of 5 mM phenylcyclopropane (PCP)/50 mM Selectfluor and 20 mM PCP/20mM 3,3',4,4'-benzophenonetetracarboxylic dianhydride (BTDA) were prepared with purified acetonitrile (Solvent-Purification System PureSolv MD 5)) and degassed with nitrogen. Samples were stirred continuously in 1 cm cuvettes for optical measurements. Measurements were also performed with mixtures of PCP/NFSI (5 mM/10 mM and 5 mM/50 mM in acetonitrile); these did not result in an observable absorption of the radical cation (PCP $^+$ ), most likely due to the strong absorption of NFSI at 266 nm that results predominately in direct excitation of NFSI rather than PCP. Additional control experiments were undertaken for 5 mM solutions of PCP (only) in acetonitrile to interrogate the excited-state kinetics of PCP.



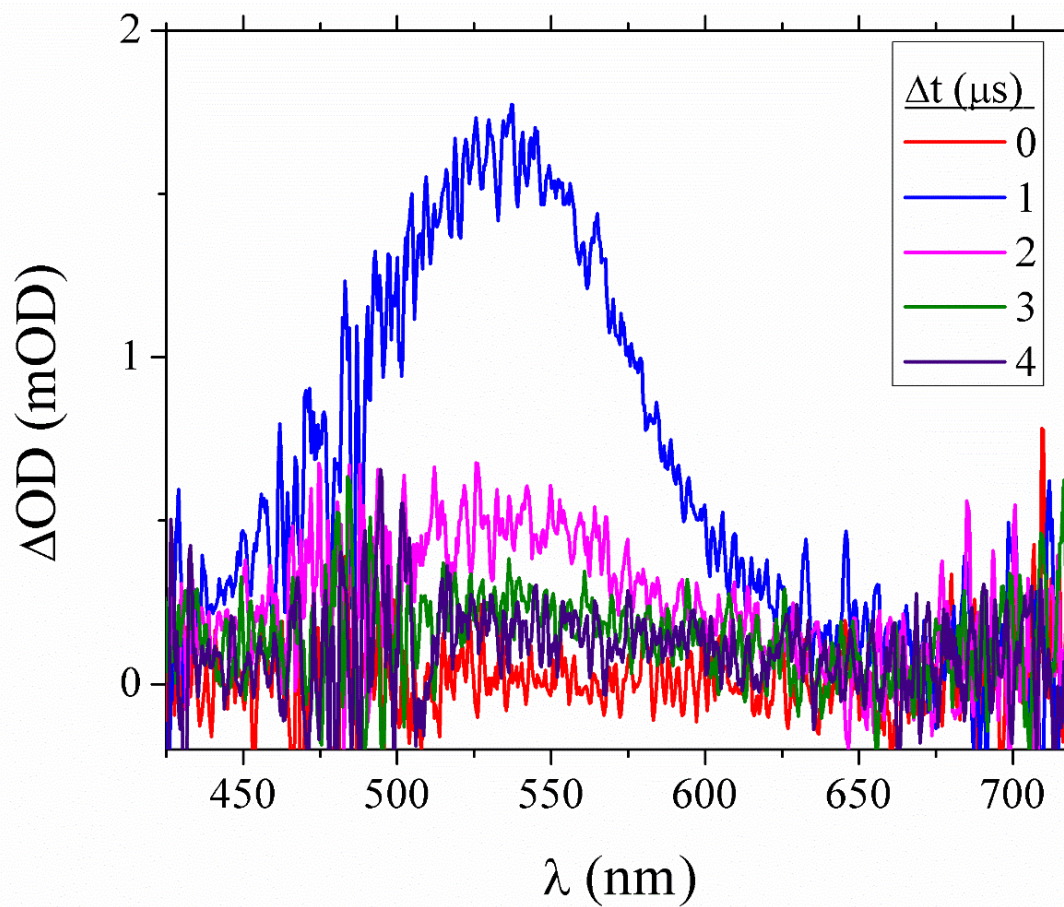
Our transient-absorption set-up has been described in detail elsewhere.<sup>56</sup> Briefly, an amplified Ti:Sapphire laser (Coherent Legend Elite, 800 nm, 35 fs FWHM, 1 kHz, 4.0 W) was frequency tripled to produce excitation pulses at 266 nm (10 mW). The excitation beam was focused at the sample to a 1 mm spot size. Three optical probe sources were used to interrogate kinetics on various timescales (fs, ns,  $\mu$ s): Femtosecond probe pulses were produced by using 800 nm to drive white-light generation in a 2 mm CaF<sub>2</sub> plate (United Crystals); nanosecond pulses were generated with a pulsed 520 or 639 nm laser diode (Osram PL520, Opnext HL6358MG,  $\sim$ 2 ns FWHM) driven by a diode pulser (Highland Technologies T165); and microsecond pulses were generated with a white-light LED (Thorlabs LEDWE-15) driven by an electronic delay generator (Berkeley Nucleonics BNC 555, 500 ns FWHM). Femtosecond probe pulses were delayed by up to 50 ns by passing the probe continuum through  $\sim$  5 meters of fiber optic cable.



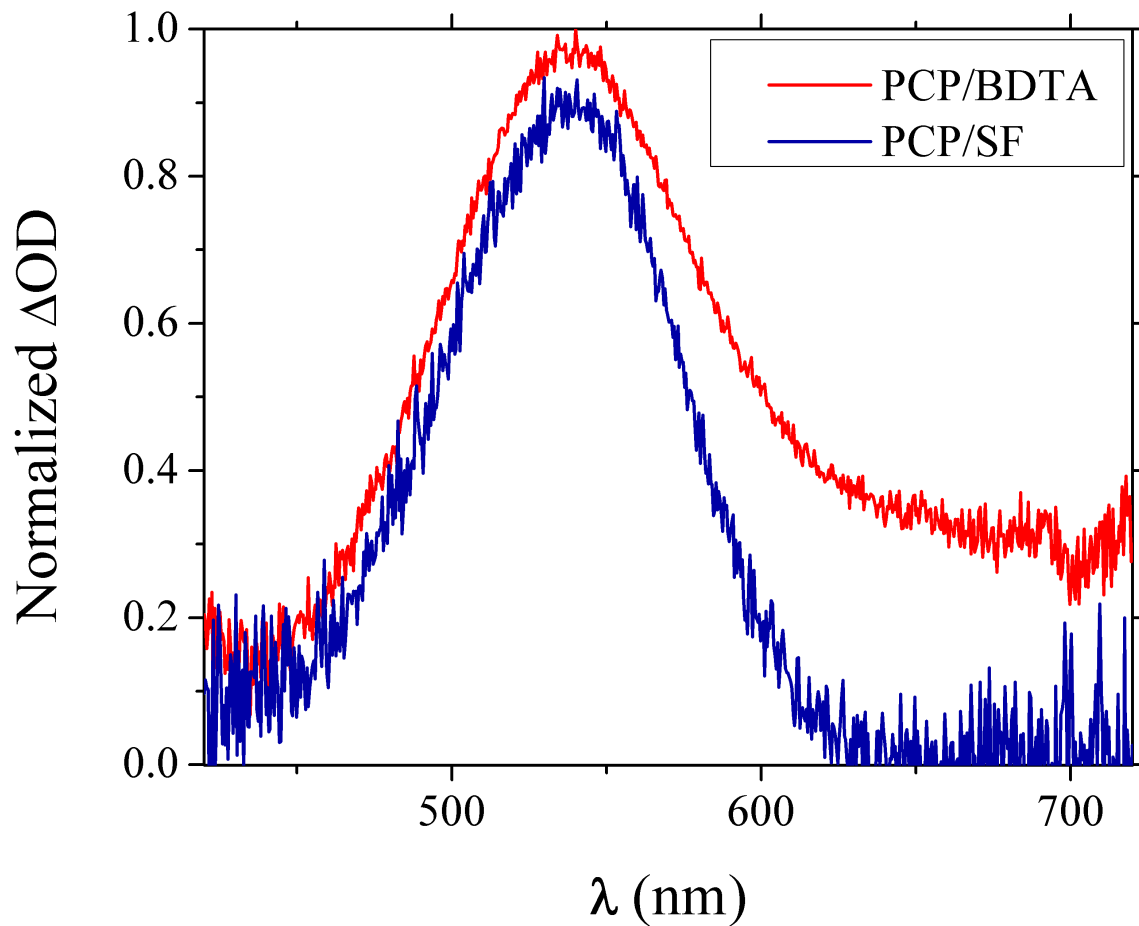
**Figure 12.21** fs-TAS of PCP in acetonitrile following 266 nm photoexcitation to illustrate the evolution of S<sub>1</sub> PCP (no quencher). Spectra have been referenced to  $\Delta$ OD of 0 at 600 nm to highlight evolution in spectral shape.



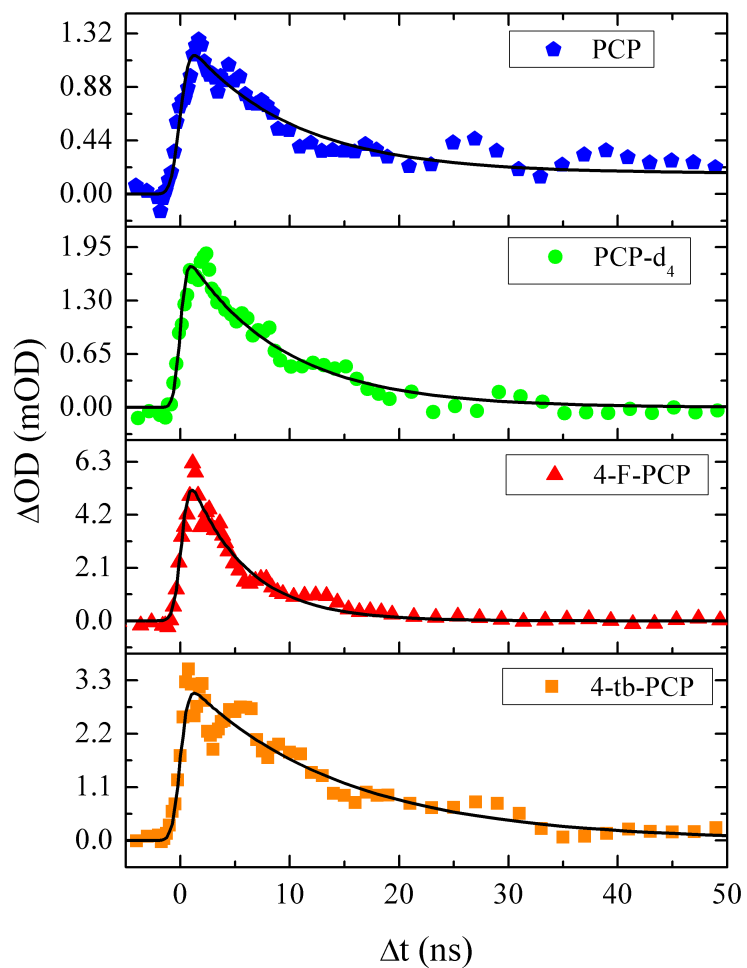
**Figure 12.22** Comparison of  $S_1$  lifetime of PCP at 700 nm in the absence and presence of Selectfluor following 266 nm excitation. The trace of PCP (no quencher) was fit with a convoluted exponential decay with a constant offset ( $\tau=318.7$  ps, offset=0.8). The trace of the PCP/Selectfluor mixture was fit with a convoluted exponential decay ( $\tau=869.2$  ps) that is in close agreement with the predicted  $S_1$  lifetime ( $\sim 0.8$  ns) in the presence of 50 mM Selectfluor by the Stern-Volmer analysis.



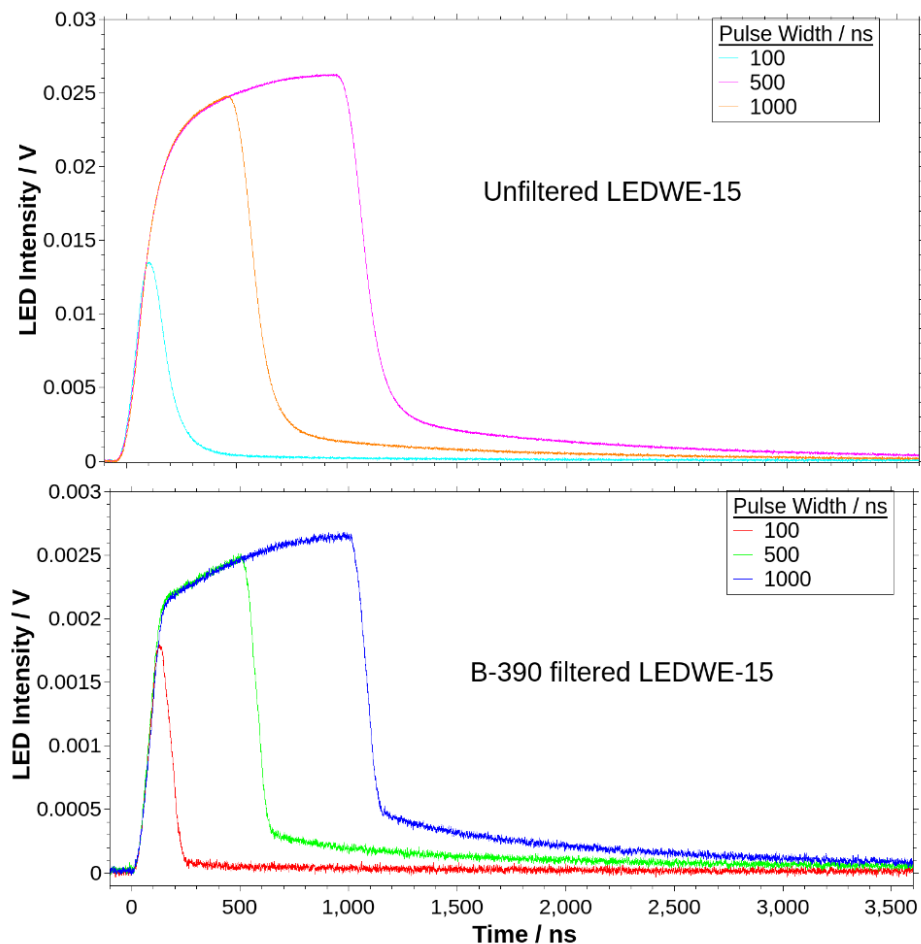
**Figure 12.23**  $\mu$ s-TAS of PCP/Selectfluor in MeCN following photoexcitation with 266 nm.



**Figure 12.24** Comparison of the  $\text{PCP}^+$  absorption spectrum as probed  $\Delta t=50$  ns following 266 nm photoexcitation of PCP/Selectfluor and 350 nm photoexcitation of PCP/BDTA; the latter has been translated vertically for clarity. An absorption maximum at 540 nm is observed under both conditions; underlying absorption for the PCP/BDTA mixture is due to the generation of  $\text{BDTA}^-$  which absorbs at 710 nm.<sup>57</sup>



**Figure 12.25** ns-TAS (probed at 639 nm) of PCP and derivatives (no added quencher) following photoexcitation with 266 nm. PCP and analogs were fit with a convoluted exponential decay, with PCP requiring an additional constant offset parameter of 0.17 mOD; decay lifetimes are given in the main text.

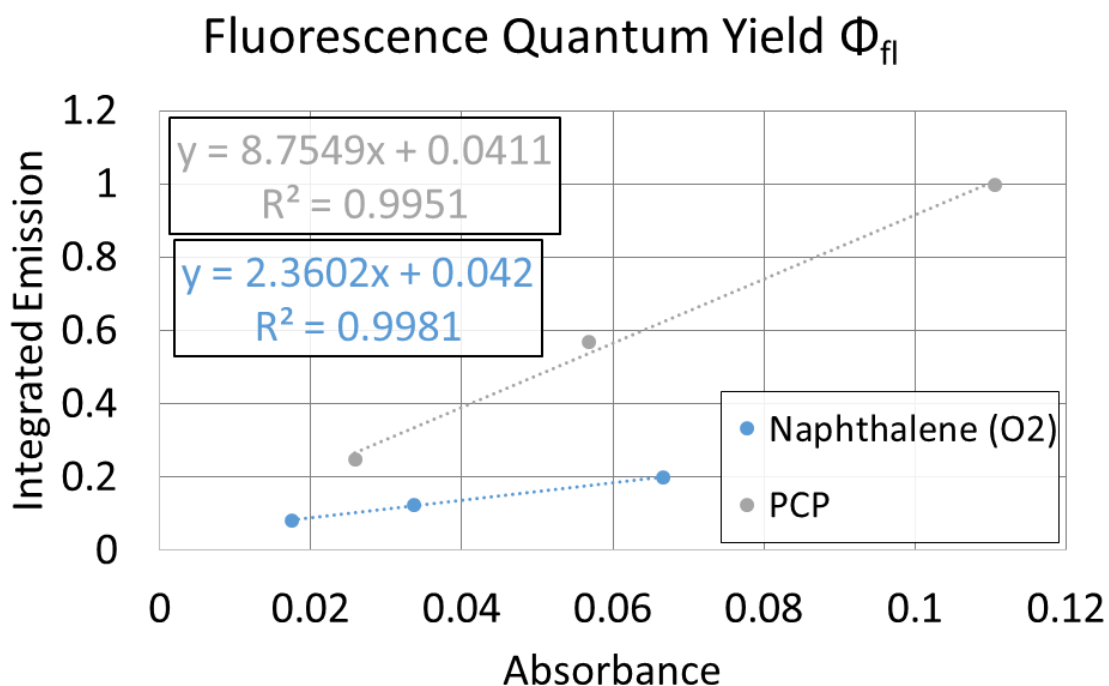


**Figure 12.26** Temporal profile of the  $\mu$ s-TA LED probe light source. The time-resolution of the LED is determined by the electronic response of the LED and the adjustable pulse-width of the delay/signal generator. Three representative pulse widths are shown above under filtered and unfiltered conditions. Comparisons of the filtered and unfiltered temporal profiles are shown to illustrate the slightly different responses of the primary (450 nm) emission and the secondary emission (450-750 nm) generated by a proprietary phosphor blend.

**Fluorescence Quantum Yield & Stern-Volmer Analysis.** Stern-Volmer analysis and fluorescence quantum yields were determined using a steady-state UV-vis (Stellarnet Black Comet) and fluorimeter (Perkin Elmer LS-5b); dispersed fluorescence was collected for excitation at 270 nm. Stock solutions of phenylcyclopropane and its analogs were prepared for both measurements. For Stern-Volmer experiments various quantities of Selectfluor were added to aliquots of stock solutions to maintain a constant optical

density of ~0.1 at 270 nm; all samples were degassed with nitrogen for 15 min. For fluorescence quantum yield measurements solutions were diluted to various concentrations; optical densities were measured by UV-vis. For both measurements, fluorescence spectra were integrated for analysis by linear least-squares regression. Stern-Volmer measurements were analyzed using Eq. 1 in Chapter 8; the fluorescence quantum yield of phenylcyclopropane was determined to be 0.12 using Eq. 1 *vide infra* where  $\Delta I/\Delta Abs \equiv$  slope of integrated emission as a function of absorbance and  $n \equiv$  refractive index of solvent.<sup>58</sup>

$$\Phi_{fl} = \frac{\frac{\Delta I}{\Delta Abs}}{\frac{\Delta I_{Ref}}{\Delta Abs_{Ref}}} \frac{n}{n_{Ref}} \Phi_{fl Ref} \quad (1)$$



**Figure 12.27** Fluorescence quantum yield ( $\Phi_{fl}$ ) of PCP determined using aerated naphthalene as a reference.<sup>59</sup>

## 12.9 Experimental Details for Chapter 9.

**General Peptide Synthesis Procedures.** Peptides were synthesized using a standard DCC coupling procedure;<sup>60</sup> syntheses of *N*-protected amino acids with phthalimide<sup>61</sup> or trifluoroacetate<sup>62</sup> substituents were also according to literature procedure.

*DCC Coupling:* The *N*-protected amino acid (12.0 mmol, 1.0 equiv) and HOBT (12.0 mmol, 1.0 equiv), were dissolved in EtOAc (90 mL) in a round bottom flask equipped with a stir bar. The reaction mixture was cooled to 0 °C. DCC (13.2 mmol, 1.1 equiv) was added, and the reaction mixture was stirred for 30 min at 0 °C. The reaction mixture was then warmed to room temperature, and the *C*-protected amino acid hydrochloride (12.0 mmol, 1.0 equiv) and triethylamine (12.0 mmol, 1.0 equiv) were added. The reaction mixture was stirred for an additional 2 h. Hexanes (25 mL) were added, and the reaction mixture was stored in a freezer overnight. It was then filtered through Celite to remove insoluble byproducts. The filtrate was transferred to separatory funnel, washed with 0.5 M HCl, saturated NaHCO<sub>3</sub>, and then brine. The combined organic layers were dried with MgSO<sub>4</sub>, filtered through Celite, and concentrated. Products were purified via recrystallization using Et<sub>2</sub>O/EtOAc.

*N-Protection with Phthalimide:* Amino acid (13.5 mmol, 1.0 equiv), phthalic anhydride (13.5 mmol, 1.0 equiv), and triethylamine (1.35 mmol, 0.1 equiv) were dissolved in toluene (70 mL) in an oven dried round bottom flask equipped with a stir bar and a Dean-Stark apparatus. The reaction mixture was heated to reflux for 4 h. Upon cooling, the reaction mixture was concentrated. The residue was dissolved in EtOAc, transferred to a separatory funnel, and washed with 1 M HCl. The organic layer was dried with MgSO<sub>4</sub>, filtered through Celite, and concentrated. The products were purified via column chromatography on silica gel eluting with hexanes/EtOAc.

*N-Protection with Trifluoroacetate:* Amino acid (22.0 mmol, 1.0 equiv) and triethylamine (22.0 mmol, 1.0 equiv) were dissolved in MeOH (12 mL) in an oven dried round bottom flask equipped with a stir bar. After 5 min, ethyl trifluoroacetate (28.0 mmol, 1.3 equiv) was added, and the reaction mixture was stirred for 24 h. Then, the reaction mixture was concentrated, dissolved in H<sub>2</sub>O (35 mL), acidified with conc. HCl



(4.0 mL), and stirred for 15-20 min. Subsequently, the reaction mixture was extracted with EtOAc. The combined organic layers were washed with brine, dried with MgSO<sub>4</sub>, filtered through Celite, and concentrated. The concentrate was held under reduced pressure until solid was obtained. The product was used without further purification.

*Hydroxyl Protection of Tyrosine with Trifluoroacetate:* Methyl (2,2,2-trifluoroacetyl)-L-tyrosinate (0.5 g, 1.72 mmol, 1.0 equiv) and NaHCO<sub>3</sub> (0.3 g, 3.42 mmol, 2.0 equiv) were dissolved in MeCN (10 mL) in an oven dried round bottom flask equipped with a stir bar. Trifluoroacetic anhydride (1.2 mL, 8.6 mmol, 5.0 equiv) was added; the reaction mixture was stirred at room temperature for 24 h and then concentrated. The crude residue was dissolved in DCM, transferred to a separatory funnel, washed with H<sub>2</sub>O, dried with MgSO<sub>4</sub>, filtered through Celite, and concentrated. The product was used without further purification.

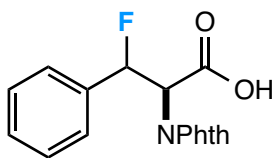
**General Fluorination Procedure.** The amino acid or peptide substrate (0.25 mmol), Selectfluor (177 mg, 0.5 mmol), dibenzosuberone (3.0 mg, 0.01 mmol), and anhydrous MeCN (3 mL) were added to an oven-dried microwave vial equipped with a stir bar under ambient air; the vial was then sealed with a septum to prevent solvent evaporation. The reaction mixture was stirred and irradiated with visible light (14-Watt CFL) for 16 h. At this time, a 0.3 mL aliquot was taken for <sup>19</sup>F NMR analysis, while the remainder of the reaction mixture was diluted with Et<sub>2</sub>O, filtered through Celite, and concentrated. The major diastereomer was isolated for compounds **2**, **4**, **7**, **8**, and **9**; all other products were isolated as a mixture of diastereomers. With the exception of **3** and **5**, all other products were purified via column chromatography on silica gel eluting with hexanes/EtOAc. Compounds **3** and **5** were purified as individual diastereomers or as mixtures via column chromatography on C18 eluting with MeCN/H<sub>2</sub>O. Compounds **4** and **9** were also purified via trituration with CHCl<sub>3</sub>.

**Gram-scale Synthesis Example.** NPhth-Gly-Phe-OEt (1.0 g, 2.63 mmol), Selectfluor (1.86 g, 5.26 mmol), dibenzosuberone (0.027 g, 0.13 mmol), and anhydrous MeCN (30 mL) were added to a round bottom flask equipped with a stir bar under ambient air. The flask was sealed with a septum to prevent solvent evaporation. The reaction mixture was stirred and irradiated with visible light (14-Watt CFL) for

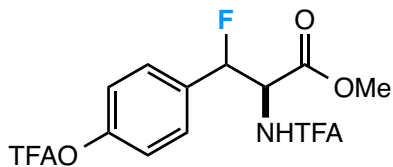
16 h. At this time, a 0.3 mL aliquot was taken for  $^{19}\text{F}$  NMR analysis, while the remainder of the reaction mixture was diluted with  $\text{Et}_2\text{O}$ , filtered through Celite, and concentrated. The crude residue was triturated with chloroform, and the major diastereomer (**9**) was obtained in 0.44 g (42% yield).

**Intermolecular Competition Experiment Procedure.** NPhth-Val-OH (0.21 g, 0.84 mmol), NPhth-Phe-OH (0.25 g, 0.84 mmol), Selectfluor (0.12 g, 0.34 mmol), dibenzosuberone (0.017 g, 0.009 mmol), and anhydrous MeCN (3.0 mL) were added to a round bottom flask equipped with a stir bar under ambient air. The flask was sealed with a septum to prevent solvent evaporation. The reaction mixture was stirred and irradiated with visible light (14-Watt CFL) for 16 h. At this time, a 0.3 mL aliquot was taken for  $^{19}\text{F}$  NMR analysis.

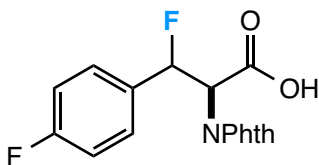
#### Characterization Data.



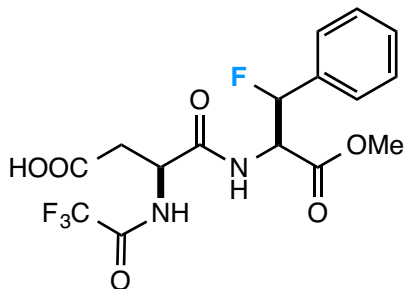
(2*R*)-2-(1,3-dioxoisindolin-2-yl)-3-fluoro-3-phenylpropanoic acid (**3**). Isolated as a mixture of diastereomers; 80% yield. Yellow oil.  $^1\text{H}$  NMR (400 MHz,  $\text{CD}_3\text{CN}$ ):  $\delta$  7.85-7.79 (2H, m), 7.74-7.69 (2H, m), 7.44-7.39 (1H, m), 7.37-7.30 (2H, m), 7.28-7.20 (2H, m), 6.36-6.20 (1H, m), 5.33-5.21 (1H, m);  $^{13}\text{C}$  NMR (400 MHz,  $\text{CD}_3\text{CN}$ ):  $\delta$  168.7, 168.0, 167.5, 137.8, 137.6, 137.0, 136.7, 136.5, 135.8, 135.7, 132.2, 131.9, 130.4, 130.38, 129.97, 129.95, 129.4, 129.3, 127.9, 127.8, 127.5, 127.4, 124.4, 124.3, 91.8 (d,  $J = 175.1$  Hz), 91.3 (d,  $J = 178.8$  Hz), 56.4 (d,  $J = 23.2$  Hz), 55.1 (d,  $J = 35.8$  Hz);  $^{19}\text{F}$  NMR (300 MHz,  $\text{CD}_3\text{CN}$ ):  $\delta$  -170.4 (1F, dd,  $J = 46.5, 15.5$  Hz), -180.6 (1F, dd,  $J = 45.9, 19.5$  Hz).



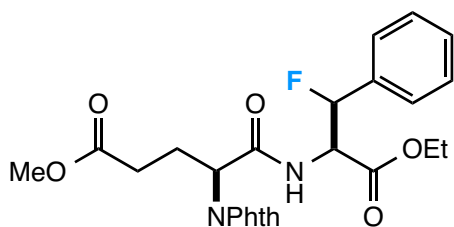
Methyl (2*R*)-3-fluoro-2-(2,2,2-trifluoroacetamido)-3-(4-(2,2,2-trifluoroacetoxy)phenyl)propanoate (**4**). Isolated major diastereomer; 41% yield (both diastereomers in 71% yield by  $^{19}\text{F}$  NMR). Pale yellow solid; m.p. 140-143 °C.  $^1\text{H}$  NMR (400 MHz,  $\text{CD}_3\text{CN}$ ):  $\delta$  8.12 (1H, d,  $J = 9.3$  Hz), 7.54-7.50 (2H, m), 7.36-7.32 (2H, m), 6.24 (1H, dd,  $J = 44.6, 3.2$  Hz), 5.11 (1H, ddd,  $J = 30.4$  Hz, 9.3, 3.0 Hz), 3.79 (3H, s);  $^{13}\text{C}$  NMR (400 MHz,  $\text{CD}_3\text{CN}$ ): 170.1, 167.38, 167.35, 157.1, 156.8, 155.8, 155.4, 149.6, 136.0, 134.8, 134.6, 130.8, 127.5, 127.4, 120.9, 91.5 (d,  $J = 178.4$  Hz), 56.8 (d,  $J = 22.1$  Hz), 52.8;  $^{19}\text{F}$  NMR (300 MHz,  $\text{CD}_3\text{CN}$ ):  $\delta$  -75.1 (3F, s), -75.6 (3F, s), -190.5 (1F, dd,  $J = 44.7, 31.0$  Hz).



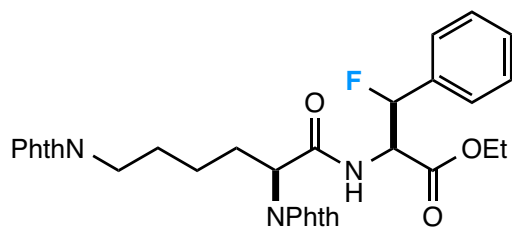
(2*R*)-2-(1,3-dioxoisindolin-2-yl)-3-fluoro-3-(4-fluorophenyl)propanoic acid (**5**). Isolated as a mixture of diastereomers; 84% yield. Yellow oil.  $^1\text{H}$  NMR (400 MHz,  $\text{CDCl}_3$ ):  $\delta$  8.90 (1H, s), 7.83-7.77 (1H, m), 7.72-7.60 (3H, m), 7.42-7.24 (2H, m), 7.01-6.94 (1H, m), 6.91-6.82 (1H, m), 6.35-6.15 (1H, m), 5.29-5.18 (1H, m); 171.1, 170.0, 167.2, 166.7, 164.27, 164.25, 164.1, 161.8, 161.78, 161.7, 134.37, 134.35, 131.3, 130.9, 128.9, 128.86, 128.83, 128.8, 128.7, 128.63, 128.55, 127.2, 123.7, 123.6, 115.5, 115.3, 90.1 (d,  $J = 177.3$  Hz), 89.3 (d,  $J = 179.1$  Hz), 55.9, 55.7, 54.6, 54.2;  $^{19}\text{F}$  NMR (300 MHz,  $\text{CDCl}_3$ ):  $\delta$  -110.7 (3F, m), -111.5 (3F, m), -168.1 (1F, dd,  $J = 46.5, 14.3$  Hz), -177.7 (1F, dd,  $J = 47.0, 14.9$  Hz).



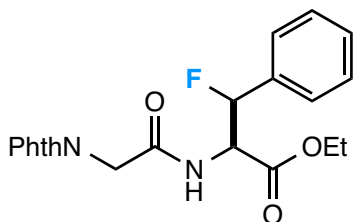
(*S*)-4-(((2*R*)-1-fluoro-3-methoxy-3-oxo-1-phenylpropan-2-yl)amino)-4-oxo-3-(2,2,2-trifluoroacetamido)butanoic acid (**6**). Isolated as a mixture of diastereomers; 78% yield. Colorless oil.  $^1\text{H}$  NMR (400 MHz,  $\text{CD}_3\text{CN}$ ):  $\delta$  7.91-7.80 (1H, m), 7.42-7.32 (5H, m), 7.18-7.11 (1H, m), 6.13-5.79 (1H, m), 5.04-4.91 (1H, m), 4.75-4.65 (1H, m), 3.74-3.66 (3H, s), 2.83-2.77 (1H, m), 2.72-2.65 (1H, m);  $^{13}\text{C}$  NMR (400 MHz,  $\text{CD}_3\text{CN}$ ):  $\delta$  172.1, 172.0, 170.0, 169.9, 169.83, 169.76, 169.5, 169.4, 158.0, 157.9, 157.6, 157.5, 136.8, 136.6, 136.5, 136.3, 130.09, 130.08, 129.78, 129.77, 129.5, 129.4, 127.0, 126.9, 126.63, 126.56, 93.5 (d,  $J = 176.9$  Hz), 93.3 (d,  $J = 178.4$  Hz), 57.8 (d,  $J = 23.6$  Hz), 53.5 (d,  $J = 35.8$  Hz), 50.9, 50.8, 35.53, 35.45;  $^{19}\text{F}$  NMR (300 MHz,  $\text{CD}_3\text{CN}$ ):  $\delta$  -175.9 (3F, s), -185.0 (1F, dd,  $J = 45.3, 16.1$ ), -190.4 (1F, dd,  $J = 45.3, 29.8$  Hz).



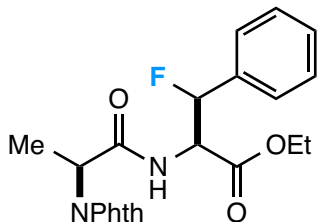
Methyl (*S*)-4-(1,3-dioxoisindolin-2-yl)-5-(((2*R*)-1-ethoxy-3-fluoro-1-oxo-3-phenylpropan-2-yl)amino)-5-oxopentanoate (**7**). Isolated as a mixture of diastereomers; 71% yield. Colorless oil.  $^1\text{H}$  NMR (400 MHz,  $\text{CDCl}_3$ ):  $\delta$  7.84-7.82 (2H, m), 7.75-7.30 (2H, m), 7.28-7.16 (5H, m), 7.08-7.06 (1H, m), 6.04 (1H, dd,  $J = 45.3, 2.5$  Hz), 5.07 (1H, ddd,  $J = 31.1, 9.2, 2.6$  Hz), 4.77 (1H, t,  $J = 7.8$  Hz), 4.22 (2H, q,  $J = 7.1$  Hz), 3.60 (3H, s), 2.45-2.40 (2H, m), 2.31-2.14 (2H, m), 1.24 (3H, s);  $^{13}\text{C}$  NMR (400 MHz,  $\text{CDCl}_3$ ):  $\delta$  172.6, 168.4, 168.3, 168.2, 167.7, 135.3, 135.1, 134.4, 134.3, 131.4, 129.2, 128.53, 128.52, 124.93, 124.85, 123.6, 92.7 (d,  $J = 179.5$  Hz), 62.1, 56.6 (d,  $J = 22.1$  Hz), 53.6, 51.7, 30.5, 24.0, 13.94;  $^{19}\text{F}$  NMR (300 MHz,  $\text{CDCl}_3$ ):  $\delta$  -192.6 (1F, dd,  $J = 45.3, 31.0$  Hz).



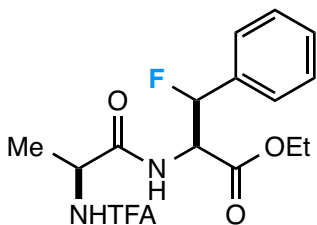
Ethyl (2*R*)-2-((*S*)-6-(1,3-dioxoisoindolin-2-yl)-2-(isoindolin-2-yl)hexanamido)-3-fluoro-3-phenylpropanoate (**8**). Isolated major diastereomer; 42% yield (both diastereomers in 61% yield by  $^{19}\text{F}$  NMR). Colorless oil.  $^1\text{H}$  NMR (400 MHz,  $\text{CDCl}_3$ ):  $\delta$  7.84-7.813 (2H, m), 7.811-7.78 (2H, m), 7.76-7.73 (2H, m), 7.70-7.67 (2H, m), 7.30-7.25 (5H, m), 7.19-7.16 (1H, m), 6.07 (1H, dd,  $J = 45.4, 2.5$  Hz), 5.08 (1H, ddd,  $J = 31.5, 9.1, 2.5$  Hz), 4.68 (1H, dd,  $J = 9.8, 6.4$  Hz), 4.30-4.18 (2H, m), 3.58 (2H, t,  $J = 7.3$  Hz), 2.42-1.97 (3H, m), 1.75-1.54 (3H, m), 1.23 (3H, t,  $J = 7.2$  Hz);  $^{13}\text{C}$  NMR (400 MHz,  $\text{CDCl}_3$ ):  $\delta$  171.1, 168.6, 168.41, 168.38, 168.2, 167.9, 135.4, 135.2, 134.3, 133.8, 132.0, 131.5, 129.2, 128.6, 128.37, 128.35, 128.34, 125.0, 124.9, 123.6, 123.1, 92.7 (d,  $J = 179.1$  Hz), 62.1, 56.6 (d,  $J = 22.9$  Hz), 54.8, 37.3, 28.1, 27.8, 23.4, 14.0;  $^{19}\text{F}$  NMR (300 MHz,  $\text{CDCl}_3$ ):  $\delta$  -193.1 (1F, dd,  $J = 45.3, 31.0$  Hz).



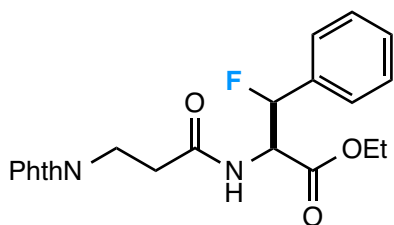
Ethyl (2*R*)-2-(2-(1,3-dioxoisoindolin-2-yl)acetamido)-3-fluoro-3-phenylpropanoate (**9**). Isolated major diastereomer; 52% yield (both diastereomers in 69% yield by  $^{19}\text{F}$  NMR). White solid; m.p. 172-176 °C.  $^1\text{H}$  NMR (400 MHz,  $\text{CDCl}_3$ ):  $\delta$  7.90-7.84 (2H, m), 7.76-7.70 (2H, m), 7.35-7.25 (5H, m), 6.54 (1H, d,  $J = 9.2$  Hz), 6.00 (1H, dd,  $J = 45.2, 2.7$  Hz), 5.08 (1H, ddd,  $J = 29.3, 9.1, 2.8$  Hz), 4.38-4.23 (4H, m), 1.29 (3H, t,  $J = 7.1$  Hz);  $^{13}\text{C}$  NMR (400 MHz,  $\text{CDCl}_3$ ):  $\delta$  168.44, 168.42, 167.4, 166.1, 135.2, 135.0, 134.2, 131.9, 128.84, 128.83, 128.46, 128.45, 125.2, 125.1, 123.6, 92.7 (d,  $J = 179.5$  Hz), 62.3, 56.6 (d,  $J = 22.9$  Hz), 40.47, 14.0;  $^{19}\text{F}$  NMR (300 MHz,  $\text{CDCl}_3$ ):  $\delta$  -191.3 (1F, dd,  $J = 45.3, 28.7$  Hz).



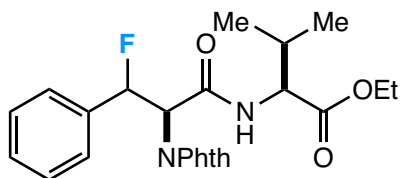
Ethyl (2*R*)-2-((*S*)-2-(1,3-dioxoisindolin-2-yl)propanamido)-3-fluoro-3-phenylpropanoate (**2**). Isolated major diastereomer; 49% yield (both diastereomers in 73% yield by  $^{19}\text{F}$  NMR). Colorless oil.  $^1\text{H}$  NMR (400 MHz,  $\text{CDCl}_3$ ):  $\delta$  7.85-7.82 (2H, m), 7.76-7.72 (2H, m), 7.28-7.21 (5H, m), 6.71 (1H, d,  $J = 8.9$  Hz), 6.04 (1H, dd,  $J = 45.3, 2.5$  Hz), 5.08 (1H, ddd,  $J = 30.6, 9.0, 2.6$  Hz), 4.84 (1H, q,  $J = 7.4$  Hz), 4.25 (2H, q,  $J = 7.1$  Hz), 1.61 (3H, d,  $J = 7.4$  Hz), 1.28 (3H, t,  $J = 7.0$  Hz);  $^{13}\text{C}$  NMR (400 MHz,  $\text{CDCl}_3$ ):  $\delta$  169.1, 168.5, 168.4, 167.6, 135.3, 135.1, 134.2, 131.7, 128.64, 128.63, 128.34, 128.33, 125.0, 124.9, 123.5, 92.7 (d,  $J = 179.1$  Hz), 62.2, 56.6 (d,  $J = 22.5$  Hz), 49.4, 14.9, 14.0;  $^{19}\text{F}$  NMR (300 MHz,  $\text{CDCl}_3$ ):  $\delta$  -194.0 (dd,  $J = 45.9, 31.0$  Hz).



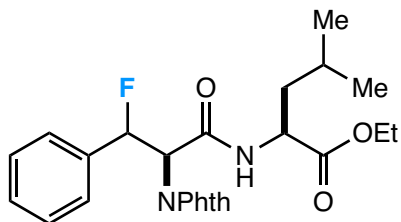
Ethyl (2*R*)-3-fluoro-3-phenyl-2-((*S*)-2-(2,2,2-trifluoroacetamido)propanamido)propanoate (**10**). Isolated as a mixture of diastereomers; 67% yield. Colorless solid; m.p. 96-98 °C.  $^1\text{H}$  NMR (400 MHz,  $\text{CDCl}_3$ ):  $\delta$  7.40-7.27 (5H, m), 7.09 (1H, d,  $J = 7.1$  Hz), 6.89-6.82 (1H, m), 6.13-5.79 (1H, m), 5.19-5.03 (1H, m), 4.66-4.50 (1H, m), 4.30 (1H, q,  $J = 7.1$  Hz), 4.16-4.08 (1H, m), 1.45-1.39 (3H, m), 1.33-1.10 (3H, m);  $^{13}\text{C}$  NMR (400 MHz,  $\text{CDCl}_3$ ):  $\delta$  170.7, 168.5, 168.4, 167.9, 167.8, 157.2, 157.0, 156.81, 156.75, 156.7, 156.4, 156.3, 156.1, 155.9, 135.09, 135.06, 134.88, 134.85, 128.99, 128.98, 128.92, 128.91, 128.51, 128.50, 128.47, 128.46, 125.17, 125.15, 125.09, 125.07, 117.04, 116.96, 114.2, 114.1, 93.0 (d,  $J = 179.1$  Hz), 92.6 (d,  $J = 182.8$  Hz), 62.5, 62.2, 57.3, 57.0, 56.9, 56.7, 49.1, 48.9, 18.4, 18.2, 14.0, 13.8;  $^{19}\text{F}$  NMR (300 MHz,  $\text{CDCl}_3$ ):  $\delta$  -75.31 (3F, s), -75.35 (3F, s), -190.9 (1F, dd,  $J = 45.9, 20.7$  Hz), -192.1 (1F, dd,  $J = 45.3, 30.4$  Hz).



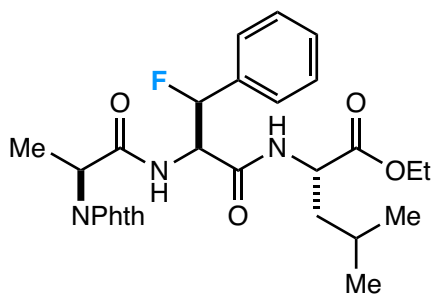
Ethyl (2*R*)-2-(3-(1,3-dioxoisindolin-2-yl)propanamido)-3-fluoro-3-phenylpropanoate (**11**). Isolated as a mixture of diastereomers; 47% yield. Beige solid; m.p. 134-138 °C. <sup>1</sup>H NMR (400 MHz, CDCl<sub>3</sub>): δ 7.80-7.76 (2H, m), 7.69-7.65 (2H, m), 7.33-7.18 (5H, m), 6.69-6.59 (1H, m), 6.04-5.7 (1H, m), 5.18-5.04 (1H, m), 4.23-4.16 (1H, m), 4.05-3.92 (2H, m), 3.86-3.75 (1H, m), 2.72-2.52 (2H, m), 1.25-1.00 (3H, m); <sup>13</sup>C NMR (400 MHz, CDCl<sub>3</sub>): δ 171.4, 169.7, 169.6, 169.3, 168.74, 168.71, 168.3, 168.07, 168.02, 167.95, 167.9, 135.8, 135.6, 135.41, 135.37, 135.2, 133.9, 133.8, 131.9, 129.2, 128.58, 128.57, 128.53, 128.52, 128.3, 128.22, 128.21, 128.20, 125.13, 125.05, 125.04, 125.0, 123.18, 123.15, 92.9 (d, *J* = 182.1 Hz), 92.8 (d, *J* = 178.8 Hz), 62.0, 61.6, 57.0, 56.8, 56.3, 56.1, 34.5, 34.4, 34.1, 34.0, 33.8, 13.9, 13.6; <sup>19</sup>F NMR (300 MHz, CDCl<sub>3</sub>): δ -191.2 (1F, dd, *J* = 45.3, 29.8 Hz), -192.5 (1F, dd, *J* = 45.9, 22.4 Hz).



Ethyl ((2*R*)-2-(1,3-dioxoisindolin-2-yl)-3-fluoro-3-phenylpropanoyl)-L-valinate (**12**). Isolated as a mixture of diastereomers with a minor impurity from valine side chain fluorination. Colorless oil. <sup>1</sup>H NMR (400 MHz, CDCl<sub>3</sub>): δ 7.94-7.87 (1H, m), 7.80-7.74 (1H, m), 7.73-7.67 (1H, m), 7.64-7.60 (1H, m), 7.55-7.50 (1H, m), 7.41-7.36 (2H, m), 7.29-7.24 (2H, m), 7.21-7.15 (1H, m), 6.56-6.33 (1H, m), 5.36-5.30 (1H, m), 4.63-4.36 (1H, m), 4.31-4.18 (1H, m), 4.15-4.01 (1H, m), 2.30-2.02 (1H, m), 1.32-1.16 (3H, m), 0.98-0.77 (6H, m); <sup>13</sup>C NMR (400 MHz, CDCl<sub>3</sub>): δ 171.2, 170.9, 167.8, 167.2, 165.84, 165.81, 165.0, 164.9, 135.7, 135.5, 135.4, 135.0, 134.8, 134.1, 131.5, 131.3, 129.83, 129.80, 129.77, 128.8, 128.62, 128.61, 127.32, 127.27, 127.1, 127.0, 123.8, 123.5, 91.9 (d, *J* = 169.9 Hz), 89.6 (d, *J* = 179.9 Hz), 61.4, 61.2, 59.3, 59.1, 57.7, 57.4, 56.4, 56.0, 31.3, 31.1, 18.9, 18.7, 17.6, 17.5, 14.1, 14.0; <sup>19</sup>F NMR (300 MHz, CDCl<sub>3</sub>): δ -164.0- -164.2 (1F, m), -174.4 (1F, dd, *J* = 47.0, 11.5 Hz).



Ethyl ((2R)-2-(1,3-dioxoisindolin-2-yl)-3-fluoro-3-phenylpropanoyl)-L-leucinate (**13**). Isolated as a mixture of diastereomers. Colorless oil.  $^1\text{H}$  NMR (400 MHz,  $\text{CDCl}_3$ ):  $\delta$  7.94-7.88 (1H, m), 7.81-7.75 (1H, m), 7.72-7.69 (1H, m), 7.65-7.60 (1H, m), 7.54-7.50 (1H, m), 7.43-7.35 (2H, m), 7.29-7.24 (2H, m), 7.08-6.67 (1H, m), 6.55-6.32 (1H, m), 5.35-5.26 (1H, m), 4.73-4.41 (1H, m), 4.29-4.02 (2H, m), 1.75-1.59 (2H, m), 1.57-1.42 (1H, m), 1.32-1.15 (3H, m), 0.98-0.92 (3H, m), 0.86-0.79 (3H, m);  $^{13}\text{C}$  NMR (400 MHz,  $\text{CDCl}_3$ ):  $\delta$  172.3, 172.1, 167.8, 167.2, 165.61, 165.59, 164.8, 164.7, 135.6, 135.4, 135.0, 134.8, 134.5, 134.1, 131.5, 131.4, 129.85, 129.82, 129.80, 129.78, 128.80, 128.64, 128.63, 127.33, 127.27, 127.10, 127.05, 123.8, 123.5, 92.0 (d,  $J = 169.9$  Hz), 89.5 (d,  $J = 179.9$  Hz), 61.5, 61.3, 59.3, 59.1, 56.2, 55.9, 51.5, 51.1, 41.7, 41.4, 26.9, 24.9, 24.7, 22.7, 22.6, 22.0, 21.8, 14.1, 14.0;  $^{19}\text{F}$  NMR (300 MHz,  $\text{CDCl}_3$ ):  $\delta$  -165.0 (1F, ddd,  $J = 47.6, 13.8, 9.2$  Hz), -176.2 (1F, dd,  $J = 47.0, 11.5$  Hz).



Ethyl ((2R)-2-((S)-2-(1,3-dioxoisindolin-2-yl)propanamido)-3-fluoro-3-phenylpropanoyl)-L-leucinate (**14**). Isolated as a mixture of diastereomers; 63% yield. White solid; m.p. 138-141 °C.  $^1\text{H}$  NMR (400 MHz,  $\text{CDCl}_3$ ):  $\delta$  7.86-7.78 (2H, m), 7.76-7.69 (2H, m), 7.39-7.22 (5H, m), 6.96-6.33 (2H, m), 6.24-5.86 (1H, m), 5.07-4.80 (2H, m), 4.58-4.42 (1H, m), 4.20-4.06 (2H, m), 1.73-1.65 (2H, m), 1.64-1.45 (4H, m), 1.28-1.14 (3H, m), 0.98-0.82 (6H, m);  $^{13}\text{C}$  NMR (400 MHz,  $\text{CDCl}_3$ ):  $\delta$  171.9, 171.7, 168.9, 168.7, 167.5, 167.43, 167.41, 167.26, 167.25, 167.03, 166.98, 135.5, 135.33, 135.27, 135.1, 134.3, 134.2, 131.7, 131.6, 129.0, 128.9, 128.7, 128.6, 128.5, 128.4, 125.7, 125.6, 125.2, 125.1, 123.48, 123.45, 92.2 (d,  $J = 180.2$  Hz), 91.8 (d,  $J = 178.0$  Hz), 61.19, 61.15, 57.6, 57.4, 57.3, 57.2, 51.30, 51.27, 49.0, 48.9, 40.9, 40.8, 24.7, 24.6,



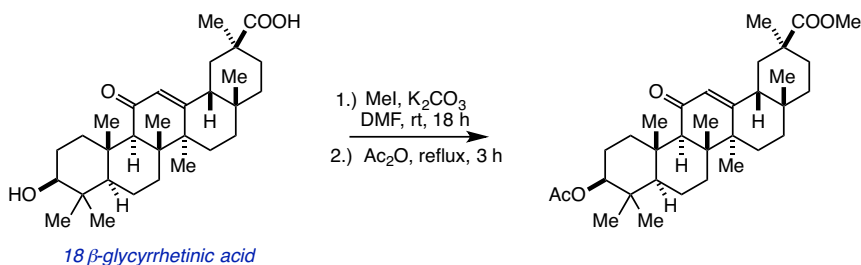
22.7, 22.6, 21.81, 21.77, 14.9, 14.8, 14.0;  $^{19}\text{F}$  NMR (300 MHz,  $\text{CDCl}_3$ ):  $\delta$  -189.0 (1F, dd,  $J = 45.3, 18.4$  Hz), -192.4 (1F, dd,  $J = 45.3, 24.7$  Hz).

### 12.10 Experimental Details for Chapter 10.

**General Fluorination Procedure.** Selectfluor (97 mg, 0.28 mmol) and the substrate (0.13 mmol) were added to an oven-dried  $\mu\text{O}$  vial equipped with a stir bar; the vial was then sealed with a cap w/ septum using a crimper and evacuated/refilled with  $\text{N}_2$  multiple times. Anhydrous  $\text{CH}_3\text{CN}$  (6 mL) was added, and the reaction mixture was irradiated at 300 nm in a Rayonet reactor while stirring. After 4 h, a 0.3 mL aliquot was taken for  $^{19}\text{F}$  NMR yield determination, and the rest of the reaction mixture was poured over  $\text{Et}_2\text{O}$ , filtered through Celite, and concentrated. The crude reaction mixture was purified initially via gradient column chromatography on silica gel eluting with  $\text{EtOAc}$ /hexanes. Analytical purity was obtained via subsequent HPLC purification.

### Synthesis of Starting Materials.

Methyl 3 $\beta$ -acetoxy-glycyrrhetinate<sup>63,64</sup>

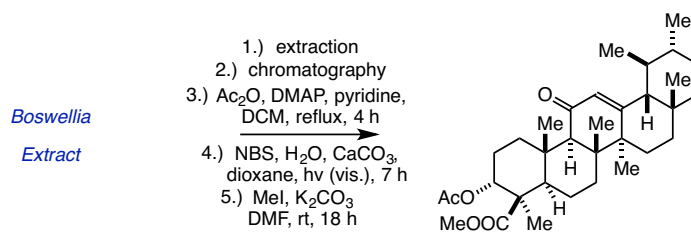


To a flame-dried round bottom equipped with a stir bar under  $\text{N}_2$  was added 18 $\beta$ -glycyrrhetic acid (2.0 g, 4.3 mmol),  $\text{K}_2\text{CO}_3$  (1.0 g, 7.2 mmol), and DMF (20 mL). The reaction mixture was stirred for 30 min at rt. Iodomethane (0.32 mL, 5.1 mmol) was then added, and the reaction mixture was stirred for 18 h. At this point, TLC indicated the complete consumption of the starting material. The reaction mixture was diluted with  $\text{CH}_2\text{Cl}_2$ , transferred to separatory funnel, and washed successively with  $\text{H}_2\text{O}$ , 1.0 M HCl,

saturated aq.  $\text{NH}_4\text{Cl}$ , and brine. The organic layer was dried over  $\text{MgSO}_4$ , filtered through Celite, concentrated, and the product (2.0 g, 92 %) was used without further purification.

Methyl 3 $\beta$ -hydroxyl-glycyrrhetinate (1.8 g, 3.7 mmol) from the previous step was dissolved in acetic anhydride and heated to reflux for 3 h. Acetic acid (4 mL) and  $\text{H}_2\text{O}$  (8 mL) were added to the hot reaction mixture, and then the reaction mixture was cooled to rt. The crystalline precipitate was collected by filtration, washed with  $\text{H}_2\text{O}$  (4 x 10 mL),  $\text{Et}_2\text{O}$  (3 mL), and dried to provide methyl 3 $\beta$ -acetoxy-glycyrrhetinate (1.87 g, 96 %) as a white solid; m.p. = 295-296 °C.  $^1\text{H}$  NMR (400 MHz,  $\text{CDCl}_3$ ): 5.62 (s, 1H), 4.47 (dd,  $J$  = 11.6, 4.9 Hz, 1H), 3.64 (s, 3H), 2.76 (dt,  $J$  = 13.7, 3.6 Hz, 1H), 2.31 (s, 1H), 2.06-2.01 (m, 1H), 2.00 (s, 3H), 1.98-1.93 (m, 2H), 1.91-1.85 (m, 1H), 1.82-1.74 (m, 1H), 1.71-1.51 (m, 5H), 1.48-1.34 (m, 3H), 1.32 (s, 3H), 1.28-1.22 (m, 2H), 1.17-1.14 (m, 1H), 1.11 (s, 3H), 1.10 (s, 3H), 1.08 (s, 3H), 1.05-0.95 (m, 2H), 0.83 (s, 6H), 0.78-0.74 (m, 1H), 0.76 (s, 3H);  $^{13}\text{C}\{^1\text{H}\}$  NMR (100 MHz,  $\text{CDCl}_3$ ): 199.9, 176.8, 170.8, 169.1, 128.4, 80.5, 61.6, 54.9, 51.6, 48.3, 45.3, 43.9, 43.1, 40.9, 38.7, 37.9, 37.6, 36.8, 32.6, 31.7, 31.0, 28.4, 28.2, 27.9, 26.4, 26.3, 23.4, 23.2, 21.2, 18.6, 17.3, 16.6, 16.3.  $\nu_{\text{max}}$  ( $\text{CaF}_2$ ,  $\text{CHCl}_3$ ): 1724 (br), 1653  $\text{cm}^{-1}$ .  $\lambda_{\text{max}}$  ( $\text{CH}_3\text{CN}$ ): 334 nm. HRMS (ESI)  $m/z$   $\text{C}_{33}\text{H}_{50}\text{O}_5\text{Na}^+$ : calc 549.355046, observed 549.354488.

Methyl 3 $\alpha$ -acetoxy-11-oxo- $\beta$ -boswellate<sup>63,65</sup>



Crude *Boswellia* resin from 90 soft gels (500 mg each) of Now Foods® - *Boswellia* extract was dissolved in  $\text{CH}_2\text{Cl}_2$  (100 mL). The solution was washed with  $\text{H}_2\text{O}$  (2 x 100 mL), dried with  $\text{MgSO}_4$ , and concentrated. The crude mixture was purified from the majority of other ingredients by gradient column chromatography on silica gel eluting with hexanes to 40:60 EtOAc:hexanes (collected all fractions containing  $R_f$  = 0.6 at 40:60 EtOAc:hexanes).

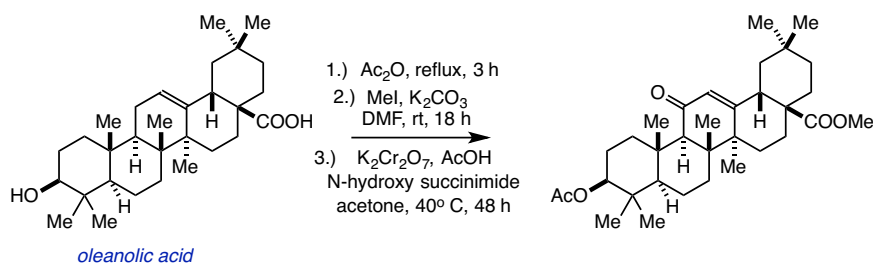
A portion of the crude mixture (10 g) from the previous step was added to a round bottom flask equipped with a stir bar and a reflux condenser under N<sub>2</sub>. Dichloromethane (12 mL), pyridine (6.4 mL), DMAP (1.2 g), and acetic anhydride (5.0 mL) were added successively. The reaction mixture was heated to 50 °C for 4 h. The reaction was quenched with 150 mL of cold 1M HCl. The reaction mixture was extracted into Et<sub>2</sub>O (3 x 150 mL), and the combined organic layers were dried with MgSO<sub>4</sub>, filtered through Celite, and concentrated.

The crude mixture (2.0 g) from the previous procedure, NBS (1.7 g), CaCO<sub>3</sub> (1.5 g), and H<sub>2</sub>O (14 mL) were added to a flame-dried round bottom flask equipped with a stir bar under N<sub>2</sub>. The flask was evacuated and refilled with N<sub>2</sub> several times. Anhydrous dioxane (140 mL) was added to the flask via syringe under N<sub>2</sub> atmosphere. The reaction mixture was stirred vigorously for 7 h and irradiated with two 14-Watt compact fluorescent lights. The mixture was diluted with EtOAc (150 mL), transferred to a separatory funnel, and the organic layer was washed with H<sub>2</sub>O (2 x 150 mL), dried with MgSO<sub>4</sub>, filtered through Celite, and concentrated. The crude mixture was purified by gradient column chromatography on silica gel eluting with 10:90 to 35:55 EtOAc:hexanes to give 3 $\alpha$ -acetoxy-11-oxo- $\beta$ -boswellic acid as a beige solid.

The 3 $\alpha$ -acetoxy-11-oxo- $\beta$ -boswellic acid from the previous step (1.5 g, 2.9 mmol), K<sub>2</sub>CO<sub>3</sub> (0.69 g, 5.0 mmol) and DMF (15 mL) were added to a flame-dried round bottom flask equipped with a stir bar under N<sub>2</sub>. The reaction mixture was stirred for 30 min, and then iodomethane (0.22 mL, 3.5 mmol) was added dropwise via syringe. The reaction mixture stirred for 22 h at rt. The reaction mixture was then diluted with EtOAc, transferred to a separatory funnel, washed with H<sub>2</sub>O, dried with MgSO<sub>4</sub>, filtered through Celite, and concentrated. The crude residue was purified by gradient column chromatography on silica gel eluting with hexanes to 15:85 EtOAc:hexanes and recrystallized in MeOH to provide methyl 3 $\alpha$ -acetoxy-11-oxo- $\beta$ -boswellate as a white solid; m.p. = 181-182 °C. <sup>1</sup>H NMR (400 MHz, CDCl<sub>3</sub>): 5.53 (s, 1H), 5.32 (t, *J* = 2.8 Hz, 1H), 3.65 (s, 3H), 2.52 (dt, *J* = 12.7 Hz, 3.6 Hz, 1H), 2.40 (s, 1H), 2.24-2.05 (m, 2H), 2.07 (s, 3H), 1.92-1.74 (m, 3H), 1.73-1.56 (m, 3H), 1.54-1.35 (m, 6H), 1.33 (s, 3H), 1.30-1.19 (m, 4H), 1.17 (s, 6H), 1.03 (s, 3H), 0.99-0.96 (m, 1H), 0.93 (s, 3H), 0.89-0.85 (m, 1H), 0.81 (s, 3H), 0.79 (d, *J* = 6.5 Hz, 3H); <sup>13</sup>C{<sup>1</sup>H} NMR (100 MHz, CDCl<sub>3</sub>): 199.2, 176.0, 170.2, 164.9, 130.5, 73.2, 60.2, 59.0, 51.5, 50.4, 46.6, 45.0 43.7, 40.9, 39.3, 39.2, 37.1, 34.6, 33.9, 32.8, 30.9, 28.8, 27.5, 27.2, 23.8, 23.6, 21.3, 21.1, 20.5,

18.7, 18.3, 17.4, 13.1.  $\nu_{\max}$  (CaF<sub>2</sub>, CHCl<sub>3</sub>): 1726 (br), 1652 cm<sup>-1</sup>.  $\lambda_{\max}$  (CH<sub>3</sub>CN): 335 nm. HRMS (ESI) m/z C<sub>33</sub>H<sub>50</sub>O<sub>5</sub>H<sup>+</sup>: calc 527.373101, observed 527.372703.

Methyl 3 $\beta$ -acetyl-11-keto-oleanolate<sup>63,64,66</sup>



To a flame-dried round bottom equipped with a stir bar under N<sub>2</sub> was added oleanolic acid (3.0 g, 6.6 mmol), K<sub>2</sub>CO<sub>3</sub> (1.5 g, 11.1 mmol), and DMF (30 mL). The reaction mixture was stirred for 30 min at rt. Iodomethane (0.49 mL, 8.4 mmol) was then added, and the reaction mixture was stirred for 18 h. At this point, TLC indicated the complete consumption of the starting material. The reaction mixture was diluted with CH<sub>2</sub>Cl<sub>2</sub>, transferred to separatory funnel, and washed successively with H<sub>2</sub>O, 1.0 M HCl, saturated aq. NH<sub>4</sub>Cl, and brine. The organic layer was dried over MgSO<sub>4</sub>, filtered through Celite, concentrated, and the product (2.85 g, 92 %) was used without a further purification.

Oleanolic acid methyl ester (2.8 g, 6.0 mmol) from the previous step was dissolved in acetic anhydride, and the reaction mixture was stirred and heated to reflux for 3 h. Acetic acid (7 mL) and H<sub>2</sub>O (12 mL) were then added to the hot reaction mixture, and then the reaction mixture was cooled to rt. The crystalline precipitate was collected by filtration, washed with H<sub>2</sub>O (4 x 15 mL) and Et<sub>2</sub>O (4 mL), and then dried to provide methyl 3 $\beta$ -acetyl-oleanolate (2.93 g, 96 %).

Methyl 3 $\beta$ -acetyloleanolate (2.0 g, 3.9 mmol) from the previous step was dissolved in a mixture of acetone (200 mL) and acetic acid (20 mL) in a round-bottom flask equipped with a stir bar and condenser. The reaction mixture was treated with *N*-hydroxysuccinimide (4.49 g, 39 mmol) and K<sub>2</sub>Cr<sub>2</sub>O<sub>7</sub> (4.6 g, 16 mmol), then stirred at 40 °C for 48 h. The reaction mixture was cooled to rt, quenched with aq. 10 % sodium metabisulfite solution (v/v), filtered through Celite and extracted into Et<sub>2</sub>O. The combined organic

layers were washed with sat. NaHCO<sub>3</sub> and brine, then dried with MgSO<sub>4</sub>, and concentrated. The crude residue was recrystallized in MeOH to provide methyl 3 $\beta$ -acetyl-11-keto-oleanolate (1.52 g, 74 %) as a white solid; m.p. = 235.5-237 °C. <sup>1</sup>H NMR (400 MHz, CDCl<sub>3</sub>): 5.63 (s, 1H), 4.5 (dd, *J* = 11.6, 4.8 Hz, 1H), 3.62 (s, 3H), 3.02-2.97 (m, 1H), 2.82 (dt, *J* = 13.7, 3.6 Hz, 1H), 2.33 (s, 1H), 2.08-2.00 (m, 1H), 2.04 (s, 3H), 1.76-1.52 (m, 9H), 1.45-1.30 (m, 3H), 1.35 (s, 3H), 1.28-1.17 (m, 3H), 1.12 (s, 3H), 1.09-1.01 (m, 1H), 0.93 (s, 3H), 0.92 (s, 3H), 0.90 (s, 3H), 0.86 (s, 6H), 0.86-0.76 (m, 1H); <sup>13</sup>C{<sup>1</sup>H} NMR (100 MHz, CDCl<sub>3</sub>): 200.0, 177.3, 170.8, 168.5, 127.7, 80.5, 61.5, 54.9, 51.7, 46.1, 44.9, 44.1, 43.3, 41.5, 38.6, 37.9, 37.0, 33.6, 32.74, 32.69, 31.5, 30.5, 27.9, 27.6, 23.43, 23.39, 23.3, 22.8, 21.2, 18.8, 17.2, 16.6, 16.1.  $\nu_{\max}$  (CaF<sub>2</sub>, CHCl<sub>3</sub>): 1721 (br), 1651 cm<sup>-1</sup>.  $\lambda_{\max}$  (CH<sub>3</sub>CN): 292, 332 nm. HRMS (ESI) *m/z* C<sub>33</sub>H<sub>50</sub>O<sub>5</sub>Na<sup>+</sup>: calc 549.355046, observed 549.354462.

### 3-Methyl-2-cholesten-1-one<sup>67,68</sup>

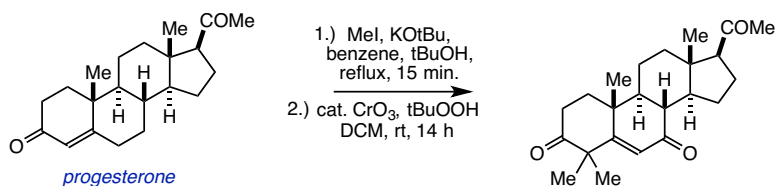


To a flame-dried three-neck round bottom equipped with a stir bar and reflux condenser under N<sub>2</sub> was added Pd(TFA)<sub>2</sub> (0.416 g, 1.25 mmol), a suspension of 5 $\alpha$ -cholestan-3-one (9.7 g, 25 mmol) in AcOH (125 mL), and DMSO (0.18 mL, 2.5 mmol). The reaction mixture was stirred, and the N<sub>2</sub> atmosphere was replaced with an O<sub>2</sub> balloon. The reaction mixture was then heated to 80 °C for 16 h. Upon cooling, the reaction mixture was neutralized with saturated aq. NaHCO<sub>3</sub> and extracted into CHCl<sub>3</sub> (x3). The combined organic layers were dried with MgSO<sub>4</sub>, filtered through Celite, and concentrated. The crude residue was purified via gradient column chromatography eluting with hexanes to 15:85 EtOAc:hexanes to provide 1-cholesten-3-one (8.7 g, 90 %).

The product from the previous step, 1-cholesten-3-one (2.1 g, 5.5 mmol), was added to a flame-dried three-neck round bottom equipped with a stir bar and reflux condenser under N<sub>2</sub>, followed by Et<sub>2</sub>O (25 mL). The reaction mixture was stirred and cooled to 0 °C. A 1.6 M solution of methyllithium in Et<sub>2</sub>O (14

mL, 22 mmol) was added drop wise while stirring. After addition, the reaction mixture was stirred for 1 h and let gradually warm to rt. The reaction mixture subsequently was cooled to 0 °C and quenched with saturated aq. NH<sub>4</sub>Cl slowly while stirring. The organic layer was separated and washed with H<sub>2</sub>O and brine, then dried with MgSO<sub>4</sub>, filtered through Celite, and concentrated in a round bottom flask. To the crude reaction mixture was added a stir bar, pyridinium dichromate (5.0 g, 13 mmol), and CH<sub>2</sub>Cl<sub>2</sub> (75 mL) under N<sub>2</sub>. The reaction mixture was stirred at rt for 16 h, then diluted with Et<sub>2</sub>O, filtered through a pad of Celite and silica gel, then concentrated. The crude residue was purified via gradient column chromatography eluting with hexanes to 25:75 EtOAc:hexanes to provide 3-methyl-2-cholesten-1-one (1.2 g, 55 %) as a white solid; m.p. = 110-111 °C. <sup>1</sup>H NMR (400 MHz, CDCl<sub>3</sub>): 5.57 (s, 1H), 2.44-2.35 (m, 1H), 2.09 (dd, *J* = 18.8, 11.1 Hz, 1H), 1.98-1.87 (m, 2H), 1.79 (s, 3H), 1.76-1.69 (m, 2H), 1.58-1.35 (m, 5H), 1.32-1.14 (m, 9H), 1.11-0.99 (m, 6H), 0.97-0.92 (m, 1H), 0.96 (s, 3H), 0.86 (d, *J* = 6.5 Hz, 3H), 0.82 (d, *J* = 6.7 Hz, 3H), 0.80 (d, *J* = 6.7 Hz, 3H), 0.62 (s, 3H); <sup>13</sup>C {<sup>1</sup>H} NMR (100 MHz, CDCl<sub>3</sub>): 205.9, 155.9, 125.5, 56.3, 47.4, 45.9, 42.9, 42.4, 40.1, 39.4, 36.6, 36.1, 36.0, 35.7, 30.6, 27.99, 27.97, 27.8, 24.1, 23.8, 23.4, 23.0, 22.7, 22.4, 18.5, 12.2, 10.5.  $\nu_{\max}$  (CaF<sub>2</sub>, CHCl<sub>3</sub>): 1663 cm<sup>-1</sup>.  $\lambda_{\max}$  (CH<sub>3</sub>CN): 331 nm. HRMS (ESI) *m/z* C<sub>28</sub>H<sub>46</sub>ONa<sup>+</sup>: calc 421.344087, 421.343781.

#### 4,4-Dimethyl-5-pregnen-3,7,20-trione<sup>69,70</sup>

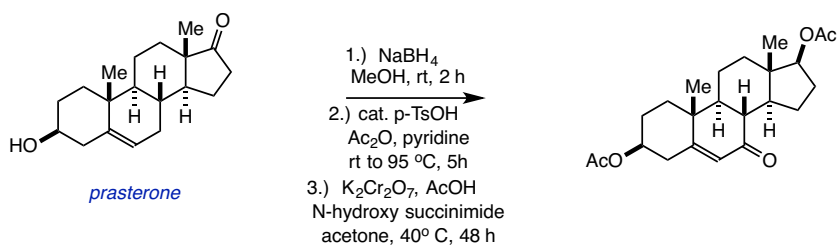


To a flame-dried three-neck round bottom equipped with a stir bar and reflux condenser under N<sub>2</sub> was added progesterone (6.0 g, 19 mmol) and benzene (160 mL). The reaction mixture was stirred and heated to reflux. A solution of KOtBu (6.4 g, 57 mmol) in tBuOH (74 mL) was added drop wise, immediately followed by a solution of iodomethane (24 mL, 382 mmol) in benzene (120 mL); the reaction mixture was stirred at reflux for 10 min and then cooled to rt. The reaction mixture was quenched with H<sub>2</sub>O (5.3 mL),

diluted with Et<sub>2</sub>O, filtered through Celite, and concentrated. The crude residue was recrystallized from MeOH three times to provide 4,4-dimethyl-5-pregnen-3,20-dione (3.9 g, 62 %).

To a flame-dried three-neck round bottom equipped with a stir bar and reflux condenser under N<sub>2</sub> was added CrO<sub>3</sub> (0.035 g, 0.35 mmol) and CH<sub>2</sub>Cl<sub>2</sub> (55 mL), followed by a 5-6 M solution of tBuOOH in decane (9.8 mL, 49 mmol). The product from the previous step, 4,4-dimethyl-5-pregnen-3,20-dione (2.4 g, 7.0 mmol), was then added as a solution in CH<sub>2</sub>Cl<sub>2</sub> (25 mL). The reaction mixture was stirred at rt for 14 h, then filtered through neutral alumina and concentrated. The crude residue was purified via gradient column chromatography eluting with hexanes to 45:55 EtOAc:hexanes to provide 4,4-dimethyl-5-pregnen-3,7,20-trione (1.4 g, 55 %) as a beige solid; m.p. = 194-198 °C. <sup>1</sup>H NMR (400 MHz, CDCl<sub>3</sub>): 5.72 (s, 1H), 2.53-2.38 (m, 2H), 2.36-2.28 (m, 2H), 2.19-2.13 (m, 1H), 2.03-1.90 (m, 3H), 1.96 (s, 3H), 1.72-1.66 (m, 1H), 1.64-1.51 (m, 3H), 1.45-1.35 (m, 1H), 1.33-1.19 (m, 3H), 1.15 (s, 3H), 1.13 (s, 3H), 0.92 (s, 3H), 0.49 (s, 3H); <sup>13</sup>C{<sup>1</sup>H} NMR (100 MHz, CDCl<sub>3</sub>): 212.1, 208.8, 200.5, 173.8, 123.9, 61.7, 49.8, 49.0, 48.6, 44.2, 44.0, 38.4, 37.3, 32.7, 31.1, 30.6, 28.6, 26.0, 25.7, 23.2, 21.1, 16.1, 12.9. ν<sub>max</sub> (CaF<sub>2</sub>, CHCl<sub>3</sub>): 1704 (br), 1666 cm<sup>-1</sup>. λ<sub>max</sub> (CH<sub>3</sub>CN): 334, 288 nm. HRMS (ESI) m/z C<sub>23</sub>H<sub>32</sub>O<sub>3</sub>Na<sup>+</sup>: calc 379.224366, observed 379.224193.

3β,17β-Diacetoxyandrost-5-ene-7-one<sup>66,71,72</sup>



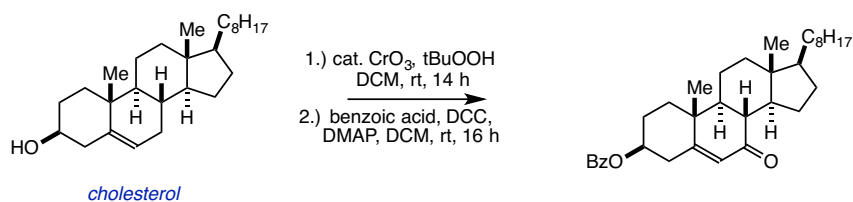
To a flame-dried round bottom equipped with a stir bar under N<sub>2</sub> was added prasterone (4.00 g, 13.9 mmol) and MeOH (75 mL). The reaction mixture was treated with NaBH<sub>4</sub> (0.53 g, 13.9 mmol) in portions over 10 min, and then stirred for an additional 2 h. The resulting white precipitate was collected by filtration and dried to provide 5-androstenediol (3.50 g, 87 %).

The 5-androstenediol from the previous step (3.1 g, 10.7 mmol), *p*-TsOH•H<sub>2</sub>O (60 mg, 0.30 mmol), and acetic anhydride (4.6 mL) were dissolved in pyridine (6.0 mL) under N<sub>2</sub>. After stirring for 1 h, the reaction mixture was heated to 95 °C and stirred for an additional 3.5 h. The reaction mixture was then cooled to rt and diluted with H<sub>2</sub>O (150 mL). The white precipitate was collected by filtration, washed with H<sub>2</sub>O, and dried to provide androstenediol-3,17-diacetate (3.52 g, 85 %).

Androstenediol-3,17-diacetate (1.93 g, 5.2 mmol) was dissolved in a mixture of acetone (200 mL) and acetic acid (20 mL) in a round-bottom flask equipped with a stir bar and reflux condenser under N<sub>2</sub>. The reaction mixture was treated with *N*-hydroxysuccinimide (5.93 g, 52 mmol) and K<sub>2</sub>Cr<sub>2</sub>O<sub>7</sub> (6.06 g, 21 mmol), and then the reaction mixture was stirred at 40 °C for 48 h. The reaction mixture was cooled to rt, quenched with aq. 10 % sodium metabisulfite solution (v/v), filtered through Celite, and extracted into Et<sub>2</sub>O. The combined organic layers were washed with saturated aq. NaHCO<sub>3</sub> and brine, and then dried with MgSO<sub>4</sub> and concentrated. The crude residue was recrystallized in MeOH to provide 3β,17β-diacetoxyandrost-5-ene-7-one (1.64 g, 82 %) as a white solid; m.p. = 222-223 °C. <sup>1</sup>H NMR (400 MHz, CDCl<sub>3</sub>): 5.7 (d, *J* = 1.8 Hz, 1H), 4.74-4.65 (m, 1H), 4.63-4.59 (m, 1H), 2.55 (ddd, *J* = 14.0, 5.1, 2.2 Hz, 1H), 2.49-2.39 (m, 2H), 2.29-2.14 (m, 2H), 2.03 (s, 3H), 2.02 (s, 3H), 2.00-1.93 (m, 2H), 1.77-1.68 (m, 2H), 1.67-1.57 (m, 2H), 1.54-1.47 (m, 3H), 1.43-1.35 (m, 1H), 1.30-1.25 (m, 1H), 1.20 (s, 3H), 1.18-1.11 (m, 1H), 0.80 (s, 3H); <sup>13</sup>C{<sup>1</sup>H} NMR (100 MHz, CDCl<sub>3</sub>): 201.1, 171.1, 170.2, 164.3, 126.5, 81.9, 72.0, 49.7, 45.0, 44.7, 43.0, 38.3, 37.8, 36.0, 35.8, 27.5, 27.3, 25.8, 21.2, 21.1, 20.7, 17.3, 12.0.  $\nu_{\max}$  (CaF<sub>2</sub>, CHCl<sub>3</sub>): 1729 (br), 1669 cm<sup>-1</sup>.  $\lambda_{\max}$  (CH<sub>3</sub>CN): 329 nm. HRMS (ESI) *m/z* C<sub>23</sub>H<sub>32</sub>O<sub>5</sub>Na<sup>+</sup>: calc 411.214195, observed 411.214375.



7-Keto-cholesteryl benzoate<sup>70,73</sup>

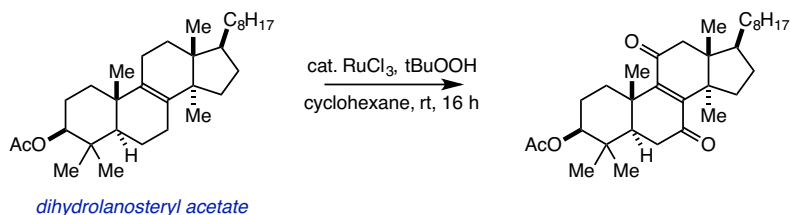


To a flame-dried three-neck round bottom equipped with a stir bar and reflux condenser under N<sub>2</sub> was added CrO<sub>3</sub> (0.050 g, 0.50 mmol) and CH<sub>2</sub>Cl<sub>2</sub> (80 mL), followed by a 70 % solution by weight of tBuOOH in H<sub>2</sub>O (9.0 mL, 70 mmol). Cholesterol (3.4 g, 10 mmol), was then added as a solution in CH<sub>2</sub>Cl<sub>2</sub> (35 mL). The reaction mixture was stirred at rt for 14 h, then filtered through neutral alumina and concentrated. The crude residue was purified via gradient column chromatography eluting with hexanes to 40:60 EtOAc:hexanes to provide 7-keto-cholesterol (1.6 g, 40 %)

To a flame-dried round bottom equipped with a stir bar was added benzoic acid (0.52 g, 4.3 mmol), 4-dimethylaminopyridine (0.05 g, 0.39 mmol), and CH<sub>2</sub>Cl<sub>2</sub> (15 mL) under N<sub>2</sub>. The reaction mixture was stirred and cooled to 0 °C. Dicyclohexylcarbodiimide (0.96 g, 4.6 mmol) was added to the reaction mixture; after 15 min., a solution of the product from the previous reaction, 7-keto-cholesterol (1.6 g, 3.9 mmol), in CH<sub>2</sub>Cl<sub>2</sub> (15 mL) was also added. The reaction mixture was stirred at rt for 16 h, then filtered through Celite to remove dicyclohexylurea byproduct. The filtrate was diluted with hexanes and washed consecutively with saturated aq. NaHCO<sub>3</sub> (x3), 1 M HCl (x3), and brine. The organic layer was dried with MgSO<sub>4</sub>, filtered through Celite, and concentrated. The crude residue was purified via column chromatography eluting with 15:85 EtOAc:hexanes to provide 7-keto-cholesteryl benzoate (0.89 g, 46 %) as a beige solid; m.p. = 144-146 °C. <sup>1</sup>H NMR (400 MHz, CDCl<sub>3</sub>): 8.04-7.99 (m, 2H), 7.56-7.51 (m, 1H), 7.43-7.39 (m, 2H), 5.72 (d, *J* = 1.6 Hz, 1H), 4.99-4.91 (m, 1H), 2.71-2.57 (m, 2H), 2.44-2.37 (m, 1H), 2.23 (t, *J* = 11.0 Hz, 1H), 2.13-2.08 (m, 1H), 2.05-1.97 (m, 2H), 1.94-1.77 (m, 2H), 1.60-1.48 (m, 4H), 1.41-1.27 (m, 6H), 1.24 (s, 3H), 1.17-.99 (m, 7H), 0.92 (d, *J* = 6.6 Hz, 3H), 0.86 (d, *J* = 6.6 Hz, 3H), 0.85 (d, *J* = 6.6 Hz, 3H), 0.68 (s, 3H); <sup>13</sup>C {<sup>1</sup>H} NMR (100 MHz, CDCl<sub>3</sub>): 201.7, 165.6, 163.7, 132.9, 130.2, 129.5, 128.2, 126.7, 72.7, 54.7, 49.9, 49.7, 45.3, 43.0, 39.4, 38.6, 38.2, 37.7, 36.1, 35.9, 35.6, 28.4, 27.9, 27.4, 26.2, 23.7,

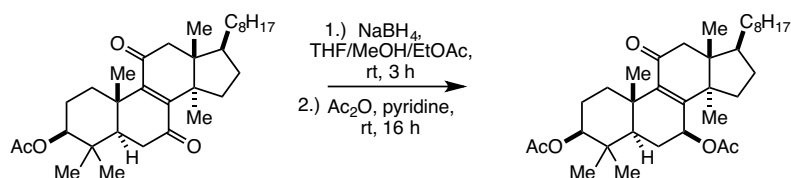
22.7, 22.5, 21.1, 18.8, 17.2, 11.9.  $\nu_{\max}$  (CaF<sub>2</sub>, CHCl<sub>3</sub>): 1714, 1668 cm<sup>-1</sup>.  $\lambda_{\max}$  (CH<sub>3</sub>CN): 332 nm. HRMS (ESI) m/z C<sub>34</sub>H<sub>48</sub>O<sub>3</sub>Na<sup>+</sup>: calc 527.349566, observed 527.349212.

7,11-Diketo-dihydrolanosteryl acetate<sup>74</sup>



To a flame-dried three-neck round bottom equipped with a stir bar under N<sub>2</sub> was added 3 $\beta$ -acetoxy-24,25-dihydrolanosteryl acetate (3.02 g, 6.6 mmol), RuCl<sub>3</sub> (0.073 g, 0.13 mmol), and cyclohexane (66 mL). A 70 % solution by weight of *t*-BuOOH in H<sub>2</sub>O (18.5 mL, 27.0 mmol) was added drop wise over 30 min via syringe pump. The reaction mixture was stirred at rt for 19 h, and then quenched with saturated aq. NaHCO<sub>3</sub> and extracted into EtOAc. The combined organic layers were dried with MgSO<sub>4</sub>, filtered through Celite, and concentrated. The crude residue was purified via gradient column chromatography on silica gel eluting with hexanes to 7.5:92.5 EtOAc:hexanes to provide 7,11-diketo-dihydrolanosteryl acetate (1.4 g, 43 %) as a yellow solid; m.p. = 142-145 °C. <sup>1</sup>H NMR (400 MHz, CDCl<sub>3</sub>): 4.48 (dd, *J* = 11.3, 5.1 Hz, 1H), 2.85 (dt, *J* = 13.8, 3.6 Hz, 1H), 2.71 (d, *J* = 15.9 Hz, 1H), 2.56 (d, *J* = 15.9 Hz, 1H), 2.49-2.37 (m, 2H), 2.16-2.03 (m, 1H), 2.00 (s, 3H), 1.97-1.84 (m, 1H), 1.74-1.54 (m, 5H), 1.52-1.42 (m, 1H), 1.39-1.29 (m, 3H), 1.27 (s, 3H), 1.26-1.16 (m, 2H), 1.12 (s, 3H), 1.10-0.93 (m, 4H), 0.90 (s, 3H), 0.85 (s, 3H), 0.83 (d, *J* = 6.7 Hz, 3H), 0.81 (d, *J* = 6.7 Hz, 3H), 0.80 (d, *J* = 6.7 Hz, 3H), 0.74 (s, 3H); <sup>13</sup>C {<sup>1</sup>H} NMR (100 MHz, CDCl<sub>3</sub>): 202.2, 201.6, 170.5, 151.5, 150.5, 79.1, 51.5, 50.0, 49.0, 48.9, 47.3, 39.4, 39.3, 37.6, 36.10, 36.09, 36.0, 33.6, 32.1, 27.8, 27.7, 27.2, 25.8, 23.9, 23.8, 22.7, 22.4, 21.1, 18.5, 17.4, 16.7, 16.4.  $\nu_{\max}$  (CaF<sub>2</sub>, CHCl<sub>3</sub>): 1727, 1672 (br) cm<sup>-1</sup>.  $\lambda_{\max}$  (CH<sub>3</sub>CN): 339 nm. HRMS (ESI) m/z C<sub>32</sub>H<sub>50</sub>O<sub>4</sub>Na<sup>+</sup>: calc 521.360131, observed 523.375432 (C<sub>32</sub>H<sub>52</sub>O<sub>4</sub>Na<sup>+</sup>).

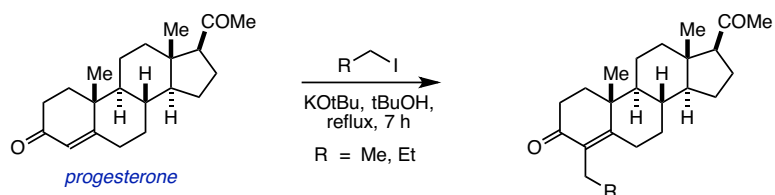
7 $\beta$ -acetoxy-11-keto-dihydrolanosteryl acetate<sup>75,76</sup>



To a flame-dried three-neck round bottom equipped with a stir bar under N<sub>2</sub> was added 3 $\beta$ -acetoxy-lanost-8-en-7,11-dione (0.49 g, 1.0 mmol), THF (0.94 mL), EtOAc (0.31 mL), MeOH (1.25 mL), and NaBH<sub>4</sub> (0.046 g, 1.2 mmol). The reaction mixture was stirred for 6 h at rt. The reaction mixture was then concentrated, and the crude residue was purified via column chromatography on silica gel eluting with EtOAc:hexanes to provide 3 $\beta$ -acetoxy-lanost-8-en-7 $\beta$ -hydroxy-11-one (0.35 g, 70 %) as a pale yellow solid.

To a flame-dried three-neck round bottom equipped with a stir bar under N<sub>2</sub> was added 3 $\beta$ -acetoxy-lanost-8-en-7 $\beta$ -hydroxy-11-one (0.67 g, 1.3 mmol), acetic anhydride (5 mL), and pyridine (5 mL). The reaction mixture was stirred for 20 h, and then diluted with CH<sub>2</sub>Cl<sub>2</sub> (10 mL). The organic layer was washed with 1M HCl (2 x 10 mL), saturated aq. NaHCO<sub>3</sub> (1 x 10 mL), and H<sub>2</sub>O (1 x 10 mL). The organic layer was dried with MgSO<sub>4</sub>, filtered through Celite, and concentrated. The crude residue was purified via gradient column chromatography on silica gel eluting with hexanes to 10:90 EtOAc:hexanes to provide 7 $\beta$ -acetoxy-11-keto-dihydrolanosteryl acetate (0.59 g, 84 %) as a white solid; m.p. = 63-65 °C. <sup>1</sup>H NMR (400 MHz, CDCl<sub>3</sub>): 5.44 (dd, *J* = 4.3, 1.4 Hz, 1H), 4.59-4.54 (m, 1H), 3.01 (dt, *J* = 13.8, 3.6 Hz, 1H), 2.68 (dd, *J* = 17.8, 0.9 Hz, 1H), 2.47 (d, *J* = 17.4 Hz, 1H), 2.07 (s, 3H), 2.04 (s, 3H), 2.02-1.92 (m, 1H), 1.82-1.63 (m, 6H), 1.56-1.45 (m, 1H), 1.42-1.29 (m, 5H), 1.27-1.20 (m, 2H), 1.18-1.10 (m, 3H), 1.17 (s, 3H), 1.08 (s, 3H), 1.03-0.96 (m, 1H), 0.87-0.84 (m, 12H), 0.83 (s, 3H), 0.78 (s, 3H); <sup>13</sup>C {<sup>1</sup>H} NMR (100 MHz, CDCl<sub>3</sub>): 200.0, 170.8, 169.9, 157.2, 143.0, 79.9, 70.4, 51.7, 50.5, 50.0, 47.5, 46.4, 39.3, 38.4, 37.3, 36.1, 36.0, 33.8, 29.9, 27.9, 27.7, 27.04, 27.01, 24.8, 24.0, 23.9, 22.7, 22.4, 21.2, 18.3, 17.1, 16.7, 16.6.  $\nu_{\max}$  (CaF<sub>2</sub>, CHCl<sub>3</sub>): 1727 (br), 1657 cm<sup>-1</sup>.  $\lambda_{\max}$  (CH<sub>3</sub>CN): 348 nm. HRMS (ESI) m/z C<sub>34</sub>H<sub>54</sub>O<sub>5</sub>Na<sup>+</sup>: calc 565.386346, observed 565.386186.

#### 4-ethyl progesterone and 4-propyl progesterone<sup>77</sup>



To a flame-dried three-neck round bottom equipped with a stir bar under N<sub>2</sub> were added progesterone (2.5 g, 8.0 mmol), KOtBu (1.6 g, 14.3 mmol) and anhydrous *t*-BuOH (120 mL). The reaction mixture was heated to reflux, and then alkyl iodide (8.0 mmol) dissolved in *t*-BuOH (120 mL) was added drop wise over 7 h. The reaction mixture was then cooled to 0 °C, diluted with H<sub>2</sub>O (80 mL), and concentrated. The crude residue was dissolved in Et<sub>2</sub>O, filtered through Celite (to remove KI), and concentrated. The crude residue was purified via column chromatography on silica gel eluting with 20:80 EtOAc:hexanes to provide the alkylated product.

#### R = Me

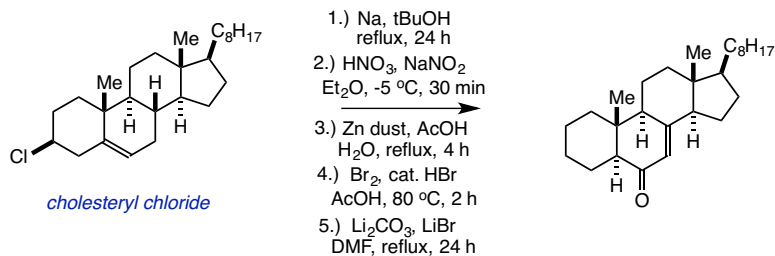
Pale yellow solid; m.p. = 109-111 °C. <sup>1</sup>H NMR (400 MHz, CDCl<sub>3</sub>): 2.70 (dt, *J* = 14.5, 3.4 Hz, 1H), 2.49 (t, *J* = 9.0 Hz, 1H), 2.38-2.21 (m, 4H), 2.19-2.07 (m, 2H), 2.08 (s, 3H), 2.04-2.01 (m, 1H), 1.93 (dt, *J* = 13.1, 4.4 Hz, 1H), 1.89-1.83 (m, 1H), 1.70-1.56 (m, 4H), 1.54-1.48 (m, 1H), 1.44-1.35 (m, 2H), 1.29-1.20 (m, 1H), 1.15-1.08 (m, 1H), 1.13 (s, 3H), 1.01-0.90 (m, 2H), 0.84 (t, *J* = 7.5 Hz, 3H), 0.62 (s, 3H); <sup>13</sup>C {<sup>1</sup>H} NMR (100 MHz, CDCl<sub>3</sub>): 209.2, 198.3, 163.2, 134.3, 63.4, 56.0, 54.1, 43.9, 38.8, 38.7, 35.3, 35.0, 33.8, 32.0, 31.4, 27.0, 24.2, 22.7, 21.0, 18.3, 17.7, 14.1, 13.3.  $\nu_{\max}$  (CaF<sub>2</sub>, CHCl<sub>3</sub>): 1699, 1657 cm<sup>-1</sup>.  $\lambda_{\max}$  (CH<sub>3</sub>CN): 335, 295 nm. HRMS (ESI) *m/z* C<sub>23</sub>H<sub>34</sub>O<sub>2</sub>Na<sup>+</sup>: calc 365.245101, observed 365.244837.

#### R = Et

Pale yellow solid; m.p. = 62.5-65 °C. <sup>1</sup>H NMR (400 MHz, CDCl<sub>3</sub>): 2.75-2.61 (m, 1H), 2.47-2.14 (m, 4H), 2.08-1.96 (m, 4H), 1.92-1.79 (m, 2H), 1.74-1.43 (m, 6H), 1.25-1.03 (m, 6H), 0.89-0.57 (m, 6H); <sup>13</sup>C {<sup>1</sup>H} NMR (100 MHz, CDCl<sub>3</sub>): 212.5, 209.3, 198.52, 198.48, 163.7, 163.6, 132.8, 132.7, 63.5, 60.9, 56.1, 54.2, 53.6, 49.8, 45.4, 43.9, 38.90, 38.85, 38.7, 35.5, 35.3, 35.1, 35.04,

33.96, 33.82, 33.79, 32.7, 32.3, 32.0, 31.4, 27.4, 27.3, 27.02, 26.96, 25.7, 24.3, 24.2, 22.9, 22.8, 21.01, 20.96, 20.7, 17.7, 14.04, 14.01, 13.3.  $\nu_{\max}$  (CaF<sub>2</sub>, CHCl<sub>3</sub>): 1700, 1658 cm<sup>-1</sup>.  $\lambda_{\max}$  (CH<sub>3</sub>CN): 335, 295 nm. HRMS (ESI) m/z C<sub>24</sub>H<sub>36</sub>O<sub>2</sub>Na<sup>+</sup>: calc 379.260751, observed 379.260480.

5 $\alpha$ -cholest-7-en-6-one<sup>78,79,80,81</sup>



A suspension of Na (7.2 g, 313 mmol) in *t*-BuOH (10.6 mL, 111 mmol) and THF (90 mL) was brought to reflux behind a blast shield. Cholesteryl chloride (8.10 g, 20.0 mmol) in THF (60 mL) was added drop wise. The reaction mixture was stirred at reflux for 24 h. Upon cooling to rt, the solution was carefully decanted onto ice and was extracted into Et<sub>2</sub>O. The combined organic layers were washed with brine and H<sub>2</sub>O, and then dried over MgSO<sub>4</sub>, filtered through Celite and concentrated to provide cholest-5-ene (6.2 g, 84 %).

Cholest-5-ene (2.0 g, 5.4 mmol) was dissolved Et<sub>2</sub>O (25 mL) in 250 mL three-neck round-bottom flask equipped with a stir bar and condenser under N<sub>2</sub>. After cooling the solution to -5 °C, aq. 60-70% HNO<sub>3</sub> (25 mL) was added drop wise over 10 min, and the reaction mixture was stirred for additional 5 min. At this point, NaNO<sub>2</sub> (0.30 g, 3.78 mmol) was added, and the reaction mixture was stirred for additional 10 min. The reaction mixture was then transferred to a separatory funnel containing 30 mL of cold water. The aqueous layer was removed without agitation, and then the Et<sub>2</sub>O layer was washed with cold H<sub>2</sub>O, 1.0 M NaOH, and then H<sub>2</sub>O. The combined organic layers were dried over Na<sub>2</sub>SO<sub>4</sub>, filtered through Celite, and concentrated. The crude residue was recrystallized in EtOH to provide 6-nitrocholest-5-ene (1.57 g, 70 %).

To a flame-dried three-neck round bottom equipped with a stir bar under N<sub>2</sub> were added 6-nitrocholest-5-ene (2.2 g, 5.3 mmol), AcOH (60 mL), and H<sub>2</sub>O (6 mL). To the reaction mixture was added Zn dust (5.2

g, 79 mmol) in portions over 30 min. The reaction mixture was then heated to reflux for 4 h. Upon cooling to rt, the precipitate was collected via filtration, dissolved in EtOAc, and filtered through Celite (to remove residual Zn). The organic layer was washed with H<sub>2</sub>O, dried with MgSO<sub>4</sub>, filtered through Celite, and concentrated to provide 5 $\alpha$ -cholestan-6-one (2.0 g, 96 %).

To a flame-dried three-neck round bottom equipped with a stir bar under N<sub>2</sub> were added 5 $\alpha$ -cholestan-6-one (1.7 g, 4.4 mmol), AcOH (75 mL), and a few drops of HBr dissolved in ~ 1.0 mL of AcOH. The reaction mixture was slowly treated with a solution of Br<sub>2</sub> (0.3 mL, 5.7 mmol) in AcOH (20 mL), and then heated to 80 °C for 2 h. Upon cooling to rt, cold H<sub>2</sub>O was added, and the reaction mixture was extracted into EtOAc. The combined organic layers were washed with sat. aq. NaHCO<sub>3</sub>, brine, and H<sub>2</sub>O, and then dried over MgSO<sub>4</sub>, filtered through Celite, and concentrated. The crude residue was purified via gradient column chromatography on silica gel eluting with EtOAc:hexanes to afford 7-bromo-6-oxo-5 $\alpha$ -cholestane (1.0 g, 50 %).

To a flame-dried three-neck round bottom equipped with a stir bar and reflux condenser under N<sub>2</sub> were added 7-bromo-6-oxo-5 $\alpha$ -cholestane (1.0 g, 2.2 mmol), Li<sub>2</sub>CO<sub>3</sub> (1.0 g, 13.5 mmol), LiBr (1.2 g, 13.5 mmol), and DMF (40.0 mL). The reaction mixture was stirred and heated to reflux for 24 h. The reaction mixture was cooled to rt, quenched with H<sub>2</sub>O and diluted with Et<sub>2</sub>O. The organic layer was separated, washed with H<sub>2</sub>O, 1.0 M HCl, sat. aq. NH<sub>4</sub>Cl, and brine. The organic layer was dried with MgSO<sub>4</sub>, filtered through Celite, and concentrated. The crude residue was purified via gradient column chromatography on silica gel eluting with EtOAc:hexanes followed by HPLC purification to provide 5 $\alpha$ -cholest-7-en-6-one (0.3 g, 36 %) as a white solid; m.p. = 93.5-95 °C. <sup>1</sup>H NMR (400 MHz, CDCl<sub>3</sub>): 5.69 (t, *J* = 2.2 Hz, 1H), 2.20-2.10 (m, 3H), 2.06-2.01 (m, 1H), 1.95-1.87 (m, 2H), 1.83-1.74 (m, 3H), 1.65-1.57 (m, 2H), 1.56-1.45 (m, 4H), 1.43-1.40 (m, 1H), 1.39-1.29 (m, 7H), 1.25-1.17 (m, 2H), 1.16-1.10 (m, 3H), 0.93 (d, *J* = 6.5 Hz, 3H), 0.86 (d, *J* = 6.7 Hz, 3H), 0.85 (d, *J* = 6.7 Hz, 3H), 0.83 (s, 3H), 0.59 (s, 3H); <sup>13</sup>C {<sup>1</sup>H} NMR (100 MHz, CDCl<sub>3</sub>): 201.2, 163.4, 123.1, 56.2, 55.6, 54.8, 50.5, 44.5, 39.4, 39.0, 38.9, 38.6, 35.9, 28.0, 27.7, 25.3, 23.8, 22.8, 22.5, 21.5, 21.3, 20.6, 18.8, 13.2, 12.3.  $\nu_{\max}$  (CaF<sub>2</sub>, CHCl<sub>3</sub>): 1660 cm<sup>-1</sup>.  $\lambda_{\max}$  (CH<sub>3</sub>CN): 330, 292 nm. HRMS (ESI) *m/z* C<sub>23</sub>H<sub>44</sub>ONa<sup>+</sup>: calc 407.328437, observed 407.328424.



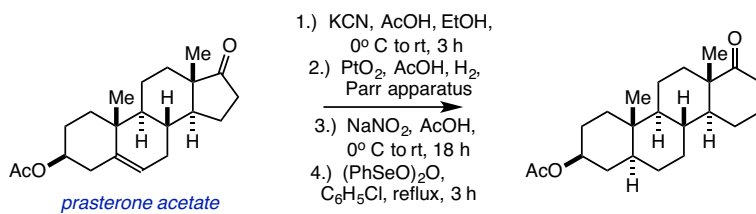
Progesterone (5.0 g, 15.9 mmol) was dissolved in pyridine (30 mL) in a flame-dried round bottom flask purged with N<sub>2</sub> and equipped with a condenser and drying tube. Sulfuryl chloride (2.57 mL, 31.8 mmol) was added to the reaction mixture drop wise at rt while stirring. The reaction mixture was stirred for additional 1 h, and then quenched with H<sub>2</sub>O and extracted into Et<sub>2</sub>O. The reaction mixture was washed successively with aq. 1.0 M HCl, 5 % aq. Na<sub>2</sub>CO<sub>3</sub>, and H<sub>2</sub>O. The organic layer was dried over Na<sub>2</sub>SO<sub>4</sub>, filtered through Celite, and concentrated. The crude residue was recrystallized in Et<sub>2</sub>O and hexanes to provide 4-chloro-progesterone (4.8 g, 87 %).

The 4-chloro-progesterone from the previous step (4.2 g, 10.9 mmol) and Zn dust (10.0 g) were added to 1,4-dioxane (180 mL) in a flame-dried round bottom under N<sub>2</sub> at 0 °C. Concentrated HCl (30.0 mL) was then added drop wise over 30 min. After stirring for additional 2.5 h, the reaction mixture was diluted with Et<sub>2</sub>O (150 mL) and filtered through Celite (washing the precipitate with Et<sub>2</sub>O); the filtrate was then transferred to a separatory funnel. The reaction mixture was washed carefully with H<sub>2</sub>O, sat. aq. NaHCO<sub>3</sub>, and brine. The organic layer was dried over MgSO<sub>4</sub>, filtered through Celite, and concentrated. The crude residue was purified via column chromatography on silica gel eluting with 10:90 EtOAc:hexanes to provide 3-chloro-3-pregnen-20-one (1.4 g, 40 %).

The 3-chloro-3-pregnen-20-one from the previous step (1.20 g, 3.58 mmol) and magnesium bis(monoperoxyphthalate) hexahydrate (1.95 g, 3.94 mmol) were dissolved in MeCN (60 mL), and the mixture was heated to reflux for 12 h. The reaction mixture was cooled to rt, filtered through Celite (washing with EtOAc), and concentrated. The residue was dissolved in Et<sub>2</sub>O and washed with 10 % aq. Na<sub>2</sub>SO<sub>3</sub>, sat. aq. NaHCO<sub>3</sub>, and H<sub>2</sub>O. The organic layer was dried over MgSO<sub>4</sub>, filtered through Celite, and concentrated. The crude residue (1.0 g, 2.85 mmol), Li<sub>2</sub>CO<sub>3</sub> (1.33 g, 18.0 mmol), and LiBr (1.6 g, 18.0

mmol) were dissolved in DMF (40 mL), and the mixture was heated to reflux for 14 h. The reaction mixture was then cooled to rt, quenched with H<sub>2</sub>O, and diluted with Et<sub>2</sub>O. The organic layer was separated and washed with H<sub>2</sub>O, 1.0 M HCl, sat. aq. NH<sub>4</sub>Cl, and brine. The organic layer was dried over MgSO<sub>4</sub>, filtered through Celite, and concentrated. The crude residue was purified via gradient column chromatography on silica gel eluting with EtOAc:hexanes to provide 5 $\alpha$ -2-pregnen-4,20-dione (0.5 g, 56 %) as a white solid; m.p. = 151-153 °C. <sup>1</sup>H NMR (400 MHz, CDCl<sub>3</sub>): 6.78-6.74 (m, 1H), 5.95 (ddd, *J* = 10.1, 3.1, 0.8 Hz, 1H), 2.49 (t, *J* = 9.0 Hz, 1H), 2.38 (dd, *J* = 18.6, 6.0 Hz, 1H), 2.22-2.10 (m, 3H), 2.08 (s, 3H), 2.04-1.94 (m, 2H), 1.77 (dq, *J* = 13.0, 3.5 Hz) 1H), 1.71-1.60 (m, 2H), 1.58-1.52 (m, 1H), 1.45-1.29 (m, 3H), 1.28-1.23 (m, 1H), 1.22-1.08 (m, 2H), 1.05-0.98 (m, 1H), 0.93-0.84 (m, 1H), 0.82 (s, 3H), 0.58 (s, 3H); <sup>13</sup>C{<sup>1</sup>H} NMR (100 MHz, CDCl<sub>3</sub>): 209.3, 201.1, 146.4, 128.7, 63.6, 56.3, 55.6, 53.9, 43.9, 40.6, 40.1, 38.7, 34.7, 31.4, 30.5, 24.2, 22.7, 20.9, 20.1, 13.3, 13.0.  $\nu_{\max}$  (CaF<sub>2</sub>, CHCl<sub>3</sub>): 1698, 1672 cm<sup>-1</sup>.  $\lambda_{\max}$  (CH<sub>3</sub>CN): 328, 275 nm. HRMS (ESI) *m/z* C<sub>21</sub>H<sub>30</sub>O<sub>2</sub>Na<sup>+</sup>: calc 337.213801, observed 337.213811.

3 $\beta$ -Acetoxy-D-homo-5 $\alpha$ -androst-16-en-17a-one<sup>86,87</sup>



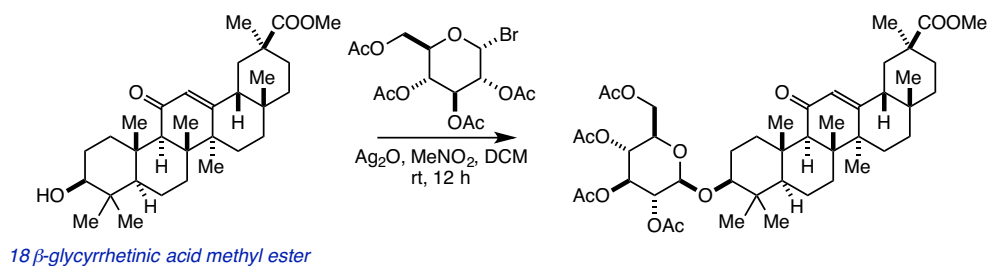
Prasterone acetate (5.0 g, 15.1 mmol) was dissolved in EtOH (150 mL) and treated with KCN (31.5 g, 484 mmol) while stirring. The reaction mixture was cooled to 0 °C and AcOH (35 mL) was added drop wise; the reaction mixture was stirred for 1 h. The reaction mixture was stirred for an additional 2 h at rt and then quenched with H<sub>2</sub>O. The white precipitate was collected by filtration, washed with H<sub>2</sub>O, washed with 2 % aq. AcOH, and then dried. The crude residue (4.8 g, 12.4 mmol), PtO<sub>2</sub> (1.0 g), and AcOH (150 mL) were shaken under H<sub>2</sub> at 40 psi in a Parr apparatus for 48 h. The solution was filtered through Celite, concentrated, and diluted with water (80 mL). Neutral impurities were removed by extracting into Et<sub>2</sub>O. The aqueous layer was then transferred to a round bottom flask, along with AcOH (10 mL), and cooled to 0



°C. Then, NaNO<sub>2</sub> (2.4 g, 34.8 mmol) dissolved in water (8 mL) was added to the reaction mixture, which was then stirred for 2 h at 0 °C. The reaction mixture was warmed to rt and stirred for additional 16 h. The precipitated white solid was collected via filtration, washed with H<sub>2</sub>O, and dried. The crude residue was purified via column chromatography eluting with EtOAc:hexanes to provide 3β-acetoxy-D-homo-5α-androstan-17a-one (2.4 g, 56 %).

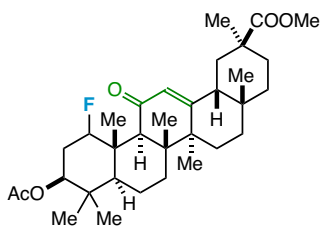
To a flame-dried three-neck round bottom equipped with a stir bar and reflux condenser under N<sub>2</sub> were added 3β-acetoxy-D-homo-5α-androst-17a-one (1.0 g, 2.9 mmol) and benzeneseleninic acid anhydride (2.1 g, 5.8 mmol). Anhydrous chlorobenzene (12 mL) was added via syringe under N<sub>2</sub> atmosphere, and the reaction mixture was stirred and heated to reflux for 2.5 h. The reaction mixture was quenched with saturated aq. NaHCO<sub>3</sub> and transferred to a separatory funnel. The crude mixture was extracted into EtOAc, and the combined organic layers were washed with H<sub>2</sub>O and brine. The crude mixture was dried with MgSO<sub>4</sub>, filtered through Celite, and concentrated. The crude residue was purified via column chromatography on silica gel eluting with 20:80 EtOAc:hexanes to provide 3β-acetoxy-D-homo-5α-androst-16-en-17a-one (0.9 g, 90 %) as a white solid; m.p. = 144-146 °C. <sup>1</sup>H NMR (400 MHz, CDCl<sub>3</sub>): 6.79-6.75 (m, 1H), 5.82-5.79 (m, 1H), 4.64-4.55 (m, 1H), 2.36 (dt, *J* = 19.4, 4.9 Hz, 1H), 1.96-1.83 (m, 2H), 1.93 (s, 3H), 1.80-1.67 (m, 3H), 1.60-1.52 (m, 2H), 1.50-1.36 (m, 3H), 1.32-1.03 (m, 6H), 0.97-0.89 (m, 1H), 0.92 (s, 3H), 0.85-0.76 (m, 1H), 0.74 (s, 3H), 0.65-0.59 (m, 1H); <sup>13</sup>C{<sup>1</sup>H} NMR (100 MHz, CDCl<sub>3</sub>): 205.3, 170.3, 147.6, 127.3, 73.2, 52.7, 46.5, 44.3, 43.7, 36.2, 35.30, 35.29, 33.6, 32.0, 30.3, 28.1, 27.10, 27.07, 21.2, 19.8, 15.5, 11.9. ν<sub>max</sub> (CaF<sub>2</sub>, CHCl<sub>3</sub>): 1722, 1667 cm<sup>-1</sup>. λ<sub>max</sub> (CH<sub>3</sub>CN): 335 nm. HRMS (ESI) m/z C<sub>22</sub>H<sub>32</sub>O<sub>3</sub>Na<sup>+</sup>: calc 367.224366, observed 367.224078.

Methyl 3 $\beta$ -(2',3',4',6'-tetra-*O*-acetyl- $\alpha$ -D-glucopyranosyloxy)-glycyrrhetinate<sup>88</sup>



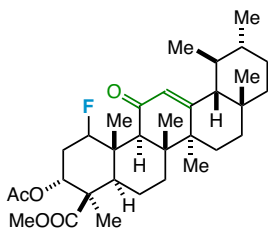
To a flame-dried amber round bottom equipped with a stir bar was added 18 $\beta$ -glycyrrhetic acid methyl ester (1.0 g, 2.1 mmol), Ag<sub>2</sub>O (0.96 g, 4.1 mmol), acetobromo- $\alpha$ -D-glucose (1.7 g, 4.1 mmol), CH<sub>2</sub>Cl<sub>2</sub> (30 mL), and CH<sub>3</sub>NO<sub>2</sub> (30 mL) under N<sub>2</sub>. The reaction mixture was stirred in the dark at rt. Three additional portions of Ag<sub>2</sub>O (0.96 g, 4.1 mmol) and acetobromo- $\alpha$ -D-glucose (1.7 g, 4.1 mmol) were added in 1 h intervals, and then the reaction mixture was stirred overnight. The reaction mixture was diluted with CHCl<sub>3</sub>, filtered through Celite, and transferred to a separatory funnel. The organic layer was washed with hot H<sub>2</sub>O (x3), dried with MgSO<sub>4</sub>, filtered through Celite, and concentrated. The crude residue was purified via column chromatography eluting with 30:70 EtOAc:hexanes to provide methyl 3 $\beta$ -(2',3',4',6'-tetra-*O*-acetyl- $\alpha$ -D-glucopyranosyloxy)-glycyrrhetinate (0.68 g, 40 %) as a white solid; m.p. = 225-226 °C. <sup>1</sup>H NMR (400 MHz, CDCl<sub>3</sub>): 5.64 (s, 1H), 5.18 (t, *J* = 9.5 Hz, 1H), 5.03-4.98 (m, 2H), 4.52 (d, *J* = 7.9 Hz, 1H), 4.24-4.20 (m, 1H), 4.08-4.05 (m, 1H), 3.69-3.64 (m, 1H), 3.66 (s, 3H), 3.09 (t, *J* = 8.0 Hz, 1H), 2.77 (dt, *J* = 13.4, 3.2 Hz, 1H), 2.29 (s, 1H), 2.04 (s, 3H), 2.00 (s, 3H), 1.99 (s, 3H), 1.98 (s, 3H), 1.92-1.87 (m, 1H), 1.84-1.73 (m, 4H), 1.65-1.52 (m, 3H), 1.42-1.36 (m, 2H), 1.40 (s, 3H), 1.33 (s, 3H), 1.30-1.27 (m, 2H), 1.18-1.15 (m, 1H), 1.12 (s, 3H), 1.10 (s, 3H), 1.09 (s, 3H), 1.01-0.97 (m, 1H), 0.95-0.87 (m, 1H), 0.91 (s, 3H), 0.78 (s, 3H), 0.74 (s, 3H), 0.69-0.66 (m, 1H); <sup>13</sup>C {<sup>1</sup>H} NMR (100 MHz, CDCl<sub>3</sub>): 200.3, 177.2, 170.9, 170.6, 169.7, 169.44, 169.39, 128.8, 103.2, 90.8, 73.2, 72.0, 71.8, 69.1, 62.6, 62.0, 55.6, 52.1, 48.7, 45.7, 44.2, 43.5, 41.4, 39.5, 39.3, 38.0, 37.1, 33.0, 32.1, 28.8, 28.6, 28.0, 27.2, 26.8, 26.7, 26.0, 23.6, 21.03, 20.99, 20.92, 20.89, 19.0, 17.7, 16.7, 16.6.  $\nu_{\max}$  (CaF<sub>2</sub>, CHCl<sub>3</sub>): 1725 (br), 1653 cm<sup>-1</sup>.  $\lambda_{\max}$  (CH<sub>3</sub>CN): 335 nm. HRMS (ESI) *m/z* C<sub>45</sub>H<sub>66</sub>O<sub>13</sub>H<sup>+</sup>: calc 815.457619, observed 815.457763.

## Characterization Data.



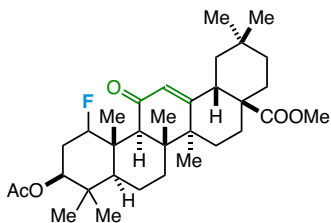
**Table 1. Compound 1.** The reaction was run according to the general procedure, and the major diastereomer was isolated. The crude material was subjected to gradient column chromatography on silica gel eluting with hexanes and EtOAc, followed by HPLC purification. Regiochemical assignment was made on the basis of 1) chemical shift in the  $^{19}\text{F}$  NMR spectrum that indicates a secondary fluoride on a cyclohexane ring, 2) disappearance of the diagnostic C1  $\text{H}_{\text{eq}}$  signal (dt at 2.76 ppm) in the  $^1\text{H}$  NMR spectrum concomitant with appearance of a  $^1\text{H}$  signal with the shift (5.58 ppm) and coupling constant ( $^2J_{\text{HF}} = 47$  Hz) that indicate a geminal fluoride, and 3) identification of  $^2J_{\text{CF}}$ - and  $^3J_{\text{CF}}$ -coupling to distinguishable peaks in the  $^{13}\text{C}$  NMR spectrum, i.e. C2, C9, C10, and C25 *vide infra*. Stereochemical assignment was made on the basis of 1) chemical shift and splitting in the  $^{19}\text{F}$  NMR spectrum that indicates  $\text{F}_{\text{ax}}$  on a cyclohexane ring and 2) accord with the calculated  $^{19}\text{F}$  NMR shift.

White solid; m.p. = 265-265.5 °C.  $^1\text{H}$  NMR (400 MHz,  $\text{CDCl}_3$ ): 5.68 (s, 1H), 5.58 (ddd,  $J = 46.6, 3.4, 2.2$  Hz, 1H), 4.92 (dd,  $J = 11.9, 5.1$  Hz, 1H), 3.69 (s, 3H), 3.13 (s, 1H), 2.12-2.06 (m, 2H), 2.05 (s, 3H), 2.04-1.91 (m, 4H), 1.83 (td,  $J = 13.6, 4.3$  Hz, 1H), 1.71-1.58 (m, 3H), 1.56-1.45 (m, 1H), 1.41-1.36 (m, 2H), 1.39 (s, 3H), 1.32-1.30 (m, 3H), 1.21-1.20 (m, 1H), 1.16 (d,  $J = 2.0$  Hz, 3H), 1.15 (s, 3H), 1.14 (s, 3H), 1.04-0.98 (m, 1H), 0.91 (s, 3H), 0.88 (s, 3H), 0.80 (s, 3H);  $^{13}\text{C}\{^1\text{H}\}$  NMR (100 MHz,  $\text{CDCl}_3$ ): 200.2, 176.9, 170.5, 169.8, 128.3, 94.1 (d,  $J = 172.9$  Hz, C1), 75.1, 52.6 (d,  $J = 8.1$  Hz, C9), 51.8, 48.4, 47.6, 45.2, 44.0, 43.5, 41.1, 40.9, 40.7, 37.9, 37.7, 32.1, 31.8, 31.1, 28.4 (d,  $J = 25.8$  Hz, C2), 28.2 (d,  $J = 21.7$  Hz, C10), 27.8, 26.5, 26.4, 23.3, 21.2, 18.9, 17.0, 16.5 (d,  $J = 5.9$  Hz, C25), 16.3;  $^{19}\text{F}$  NMR (282 MHz,  $\text{CDCl}_3$ ): -191.9 (m, 1F).  $\nu_{\text{max}}$  (ATR-IR): 1734 (br), 1653  $\text{cm}^{-1}$ . HRMS (ESI)  $m/z$   $\text{C}_{33}\text{H}_{49}\text{FO}_5\text{Na}^+$ : calc 567.345624, observed 567.345124.



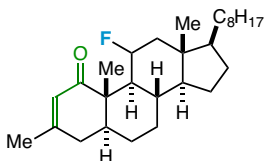
**Table 1. Compound 2.** The reaction was run according to the general procedure, and the product was isolated as a mixture of diastereomers. The crude material was subjected to gradient column chromatography on silica gel eluting with hexanes and EtOAc, followed by HPLC purification. Regiochemical and stereochemical assignments were made by analogy to compound 1.

Yellow oil.  $^1\text{H}$  NMR (400 MHz,  $\text{CDCl}_3$ ): 5.57 (s, 1H), 5.33 (t,  $J = 2.6$  Hz, 1H), 4.40-4.18 (m, 1H), 3.71-3.68 (m, 3H), 2.56-2.50 (m, 1H), 2.40 (s, 1H), 2.25-2.16 (m, 1H), 2.08 (s, 3H), 2.00-1.93 (m, 1H), 1.92-1.87 (m, 2H), 1.86-1.80 (m, 1H), 1.80-1.72 (m, 1H), 1.71-1.65 (m, 1H), 1.64-1.62 (m, 1H), 1.60-1.53 (m, 2H), 1.52-1.43 (m, 3H), 1.41-1.38 (m, 1H), 1.37-1.32 (m, 3H), 1.27-1.22 (m, 2H), 1.21-1.15 (m, 6H), 1.11-1.06 (m, 2H), 1.03 (s, 3H), 0.98-0.94 (m, 2H), 0.92-0.88 (m, 3H), 0.87-0.82 (m, 3H);  $^{13}\text{C}\{^1\text{H}\}$  NMR (100 MHz,  $\text{CDCl}_3$ ): 199.04, 198.98, 176.0, 170.2, 163.4, 162.9, 131.1, 131.0, 96.5 (d,  $J = 170.3$  Hz), 93.0 (d,  $J = 170.3$  Hz), 73.2, 60.3, 58.1, 54.1, 51.6, 50.4, 46.6, 46.2, 46.0, 45.1, 45.04, 44.97, 44.8, 44.0, 43.6, 38.7, 38.1, 37.90, 37.85, 37.8, 37.2, 35.9, 35.7, 35.6, 34.6, 32.8, 32.7, 32.0, 28.6, 28.4, 27.1, 26.5, 26.2, 26.1, 23.8, 23.6, 21.8, 21.7, 21.3, 20.8, 20.6, 18.7, 18.3, 17.1, 17.0, 15.22, 15.18, 13.1;  $^{19}\text{F}$  NMR (282 MHz,  $\text{CDCl}_3$ ): -177.7 (dm,  $J = 49.3$  Hz, 1F), -182.6 (m, 1F).  $\nu_{\text{max}}$  (ATR-IR): 1734 (br), 1662  $\text{cm}^{-1}$ . HRMS (ESI)  $m/z$   $\text{C}_{33}\text{H}_{49}\text{FO}_5\text{Na}^+$ : calc 567.345624, observed 567.345078.



**Table 1. Compound 3.** The reaction was run according to the general procedure, and the major diastereomer was isolated. The crude material was subjected to gradient column chromatography on silica gel eluting with hexanes and EtOAc, followed by HPLC purification. Regiochemical and stereochemical assignments were made by analogy to compound 1.

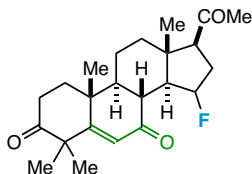
White solid; m.p. = 238-241 °C.  $^1\text{H}$  NMR (400 MHz,  $\text{CDCl}_3$ ): 5.65 (s, 1H), 5.62 (dm,  $J = 46.3$  Hz, 1H), 4.92 (dd,  $J = 12.0, 4.9$  Hz, 1H), 3.63 (s, 3H), 3.10 (s, 1H), 3.04-2.99 (m, 1H), 2.12-2.06 (m, 1H), 2.05 (s, 3H), 2.04-2.01 (m, 1H), 1.99-1.86 (m, 1H), 1.77-1.69 (m, 2H), 1.67-1.63 (m, 2H), 1.61-1.58 (m, 2H), 1.51-1.41 (m, 1H), 1.38 (s, 3H), 1.37-1.30 (m, 2H), 1.28-1.18 (m, 4H), 1.12 (d,  $J = 2.1$  Hz, 3H), 0.99-0.92 (m, 10H), 0.90 (s, 3H), 0.87 (s, 3H);  $^{13}\text{C}\{^1\text{H}\}$  NMR (100 MHz,  $\text{CDCl}_3$ ): 200.3, 177.5, 170.5, 169.2, 127.6, 95.0 (d,  $J = 172.5$  Hz, C1), 75.1, 52.6 (d,  $J = 8.1$  Hz, C9), 51.9, 47.7, 46.2, 44.8, 44.2, 43.8, 41.6, 41.0, 40.9, 37.9, 33.7, 32.8, 32.2, 31.6, 30.7, 28.3, 28.1, 27.8, 23.5, 23.4, 22.9, 21.2, 19.1, 16.9, 16.4, 16.3;  $^{19}\text{F}$  NMR (282 MHz,  $\text{CDCl}_3$ ): -192.2 (m, 1F).  $\nu_{\text{max}}$  (ATR-IR): 1734 (br), 1652  $\text{cm}^{-1}$ . HRMS (ESI)  $m/z$   $\text{C}_{33}\text{H}_{49}\text{FO}_5\text{Na}^+$ : calc 567.345624, observed 567.345195.



**Table 1. Compound 4.** The reaction was run according to the general procedure, and the major diastereomer was isolated. The crude material was subjected to gradient column chromatography on silica gel eluting with hexanes and EtOAc, followed by HPLC purification. Regiochemical assignment was made on the basis of 1) chemical shift in the  $^{19}\text{F}$  NMR spectrum that indicates a secondary fluoride on a cyclohexane ring, 2) identification of  $^3J_{\text{HF}}$ -coupling (10.3 Hz) to the diagnostic C9  $\text{H}_{\text{ax}}$  signal (ddd at 2.35) as confirmed by a  $^1\text{H}\{^{19}\text{F}\}$  NMR spectrum, and 3) downfield shifts of the C18 ( $\Delta\delta = 0.11$  ppm) and C19 ( $\Delta\delta = 0.21$  ppm) Me signals in the  $^1\text{H}$  NMR spectrum with respect to the starting material. Stereochemical assignment was made on the basis of 1) chemical shift and splitting in the  $^{19}\text{F}$  NMR spectrum that indicates  $\text{F}_{\text{eq}}$  on a cyclohexane ring, 2) identification of antiperiplanar vicinal coupling in the  $^1\text{H}$  NMR spectrum of  $\text{H}_{\text{ax}}$  at the C11 position to the axial hydrogen atoms at C9 and C12 (i.e. t,  $^3J_{\text{HH}} = 11.3$  Hz), 3) lack of long-range coupling of fluorine to the C18 and C19 Me hydrogen atoms in the  $^1\text{H}$  NMR spectrum, and 4) accord with the calculated  $^{19}\text{F}$  NMR shift.

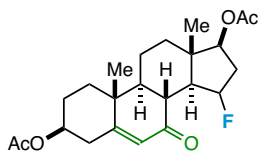
White solid; m.p. = 120-123 °C.  $^1\text{H}$  NMR (400 MHz,  $\text{CDCl}_3$ ): 5.71-5.70 (m, 1H), 4.56 (dtd,  $J = 48.2, 11.3, 4.2$  Hz, 1H), 2.35 (ddd,  $J = 11.7, 10.3, 4.1$  Hz, 1H), 2.21-2.13 (m, 1H), 2.02 (dd,  $J = 18.9, 4.9$  Hz, 1H), 1.96-1.85 (m, 2H), 1.82 (s, 3H), 1.81-1.74 (m, 1H), 1.71-1.58 (m, 3H), 1.56-1.44 (m, 3H), 1.40-1.19 (m,

8H), 1.17 (s, 3H), 1.16-0.94 (m, 5H), 0.92 (d,  $J = 6.6$  Hz, 3H), 0.87-0.85 (m, 6H), 0.74 (s, 3H);  $^{13}\text{C}\{^1\text{H}\}$  NMR (100 MHz,  $\text{CDCl}_3$ ): 204.6, 152.9, 125.5, 91.3 (d,  $J = 181.2$  Hz, C11), 56.3, 55.9, 49.4, 49.2, 46.6, 46.5, 46.4, 43.4, 43.34, 43.28, 39.4, 36.5, 35.9, 35.7, 34.7, 34.6, 29.7, 28.4, 28.01, 27.97, 23.9, 23.4, 22.8, 22.7, 22.5, 18.4, 13.7, 10.4;  $^{19}\text{F}$  NMR (282 MHz,  $\text{CDCl}_3$ ): -178.3 (dm,  $J = 48.2$  Hz, 1F).  $\nu_{\text{max}}$  (ATR-IR):  $1684\text{ cm}^{-1}$ . HRMS (ESI)  $m/z$   $\text{C}_{28}\text{H}_{45}\text{FONa}^+$ : calc 439.334665, observed 439.334655.



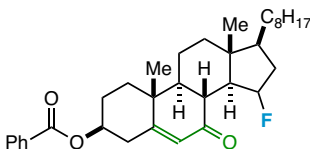
**Table 1. Compound 5.** The reaction was run according to the general procedure, and the major diastereomer was isolated. The crude material was subjected to gradient column chromatography on silica gel eluting with hexanes and EtOAc, followed by HPLC purification. Regiochemical assignment was made on the basis of 1) chemical shift in the  $^{19}\text{F}$  NMR spectrum that indicates a secondary fluoride, 2)  $^2J_{\text{HF}}$ -coupling in the  $^1\text{H}$  and  $^{19}\text{F}$  NMR spectra that indicates cyclopentane ring fluorination (52.8 Hz), and 3) identification of  $^2J_{\text{CF}}$ -coupling to distinguishable peaks in the  $^{13}\text{C}$  NMR spectrum, i.e. C14 and C16 *vide infra*. Stereochemical assignment was made on the basis of 1) chemical shift and splitting in the  $^{19}\text{F}$  NMR spectrum and 2) accord with the calculated  $^{19}\text{F}$  NMR shift. Assignments were confirmed by X-ray crystallography.

White solid; m.p. = 191-192 °C.  $^1\text{H}$  NMR (400 MHz,  $\text{CDCl}_3$ ): 6.03 (s, 1H), 5.40 (dm,  $J = 52.9$  Hz, 1H), 2.84-2.66 (m, 2H), 2.64-2.60 (m, 2H), 2.39 (t,  $J = 11.5$  Hz, 1H), 2.16 (s, 3H), 2.15-1.96 (m, 3H), 1.93-1.73 (m, 5H), 1.58-1.55 (m, 1H), 1.34 (s, 6H), 1.07 (s, 3H), 0.72 (s, 3H);  $^{13}\text{C}\{^1\text{H}\}$  NMR (100 MHz,  $\text{CDCl}_3$ ): 212.2, 207.7, 198.1, 174.7, 125.0, 93.2 (d,  $J = 178.0$  Hz, C15), 59.7, 58.8 (d,  $J = 19.9$  Hz, C14), 50.3, 49.5, 45.92, 45.86, 42.7, 38.2 (d,  $J = 22.5$  Hz, C16), 33.5, 33.3, 33.2, 31.5, 30.9, 28.4, 26.3, 21.6, 17.7, 14.3;  $^{19}\text{F}$  NMR (282 MHz,  $\text{CDCl}_3$ ): -162.8 (dm,  $J = 52.8$  Hz, 1F).  $\nu_{\text{max}}$  (ATR-IR): 1706 (br),  $1669\text{ cm}^{-1}$ . HRMS (ESI)  $m/z$   $\text{C}_{23}\text{H}_{31}\text{FO}_3\text{Na}^+$ : calc 397.214944, observed 397.214956.



**Table 1. Compound 6.** The reaction was run according to the general procedure, and the major diastereomer was isolated. The crude material was subjected to gradient column chromatography on silica gel eluting with hexanes and EtOAc, followed by HPLC purification. Regiochemical and stereochemical assignments were made by analogy to compound 5.

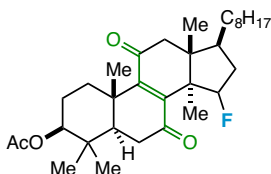
White solid; m.p. = 215-216.5 °C.  $^1\text{H}$  NMR (400 MHz,  $\text{CDCl}_3$ ): 5.80 (d,  $J = 2.0$  Hz, 1H), 5.24 (dm,  $J = 52.2$  Hz, 1H), 4.89 (t,  $J = 9.1$  Hz, 1H), 4.77-4.69 (m, 1H), 2.62 (ddd,  $J = 14.3, 5.0, 2.2$  Hz, 1H), 2.51-2.33 (m, 3H), 2.22-2.08 (m, 1H), 2.07-2.04 (m, 6H), 2.03-1.94 (m, 2H), 1.77-1.58 (m, 5H), 1.55-1.44 (m, 1H), 1.37-1.23 (m, 2H), 1.17 (s, 3H), 0.83 (s, 3H);  $^{13}\text{C}\{^1\text{H}\}$  NMR (100 MHz,  $\text{CDCl}_3$ ): 198.0, 170.7, 170.2, 164.9, 127.1, 92.1 (d,  $J = 181.0$  Hz, C15), 78.5 (d,  $J = 1.8$  Hz, C17), 71.7, 53.4 (d,  $J = 19.5$  Hz, C14), 50.3, 45.1, 45.0, 43.1, 37.9, 37.7, 36.9, 36.6, 36.0, 35.7, 27.3, 21.2, 21.0, 20.8, 17.9, 13.2;  $^{19}\text{F}$  NMR (282 MHz,  $\text{CDCl}_3$ ): -162.7 (m, 1F).  $\nu_{\text{max}}$  (ATR-IR): 1733 (br), 1675  $\text{cm}^{-1}$ . HRMS (ESI)  $m/z$   $\text{C}_{23}\text{H}_{31}\text{FO}_5\text{Na}^+$ : calc 429.204773, observed 429.204889.



**Table 1. Compound 7.** The reaction was run according to the general procedure, and the major diastereomer was isolated. The crude material was subjected to gradient column chromatography on silica gel eluting with hexanes and EtOAc, followed by HPLC purification. Regiochemical and stereochemical assignments were made by analogy to compound 5.

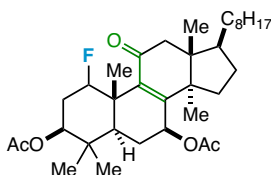
White solid; m.p. = 144.5-146 °C.  $^1\text{H}$  NMR (400 MHz,  $\text{CDCl}_3$ ): 8.05-8.03 (m, 2H), 7.59-7.55 (m, 1H), 7.46-7.43 (m, 2H), 5.85 (d,  $J = 2.0$  Hz, 1H), 5.29 (dm,  $J = 53.2$  Hz, 1H), 5.04-4.96 (m, 1H), 2.78-2.73 (m, 1H), 2.67-2.60 (m, 1H), 2.33 (t,  $J = 11.3$  Hz, 1H), 2.20-2.09 (m, 1H), 2.08-1.97 (m, 2H), 1.95-1.79 (m, 2H), 1.78-1.71 (m, 1H), 1.70-1.58 (m, 4H), 1.57-1.44 (m, 3H), 1.44-1.23 (m, 5H), 1.20 (s, 3H), 1.16-1.04 (m, 3H), 0.94 (d,  $J = 6.5$  Hz, 3H), 0.87 (d,  $J = 6.7$  Hz, 3H), 0.86 (d,  $J = 6.6$  Hz, 3H), 0.74 (s, 3H);  $^{13}\text{C}\{^1\text{H}\}$

NMR (100 MHz, CDCl<sub>3</sub>): 198.6, 165.8, 164.6, 133.0, 130.2, 129.6, 128.4, 127.6, 94.0 (d, *J* = 175.8 Hz, C15), 72.4, 58.4 (d, *J* = 18.4 Hz, C14), 52.7, 50.6, 45.2, 45.1, 43.2, 39.4, 39.2, 38.0, 37.8, 37.7, 36.0, 35.7, 34.9, 28.0, 27.4, 23.8, 22.8, 22.5, 21.3, 18.5, 18.0, 13.0; <sup>19</sup>F NMR (282 MHz, CDCl<sub>3</sub>): -160.7 (m, 1F).  $\nu_{\max}$  (ATR-IR): 1717, 1675 cm<sup>-1</sup>. HRMS (ESI) *m/z* C<sub>34</sub>H<sub>47</sub>FO<sub>3</sub>Na<sup>+</sup>: calc 545.340145, observed 545.339881.



**Table 1. Compound 8.** The reaction was run according to the general procedure, and the major diastereomer was isolated. The crude material was subjected to gradient column chromatography on silica gel eluting with hexanes and EtOAc, followed by HPLC purification. Regiochemical and stereochemical assignments were made by analogy to compound 5.

Pale yellow solid; m.p. = 126-129 °C. <sup>1</sup>H NMR (400 MHz, CDCl<sub>3</sub>): 5.38 (dm, *J* = 53.1 Hz, 1H), 4.53 (dd, *J* = 11.4, 5.1 Hz, 1H), 2.93 (dt, *J* = 13.9, 3.7 Hz, 1H), 2.80-2.75 (m, 1H), 2.65-2.40 (m, 4H), 2.06 (s, 3H), 1.82-1.60 (m, 5H), 1.57-1.55 (m, 1H), 1.47-1.36 (m, 4H), 1.31-1.21 (m, 1H), 1.19-1.15 (m, 6H), 1.14 (d, *J* = 2.2 Hz, 3H), 1.01 (d, *J* = 3.8 Hz, 3H), 0.96 (s, 3H), 0.91-0.86 (m, 12H); <sup>13</sup>C{<sup>1</sup>H} NMR (100 MHz, CDCl<sub>3</sub>): 201.6, 201.5, 170.8, 152.2, 147.9, 96.2 (d, *J* = 186.5 Hz, C15), 79.2, 52.7 (d, *J* = 17.3 Hz, C14), 52.4, 51.1, 49.4, 46.57, 46.55, 40.1, 39.3, 37.9, 37.0 (d, *J* = 20.6 Hz, C16), 36.2, 36.1, 35.5, 33.6, 28.0, 27.9, 23.9, 22.8, 22.6, 22.54, 22.48, 21.2, 18.4, 17.6, 17.2, 17.1, 16.6; <sup>19</sup>F NMR (282 MHz, CDCl<sub>3</sub>): -159.1 (m, 1F).  $\nu_{\max}$  (ATR-IR): 1734, 1679 (br) cm<sup>-1</sup>. HRMS (ESI) *m/z* C<sub>32</sub>H<sub>49</sub>FO<sub>4</sub>Na<sup>+</sup>: calc 539.350709, observed 539.350584.

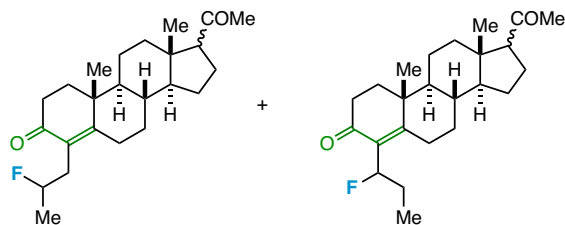


**Table 1. Compound 9.** The reaction was run according to the general procedure, and the major diastereomer was isolated. The crude material was subjected to gradient column chromatography on silica



gel eluting with hexanes and EtOAc, followed by HPLC purification. Regiochemical and stereochemical assignments were made by analogy to compound **1**.

Clear oil.  $^1\text{H}$  NMR (400 MHz,  $\text{CDCl}_3$ ): 5.99 (dm,  $J = 45.4$  Hz, 1H), 5.45-5.44 (m, 1H), 5.11-5.06 (m, 1H), 4.99 (dd,  $J = 12.2, 4.7$  Hz, 1H), 2.74 (d,  $J = 17.8$  Hz, 1H), 2.51 (d,  $J = 17.5$  Hz, 1H), 2.22-2.12 (m, 1H), 2.10 (s, 3H), 2.06 (s, 4H), 2.03-1.93 (m, 2H), 1.91-1.70 (m, 8H), 1.68-1.55 (m, 3H), 1.47-1.31 (m, 5H), 1.28-1.23 (m, 1H), 1.21 (s, 3H), 1.09 (s, 3H), 0.95-0.91 (m, 2H), 0.89-0.85 (m, 8H), 0.84-0.30 (m, 1H), 0.79 (s, 3H);  $^{13}\text{C}\{^1\text{H}\}$  NMR (151 MHz,  $\text{CDCl}_3$ ): 200.1, 170.5, 170.1, 159.3, 139.8, 92.2 (d,  $J = 172.1$  Hz, C1), 70.5, 69.9, 51.8, 51.4, 51.0, 50.6, 50.0, 47.7, 42.7, 39.7, 37.4, 37.2, 36.2, 36.0, 34.0, 33.9, 30.0, 29.7, 29.1, 27.9, 27.6, 27.2, 25.8, 24.9, 21.3, 18.4, 17.7, 17.1, 16.8, 16.4;  $^{19}\text{F}$  NMR (282 MHz,  $\text{CDCl}_3$ ): -189.3 (m, 1F).  $\nu_{\text{max}}$  (ATR-IR): 1740 (br), 1662  $\text{cm}^{-1}$ . HRMS (ESI)  $m/z$   $\text{C}_{34}\text{H}_{53}\text{FO}_5\text{Na}^+$ : calc 583.376924, observed 583.377088.



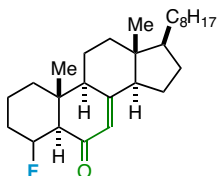
**Table 1. Compound 10a.** The reaction was run according to the general procedure, and the product was isolated as a mixture of diastereomers. The crude material was subjected to gradient column chromatography on silica gel eluting with hexanes and EtOAc, followed by HPLC purification. Regiochemical assignment was made on the basis of 1) chemical shift and complex splitting in the  $^{19}\text{F}$  NMR spectrum that indicate a secondary fluoride in the homoallylic position (dm,  $^2J_{\text{HF}} \approx 49$  Hz) and 2) identification of  $^3J_{\text{HF}}$ - and  $^3J_{\text{HF}}$ -coupling to the diagnostic side chain Me hydrogen atoms, i.e. dd,  $J = 23.8, 6.2$  Hz at 1.32 ppm (Me, isomer 1) and dd,  $J = 23.9, 6.2$  Hz at 1.29 ppm (Me, isomer 2). No stereochemical assignment was made.

Clear oil.  $^1\text{H}$  NMR (400 MHz,  $\text{CDCl}_3$ ): 4.60 (dm,  $J = 48.9$  Hz, 1H), 2.87-2.80 (m, 1H), 2.77-2.56 (m, 2H), 2.55-2.50 (m, 1H), 2.44-2.36 (m, 1H), 2.28-2.14 (m, 2H), 2.12 (s, 3H), 2.11-2.04 (m, 1H), 2.03-1.97 (m, 1H), 1.91-1.84 (m, 1H), 1.74-1.62 (m, 5H), 1.47-1.39 (m, 2H), 1.35-1.25 (m, 4H), 1.21-1.19 (m, 3H), 1.18-1.11 (m, 1H), 1.08-0.96 (m, 3H), 0.67 (s, 3H);  $^{13}\text{C}$  NMR (151 MHz,  $\text{CDCl}_3$ ): 209.4, 198.6, 166.9, 128.3,

93.5, 91.7, 90.5, 89.7, 64.0, 63.1, 60.5, 56.5, 55.7, 54.4, 53.9, 45.5, 44.3, 44.0, 40.1, 39.6, 39.4, 38.8, 35.9, 35.7, 35.1, 34.9, 34.6, 34.3, 33.8, 32.9, 32.7, 32.6, 31.9, 31.0, 29.7, 28.9, 28.1, 27.2, 25.1, 24.2, 23.7, 23.4, 22.9, 22.0, 21.6, 21.5, 21.1, 20.8, 20.6, 20.2, 19.1, 18.3, 17.4, 16.6, 14.6, 13.8, 13.0;  $^{19}\text{F}$  NMR (282 MHz,  $\text{CDCl}_3$ ): -172.0 (m, 1F).  $\nu_{\text{max}}$  (ATR-IR): 1704, 1662  $\text{cm}^{-1}$ . HRMS (ESI)  $m/z$   $\text{C}_{24}\text{H}_{35}\text{FO}_2\text{Na}^+$ : calc 397.251330, observed 397.251200.

**Compound 10b.** The reaction was run according to the general procedure, and the major diastereomer was isolated. The crude material was subjected to gradient column chromatography on silica gel eluting with hexanes and EtOAc, followed by HPLC purification. Regiochemical assignment was made on the basis of 1) chemical shift and splitting in the  $^{19}\text{F}$  NMR spectrum that indicate a secondary fluoride in the allylic position (ddd,  $^2J_{\text{HF}} \approx 49$  Hz,  $^3J_{\text{HF}} \approx 30$ , 12 Hz) and 2) analogy to compound **14**. No stereochemical assignment was made.

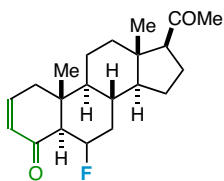
Clear oil.  $^1\text{H}$  NMR (400 MHz,  $\text{CDCl}_3$ ): 5.69 (ddd,  $J = 47.6, 9.2, 5.0$  Hz, 1H), 3.13 (dt,  $J = 13.9, 3.2$  Hz, 1H), 2.56-2.50 (m, 1H), 2.41-2.30 (m, 2H), 2.28-2.16 (m, 1H), 2.12 (s, 3H), 2.10-1.84 (m, 5H), 1.76-1.59 (m, 6H), 1.47-1.38 (m, 2H), 1.34-1.22 (m, 1H), 1.21 (s, 3H), 1.19-1.02 (m, 3H), 0.96 (t,  $J = 7.5$  Hz, 3H), 0.67 (s, 3H);  $^{19}\text{F}$  NMR (282 MHz,  $\text{CDCl}_3$ ): -186.5 (ddd,  $J = 47.6, 30.4, 12.0$  Hz, 1F).  $\nu_{\text{max}}$  (ATR-IR): 1705, 1666  $\text{cm}^{-1}$ . HRMS (ESI)  $m/z$   $\text{C}_{24}\text{H}_{35}\text{FO}_2\text{Na}^+$ : calc 397.251330, observed 397.251294.



**Table 1. Compound 11.** The reaction was run according to the general procedure, and the product was isolated as a mixture of diastereomers. The crude material was subjected to gradient column chromatography on silica gel eluting with hexanes and EtOAc, followed by HPLC purification. Regiochemical assignment was made on the basis of 1) chemical shift in the  $^{19}\text{F}$  NMR spectrum that indicates a secondary fluoride on a cyclohexane ring and 2) identification of  $^3J_{\text{HF}}$ - and  $^3J_{\text{HH}}$ -coupling to the hydrogen atom at C5 in the  $^1\text{H}$  NMR spectrum consistent with fluorine in the C4 position, i.e. dd,  $J = 13.1, 9.7$  Hz at 2.39 ppm. Stereochemical assignment was made on the basis of 1) chemical shift and splitting in

the  $^{19}\text{F}$  NMR spectrum that indicates  $F_{\text{eq}}$  on a cyclohexane ring and 2) accord with the calculated  $^{19}\text{F}$  NMR shift.

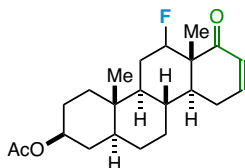
White solid; m.p. = 156-158 °C.  $^1\text{H}$  NMR (400 MHz,  $\text{CDCl}_3$ ): 5.75-5.74 (m, 1H), 5.01 (dm,  $J = 47.7$  Hz, 1H), 2.39 (dd,  $J = 13.1, 9.7$  Hz, 1H), 2.30-2.21 (m, 2H), 2.15- 1.86 (m, 4H), 1.78-1.69 (m, 3H), 1.63-1.49 (m, 6H), 1.48-1.42 (m, 3H), 1.40-1.31 (m, 6H), 1.29-1.22 (m, 2H), 1.05-0.97 (m, 2H), 0.93 (d,  $J = 6.4$  Hz, 3H), 0.88-0.86 (m, 6H), 0.84 (s, 3H);  $^{13}\text{C}\{^1\text{H}\}$  NMR (151 MHz,  $\text{CDCl}_3$ ): 198.6, 162.5, 123.2, 87.2 (d,  $J = 169.8$  Hz, C4), 59.2, 56.3, 55.6, 50.9, 44.8, 41.2, 39.4, 38.8, 37.4, 36.0, 31.9, 31.8, 29.7, 28.0, 27.7, 23.9, 22.8, 22.5, 21.7, 19.2, 18.8, 15.0, 12.3;  $^{19}\text{F}$  NMR (282 MHz,  $\text{CDCl}_3$ ): -174.1 (m, 1F).  $\nu_{\text{max}}$  (ATR-IR): 1684  $\text{cm}^{-1}$ . HRMS (ESI)  $m/z$   $\text{C}_{27}\text{H}_{43}\text{FONa}^+$ : calc 425.319015, observed 425.318928.



**Table 1. Compound 12.** The reaction was run according to the general procedure, and the major diastereomer was isolated. The crude material was subjected to gradient column chromatography on silica gel eluting with hexanes and EtOAc, followed by HPLC purification. Regiochemical assignment was made on the basis of 1) chemical shift in the  $^{19}\text{F}$  NMR spectrum that indicates a secondary fluoride on a cyclohexane ring, 2) identification of  $^2J_{\text{HF}}$ - and  $^3J_{\text{HH}}$ -coupling constants consistent with fluorine in the C6 position, and 3) identification of  $^2J_{\text{CF}}$ - and  $^3J_{\text{CF}}$ -coupling to distinguishable peaks in the  $^{13}\text{C}$  NMR spectrum, e.g. diagnostic coupling to C5 *vide infra*. Stereochemical assignment was made on the basis of 1) chemical shift and splitting in the  $^{19}\text{F}$  NMR spectrum, 2) identification of antiperiplanar vicinal coupling in the  $^1\text{H}$  NMR spectrum of  $\text{H}_{\text{ax}}$  at the C6 position to the axial hydrogen atoms at C5 and C7 (i.e.  $^3J_{\text{HH}} = 11.2, 9.9$  Hz), and 3) accord with the calculated  $^{19}\text{F}$  NMR shift.

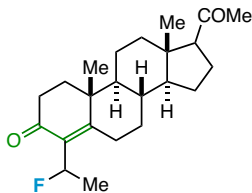
White solid; m.p. = 184-186 °C.  $^1\text{H}$  NMR (400 MHz,  $\text{CDCl}_3$ ): 6.76-6.71 (m, 1H), 6.04 (ddd,  $J = 10.1, 2.8, 1.4$  Hz, 1H), 4.94 (dddd,  $J = 47.7, 11.2, 9.9, 5.6$  Hz, 1H), 2.56-2.47 (m, 2H), 2.35-2.32 (m, 2H), 2.28-2.14 (m, 2H), 2.12 (s, 3H), 2.10-2.06 (m, 1H), 1.78-1.66 (m, 2H), 1.58-1.55 (m, 1H), 1.49-1.33 (m, 3H), 1.31-1.08 (m, 4H), 0.85 (s, 3H), 0.62 (s, 3H);  $^{13}\text{C}\{^1\text{H}\}$  NMR (100 MHz,  $\text{CDCl}_3$ ): 209.1, 198.5, 145.1, 129.3, 86.6 (d,  $J = 172.5$  Hz, C6), 63.4, 59.5 (d,  $J = 14.7$  Hz, C5), 56.0, 52.7, 43.9, 42.0 (d,  $J = 7.4$  Hz), 41.1, 38.4,

37.1 (d,  $J = 18.8$  Hz), 33.2 (d,  $J = 11.1$  Hz), 31.4, 24.2, 22.8, 20.7, 14.0, 13.2;  $^{19}\text{F}$  NMR (282 MHz,  $\text{CDCl}_3$ ): -175.1 (dm,  $J = 47.7$  Hz, 1F).  $\nu_{\text{max}}$  (ATR-IR): 1690 (br)  $\text{cm}^{-1}$ . HRMS (ESI)  $m/z$   $\text{C}_{21}\text{H}_{29}\text{FO}_2\text{Na}^+$ : calc 355.204379, observed 355.204463.



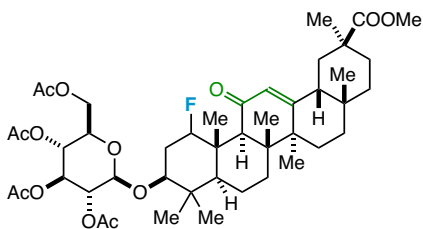
**Table 1. Compound 13.** The reaction was run according to the general procedure, and the major diastereomer was isolated. The crude material was subjected to gradient column chromatography on silica gel eluting with hexanes and EtOAc, followed by HPLC purification. Regiochemical assignment was made on the basis of 1) chemical shift in the  $^{19}\text{F}$  NMR spectrum that indicates a secondary fluoride on a cyclohexane ring, 2) identification of  $^4J_{\text{HF}}$ -coupling to the distinguishable C18 Me hydrogen atoms in the  $^1\text{H}$  NMR spectrum, and 3) identification of  $^2J_{\text{CF}}$ - and  $^3J_{\text{CF}}$ -coupling to distinguishable peaks in the  $^{13}\text{C}$  NMR spectrum, i.e. C11, C13, C17a, and C18 *vide infra*. Stereochemical assignment was made on the basis of 1) chemical shift and splitting in the  $^{19}\text{F}$  NMR spectrum that indicates  $\text{F}_{\text{ax}}$  on a cyclohexane ring and 2) accord with the calculated  $^{19}\text{F}$  NMR shift.

White solid; m.p. = 135-137 °C.  $^1\text{H}$  NMR (400 MHz,  $\text{CDCl}_3$ ): 6.92-6.87 (m, 1H), 5.98-5.95 (m, 1H), 5.17 (dm,  $J = 46.8$  Hz, 1H), 4.72-4.64 (m, 1H), 2.56-2.49 (m, 1H), 2.16-2.09 (m, 1H), 2.05-1.96 (m, 2H), 2.02 (s, 3H), 1.89-1.80 (m, 2H), 1.73-1.63 (m, 2H), 1.58-1.18 (m, 8H), 1.10-0.97 (m, 2H), 0.96 (d,  $J = 1.1$  Hz, 3H), 0.82 (s, 3H);  $^{13}\text{C}\{^1\text{H}\}$  NMR (100 MHz,  $\text{CDCl}_3$ ): 201.0 (d,  $J = 0.7$  Hz, C17a), 170.6, 148.2, 128.2, 91.0 (d,  $J = 172.5$  Hz, C12), 73.3, 48.3 (d,  $J = 19.2$  Hz, C13), 45.9, 43.9, 39.8, 36.1, 35.2, 34.7, 33.8, 30.1, 28.2, 27.2, 26.3, 25.4 (d,  $J = 21.4$  Hz, C11), 21.4, 14.9 (d,  $J = 7.0$  Hz, C18), 11.9;  $^{19}\text{F}$  NMR (282 MHz,  $\text{CDCl}_3$ ): -185.6 (m, 1F).  $\nu_{\text{max}}$  (ATR-IR): 1734, 1684  $\text{cm}^{-1}$ . HRMS (ESI)  $m/z$   $\text{C}_{22}\text{H}_{31}\text{FO}_3\text{Na}^+$ : calc 385.214944, observed 385.214903.



**Table 1. Compound 14.** The reaction was run according to the general procedure, and the product was isolated as a mixture of diastereomers. The crude material was subjected to gradient column chromatography on silica gel eluting with hexanes and EtOAc, followed by HPLC purification. Regiochemical assignment was made on the basis of 1) chemical shift and splitting in the  $^{19}\text{F}$  NMR spectrum that indicate a secondary fluoride in the allylic position (dq,  $^2J_{\text{HF}} \approx 45$  Hz,  $^3J_{\text{HF}} \approx 22$  Hz) and 2) identification of  $^3J_{\text{HH}}$ - and  $^3J_{\text{HF}}$ -coupling to the diagnostic side chain Me hydrogen atoms, i.e. dd,  $J = 22.2$ , 6.7 Hz at 1.48 ppm (Me, minor isomer) and dd,  $J = 22.3$ , 6.7 Hz at 1.46 ppm (Me, major isomer). No stereochemical assignment was made.

White solid; m.p. = 123.5-125 °C.  $^1\text{H}$  NMR (400 MHz,  $\text{CDCl}_3$ ): 6.01-5.83 (m, 1H), 3.19-3.13 (m, 1H), 2.52 (t,  $J = 9.0$  Hz, 1H), 2.45-2.34 (m, 2H), 2.26-1.85 (m, 8H), 1.75-1.61 (m, 4H), 1.59-1.54 (m, 1H), 1.53-1.42 (m, 3H), 1.32-1.23 (m, 1H), 1.21 (s, 3H), 1.19-1.12 (m, 2H), 1.10-1.02 (m, 2H), 0.95-0.86 (m, 1H), 0.67 (s, 3H);  $^{13}\text{C}\{^1\text{H}\}$  NMR (100 MHz,  $\text{CDCl}_3$ ): 209.7, 209.6, 197.4, 197.3, 169.7, 168.5, 133.0, 132.9, 132.4, 132.2, 86.8 (d,  $J = 166.2$  Hz), 86.0 (d,  $J = 167.0$  Hz), 63.84, 63.82, 56.42, 56.37, 54.9, 44.28, 44.26, 40.08, 40.07, 40.03, 40.02, 39.10, 39.08, 35.7, 35.1, 35.0, 33.84, 33.83, 32.6, 32.3, 31.82, 31.80, 27.6, 27.5, 24.62, 24.61, 23.3, 23.2, 21.6, 21.4, 21.3, 21.2, 17.84, 17.82, 13.7;  $^{19}\text{F}$  NMR (282 MHz,  $\text{CDCl}_3$ ): -174.7 (dq,  $J = 44.2$ , 21.8 Hz, 1F), -178.0 (dq,  $J = 44.7$ , 22.4 Hz, 1F).  $\nu_{\text{max}}$  (ATR-IR): 1704, 1669  $\text{cm}^{-1}$ . HRMS (ESI) m/z  $\text{C}_{23}\text{H}_{33}\text{FO}_2\text{Na}^+$ : calc 383.235680, observed 383.235663.



**Fig. 3. Compound 15.** The reaction was run according to the general procedure, and the major diastereomer was isolated. The crude material was subjected to gradient column chromatography on silica gel eluting with hexanes and EtOAc, followed by HPLC purification. Regiochemical and stereochemical assignments were made by analogy to compound 1.

White solid; m.p. = 225-226 °C.  $^1\text{H}$  NMR (400 MHz,  $\text{CDCl}_3$ ): 5.70 (s, 1H), 5.60 (dm,  $J = 46.9$  Hz, 1H), 5.25-5.19 (m, 1H), 5.08-5.00 (m, 2H), 4.54 (d,  $J = 8.0$  Hz, 1H), 4.28 (dd,  $J = 12.1, 6.4$  Hz, 1H), 4.11 (dd,  $J = 12.1, 2.3$  Hz, 1H), 3.76-3.72 (m, 1H), 3.71 (s, 3H), 3.50 (dd,  $J = 7.3, 4.8$  Hz, 1H), 3.08 (s, 1H), 2.39-2.34 (m, 1H), 2.18-2.11 (m, 1H), 2.10 (s, 3H), 2.06-2.03 (m, 7H), 2.02 (s, 3H), 2.01-1.93 (m, 2H), 1.89-1.80 (m, 1H), 1.69-1.60 (m, 3H), 1.55-1.41 (m, 3H), 1.40-1.39 (m, 3H), 1.38-1.18 (m, 7H), 1.16-1.12 (m, 8H), 1.11-1.07 (m, 1H), 1.00-0.98 (m, 2H), 0.83 (s, 3H), 0.79 (s, 3H);  $^{13}\text{C}\{^1\text{H}\}$  NMR (151 MHz,  $\text{CDCl}_3$ ): 200.2, 176.9, 170.8, 170.4, 169.8, 169.5, 169.2, 128.4, 102.9, 94.8 (d,  $J = 169.8$  Hz, C1), 84.7, 72.9, 71.7, 68.8, 62.3, 52.6, 51.8, 48.5, 47.8, 45.2, 44.1, 43.5, 43.2, 41.1, 40.7, 38.9, 37.8, 32.7, 32.1, 31.9, 31.1, 30.5, 29.7, 28.6, 28.4, 27.8, 27.3, 26.5, 23.3, 22.7, 20.7, 18.9, 17.0, 16.5, 15.9;  $^{19}\text{F}$  NMR (282 MHz,  $\text{CDCl}_3$ ): -191.8 (m, 1F).  $\nu_{\text{max}}$  (ATR-IR): 1751 (br), 1653  $\text{cm}^{-1}$ . HRMS (ESI)  $m/z$   $\text{C}_{45}\text{H}_{65}\text{FO}_{13}\text{H}^+$ : calc 855.430141, observed 855.429804.

### 12.11 Experimental Details for Chapter 11.

**Single Crystal X-ray Crystallography.** All reflection intensities were measured at 110(2) K using a SuperNova diffractometer (equipped with Atlas detector) with Cu  $K\alpha$  radiation ( $\lambda = 1.54178$  Å) under the program CrysAlisPro (Version 1.171.36.32 Agilent Technologies, 2013). The same program was used to refine the cell dimensions and for data reduction. The structure was solved with the program SHELXS-2014/7 (Sheldrick, 2015) and was refined on  $F^2$  with SHELXL-2014/7 (Sheldrick, 2015). Analytical numeric absorption correction using a multifaceted crystal model was applied using CrysAlisPro. The temperature of the data collection was controlled using the system Cryojet (manufactured by Oxford

Instruments). The H atoms were placed at calculated positions using the instructions AFIX 13, AFIX 23, AFIX 43, AFIX 137 or AFIX 147 with isotropic displacement parameters having values 1.2 or 1.5  $U_{eq}$  of the attached C or O atoms. The structure is ordered.

The absolute configuration was established by anomalous-dispersion effects in diffraction measurements on the crystal, and the Flack and Hooft parameters refine to 0.004(5) and 0.000(2), respectively.

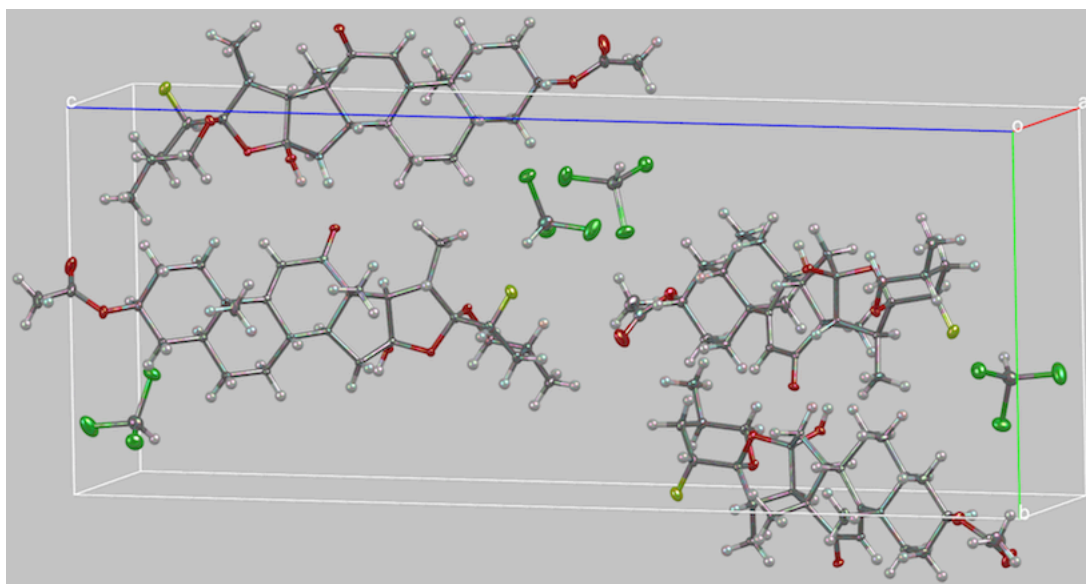
**Table 12.13** Crystallographic Data for **2**:CHCl<sub>3</sub>.

	2:CHCl <sub>3</sub>
Crystal data	
Chemical formula	C <sub>29</sub> H <sub>41</sub> FO <sub>6</sub> ·CHCl <sub>3</sub>
$M_r$	623.98
Crystal system, space group	Orthorhombic, $P2_12_12_1$
Temperature (K)	110
$a, b, c$ (Å)	6.62124 (7), 13.29651 (13), 34.1798 (4)
$V$ (Å <sup>3</sup> )	3009.17 (6)
$Z$	4
Radiation type	Cu $K\alpha$
$\mu$ (mm <sup>-1</sup> )	3.16
Crystal size (mm)	0.68 × 0.43 × 0.12
Data collection	
Diffractometer	SuperNova, Dual, Cu at zero, Atlas
Absorption correction	Analytical <i>CrysAlis PRO</i> , Agilent Technologies, Version 1.171.36.32 (release 02-

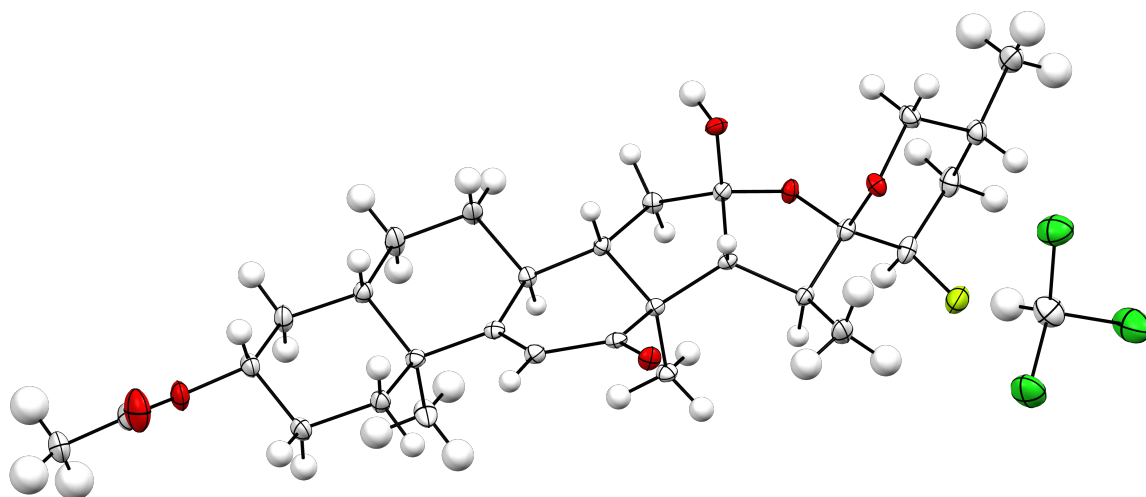
	08-2013 CrysAlis171 .NET) (compiled Aug 2 2013,16:46:58) Analytical numeric absorption correction using a multifaceted crystal model based on expressions derived by R.C. Clark & J.S. Reid. (Clark, R. C. & Reid, J. S. (1995). Acta Cryst. A51, 887-897)
$T_{\min}, T_{\max}$	0.295, 0.719
No. of measured, independent and observed [ $I > 2s(I)$ ] reflections	19696, 5910, 5798
$R_{\text{int}}$	0.026
$(\sin \theta/\lambda)_{\text{max}}$ ( $\text{\AA}^{-1}$ )	0.616
Refinement	
$R[F^2 > 2s(F^2)], wR(F^2), S$	0.035, 0.101, 1.09
No. of reflections	5910
No. of parameters	367
H-atom treatment	H-atom parameters constrained
$D\rho_{\text{max}}, D\rho_{\text{min}}$ ( $\text{e \AA}^{-3}$ )	0.65, -0.45
Absolute structure	Flack x determined using 2420 quotients $[(I^+)-(I^-)]/[(I^+)+(I^-)]$ (Parsons, Flack and Wagner, Acta Cryst. B69 (2013) 249-259).
Absolute structure Flack parameter	0.004 (5)

Computer programs: *CrysAlis PRO*, Agilent Technologies, Version 1.171.36.32 (release 02-08-2013 CrysAlis171 .NET) (compiled Aug 2 2013, 16:46:58), *SHELXS2014/7* (Sheldrick, 2015), *SHELXL2014/7* (Sheldrick, 2015), *SHELXTL* v6.10 (Sheldrick, 2008).<sup>89</sup>





**Figure 12.28** Packing diagram screenshot for **2:CHCl<sub>3</sub>** crystal.



**Figure 12.29** Thermal ellipsoid plot for **2:CHCl<sub>3</sub>** crystal (50% probability level).

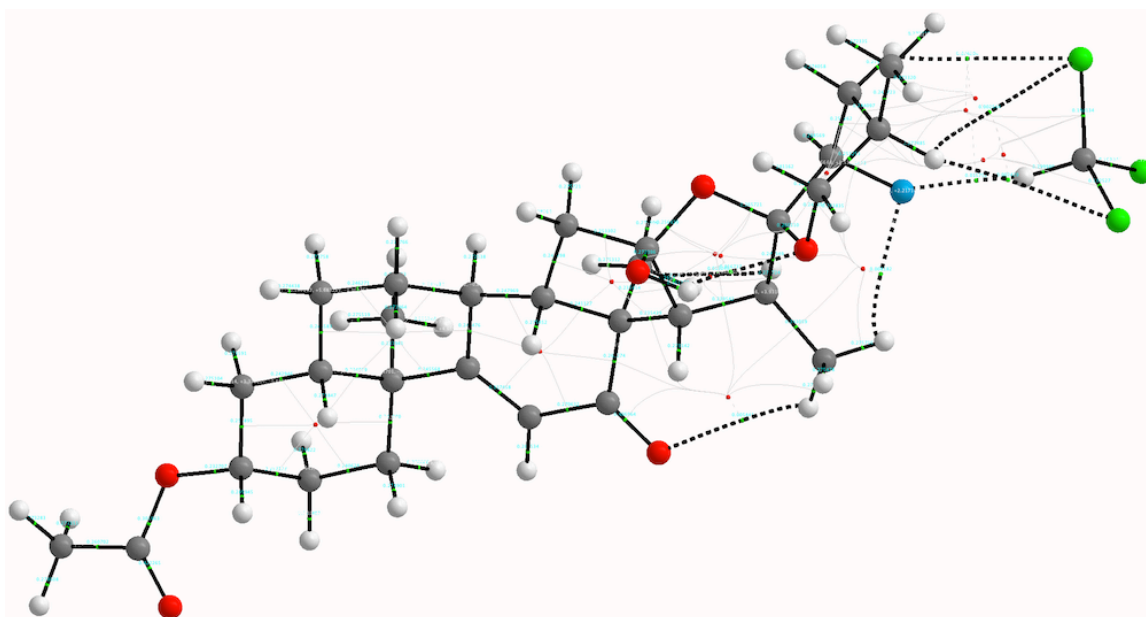


Figure 12.30 AIM analysis screenshot.

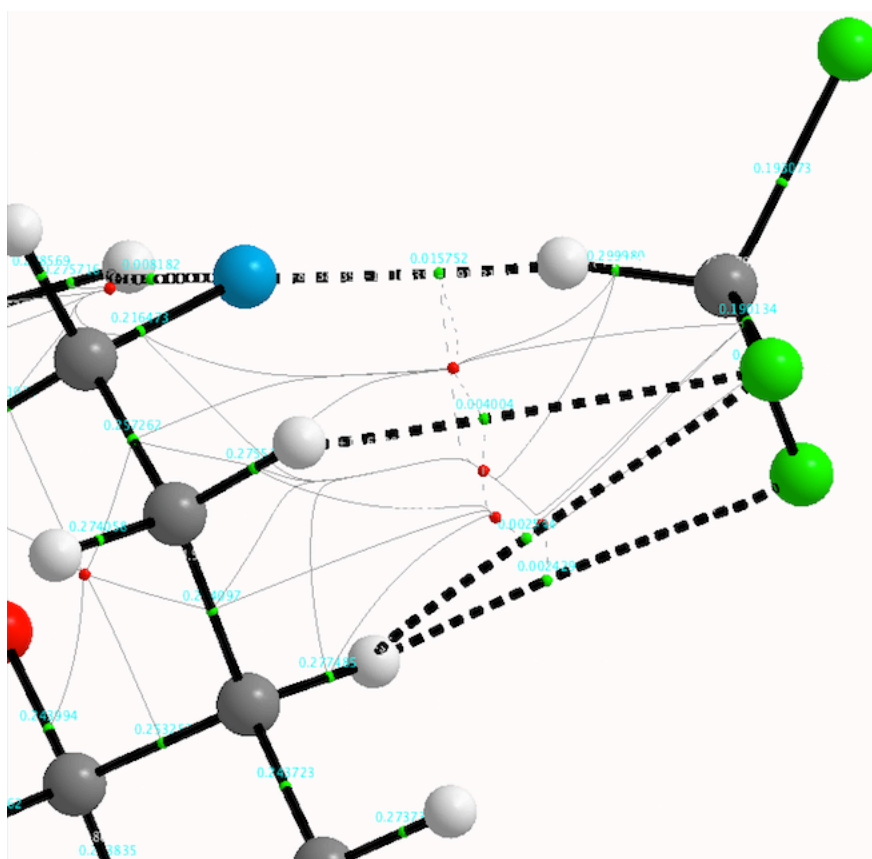
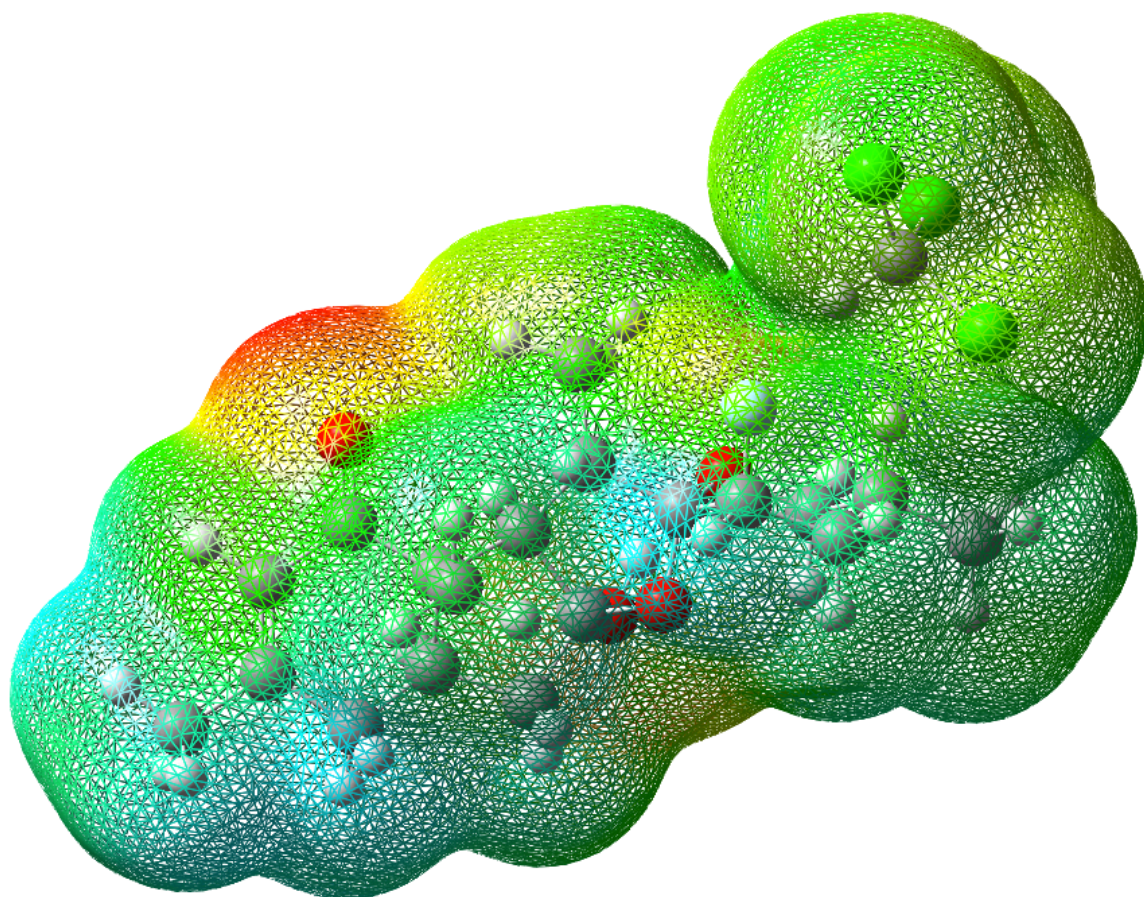
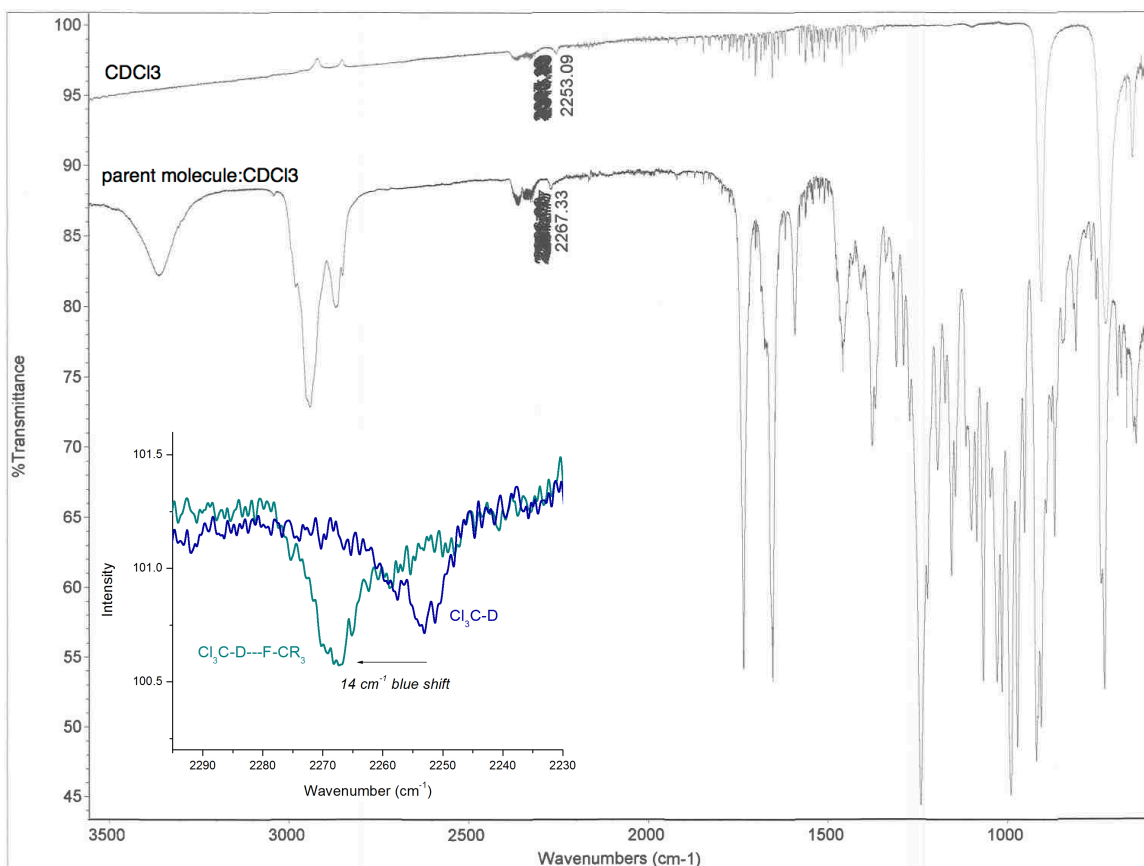


Figure 12.31 AIM analysis screenshot (zoomed in).



**Figure 12.32** Pruned parent molecule 2 (CAM-B3LYP/6-311++G\*\*) electrostatic potential map (EPM).



**Figure 12.33** Overlay of IR spectra of  $\text{CDCl}_3$  and 1:1 parent molecule **2**: $\text{CDCl}_3$ .

### Characterization Data.

*9,11-dehydrohecogenin acetate.* Hecogenin acetate **1** (1.4 g, 2.9 mmol) and benzeneseleninic acid anhydride (2.1 g, 5.8 mmol) were added to a flame-dried three-neck round bottom equipped with a stir bar and reflux condenser under  $\text{N}_2$ . Anhydrous chlorobenzene (12 mL) was added via syringe, and the reaction mixture was stirred and heated to reflux for 3 h. The reaction mixture was quenched with saturated aq.  $\text{NaHCO}_3$  and transferred to a separatory funnel. The crude mixture was extracted into EtOAc, and the combined organic layers were washed with  $\text{H}_2\text{O}$  and brine. The crude mixture was dried with  $\text{MgSO}_4$ , filtered through Celite, and concentrated. The crude residue was purified via gradient column chromatography on silica gel eluting with 10:90 to 20:80 EtOAc:hexanes to provide 9,11-dehydrohecogenin acetate as a pale white solid (1.0 g, 73% yield); m.p. = 213-215 °C.  $^1\text{H}$  NMR ( $\text{CDCl}_3$ )  $\delta$  5.65 (1H, d,  $J = 2.0$  Hz), 4.67-4.59 (1H, m), 4.38-4.32 (1H, m), 3.43 (1H, ddd,  $J = 10.8, 4.2, 2.0$  Hz), 3.31 (1H, t,  $J = 11.0$  Hz), 2.51-2.44 (1H, m), 2.35 (1H, dd,  $J = 8.8, 7.2$  Hz), 2.18-2.12 (1H, m), 2.02-1.89 (2H,

m), 1.99 (3H, s), 1.82-1.33 (16H, m), 1.09-1.02 (7H, m), 0.88 (3H, s), 0.75 (3H, d,  $J = 6.4$  Hz);  $^{13}\text{C}\{^1\text{H}\}$  NMR ( $\text{CDCl}_3$ )  $\delta$  204.6, 170.4, 170.3, 119.9, 109.2, 79.6, 72.5, 66.8, 53.6, 52.2, 50.9, 42.4, 42.3, 39.1, 36.7, 34.4, 33.6, 32.3, 31.3, 31.2, 30.1, 28.7, 27.4, 27.1, 21.2, 18.3, 17.0, 14.9, 13.0;  $\nu_{\text{max}}$  ( $\text{CaF}_2$ ,  $\text{CHCl}_3$ ): 1726, 1669  $\text{cm}^{-1}$ ; HRMS (ESI/ion-trap)  $m/z$ :  $[\text{M} + \text{Na}]^+$  Calcd for  $\text{C}_{29}\text{H}_{42}\text{O}_5\text{Na}^+$  493.2925; Found 493.2900.

*23 $\beta$ -fluoro-16 $\alpha$ -hydroxy-9,11-dehydrohecogenin acetate (2)*. Selectfluor (195 mg, 0.55 mmol) and 9,11-dehydrohecogenin acetate (118 mg, 0.25 mmol) were added to an oven-dried  $\mu\omega$  vial equipped with a stir bar; the vial was then sealed with a cap w/ septum using a crimper and evacuated/refilled with  $\text{N}_2$  multiple times. Anhydrous  $\text{CH}_3\text{CN}$  (6.0 mL) was added, and the reaction mixture was irradiated at 300 nm in a Rayonet reactor while stirring. After 4 h, an aliquot was taken for  $^{19}\text{F}$  NMR analysis. The reaction mixture was then poured over  $\text{Et}_2\text{O}$ , filtered through Celite, and concentrated. The crude reaction mixture was purified via gradient column chromatography on silica gel eluting with EtOAc/hexanes to provide **2** as a white solid (40 mg, 32% yield); m.p. = 196-198  $^\circ\text{C}$ .<sup>90</sup>  $^1\text{H}$  NMR ( $\text{CDCl}_3$ )  $\delta$  5.71 (1H, d,  $J = 2.0$  Hz), 4.70-4.62 (1H, m), 4.34 (1H, dm,  $J = 47.5$  Hz), 3.66-3.54 (2H, m), 3.35 (1H, br s), 2.50-2.43 (1H, m), 2.36 (1H, d,  $J = 6.8$  Hz), 2.25 (1H, quin,  $J = 6.9$  Hz), 2.20-2.11 (1H, m), 2.09-2.05 (2H, m), 2.01 (3H, s), 2.00-1.92 (3H, m), 1.79-1.73 (3H, m), 1.71-1.40 (7H, m), 1.25 (3H, dd,  $J = 6.9, 0.7$  Hz), 1.22-1.12 (1H, m), 1.08 (3H, s), 0.90 (3H, s), 0.82 (3H, d,  $J = 6.7$  Hz);  $^{13}\text{C}\{^1\text{H}\}$  NMR ( $\text{CDCl}_3$ )  $\delta$  203.7, 170.7, 170.5, 119.8, 115.8, 108.0 (d,  $J = 26.2$  Hz), 89.9 (d,  $J = 172.9$  Hz), 72.5, 67.5, 63.4, 52.3, 51.4, 42.4, 42.0, 39.3, 38.2, 36.5, 34.4, 34.1 (d,  $J = 20.3$  Hz), 33.7, 32.2, 27.4, 27.2, 24.0, 21.3, 18.3, 16.5, 14.5, 13.9;  $^{19}\text{F}$  NMR ( $\text{CDCl}_3$ )  $\delta$  -194.0 (1F, m);  $\nu_{\text{max}}$  ( $\text{CaF}_2$ ,  $\text{CHCl}_3$ ): 3560 (br), 1728, 1674  $\text{cm}^{-1}$ .

## 12.12 References.

<sup>1</sup> D. Naumann and J. Kischkewitz, *J. Fluorine Chem.*, 1990, **47**, 283-299.

<sup>2</sup> ACD/NMR Processor Academic Edition, version 12.0, Advanced Chemistry Development, Inc., Toronto, ON, Canada, www.acdlabs.com, **2012**.

<sup>3</sup> A. Huczynski, J. Rutkowski, and B. Brzezinski, *Struct. Chem.*, 2011, **22**, 627-634.

<sup>4</sup> Merrick, J. P.; Moran, D.; Radom, L. *J. Phys. Chem. A* **2007**, *111*, 11683–11700.

<sup>5</sup> Aoyama, M.; Fukuhara, T.; Hara, S. *J. Org. Chem.* **2008**, *73*, 4186-4189.

<sup>6</sup> Olah, G. A.; Li, X.-Y.; Wang, Q.; Prakash, G. K. S. *Synthesis*, **1993**, *7*, 693-699.

- 
- <sup>7</sup> Schneider, H.-J.; Gschwendtner, W.; Heiske, D.; Hoppen, V.; Thomas, F. *Tetrahedron* **1977**, *33*, 1769-1773.
- <sup>8</sup> Matsui, T.; Deguchi, M.; Yoshizawa, H. *U.S. Pat. Appl. Publ.* **2005**, US 20050158623 A1 20050721
- <sup>9</sup> Chambers, R. D.; Kenwright, A. M.; Parsons, M.; Sandford, G.; Moilliet, J. S. *Perkin Trans. 1* **2002**, *19*, 2190-2197.
- <sup>10</sup> Kobayashi, S.; Yoneda, A.; Fukuhara, T.; Hara, S. *Tetrahedron*, **2004**, *60*, 6923-6930.
- <sup>11</sup> Luo, H.-Q.; Loh, T.-P. *Tetrahedron Lett.* **2009**, *50*, 1554-1556.
- <sup>12</sup> Hu, J.; He, Z. *Faming Zhuanli Shenqing* **2011**, CN102219638.
- <sup>13</sup> Yin, J.; Zarkowsky, D. S.; Thomas, D. W.; Zhao, M. M.; Huffman, M. A. *Org. Lett.* **2004**, *6*, 1465-1468.
- <sup>14</sup> Ramsden, C. A.; Shaw, M. M. *Tetrahedron Lett.* **2009**, *50*, 3321-3324.
- <sup>15</sup> Bloom, S.; Pitts, C. R.; Miller, D. C.; Haselton, N.; Holl, M. G.; Urheim, E.; Lectka, T. *Angew. Chem. Int. Ed.* **2012**, *51*, 10580-10583.
- <sup>16</sup> Dahbi, A.; Hamman, S.; Beguin, C. G. *Magn. Reson. Chem.* **1986**, *24*, 337-342.
- <sup>17</sup> Blessley, G.; Holden, P.; Brown, J. M.; Gouverneur, V.; Walker, M. *Org. Lett.* **2012**, *14*, 2754-2757.
- <sup>18</sup> Cazorla, C.; Melay, E.; Andrioletti, B.; Lemaire, M. *Tetrahedron Lett.* **2009**, *50*, 3936-3938.
- <sup>19</sup> For an early review on spin trapping reagents and techniques, see: Janzen, E. G. *Acc. Chem. Res.* **1971**, *4*, 31-40.
- <sup>20</sup> Huczynski, A.; Rutkowski, J.; Brzezinski, B. *Struct. Chem.* **2011**, *22*, 627-634.
- <sup>21</sup> For iodide redox processes, see: (a) Oskam, G.; Bergeron, B. V.; Meyer, G. J.; Searson, P. C. *J. Phys. Chem. B* **2001**, *105*, 6867-6873. (b) Datta, J.; Bhattacharya, A.; Kundu, K. K. *Bull. Chem. Soc. Jpn.* **1988**, *61*, 1735-1742. (c) Macagno, V. A.; Giordano, M. C.; Arvia, A. J. *Electrochim. Acta* **1969**, *14*, 335-337.
- <sup>22</sup> Prakash, T. *Adv. Matt. Lett.* **2011**, *2*, 131-135.
- <sup>23</sup> Pyridylmethanimine copper(I) catalysts were synthesized according to literature procedure from both amine functionalized silica gel and amino functional cross-linked poly(styrene) beads, pyridine-2-carbaldehyde, and cuprous chloride. See: (a) Clark, A. J.; Filik, R. P.; Haddleton, D. M.; Radigue, A.; Sanders, C. J.; Thomas, G. H.; Smith, M. E. *J. Org. Chem.* **1999**, *64*, 8954-8957. (b) Haddleton, D. M.; Kukulj, D.; Radigue, A. P. *Chem. Commun.* **1999**, 99-100.
- <sup>24</sup> An attempt was made to grow crystals of the 2:1 bis(imine) ligand:copper species to confirm 2:1 binding, but only the aforementioned polymeric structure crystallized.
- <sup>25</sup> Tan, K.-T.; Chng, S.-S.; Cheng, H.-S.; Loh, T.-P. *J. Am. Chem. Soc.* **2003**, *125*, 2958-2963.
- <sup>26</sup> Not optimized.
- <sup>27</sup> Shindo, M.; Sugioka, T.; Shishido, K. *Tetrahedron Lett.* **2004**, *45*, 9265-9268.
- <sup>28</sup> Adapted from: Padwa, A.; Rodriguez, A.; Tohidi, M.; Fukunaga, T. *J. Am. Chem. Soc.* **1983**, *105*, 933-943.
- <sup>29</sup> For instance: Moncol, J.; Mudra, M.; Lönnecke, P.; Hewitt, M.; Valko, M.; Morris, H.; Svorec, J.; Melnik, M.; Mazur, M.; Koman, M. *Inorg. Chim. Acta.* **2007**, *360*, 3213-3225.
- <sup>30</sup> Schneider, H.-J.; Gschwendtner, W.; Heiske, D.; Hoppen, V.; Thomas, F. *Tetrahedron* **1977**, *33*, 1769-1773.
- <sup>31</sup> Beaulieu, F.; Beaugard, L.; Courchesne, G.; Couturier, M.; LaFlamme, F.; L'Heureux, A. *Org. Lett.* **2009**, *11*, 5050-5053.
- <sup>24</sup> Aoyama, M.; Fukuhara, T.; Hara, S. *J. Org. Chem.* **2008**, *73*, 4186-4189.

- 
- <sup>25</sup> York, C.; Prakash, G. K. S.; Olah, G. A. *Tetrahedron* **1996**, *52*, 9-14.
- <sup>26</sup> Bloom, S.; Sharber, S. A.; Holl, M. G.; Knippel, J. L.; Lectka, T. *J. Org. Chem.* **2013**, *78*, 11082-11086.
- <sup>27</sup> ACD/NMR Processor Academic Edition, version 12.0, Advanced Chemistry Development, Inc., Toronto, ON, Canada, www.acdlabs.com, **2012**.
- <sup>32</sup> Bloom, S.; Knippel, J. L.; Lectka, T. *Chem. Sci.* **2014**, *5*, 1175-1178.
- <sup>33</sup> Amaoka, Y.; Nagatomo, M.; Inoue, M. *Org. Lett.* **2013**, *15*, 2160-2163.
- <sup>34</sup> Aoyama, M.; Fukuhara, T.; Hara, S. *J. Org. Chem.* **2008**, *73*, 4186-4189.
- <sup>35</sup> York, C.; Prakash, G. K. S.; Olah, G. A. *Tetrahedron* **1996**, *52*, 9-14.
- <sup>36</sup> Bloom, S.; Pitts, C. R.; Woltornist, R.; Griswold, A.; Holl, M. G.; Lectka, T. *Org. Lett.* **2013**, *15*, 1722-1724.
- <sup>37</sup> Bloom, S.; Sharber, S. A.; Holl, M. G.; Knippel, J. L.; Lectka, T. *J. Org. Chem.* **2013**, *78*, 11082-11086.
- <sup>38</sup> Liu, W.; Huang, X.; Cheng, M.-J.; Nielsen, R. J.; Goddard III, W. A.; Groves, J. T. *Science* **2012**, *337*, 1322-1325.
- <sup>39</sup> J. Lee, H. Kim, J. K. Cha, *J. Am. Chem. Soc.* **1996**, *118*, 4198-4199.
- <sup>40</sup> O. G. Kulinkovich, S. V. Sviridov, D. A. Vasilevski, *Synthesis*, **1990**, 234.
- <sup>41</sup> U. M. Dzhemilev, A. G. Ibragimov, L. O. Khafizova, R. R. Gubaidullin (Uchrezhdenie Rossijskoj akademii nauk Institut neftekhimii i kataliza RAN), RU 2433990 C2, **2011**.
- <sup>42</sup> L. O. Khafizova, R. R. Gubaidullin, U. M. Dzhemilev, *Tetrahedron* **2011**, *67*, 9142-9147.
- <sup>43</sup> J. Jiao, L. X. Nguyen, D. R. Patterson, R. A. Flowers II, *Org. Lett.* **2007**, *9*, 1323-1326.
- <sup>44</sup> S. Bloom, C. R. Pitts, R. Woltornist, A. Griswold, M. G. Holl, T. Lectka, *Org. Lett.* **2013**, *15*, 1722-1724.
- <sup>45</sup> W. Liu, X. Huang, M. Cheng, R. J. Nielson, W. A. Goddard III, J. T. Groves, *Science*, **2012**, *337*, 1322-1325.
- <sup>46</sup> M. Kawatsura and J. F. Hartwig, *J. Am. Chem. Soc.*, 1999, **121**, 1473-1478.
- <sup>47</sup> a) G. F. Woods and F. Scotti, *J. Org. Chem.*, 1961, **26**, 312-318. b) E. Pinard, S. M. Ceccarelli, H. Stalder, and D. Alberati, *Bioorg. Med. Chem. Lett.*, 2006, **16**, 349-352.
- <sup>48</sup> M. Ceylan, S. Yalcin, H. Secen, Y. Suetbeyaz, and M. Balci, *J. Chem. Res-S.*, 2003, **1**, 21-23.
- <sup>49</sup> M. C. Willis, D. Taylor, and A. T. Gillmore, *Tetrahedron*, 2006, **62**, 11513-11520.
- <sup>50</sup> C. Djerassi, G. von Mutzenbecher, J. Fajkos, D. H. Williams, and H. Budzikiewicz, *J. Am. Chem. Soc.*, 1965, **87**, 817-826.
- <sup>51</sup> J.-B. Xia, C. Zhu, and C. Chen, *J. Am. Chem. Soc.*, 2013, **135**, 17494-17500.
- <sup>52</sup> Adapted from: Lorenz, J. C.; Long, J.; Yang, Z.; Xue, S.; Xie, Y.; Shi, Y. *J. Org. Chem.* **2004**, *69*, 327-334.
- <sup>53</sup> Adapted from: Wallace, D. J.; Chen, C. *Tetrahedron Lett.* **2002**, *43*, 6987-6990.
- <sup>54</sup> Adapted from: Shaikh, T. M.; Hong, F.-E. *Beilstein J. Org. Chem.* **2013**, *9*, 1578-1588.
- <sup>55</sup> Adapted from: Yao, Q.; Kinney, E. P.; Yang, Z. *J. Org. Chem.* **2003**, *68*, 7528-7531.
- <sup>56</sup> (a) Molloy, M. S.; Snyder, J. A.; Bragg, A. E. *J. Phys. Chem. A* **2014**, *118*, 3913-3925. (b) Snyder, J. A.; Bragg, A. E. *J. Phys. Chem. A* **2015**, *119*, 3972-3985.

- 
- <sup>57</sup> Godbout, J. T.; Zuilhof, H.; Heim, G.; Gould, I. R.; Goodman, J. L.; Dinnocenzo, J. P.; Kelley, A. M. *J. Raman Spectrosc.* **2000**, *31*, 233–241.
- <sup>58</sup> Brouwer, A. M. *Pure Appl. Chem.* **2011**, *83*, 2213–2228.
- <sup>59</sup> Hautala, R. R.; Schore, N. E.; Turro, N. J. *J. Am. Chem. Soc.* **1973**, *95*, 5508–5514.
- <sup>60</sup> Rich, D. H.; Singh, J. The carbodiimide method. In *The Peptides: Analysis, Synthesis, Biology*; Gross, E., Meienhofer, J., Eds.; Academic: New York, 1979; pp 241–261.
- <sup>61</sup> Satzinger, G. *Arzneim-Forsch. Drug Res.* **1994**, *44*, 261–266.
- <sup>62</sup> Curphey, T. J. *J. Org. Chem.* **1979**, *44*, 2805–2807.
- <sup>63</sup> Csuk, R.; Schwarz, S.; Kluge, R.; Ströhl, D. *Eur. J. Org. Chem.* **2010**, *45*, 5718–5723.
- <sup>64</sup> Beseda, I.; Czollner, L.; Shah, P. S.; Khunt, R.; Gaware, R.; Kosma, P.; Stanetty, C.; del Ruiz-Ruiz, M. C.; Amer, H.; Mereiter, K.; Da Cunha, T.; Odermatt, A.; Claben-Houben, D.; Jordis, U. *Bioorg. Med. Chem.* **2010**, *18*, 433–454.
- <sup>65</sup> Jauch, J.; Bergmann, J. *Eur. J. Org. Chem.* **2003**, *24*, 4752–4756.
- <sup>66</sup> Siewert, B.; Wiemann, J.; Köwitsch, A.; Csuk, R. *Eur. J. Med. Chem.* **2014**, *72*, 84–101.
- <sup>67</sup> Diao, T.; Stahl, S. S. *J. Am. Chem. Soc.* **2011**, *133*, 14566–14569.
- <sup>68</sup> Frelek, J.; Szczepek, W. J.; Weiss, H. P.; Reiss, G. J.; Frank, W.; Brechtel, J.; Schultheis, B.; Kuball, H.-G. *J. Am. Chem. Soc.* **1998**, *120*, 7010–7019.
- <sup>69</sup> Sondheimer, F.; Mazur, Y. *J. Am. Chem. Soc.* **1957**, *79*, 2906–2910.
- <sup>70</sup> Muzart, J. *Tetrahedron Lett.* **1987**, *28*, 4665–4668.
- <sup>71</sup> Liu, X.-K.; Ye, B.-J.; Wu, Y.; Nan, J.-X.; Lin, Z.-H.; Piao, H.-R. *Chem. Biol. Drug. Des.* **2012**, *79*, 523–529.
- <sup>72</sup> Zheng, Y.; Li, Y. *J. Org. Chem.* **2003**, *68*, 1603–1606.
- <sup>73</sup> Roleira, F. M. F.; Tavares da Silva, E. J.; Carvalho, R. A.; Marques, M. P. M. *Lett. Drug Des. Discov.* **2010**, *7*, 610–617.
- <sup>74</sup> Shingate, B. B.; Hazra, B. G.; Salunke, D. B.; Pore, V. S.; Shirazi, F. S.; Deshpande, M. V. *Tetrahedron* **2013**, *69*, 11155–11163.
- <sup>75</sup> Dias, J. R.; Martin, D. E.; Wilcox, H. E. *J. Prakt. Chem.* **1992**, *334*, 474–476.
- <sup>76</sup> Takatsuto, S.; Ikekawa, N. *Chem. Pharm. Bull.* **1987**, *35*, 986–995.
- <sup>77</sup> Brown, B. R.; Trown, P. W.; Woodhouse, J. M. *J. Chem. Soc.* **1961**, 2478–2485.
- <sup>78</sup> Valente, C.; Eadon, G. *J. Org. Chem.* **1984**, *49*, 44–51.
- <sup>79</sup> Rowland, A. T. *Steroids* **1975**, *26*, 251–254.
- <sup>80</sup> Dodson, R. M.; Riegel, B. *J. Org. Chem.* **1948**, *13*, 424–437.
- <sup>81</sup> Kametani, T.; Tsubuki, M.; Higurashi, K.; Honda, T. *J. Org. Chem.* **1986**, *51*, 2932–2939.
- <sup>82</sup> Mori, H. *Chem. Pharm. Bull.* **1962**, *10*, 429–432.
- <sup>83</sup> Logashenko, E. B.; Salomatina, O. V.; Markov, A. V.; Korchagina, D. V.; Salakhutdinov, N. F.; Tolstikov, G. A.; Vlassov, V. V.; Zenkova, M. A. *ChemBioChem* **2011**, *12*, 784–794.
- <sup>84</sup> Kasal, A.; Budešínský, M.; Mareš, P.; Křištofiková, Z.; Leitão, A. J.; Sá e Melo, M. L.; Silva, M. M. C. *Steroids* **2016**, *105*, 12–18.
- <sup>85</sup> Templeton, J. F.; Majid, S.; Marr, A.; Marat, K. *J. Chem. Soc., Perkin Trans. 1*, **1990**, 2581–2584.



---

<sup>86</sup> Kirk, D. N.; Klyne, W.; Peach, C. M.; Wilson, M. A. *J. Chem. Soc. C* **1970**, 1454-1460.

<sup>87</sup> Barton, D. H. R.; Lester, D. J.; Ley, S. V. *J. Chem. Soc., Perkin Trans. 1*, **1980**, 2209-2212.

<sup>88</sup> Atopkina, L. N.; Denisenko, V. A. *Chem. Nat. Compd.* **2015**, *51*, 711-715.

<sup>89</sup> Sheldrick, G. M. *Acta Cryst.* **2015**, *C71*, 3-8.

<sup>90</sup> Determined for 2:CHCl<sub>3</sub> crystal.

## Vita

On August 19<sup>th</sup>, 1988, Bambi Marangio-Pitts, wife of Kenneth G. Pitts, endured 18 hours of hard labor to bring Cody Ross Pitts into this world. After his arrival, Cody attempted to grow up in Waterbury, Connecticut – "The Brass City" – where he attended St. Mary's School (as did his younger brother, Casey Joshua Pitts, and sister, Kendelle Rose Pitts) before moving on to Southington High School. Throughout these early academic years, if you told him he was going to be a chemist, he might have laughed in your face. Instead, Cody attended Monmouth University in New Jersey as an undergraduate student with aspirations to study marine biology and theatre... but then he took organic chemistry. Whether it was the fault of the subject matter or Prof. Massimiliano Lamberto himself, Cody felt compelled to switch his major to chemistry after Prof. Lamberto's Organic Chemistry I course in the spring of his sophomore year. Ultimately, he graduated in 2010 with this major in chemistry and minors in both physics and musical theatre at the top of his class with a cumulative 4.0 GPA and an Honors thesis comprised of work in Prof. Lamberto's laboratory of synthetic organic chemistry. Yet, to make sure graduate school was what he *really* wanted to do, he took a year off to clear his head, spend time with his grandparents (Rosario and Julia Marangio), work as an EMT, and continue to pursue a career in acting on the side (as acting has always played a role in this character's life, and always will). Having heard in a movie that if you truly love something, you should let it go, Cody let go of organic chemistry for just a couple months and found himself sprinting back to it. It was meant to be. He thus applied and was accepted to Johns Hopkins University, where he knew immediately that he needed to work with Prof. Thomas Lectka. Cody joined the Lectka laboratory at an extremely exciting time, as the universe was ready for a mild radical fluorination reaction to be discovered (though whether or not the universe wanted Steven Bloom and Cody to do it is another story). In his graduate career, Cody has had the pleasure of developing various synthetic methods and studying intricate reaction mechanisms in the blossoming field of practical radical fluorination chemistry. Perhaps even more than discovering this new chemistry, he loved teaching others about it. Upon graduation from Johns Hopkins, he and his remarkable wife, Katrina Lynne Pitts, are moving first to Switzerland, where Cody will be pursuing postdoctoral research with Prof. Antonio Togni at ETH-Zürich, and then to California, where Cody will be pursuing postdoctoral research with Prof. Phil Baran at The Scripps Research Institute. Then, he will finally get a real job in academia and pursue who knows what.